WADC TECHNICAL REPORT 54-592, Part 2

EFFECTS OF STRUCTURAL FLEXIBILITY ON GUST LOADING OF AIRCRAFT

Part 2 - DYNAMIC STRESSES IN SWEPT-WING AIRPLANES

A. A. Kirsch, J. M. Calligeros and K. A. Foss
Massachusetts Institute of Technology

August 1955

Aircraft Laboratory
Contract No. AF 33(616)-2425
RDO No. R451-344 SR-1a

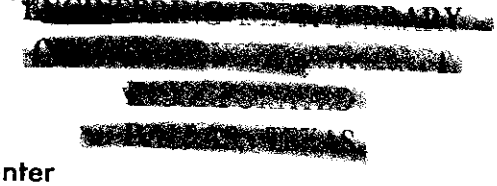

Wright Air Development Center
Air Research and Development Command
United States Air Force
Wright-Patterson Air Force Base, Ohio

FOREWORD

The trend toward highly flexible aircraft with swept wings has raised some questions as to the applicability of existing methods for calculating the structural stresses due to gust loading. It was consequently decided by the Wright Air Development Center, U. S. Air Force, to initiate research to provide information on the effects of structural flexibility on the gust loading of swept-wing aircraft and to develop methods for computing these effects.

The present report is the second and concluding part to be issued on this research. It was prepared by the Aeroelastic and Structures Research Laboratory, Massachusetts Institute of Technology, under U. S. A. F. Contract No. 33(616)-2425 with Professor T. H. H. Pian as project supervisor and Mr. K. A. Foss as project leader. The contract is being administered by the Aircraft Laboratory, Directorate of Laboratories, Wright Air Development Center, with Mr. H. E. Kugel acting as project engineer and Mr. W. Boccius as scientist advisor.

The authors wish to acknowledge the work of Mr. R. E. Storey at the beginning of this investigation. They also wish to thank the personnel of the Computing Section of the Aeroelastic and Structures Research Laboratory for performing many of the computations, Mr. H. W. Gewehr for preparing the figures and Miss I. G. Ellis for typing the manuscript.

ABSTRACT

A simplified numerical method is presented for finding the transient stresses in a swept-wing airplane after entry into a gust. The effects of the pitching motion of the airplane and of the unsteady downwash at the tail on the transient stresses are included. Some sample calculations indicate that more degrees of freedom are necessary in the analysis of gust loads on a flexible swept-wing airplane than for an unswept-wing airplane, and that the alleviation of gust loads commonly attributed to flexible swept wings is always at least partially cancelled by the increased pitching motion of the airplane.

PUBLICATION REVIEW

This report has been reviewed and is approved.

FOR THE COMMANDER:

for E. H. Schwartz
D. D. McKee
Colonel, USAF
Chief, Aircraft Laboratory
Directorate of Laboratories

TABLE OF CONTENTS

LIST OF ILLUSTRATIONS

GLOSSARY OF SYMBOLS

A	Cross-sectional area of body of revolution equivalent to fuselage
AR	Aspect ratio
a	Lift-curve slope
b	Span of lifting surface
C_{ij}	Flexibility influence coefficient
C_L	Lift coefficient, based on wing area
$\frac{dC_{mf}}{d\alpha}$	Moment-curve slope of fuselage, based on wing area and mean geometric chord
c	Local chord
$\bar{c}$	Mean geometric chord
F	Gust profile function = $\frac{w}{w_{MAX}}$
f	Gust forcing function
k_y	Pitching radius of gyration of airplane
K_{ij}	Stiffness influence coefficient
L	Lift
l	Distance in streamwise direction measured in mean geometric chords
M	Mass of airplane, or generalized mass
P_t	Tail parameter = $\frac{S_t a_t}{S a_w}$
Q_i	Generalized force
q_i	Generalized coordinate

s	Dimensionless time= $\frac{Ut}{\bar{c}/2}$
s_g	Gust-gradient distance, distance to gust peak in mean geometric wing semichords
S	Area of lifting surface
t	Time from beginning of gust penetration
U	True airspeed of airplane
V_f	Volume of body of revolution equivalent to fuselage
w	Vertical velocity of gust
y	Spanwise coordinate, measured perpendicular from center line of airplane
q_0	Vertical displacement of center of gravity of airplane, positive up
α	Angle of attack
β	Sweep parameter
γ	Ratio of mean geometric wing chord to mean geometric tail chord $= \frac{\bar{c}}{\bar{c}_t}$
ϵ	Increment of s for numerical integration
$\frac{d\epsilon}{d\alpha}$	Downwash parameter
φ	Indicial lift growth on horizontal tail due to downwash from wing
η	Dimensionless spanwise coordinate = $\frac{y}{b/2}$
q_1	Pitch angle
λ	Taper ratio
μ	Dimensionless mass parameter = $\frac{M}{\rho S \frac{\bar{c}}{2} a_w}$
φ_0	Dimensionless vertical displacement coordinate $= \frac{q_0}{\bar{c}/2}$
ρ	Mass density of air

φ	Wagner lift-growth function
ψ	Kussner lift-growth function
Θ	Sweep angle of elastic axis
Λ	Sweep angle of fractional-chord line

Subscripts

f	Fuselage
w	Wing
t	Horizontal tail
Λ	Includes effects of sweep

Superscripts

G	Due to gust
L	For lift
α	Due to angle of attack (or motion)

Notation

$(')$	Differentiation with respect to s
$(\dot{})$	Differentiation with respect to t
$[\ ]$	Rectangular matrix
$\{\ \}$	Column matrix
$[\ \searrow]$	Diagonal matrix

INTRODUCTION

The inclusion of the effects of structural flexibility in methods for computing the gust loads on aircraft has been the subject of considerable research in recent years, e. g., References 1, 2, 3 and 4. In Reference 5 good agreement has been found for the dynamic overstress in wing-root bending moment between flight experiments and a theoretical method which considers only a rigid-body heaving and one wing-bending degree of freedom. This study was confined to airplanes with unswept wings. A similar analytical method has been developed in References 6 and 7 for airplanes with swept wings; however, the neglect of the airplane pitching degree of freedom may be a severe limitation because of the elastic and aerodynamic coupling between this degree of freedom and the bending motion of a swept wing. The present report is concerned with the importance of including additional degrees of freedom.

In Section I the equations of motion are formulated for the response of a flexible swept-wing airplane to a discrete gust. Structural vibrations are taken into account through the use of assumed modes of deformation.

The numerical procedure developed in Reference 8 (Part 1 of the present report) for computing gust-response time histories has been extended to include the assumed vibrational degrees of freedom. Since this method involves a step-by-step recurrence relationship, it is particularly adaptable to automatic digital computing machinery.

In Section IV the dynamic stresses in the swept wing of an example airplane are found. The effects of neglecting certain degrees of freedom and of using quasi-

steady aerodynamics for the damping forces are investigated.

The effect of the side-bending vibration of an underslung nacelle on the bending moment at the root of an example wing is investigated in Appendix C; and the contribution of the downwash behind a vibrating wing on the horizontal tail gust loads is investigated in Appendix D.

In Appendix E, the relative accuracy of three different methods for computing transient stresses is illustrated by theoretical considerations of convergence and by numerical examples. A modification of the mode-acceleration method which combines both accuracy and simplicity is proposed.

A parametric study is made in Appendix F in an attempt to find the optimum spanwise location for a heavy concentrated mass such as a nacelle insofar as dynamic overstresses are concerned.

I EQUATIONS OF MOTION

The motion of a continuous elastic system such as an aircraft structure involves an infinite number of degrees of freedom; and so, except for very simple cases, the motion of such a structure must be described approximately by a finite number of judiciously chosen degrees of freedom. In practice, an aircraft structure is usually reduced to a system with a finite number of degrees of freedom by one of the following approaches:

(1) Approximation of the structure by a system of elastically connected discrete mass particles each with its own equation of motion (Reference 2).

(2) The use of assumed modes of deformation together with generalized coordinates (Reference 7).

(3) The use of natural modes of vibration together with normal coordinates (Reference 1).

Each of the three approaches results in a set of simultaneous linear differential equations; and, when aerodynamic damping forces are taken into account, these equations are coupled together. Even though inertial coupling terms are eliminated by the discrete mass approach and both inertial and elastic coupling terms are eliminated by the normal mode approach, the ease of solution of the equations of motion depends primarily upon the number of degrees of freedom required because these equations are coupled together by aerodynamic terms in any case. Since mode shape methods are

preferable for the purpose of computing aerodynamic forces, and since fewer mode shapes than lumped masses are usually required to adequately describe the vibrations of a continuous system, the discrete mass approach appears to be the least desirable. The natural modes and frequencies of an airplane are not always available in the early stages of design and are tedious to compute, particularly when the weight condition is varied; consequently, the assumed mode approach has been chosen for the analysis which follows.

The equations of motion of a flexible airplane are easily derived in terms of generalized coordinates through the use of Lagrange's Equation in the following form:

$$\frac{d}{dt}\left(\frac{\partial T}{\partial \dot{q}_i}\right) - \frac{\partial T}{\partial q_i} + \frac{\partial U_i}{\partial q_i} = Q_i \qquad (1.1)$$

where

q_i is a generalized coordinate

T is the kinetic energy of the system

U_i is the internal energy of the system

Q_i is a generalized force

In the present analysis, two rigid body and five deformation modes, ϕ_i, are considered which will represent the flexible airplane under dynamic loading. While only the fundamental cantilever deformation modes are used presently for the purpose of simplification, additional modes can be incorporated without difficulty. The kinetic energy expression for this system is

$$T = \frac{1}{2}\int_{-\frac{\bar{c}}{2}\ell_{c.g.}}^{\frac{\bar{c}}{2}\ell_f} m_f(\bar{x})\,V_f^2\,d\bar{x} + \int_0^{b/2} m_w(y)\,V_w^2\,dy + \int_0^{b_t/2} m_t(y)\,V_t^2\,dy$$

$$+\frac{1}{2}\int_{-\frac{\bar{c}}{2}\ell_{c.g.}}^{\frac{\bar{c}}{2}\ell_f} I_f(\bar{x})\,\dot{\theta}_f^2\,d\bar{x} + \int_0^{b/2} I_w(y)\,\dot{\theta}_w^2\,dy + \int_0^{b_t/2} I_t(y)\,\dot{\theta}_t^2\,dy \qquad (1.2)$$

where

$m_f(\bar{x})$	is the mass per unit length along the fuselage
$m_w(y)$	is the mass per unit length of the wing in the y direction
$m_t(y)$	is the mass per unit length of the horizontal tail in the y direction
$I_f(\bar{x})$	is the local moment of inertia of the fuselage about the local y-axis
$I_w(y)$	is the local moment of inertia of the wing about the local c. g.
$I_t(y)$	is the local moment of inertia of the horizontal tail about the local c. g.
V_f, V_w, V_t	are the velocities of the fuselage, wing and horizontal tail, respectively, at the local c. g. 's
$\dot{\theta}_f, \dot{\theta}_w, \dot{\theta}_t$	are the rotary velocities of the fuselage, wing and horizontal tail, respectively, about the local c. g. 's

and, in terms of the displacements $\phi_i(y)\,q_i(t)$, the internal energy of the system is

$$U_i = \tfrac{1}{2}\int_{-\frac{\bar{c}}{2}\ell_{c.g.}}^{\frac{\bar{c}}{2}\ell_f} EI_f(\bar{x})\left(\frac{d^2\phi_2}{d\bar{x}^2}\right)^2 q_2^2\, d\bar{x} + \int_0^{\frac{b}{2\cos\Phi}} EI_w(\bar{y})\left(\frac{d^2\phi_3}{d\bar{y}^2}\right)^2 q_3^2\, d\bar{y}$$

$$+ \int_0^{\frac{b}{2\cos\Phi}} GJ_w(\bar{y})\left(\frac{d\phi_4}{d\bar{y}}\right)^2 q_4^2\, d\bar{y} + \int_0^{\frac{b_t}{2\cos\Phi_t}} EI_t(\bar{y})\left(\frac{d^2\phi_5}{d\bar{y}^2}\right)^2 q_5^2\, d\bar{y}$$

$$+ \int_0^{\frac{b_t}{2\cos\Phi_t}} GJ_t(\bar{y})\left(\frac{d\phi_6}{d\bar{y}}\right)^2 q_6^2\, d\bar{y} \qquad (1.3)$$

where the subscripts

2, 3, 4, 5, 6	refer to the fuselage bending, first wing bending, first wing torsion, first horizontal tail bending, first horizontal tail torsion modes, respectively

and

EI_f, EI_w, EI_t	are the bending stiffnesses of the fuselage, wing, and horizontal tail, respectively
GJ_w, GJ_t	are the torsional stiffnesses of the wing and horizontal tail, respectively

Appendix A. 4 gives the internal energy expressions when influence or stiffness coefficients are used instead of the EI and GJ distributions.

The generalized forces and moments are obtained from the virtual work expression which is

$$Q_i \delta q_i = \int_{-\frac{\bar{c}}{2}\ell_{c.g.}}^{\frac{\bar{c}}{2}\ell_f} \left[\left(\ell_f^{\alpha} + \ell_f^{\Theta} \right) d\bar{x} \right] \delta \left(q_0 - \bar{x} q_1 + \phi_2(\bar{x}) q_2 \right)$$

$$+ 2 \int_0^{\frac{b}{2}} \left[\left(\ell_w^{\alpha} + \ell_w^{\Theta} \right) dy \right] \delta \left(q_0 + k_1(y) q_1 + \left[\phi_2\left(\tfrac{\bar{c}}{2}\ell_w\right) + \left(\frac{d\phi_2}{d\bar{x}}\right)_{\frac{\bar{c}}{2}\ell_w} k_2(y) \right] q_2 \right.$$

$$\left. + \phi_3(y) q_3 + \left[k_1(y) - k_w(y) \right] \left[\phi_4(y) \cos \Theta q_4 - \frac{d\phi_3}{dy} \sin \Theta \cos \Theta q_3 \right] \right)$$

$$+ 2 \int_0^{\frac{b_t}{2}} \left[\left(\ell_t^{\alpha} + \ell_t^{\Theta} + \ell_{tw}^{\alpha} + \ell_{tw}^{\Theta} \right) dy \right] \delta \left(q_0 - k_3(y) q_1 + \left[\phi_2\left(\tfrac{\bar{c}}{2}\ell_t\right) + \left(\frac{d\phi_2}{d\bar{x}}\right)_{\frac{\bar{c}}{2}\ell_t} k_4(y) \right] q_2 \right.$$

$$\left. + \phi_5(y) q_5 + \left[k_5(y) - k_3(y) \right] \left[\phi_6(y) \cos \Theta_t q_6 - \frac{d\phi_5}{dy} \sin \Theta_t \cos \Theta_t q_5 \right] \right) \qquad (1.4)$$

where

$$k_1 = \frac{\bar{c}}{2} \left(\ell_1 - \eta \, AR \tan \Lambda_1 \right) \qquad k_w = \frac{\bar{c}}{2} \left(\ell_w - \eta \, AR \tan \Theta \right)$$

$$k_2 = \frac{\bar{c}}{2} \left(\ell_1 - \ell_w - \eta \, AR \tan \Lambda_1 \right) \qquad k_4 = \frac{\bar{c}}{2} \left(\ell_{1t} - \ell_t + \eta \frac{AR_t}{\gamma} \tan \Lambda_{1t} \right)$$

$$k_3 = \frac{\bar{c}}{2} \left(\ell_{1t} + \eta \frac{AR_t}{\gamma} \tan \Lambda_{1t} \right) \qquad k_5 = \frac{\bar{c}}{2} \left(\ell_t + \eta \frac{AR_t}{\gamma} \tan \Theta_t \right)$$

$\bar{x}$ is the distance from the center of gravity of the airplane to a local fuselage mass, positive aft.

Figure 1.1 shows the definitions of the distances ℓ_1, ℓ_w, ℓ_t, ℓ_{1t} and the sweep angles Λ_1, Λ_{1t}, Θ and Θ_t.

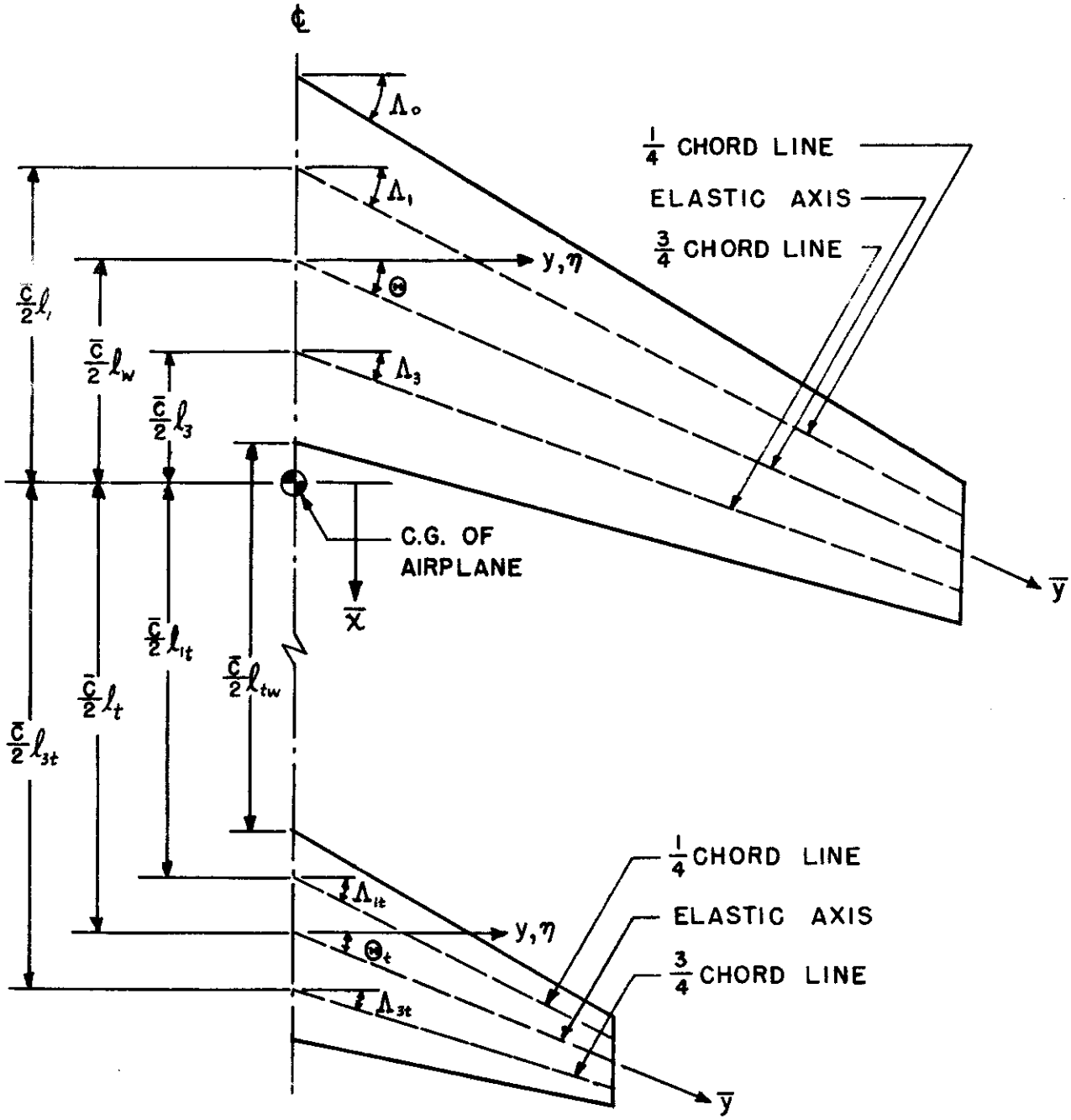

FIGURE 1.1 DEFINITION OF DISTANCES AND SWEEP ANGLES

The linear and angular velocities to be introduced into equation (1.2) are given by

$$V_f = \dot{q}_0 - \bar{x}\dot{q}_1 + \phi_2(\bar{x})\dot{q}_2 \tag{1.5}$$

$$V_w = \dot{q}_0 + C_1(y)\dot{q}_1 + \left[\phi_2\left(\tfrac{\bar{c}}{2}\ell_w\right) + \left(\frac{d\phi_2}{d\bar{x}}\right)_{\frac{\bar{c}}{2}\ell_w} C_2(y)\right]\dot{q}_2 + \phi_3(y)\dot{q}_3$$

$$+ \tfrac{\bar{c}}{2} x_{c.g.w}\phi_4(y)\cos\Theta\,\dot{q}_4 - \tfrac{\bar{c}}{2} x_{c.g.w}\frac{d\phi_3}{dy}\sin\Theta\cos\Theta\,\dot{q}_3 \tag{1.6}$$

$$V_t = \dot{q}_0 - C_3(y)\dot{q}_1 + \left[\phi_2\left(\tfrac{\bar{c}}{2}\ell_t\right) - \left(\frac{d\phi_2}{d\bar{x}}\right)_{\frac{\bar{c}}{2}\ell_t} C_4(y)\right]\dot{q}_2 + \phi_5(y)\dot{q}_5$$

$$+ \tfrac{\bar{c}}{2} x_{c.g.t}\phi_6(y)\cos\Theta_t\,\dot{q}_6 - \tfrac{\bar{c}}{2} x_{c.g.t}\frac{d\phi_5}{dy}\sin\Theta_t\cos\Theta_t\,\dot{q}_5 \tag{1.7}$$

$$\dot{\theta}_f = \dot{q}_1 - \frac{d\phi_2}{d\bar{x}}\dot{q}_2 \tag{1.8}$$

$$\dot{\theta}_w = \dot{q}_1 + \left(\frac{d\phi_2}{d\bar{x}}\right)_{\frac{\bar{c}}{2}\ell_w}\dot{q}_2 - \frac{d\phi_3}{dy}\sin\Theta\cos\Theta\,\dot{q}_3 + \phi_4(y)\cos\Theta\,\dot{q}_4 \tag{1.9}$$

$$\dot{\theta}_t = \dot{q}_1 - \left(\frac{d\phi_2}{d\bar{x}}\right)_{\frac{\bar{c}}{2}\ell_t}\dot{q}_2 - \frac{d\phi_5}{dy}\sin\Theta_t\cos\Theta_t\dot{q}_5 + \phi_6(y)\cos\Theta_t\,\dot{q}_6 \tag{1.10}$$

where

$\tfrac{\bar{c}}{2}x_{c.g.w}, \tfrac{\bar{c}}{2}x_{c.g.t}$ is the streamwise distance from the elastic axis to the local c. g. of the wing and horizontal tail, respectively, positive if in front of the elastic axis

$$C_1(\eta) = \frac{\bar{c}}{2}\left(x_{c.g.w} + \ell_w - \eta\, AR \tan \Theta\right)$$

$$C_2(\eta) = \frac{\bar{c}}{2}\left(x_{c.g.w} - \eta\, AR \tan \Theta\right)$$

$$C_3(\eta) = \frac{\bar{c}}{2}\left(\ell_t - x_{c.g.t} + \eta \frac{AR_t}{\gamma} \tan \Theta_t\right)$$

$$C_4(\eta) = \frac{\bar{c}}{2}\left(x_{c.g.t} - \eta \frac{AR_t}{\gamma} \tan \Theta_t\right)$$

As mentioned previously, the mode shapes, ϕ_i , in equations (1.5) through (1.10) must be cantilevered; e.g., ϕ_3 and ϕ_4 are zero at the wing root and ϕ_2 is zero at the airplane c.g.

Substituting equation (1.2), (1.3), (1.4) and the velocities into equation (1.1), the equations of motion become

$$M_{00}\ddot{q}_0 + M_{02}\ddot{q}_2 + M_{03}\ddot{q}_3 + \frac{\bar{c}}{2}M_{04}\ddot{q}_4 + M_{05}\ddot{q}_5 + \frac{\bar{c}}{2}M_{06}\ddot{q}_6 = Q_0 \qquad (1.11)$$

$$\left(\frac{\bar{c}}{2}\right)^2 M_{11}\ddot{q}_1 + \frac{\bar{c}}{2}M_{12}\ddot{q}_2 + \frac{\bar{c}}{2}M_{13}\ddot{q}_3 + \left(\frac{\bar{c}}{2}\right)^2 M_{14}\ddot{q}_4 + \frac{\bar{c}}{2}M_{15}\ddot{q}_5 + \left(\frac{\bar{c}}{2}\right)^2 M_{16}\ddot{q}_6 = Q_1 \qquad (1.12)$$

$$M_{20}\ddot{q}_0 + \frac{\bar{c}}{2}M_{21}\ddot{q}_1 + M_{22}\ddot{q}_2 + M_{23}\ddot{q}_3 + \frac{\bar{c}}{2}M_{24}\ddot{q}_4 + M_{25}\ddot{q}_5 + \frac{\bar{c}}{2}M_{26}\ddot{q}_6 + K_{22}q_2 = Q_2 \qquad (1.13)$$

$$M_{30}\ddot{q}_0 + \frac{\bar{c}}{2}M_{31}\ddot{q}_1 + M_{32}\ddot{q}_2 + M_{33}\ddot{q}_3 + \frac{\bar{c}}{2}M_{34}\ddot{q}_4 + K_{33}q_3 = Q_3 \qquad (1.14)$$

$$\tfrac{\bar{c}}{2} M_{40}\ddot{q}_0 + \left(\tfrac{\bar{c}}{2}\right)^2 M_{41}\ddot{q}_1 + \tfrac{\bar{c}}{2} M_{42}\ddot{q}_2 + \tfrac{\bar{c}}{2} M_{43}\ddot{q}_3 + \left(\tfrac{\bar{c}}{2}\right)^2 M_{44}\ddot{q}_4 + K_{44} q_4 = Q_4 \qquad (1.15)$$

$$M_{50}\ddot{q}_0 + \tfrac{\bar{c}}{2} M_{51}\ddot{q}_1 + M_{52}\ddot{q}_2 + M_{55}\ddot{q}_5 + \tfrac{\bar{c}}{2} M_{56}\ddot{q}_6 + K_{55} q_5 = Q_5 \qquad (1.16)$$

$$\tfrac{\bar{c}}{2} M_{60}\ddot{q}_0 + \left(\tfrac{\bar{c}}{2}\right)^2 M_{61}\ddot{q}_1 + \tfrac{\bar{c}}{2} M_{62}\ddot{q}_2 + \tfrac{\bar{c}}{2} M_{65}\ddot{q}_5 + \left(\tfrac{\bar{c}}{2}\right)^2 M_{66}\ddot{q}_6 + K_{66} q_6 = Q_6 \qquad (1.17)$$

where

$M_{ij} = M_{ji}$ are generalized masses defined in Appendix A.

$$K_{22} = \int_{-\frac{\bar{c}}{2}\ell_{c.g.}}^{\frac{\bar{c}}{2}\ell_f} EI_f(\bar{x}) \left(\frac{d^2\phi_2}{d\bar{x}^2}\right)^2 d\bar{x} \qquad K_{33} = 2\int_0^{\frac{b}{2\cos\Phi}} EI_w(\bar{y}) \left(\frac{d^2\phi_3}{d\bar{y}^2}\right)^2 d\bar{y}$$

$$K_{44} = 2\int_0^{\frac{b}{2\cos\Phi}} GJ_w(\bar{y}) \left(\frac{d\phi_4}{d\bar{y}}\right)^2 d\bar{y} \qquad K_{55} = 2\int_0^{\frac{b_t}{2\cos\Phi_t}} EI_t(\bar{y}) \left(\frac{d^2\phi_5}{d\bar{y}^2}\right)^2 d\bar{y}$$

$$K_{66} = 2\int_0^{\frac{b_t}{2\cos\Phi_t}} GJ_t(\bar{y}) \left(\frac{d\phi_6}{d\bar{y}}\right)^2 d\bar{y}$$

and, from equation (1.4), the generalized forces are

$$Q_0 = \int_{-\frac{\bar{c}}{2}\ell_{c.g.}}^{\frac{\bar{c}}{2}\ell_f} (\ell_f^\alpha + \ell_f^c)\, d\bar{x} + 2\int_0^{b/2} (\ell_w^\alpha + \ell_w^c)\, dy + 2\int_0^{\frac{b_t}{2}} (\ell_t^\alpha + \ell_t^c + \ell_{tw}^\alpha + \ell_{tw}^c)\, dy$$

$$Q_1 = -\int_{-\frac{\bar{c}}{2}\ell_{c.g.}}^{\frac{\bar{c}}{2}\ell_f} (\ell_f^\alpha + \ell_f^c)\,\bar{x}\, d\bar{x} + 2\int_0^{\frac{b}{2}} (\ell_w^\alpha + \ell_w^c)\, k_1(y)\, dy + 2\int_0^{\frac{b_t}{2}} (\ell_t^\alpha + \ell_t^c + \ell_{tw}^\alpha + \ell_{tw}^c)\, k_3(y)\, dy$$

$$Q_2 = \int_{-\frac{\bar{c}}{2}\ell_{c.g.}}^{\frac{\bar{c}}{2}\ell_f} (\ell_f^\alpha + \ell_f^c)\,\phi_2(\bar{x})\, d\bar{x} + 2\int_0^{b/2} (\ell_w^\alpha + \ell_w^c)\left[\phi_2\left(\tfrac{\bar{c}}{2}\ell_w\right) + \left(\frac{d\phi_2}{d\bar{x}}\right)_{\frac{\bar{c}}{2}\ell_w} k_2(y)\right] dy$$

$$+2\int_0^{\frac{b_t}{2}} (\ell_t^\alpha + \ell_t^c + \ell_{tw}^\alpha + \ell_{tw}^c)\left[\phi_2\left(\tfrac{\bar{c}}{2}\ell_t\right) + \left(\frac{d\phi_2}{d\bar{x}}\right)_{\frac{\bar{c}}{2}\ell_t} k_4(y)\right] dy$$

$$Q_3 = 2\int_0^{\frac{b}{2}} (\ell_w^\alpha + \ell_w^c)\left[\phi_3(y) - \frac{d\phi_3}{dy}\sin\Theta\cos\Theta\left(k_1(y) - k_w(y)\right)\right] dy$$

$$Q_4 = 2\int_0^{b/2} (\ell_w^\alpha + \ell_w^c)\left[k_1(y) - k_w(y)\right]\phi_4(y)\cos\Theta\, dy$$

$$Q_5 = 2\int_0^{\frac{b_t}{2}} (\ell_t^\alpha + \ell_t^c + \ell_{tw}^\alpha + \ell_{tw}^c)\left[\phi_5(y) - \frac{d\phi_5}{dy}\sin\Theta_t\cos\Theta_t\left(k_5(y) - k_3(y)\right)\right] dy$$

$$Q_6 = 2\int_0^{\frac{b_t}{2}} (\ell_t^\alpha + \ell_t^c + \ell_{tw}^\alpha + \ell_{tw}^c)\left[k_5(y) - k_3(y)\right]\phi_6(y)\cos\Theta_t\, dy$$

Integrated forms of the generalized forces are derived in Appendix A which include the effects of unsteady flow and of the lag in downwash behind the vibrating wing. After introducing these aerodynamic terms and the dimensionless time $s = \frac{Ut}{\bar{c}/2}$, the equations of motion can be written in dimensionless form as

$$\left\{2\mu_{00}\xi_0'' + 2\mu_{02}\xi_2'' + 2\mu_{03}\xi_3'' + 2\mu_{04}q_4'' + 2\mu_{05}\xi_5'' + 2\mu_{06}q_6''\right\}_s$$

$$-\left\{a_{01}q_1 + \frac{\bar{c}}{2}a_{02}\xi_2 + \frac{\bar{c}}{2}a_{03}\xi_3 + a_{04}q_4 + \frac{\bar{c}}{2}b_{00}\xi_0' + b_{01}q_1' + \frac{\bar{c}}{2}b_{02}\xi_2'\right.$$

$$\left. + \frac{\bar{c}}{2}b_{03}\xi_3' + b_{04}q_4'\right\}_s - P_t\left\{c_{01}q_1 + \frac{\bar{c}}{2}c_{02}\xi_2 + \frac{\bar{c}}{2}c_{05}\xi_5 + c_{06}q_6\right.$$

$$\left. + \frac{\bar{c}}{2}d_{00}\xi_0' + d_{01}q_1' + \frac{\bar{c}}{2}d_{02}\xi_2' + \frac{\bar{c}}{2}d_{05}\xi_5' + d_{06}q_6'\right\}_s$$

$$+ \bar{b}\,P_t\left(\frac{d\varepsilon}{d\alpha}\right)\left\{q_1 + \frac{\bar{c}}{2}g_2\xi_2 + \frac{\bar{c}}{2}b_0\xi_0' + f_1q_1' + \frac{\bar{c}}{2}f_2\xi_2'\right\}_s$$

$$+ \bar{h}\,P_t\left(\frac{d\varepsilon}{d\alpha}\right)\left\{q_1 + \frac{\bar{c}}{2}g_2\xi_2 + \frac{\bar{c}}{2}b_0\xi_0' + f_1q_1' + \frac{\bar{c}}{2}f_2\xi_2'\right\}_{s-s_n}$$

$$+ \bar{d}\,P_t\left(\frac{d\varepsilon}{d\alpha}\right)\left\{\frac{\bar{c}}{2}e_3\xi_3 + e_1q_1' + \frac{\bar{c}}{2}e_2\xi_2' + \frac{\bar{c}}{2}f_3\xi_3'\right\}_{s-s_n}$$

$$+ \bar{e}\,P_t\left(\frac{d\varepsilon}{d\alpha}\right)\left\{\frac{\bar{c}}{2}e_3\xi_3'\right\}_{s-s_n} + \bar{f}\,P_t\left(\frac{d\varepsilon}{d\alpha}\right)\left\{e_4q_4 + f_4q_4'\right\}_{s-s_n}$$

$$+ \bar{g}\,P_t\left(\frac{d\varepsilon}{d\alpha}\right)\left\{d_4q_4'\right\}_{s-s_n} + T_s^{(1)} + T_s^{(2)} + P_tT_s^{(\gamma 1)} + P_tT_s^{(\gamma 2)} = f_s^0$$

(1.18)

$$\left\{ 2\mu_{11}\ddot{q}_1 + 2\mu_{12}\ddot{\zeta}_2 + 2\mu_{13}\ddot{\zeta}_3 + 2\mu_{14}\ddot{q}_4 + 2\mu_{15}\ddot{\zeta}_5 + 2\mu_{16}\ddot{q}_6 \right\}_s$$

$$-\left\{ a_{11}q_1 + \frac{\bar{c}}{2}a_{12}\zeta_2 + \frac{\bar{c}}{2}a_{13}\zeta_3 + a_{14}q_4 + \frac{\bar{c}}{2}b_{10}\dot{\zeta}_0 + b_{11}\dot{q}_1 + \frac{\bar{c}}{2}b_{12}\dot{\zeta}_2 \right.$$

$$\left. + \frac{\bar{c}}{2}b_{13}\dot{\zeta}_3 + b_{14}\dot{q}_4 \right\}_s + P_t\left\{ c_{11}q_1 + \frac{\bar{c}}{2}c_{12}\zeta_2 + \frac{\bar{c}}{2}c_{15}\zeta_5 + c_{16}q_6 \right.$$

$$\left. + \frac{\bar{c}}{2}d_{10}\dot{\zeta}_0 + d_{11}\dot{q}_1 + \frac{\bar{c}}{2}d_{12}\dot{\zeta}_2 + \frac{\bar{c}}{2}d_{15}\dot{\zeta}_5 + d_{16}\dot{q}_6 \right\}_s$$

$$-\frac{2}{a_w}\frac{dC_{m_\beta}}{d\alpha}\left\{ q_1 + \frac{\bar{c}}{2}a_2\zeta_2 + \frac{\bar{c}}{2}a_0\dot{\zeta}_0 + b_1\dot{q}_1 + \frac{\bar{c}}{2}b_2\dot{\zeta}_2 \right\}_s$$

$$-\bar{b}\,P_t\left(\frac{d\varepsilon}{d\alpha}\right)C_{11}\left\{ q_1 + \frac{\bar{c}}{2}g_2\zeta_2 + \frac{\bar{c}}{2}b_0\dot{\zeta}_0 + f_1\dot{q}_1 + \frac{\bar{c}}{2}f_2\dot{\zeta}_2 \right\}_s$$

$$-\bar{h}\,P_t\left(\frac{d\varepsilon}{d\alpha}\right)C_{11}\left\{ q_1 + \frac{\bar{c}}{2}g_2\zeta_2 + \frac{\bar{c}}{2}b_0\dot{\zeta}_0 + f_1\dot{q}_1 + \frac{\bar{c}}{2}f_2\dot{\zeta}_2 \right\}_{s-s_n}$$

$$-\bar{d}\,P_t\left(\frac{d\varepsilon}{d\alpha}\right)C_{11}\left\{ \frac{\bar{c}}{2}e_3\zeta_3 + e_1\dot{q}_1 + \frac{\bar{c}}{2}e_2\dot{\zeta}_2 + \frac{\bar{c}}{2}f_3\dot{\zeta}_3 \right\}_{s-s_n}$$

$$-\bar{e}\,P_t\left(\frac{d\varepsilon}{d\alpha}\right)C_{11}\left\{ \frac{\bar{c}}{2}c_3\dot{\zeta}_3 \right\}_{s-s_n} - \bar{f}\,P_t\left(\frac{d\varepsilon}{d\alpha}\right)C_{11}\left\{ e_4q_4 + f_4\dot{q}_4 \right\}_{s-s_n}$$

$$-\bar{g}\,P_t\left(\frac{d\varepsilon}{d\alpha}\right)C_{11}\left\{ d_4\dot{q}_4 \right\}_{s-s_n} + T_s^{(1)} + T_s^{(4)} - P_t T_s^{(13)} - P_t T_s^{(14)} = f_s' \qquad (1.19)$$

$$\left\{2\mu_{20}\ddot{\xi}_0 + 2\mu_{21}\ddot{q}_1 + 2\mu_{22}\ddot{\xi}_2 + 2\mu_{23}\ddot{\xi}_3 + 2\mu_{24}\ddot{q}_4 + 2\mu_{25}\ddot{\xi}_5 + 2\mu_{26}\ddot{q}_6\right\}_s$$

$$+ k_{22}\xi_2 - \left\{a_{21}q_1 + \frac{\bar{c}}{2}a_{22}\xi_2 + \frac{\bar{c}}{2}a_{23}\xi_3 + a_{24}q_4 + \frac{\bar{c}}{2}b_{20}\dot{\xi}_0 + b_{21}\dot{q}_1\right.$$

$$\left. + \frac{\bar{c}}{2}b_{22}\dot{\xi}_2 + \frac{\bar{c}}{2}b_{23}\dot{\xi}_3 + b_{24}\dot{q}_4\right\}_s - P_t\left\{c_{21}q_1 + \frac{\bar{c}}{2}c_{22}\xi_2 + \frac{\bar{c}}{2}c_{25}\xi_5\right.$$

$$\left. + c_{26}q_6 + \frac{\bar{c}}{2}d_{20}\dot{\xi}_0 + d_{21}\dot{q}_1 + \frac{\bar{c}}{2}d_{22}\dot{\xi}_2 + \frac{\bar{c}}{2}d_{25}\dot{\xi}_5 + d_{26}\dot{q}_6\right\}_s$$

$$+ \frac{1}{a_w}\frac{dC_{mf}}{d\alpha}\left\{c_1q_1 + \frac{\bar{c}}{2}c_2\xi_2 + \frac{\bar{c}}{2}d_0\dot{\xi}_0 + d_1\dot{q}_1 + \frac{\bar{c}}{2}d_2\dot{\xi}_2\right\}_s$$

$$+ \tilde{b}\,P_t\left(\frac{d\varepsilon}{d\alpha}\right)c_{21}\left\{q_1 + \frac{\bar{c}}{2}g_2\xi_2 + \frac{\bar{c}}{2}b_0\dot{\xi}_0 + f_1\dot{q}_1 + \frac{\bar{c}}{2}f_2\dot{\xi}_2\right\}_s$$

$$+ \tilde{h}\,P_t\left(\frac{d\varepsilon}{d\alpha}\right)c_{21}\left\{q_1 + \frac{\bar{c}}{2}g_2\xi_2 + \frac{\bar{c}}{2}b_0\dot{\xi}_0 + f_1\dot{q}_1 + \frac{\bar{c}}{2}f_2\dot{\xi}_2\right\}_{s-s_m}$$

$$+ \tilde{d}\,P_t\left(\frac{d\varepsilon}{d\alpha}\right)c_{21}\left\{\frac{\bar{c}}{2}e_3\xi_3 + e_1\dot{q}_1 + \frac{\bar{c}}{2}e_2\dot{\xi}_2 + \frac{\bar{c}}{2}f_3\dot{\xi}_3\right\}_{s-s_m}$$

$$+ \tilde{e}\,P_t\left(\frac{d\varepsilon}{d\alpha}\right)c_{21}\left\{\frac{\bar{c}}{2}c_3\dot{\xi}_3\right\}_{s-s_m} + \tilde{f}\,P_t\left(\frac{d\varepsilon}{d\alpha}\right)c_{21}\left\{e_4q_4 + f_4\dot{q}_4\right\}_{s-s_m}$$

$$+ \tilde{g}\,P_t\left(\frac{d\varepsilon}{d\alpha}\right)c_{21}\left\{d_4\dot{q}_4\right\}_{s-s_m} + T_s^{(5)} + T_s^{(6)} + P_tT_s^{(\gamma 5)} + P_tT_s^{(\gamma 6)} = f_s^2$$

(1.20)

$$\left\{ 2\mu_{30}\ddot{\xi}_0 + 2\mu_{31}\ddot{q}_1 + 2\mu_{32}\ddot{\xi}_2 + 2\mu_{33}\ddot{\xi}_3 + 2\mu_{34}\ddot{q}_4 \right\}_s + k_{33}\xi_3$$

$$- \left\{ a_{31}q_1 + \frac{\bar{c}}{2}a_{32}\xi_2 + \frac{\bar{c}}{2}a_{33}\xi_3 + a_{34}q_4 + \frac{\bar{c}}{2}b_{30}\dot{\xi}_0 + b_{31}\dot{q}_1 + \frac{\bar{c}}{2}b_{32}\dot{\xi}_2 \right.$$

$$\left. + \frac{\bar{c}}{2}b_{33}\dot{\xi}_3 + b_{34}\dot{q}_4 \right\} + T_s^{(7)} + T_s^{(8)} = f_s^3 \qquad (1.21)$$

$$\left\{ 2\mu_{40}\ddot{\xi}_0 + 2\mu_{41}\ddot{q}_1 + 2\mu_{42}\ddot{\xi}_2 + 2\mu_{43}\ddot{\xi}_3 + 2\mu_{44}\ddot{q}_4 \right\}_s + k_{44}q_4$$

$$- \left\{ a_{41}q_1 + \frac{\bar{c}}{2}a_{42}\xi_2 + \frac{\bar{c}}{2}a_{43}\xi_3 + a_{44}q_4 + \frac{\bar{c}}{2}b_{40}\dot{\xi}_0 + b_{41}\dot{q}_1 + \frac{\bar{c}}{2}b_{42}\dot{\xi}_2 \right.$$

$$\left. + \frac{\bar{c}}{2}b_{43}\dot{\xi}_3 + b_{44}\dot{q}_4 \right\}_s + T_s^{(9)} + T_s^{(10)} = f_s^4 \qquad (1.22)$$

$$\left\{ 2\mu_{50}\ddot{\xi}_0 + 2\mu_{51}\ddot{q}_1 + 2\mu_{52}\ddot{\xi}_2 + 2\mu_{55}\ddot{\xi}_5 + 2\mu_{56}\ddot{q}_6 \right\}_s + \left\{ k_{55}\xi_5 \right\}_s$$

$$- P_t \left\{ c_{51}q_1 + \frac{\bar{c}}{2}c_{52}\xi_2 + \frac{\bar{c}}{2}c_{55}\xi_5 + c_{56}q_6 + \frac{\bar{c}}{2}d_{50}\dot{\xi}_0 + d_{51}\dot{q}_1 + \frac{\bar{c}}{2}d_{52}\dot{\xi}_2 \right.$$

$$\left. + \frac{\bar{c}}{2}d_{55}\dot{\xi}_5 + d_{56}\dot{q}_6 \right\}_s + \bar{b}P_t\left(\frac{d\varepsilon}{d\alpha}\right)c_{51}\left\{ q_1 + \frac{\bar{c}}{2}g_2\xi_2 + \frac{\bar{c}}{2}b_0\dot{\xi}_0 + f_1\dot{q}_1 \right.$$

$$\left. + \frac{\bar{c}}{2}f_2\dot{\xi}_2 \right\}_s + \bar{h}P_t\left(\frac{d\varepsilon}{d\alpha}\right)c_{51}\left\{ q_1 + \frac{\bar{c}}{2}g_2\xi_2 + \frac{\bar{c}}{2}b_0\dot{\xi}_0 + f_1\dot{q}_1 + \frac{\bar{c}}{2}f_2\dot{\xi}_2 \right\}_{s-s_n}$$

$$+ \bar{d}\, P_t\left(\frac{d\varepsilon}{d\alpha}\right) C_{51}\left\{\frac{\bar{c}}{2} e_3 \xi_3 + e_1 \dot{q}_1 + \frac{\bar{c}}{2} e_2 \dot{\xi}_2 + \frac{\bar{c}}{2} f_3 \dot{\xi}_3\right\}_{s-s_n}$$

$$+ \bar{e}\, P_t\left(\frac{d\varepsilon}{d\alpha}\right) C_{51}\left\{\frac{\bar{c}}{2} c_3 \dot{\xi}_3\right\}_{s-s_n} + \bar{f}\, P_t\left(\frac{d\varepsilon}{d\alpha}\right) C_{51}\left\{e_4 q_4 + f_4 \dot{q}_4\right\}_{s-s_n}$$

$$+ \bar{g}\, P_t\left(\frac{d\varepsilon}{d\alpha}\right) C_{51}\left\{d_4 \dot{q}_4\right\}_{s-s_n} + P_t T_5^{(x11)} + P_t T_5^{(x12)} = f_5^s$$

$$\left\{2\mu_{60} \ddot{\xi}_0 + 2\mu_{61} \ddot{q}_1 + 2\mu_{62} \ddot{\xi}_2 + 2\mu_{65} \ddot{\xi}_5 + 2\mu_{66} \ddot{q}_6\right\}_s + \left\{k_{66} q_6\right\}_s \qquad (1.23)$$

$$- P_t\left\{C_{61} q_1 + \frac{\bar{c}}{2} C_{62} \xi_2 + \frac{\bar{c}}{2} C_{65} \xi_5 + C_{66} q_6 + \frac{\bar{c}}{2} d_{60} \dot{\xi}_0 + d_{61} \dot{q}_1 + \frac{\bar{c}}{2} d_{62} \dot{\xi}_2\right.$$

$$\left. + \frac{\bar{c}}{2} d_{65} \dot{\xi}_5 + d_{66} \dot{q}_6\right\}_s + \bar{b}\, P_t\left(\frac{d\varepsilon}{d\alpha}\right) C_{61}\left\{q_1 + \frac{\bar{c}}{2} g_2 \xi_2 + \frac{\bar{c}}{2} b_0 \dot{\xi}_0 + f_1 \dot{q}_1\right.$$

$$\left. + \frac{\bar{c}}{2} f_2 \dot{\xi}_2\right\}_s + \bar{h}\, P_t\left(\frac{d\varepsilon}{d\alpha}\right) C_{61}\left\{q_1 + \frac{\bar{c}}{2} g_2 \xi_2 + \frac{\bar{c}}{2} b_0 \dot{\xi}_0 + f_1 \dot{q}_1 + \frac{\bar{c}}{2} f_2 \dot{\xi}_2\right\}_{s-s_n}$$

$$+ \bar{d}\, P_t\left(\frac{d\varepsilon}{d\alpha}\right) C_{61}\left\{\frac{\bar{c}}{2} e_3 \xi_3 + e_1 \dot{q}_1 + \frac{\bar{c}}{2} e_2 \dot{\xi}_2 + \frac{\bar{c}}{2} f_3 \dot{\xi}_3\right\}_{s-s_n}$$

$$+ \bar{e}\, P_t\left(\frac{d\varepsilon}{d\alpha}\right) C_{61}\left\{\frac{\bar{c}}{2} c_3 \dot{\xi}_3\right\}_{s-s_n} + \bar{f}\, P_t\left(\frac{d\varepsilon}{d\alpha}\right) C_{61}\left\{e_4 q_4 + f_4 \dot{q}_4\right\}_{s-s_n}$$

$$+ \bar{g}\, P_t\left(\frac{d\varepsilon}{d\alpha}\right) C_{61}\left\{d_4 \dot{q}_4\right\}_{s-s_n} + P_t T_5^{(x13)} + P_t T_5^{(x14)} = f_5^6 \qquad (1.24)$$

where

$a_{ij}, b_{ij}, c_{ij}, d_{ij}$ are aerodynamic coefficients which are functions of aspect-ratio, taper ratio, sweep angle, and mode shape. They can be interpreted as the contributions of the j^{th} motion to the i^{th} degree of freedom

$i, j = 0, 1, 2, 3, 4, 5, 6$ refer to heaving, pitching, fuselage bending, first wing bending, first wing torsion, first horizontal tail bending, first horizontal tail torsion modes, respectively

$s_n = \ell_{tw} + \frac{\beta_t}{2\gamma} + 1.6$ (see Figure A. 2)

$\bar{b}, \bar{h}, \bar{d}, \bar{e}, \bar{f}, \bar{g}$ are the values of the normalized lift-growth functions for the horizontal tail due to downwash from the wing when approximated by step functions as given in Figure A. 2. They correspond to various wing spanwise changes in angle of attack and are given in Appendix A. 3. i

$\frac{d\varepsilon}{d\alpha}$ is the steady state downwash parameter due to a certain spanwise change in angle of attack of the wing

$\frac{dC_{m_f}}{d\alpha}$ is the "moment-curve" slope for the fuselage

f_s^i are forcing functions for a sharp-edged gust

$P_t = \frac{a_t S_t}{a_w S}$

$q_i = \frac{\bar{c}}{2} \gamma_i$ are generalized displacement and rotation coordinates

$q_0(s)$ is the vertical displacement of the undeformed center of gravity of the airplane, positive up

$q_1(s)$ is the pitch-angle at the undeformed center of gravity, positive nose up

$q_2(s)$ is the displacement of the fuselage bending mode $\phi_2(\bar{x})$

$q_3(s)$ is the displacement of the wing bending mode $\phi_3(y)$

$q_4(s)$ is the displacement of the wing torsion mode $\phi_4(y)$

$q_5(s)$ is the displacement of the horizontal tail bending mode $\phi_5(y)$

$q_6(s)$ is the displacement of the horizontal tail torsion mode $\phi_6(y)$

$\mu_{ij} = \frac{M_{ij}}{\rho S \frac{\bar{c}}{2} a_w}$ are dimensionless mass parameters which have the property that $\mu_{ij} = \mu_{ji}$

$k_{ij} = 2\mu_{ij}\left(\frac{\omega_i \frac{\bar{c}}{2}}{U}\right)^2$ are dimensionless stiffness coefficients and ω_i the restrained cantilever frequencies in bending and torsion

The functions $T_s^{(i)}$ and $T_s^{(\gamma i)}$ are lift deficiency terms corresponding to the exponential terms of the Wagner function (Equation (A. 2)), and are defined by

$$T_s^{(1)} = .165 \int_0^s \alpha^{(1)} e^{-.045(s-\sigma)} \, d\sigma \tag{1.25}$$

$$T_s^{(2)} = .335 \int_0^s \alpha^{(1)} e^{-.30(s-\sigma)} \, d\sigma \tag{1.26}$$

$$T_s^{(\gamma 1)} = .165 \int_0^s \alpha^{(2)} e^{-.045\gamma(s-\sigma)} \, d\sigma \tag{1.27}$$

$$T_s^{(\gamma 2)} = .335 \int_0^s \alpha^{(2)} e^{-.30\gamma(s-\sigma)} \, d\sigma \tag{1.28}$$

$$T_s^{(3)} = .165 \int_0^s \alpha^{(3)} e^{-.045(s-\sigma)} \, d\sigma \tag{1.29}$$

$$T_s^{(4)} = .335 \int_0^s \alpha^{(3)} e^{-.30(s-\sigma)} \, d\sigma \tag{1.30}$$

$$T_s^{(\gamma 3)} = .165 \int_0^s \alpha^{(4)} e^{-.045\gamma(s-\sigma)} \, d\sigma \tag{1.31}$$

$$T_s^{(\gamma 4)} = .335 \int_0^s \alpha^{(4)} e^{-.30\gamma(s-\sigma)} \, d\sigma \tag{1.32}$$

Similar expressions are obtained for $T^{(5)}, T^{(6)}, T^{(7)}, T^{(8)}, T^{(9)}, T^{(10)}$ and $T^{(55)}, T^{(56)}$ $T^{(511)}, T^{(512)}, T^{(513)}, T^{(514)}$ by analogy. The functions $T^{(11)}, T^{(12)}, T^{(13)}, T^{(14)}, T^{(57)}, T^{(58)}, T^{(59)}, T^{(510)} = 0$ The angles of attack $\alpha^{(1)}, \alpha^{(3)}, \alpha^{(5)}, \alpha^{(7)}, \alpha^{(9)}$ correspond to the second term in braces of equations (1.18), (1.19), (1.20), (1.21) and (1.22), respectively, and $\alpha^{(2)}, \alpha^{(4)}$ $\alpha^{(6)}, \alpha^{(12)}, \alpha^{(14)}$ correspond to the third term in braces of equations (1.18), (1.19), (1.20), (1.21) and (1.24), respectively. The forcing functions f_s^i of equations (1.18) through (1.24) are derived in Appendix A for a sharp edged gust. Results for other gust profiles can be obtained through the use of Duhamel's integral. The coefficients a, b, c, d, e, f and g are derived in Appendix A where an additional mode is included for the purpose of illustration.

The above equations are for incremental values of displacement above those necessary for level flight and were derived using strip theory and the assumption that the forward velocity U remains constant.

The solution of these equations of motion by analytical means is impractical because of the convolution integrals which contain the unknown responses in their integrands and because of the complexity of the forcing functions. The solution of these equations by the simplified numerical method of Reference 8 is described in the following section.

II NUMERICAL SOLUTION OF THE EQUATIONS OF MOTION

The equations of motion, (1.18) through (1.24), in matrix form are

$$[A^1]\begin{Bmatrix} \ddot{\xi}_0 \\ \ddot{q}_1 \\ \ddot{\xi}_2 \\ \ddot{\xi}_3 \\ \ddot{q}_4 \\ \ddot{\xi}_5 \\ \ddot{q}_6 \end{Bmatrix}_s + [A^2]\begin{Bmatrix} \dot{\xi}_0 \\ \dot{q}_1 \\ \dot{\xi}_2 \\ \dot{\xi}_3 \\ \dot{q}_4 \\ \dot{\xi}_5 \\ \dot{q}_6 \end{Bmatrix}_s + [A^3]\begin{Bmatrix} \xi_0 \\ q_1 \\ \xi_2 \\ \xi_3 \\ q_4 \\ \xi_5 \\ q_6 \end{Bmatrix}_s + [A^4]\begin{Bmatrix} T^{(1)} \\ T^{(2)} \\ T^{(3)} \\ T^{(4)} \\ \vdots \\ \vdots \\ T^{(13)} \\ T^{(14)} \end{Bmatrix}_s + [A^5]\begin{Bmatrix} T^{(\gamma 1)} \\ T^{(\gamma 2)} \\ T^{(\gamma 3)} \\ T^{(\gamma 4)} \\ \vdots \\ \vdots \\ T^{(\gamma 13)} \\ T^{(\gamma 14)} \end{Bmatrix}_s = \begin{Bmatrix} f^0 \\ f^1 \\ f^2 \\ f^3 \\ f^4 \\ f^5 \\ f^6 \end{Bmatrix}_s \tag{2.1}$$

where the matrices $[A^i]$ are defined below.

It should be noticed that the above column matrices do not contain terms involving $s - s_n$. This simplification has been made by using the first two terms of the Taylor's series expansion,

$$f(x+h) = f(x) + h\, f'(x) \tag{2.2}$$

Thus, the terms involving $s - s_n$ have been approximated by

$$\left\{ \quad \right\}_{s-s_n} = \left\{ \quad \right\}_s - s_n \left\{ \quad \right\}'_s \tag{2.3}$$

This can be justified by the fact that the effects of lag in downwash due to motion of the wing are secondary effects as will be shown by numerical examples in Section IV.

The coefficients for the matrix $[A']$ are

$$A'_{00} = 2\mu_{00} - \bar{h}\, s_n P_t \left(\frac{d\varepsilon}{d\alpha}\right) \frac{\bar{c}}{2} b_0$$

$$A'_{01} = -\bar{h}\, s_n P_t \left(\frac{d\varepsilon}{d\alpha}\right) f_1 - \bar{d}\, s_n P_t \left(\frac{d\varepsilon}{d\alpha}\right) e_1$$

$$A'_{02} = 2\mu_{02} - \bar{h}\, s_n P_t \left(\frac{d\varepsilon}{d\alpha}\right) \frac{\bar{c}}{2} f_2 - \bar{d}\, s_n P_t \left(\frac{d\varepsilon}{d\alpha}\right) \frac{\bar{c}}{2} e_2$$

$$A'_{03} = 2\mu_{03} - \bar{d}\, s_n P_t \left(\frac{d\varepsilon}{d\alpha}\right) \frac{\bar{c}}{2} f_3 - \bar{e}\, s_n P_t \left(\frac{d\varepsilon}{d\alpha}\right) \frac{\bar{c}}{2} c_3$$

$$A'_{04} = 2\mu_{04} - \bar{f}\, s_n P_t \left(\frac{d\varepsilon}{d\alpha}\right) f_4 - \bar{g}\, s_n P_t \left(\frac{d\varepsilon}{d\alpha}\right) d_4$$

$$A'_{05} = 2\mu_{05}$$

$$A'_{06} = 2\mu_{06}$$

$$A'_{10} = \bar{h}\, s_n P_t \left(\frac{d\varepsilon}{d\alpha}\right) c_{11} \frac{\bar{c}}{2} b_0$$

$$A'_{11} = 2\mu_{11} + \bar{h}\, s_n P_t \left(\frac{d\varepsilon}{d\alpha}\right) c_{11} f_1 + \bar{d}\, s_n P_t \left(\frac{d\varepsilon}{d\alpha}\right) c_{11} e_1$$

$$A'_{12} = 2\mu_{12} + \bar{h}\, s_n P_t \left(\frac{d\varepsilon}{d\alpha}\right) c_{11} \frac{\bar{c}}{2} f_2 + \bar{d}\, s_n P_t \left(\frac{d\varepsilon}{d\alpha}\right) c_{11} \frac{\bar{c}}{2} e_2$$

$$A'_{13} = 2\mu_{13} + \bar{d}\, s_n P_t \left(\frac{d\varepsilon}{d\alpha}\right) c_{11} \frac{\bar{c}}{2} f_3 + \bar{e}\, s_n P_t \left(\frac{d\varepsilon}{d\alpha}\right) c_{11} \frac{\bar{c}}{2} c_3$$

$$A'_{14} = 2\mu_{14} + \bar{f}\, s_n P_t \left(\frac{d\varepsilon}{d\alpha}\right) c_{11} f_4 + \bar{g}\, s_n P_t \left(\frac{d\varepsilon}{d\alpha}\right) c_{11} d_4$$

$$A'_{15} = 2\mu_{15}$$

$$A'_{16} = 2\mu_{16}$$

$$A'_{20} = 2\mu_{02} - \bar{h}\, s_n P_t \left(\frac{d\varepsilon}{d\alpha}\right) c_{21} \frac{\bar{c}}{2} b_0$$

$$A'_{21} = 2\mu_{12} - \bar{h}\, s_n P_t \left(\frac{d\varepsilon}{d\alpha}\right) c_{21} f_1 - \bar{d}\, s_n P_t \left(\frac{d\varepsilon}{d\alpha}\right) c_{21} e_1$$

$$A'_{22} = 2\mu_{22} - \bar{h}\, s_n P_t \left(\frac{d\varepsilon}{d\alpha}\right) c_{21} \frac{\bar{c}}{2} f_2 - \bar{d}\, s_n P_t \left(\frac{d\varepsilon}{d\alpha}\right) c_{21} \frac{\bar{c}}{2} e_2$$

$$A'_{23} = 2\mu_{23} - \bar{d}\, s_n P_t \left(\frac{d\varepsilon}{d\alpha}\right) c_{21} \frac{\bar{c}}{2} f_3 - \bar{e}\, s_n P_t \left(\frac{d\varepsilon}{d\alpha}\right) c_{21} \frac{\bar{c}}{2} c_3$$

$$A'_{24} = 2\mu_{24} - \bar{f}\, s_n P_t \left(\frac{d\varepsilon}{d\alpha}\right) c_{21} f_4 - \bar{g}\, s_n P_t \left(\frac{d\varepsilon}{d\alpha}\right) c_{21} d_4$$

$$A'_{25} = 2\mu_{25}$$

$$A'_{26} = 2\mu_{26}$$

$$A'_{30} = 2\mu_{03} \qquad A'_{40} = 2\mu_{04}$$

$$A'_{31} = 2\mu_{13} \qquad A'_{41} = 2\mu_{14}$$

$$A'_{32} = 2\mu_{23} \qquad A'_{42} = 2\mu_{24}$$

$$A'_{33} = 2\mu_{33} \qquad A'_{43} = 2\mu_{34}$$

$$A'_{34} = 2\mu_{34} \qquad A'_{44} = 2\mu_{44}$$

$$A'_{35} = 0 \qquad A'_{45} = 0$$

$$A'_{36} = 0 \qquad A'_{46} = 0$$

$$A'_{50} = 2\mu_{05} - \bar{h}\, s_n P_t \left(\frac{d\varepsilon}{d\alpha}\right) c_{51} \frac{\bar{c}}{2} b_0$$

$$A'_{51} = 2\mu_{15} - \bar{h}\, s_n P_t \left(\frac{d\varepsilon}{d\alpha}\right) c_{51} f_1 - \bar{d}\, s_n P_t \left(\frac{d\varepsilon}{d\alpha}\right) c_{51} e_1$$

$$A'_{52} = 2\mu_{25} - \bar{h}\, s_n P_t \left(\frac{d\varepsilon}{d\alpha}\right) c_{51} \frac{\bar{c}}{2} f_2 - \bar{d}\, s_n P_t \left(\frac{d\varepsilon}{d\alpha}\right) c_{51} \frac{\bar{c}}{2} e_2$$

$$A'_{53} = -\bar{d}\, s_n P_t \left(\frac{d\varepsilon}{d\alpha}\right) c_{51} \frac{\bar{c}}{2} f_3 - \bar{e}\, s_n P_t \left(\frac{d\varepsilon}{d\alpha}\right) c_{51} \frac{\bar{c}}{2} c_3$$

$$A'_{54} = -\bar{f}\, s_n P_t \left(\frac{d\varepsilon}{d\alpha}\right) c_{51} e_4 - \bar{g}\, s_n P_t \left(\frac{d\varepsilon}{d\alpha}\right) c_{51} d_4$$

$$A'_{55} = 2\mu_{55}$$

$$A'_{56} = 2\mu_{56}$$

$$A'_{60} = 2\mu_{06} - \bar{h}\, s_n P_t \left(\frac{d\varepsilon}{d\alpha}\right) c_{61} \frac{\bar{c}}{2} b_0$$

$$A'_{61} = 2\mu_{16} - \bar{h}\, s_n P_t \left(\frac{d\varepsilon}{d\alpha}\right) c_{61} f_1 - \bar{d}\, s_n P_t \left(\frac{d\varepsilon}{d\alpha}\right) c_{61} e_1$$

$$A'_{62} = 2\mu_{26} - \bar{h}\, s_n P_t \left(\frac{d\varepsilon}{d\alpha}\right) c_{61} \frac{\bar{c}}{2} f_2 - \bar{d}\, s_n P_t \left(\frac{d\varepsilon}{d\alpha}\right) c_{61} \frac{\bar{c}}{2} e_2$$

$$A'_{63} = -\bar{d}\, s_n P_t \left(\frac{d\varepsilon}{d\alpha}\right) c_{61} \frac{\bar{c}}{2} f_3 - \bar{e}\, s_n P_t \left(\frac{d\varepsilon}{d\alpha}\right) c_{61} \frac{\bar{c}}{2} c_3$$

$$A'_{64} = -\bar{f}\, s_n P_t \left(\frac{d\varepsilon}{d\alpha}\right) c_{61} f_4 - \bar{g}\, s_n P_t \left(\frac{d\varepsilon}{d\alpha}\right) c_{61} d_4$$

$$A'_{65} = 2\mu_{56}$$

$$A'_{66} = 2\mu_{66}$$

The coefficients for the matrix $[A^2]$ are

$$A^2_{00} = -\frac{\bar{c}}{2} b_{00} - P_t \frac{\bar{c}}{2} d_{00} + P_t \left(\frac{d\epsilon}{d\alpha}\right) \frac{\bar{c}}{2} b_0$$

$$A^2_{01} = -b_{01} - P_t d_{01} + P_t \left(\frac{d\epsilon}{d\alpha}\right) f_1 + \bar{d} P_t \left(\frac{d\epsilon}{d\alpha}\right) e_1 - \bar{h} s_n P_t \left(\frac{d\epsilon}{d\alpha}\right)$$

$$A^2_{02} = -\frac{\bar{c}}{2} b_{02} - P_t \frac{\bar{c}}{2} d_{02} + P_t \left(\frac{d\epsilon}{d\alpha}\right) \frac{\bar{c}}{2} f_2 - \bar{h} s_n P_t \left(\frac{d\epsilon}{d\alpha}\right) \frac{\bar{c}}{2} g_2 + \bar{d} P_t \left(\frac{d\epsilon}{d\alpha}\right) \frac{\bar{c}}{2} e_2$$

$$A^2_{03} = -\frac{\bar{c}}{2} b_{03} + \bar{d} s_n P_t \left(\frac{d\epsilon}{d\alpha}\right) \frac{\bar{c}}{2} f_3 + \bar{e} P_t \left(\frac{d\epsilon}{d\alpha}\right) \frac{\bar{c}}{2} c_3 - \bar{d} s_n P_t \left(\frac{d\epsilon}{d\alpha}\right) \frac{\bar{c}}{2} e_3$$

$$A^2_{04} = -b_{04} + \bar{f} P_t \left(\frac{d\epsilon}{d\alpha}\right) f_4 + \bar{g} P_t \left(\frac{d\epsilon}{d\alpha}\right) d_4 - \bar{f} s_n P_t \left(\frac{d\epsilon}{d\alpha}\right) e_4$$

$$A^2_{05} = -P_t \frac{\bar{c}}{2} d_{05}$$

$$A^2_{06} = -P_t d_{06}$$

$$A^2_{10} = -\frac{2}{a_w} \frac{dC_{mf}}{d\alpha} \frac{\bar{c}}{2} a_0 - \frac{\bar{c}}{2} b_{10} + P_t \frac{\bar{c}}{2} d_{10} - P_t \left(\frac{d\epsilon}{d\alpha}\right) c_{11} \frac{\bar{c}}{2} b_0$$

$$A^2_{11} = -\frac{2}{a_w} \frac{dC_{mf}}{d\alpha} b_1 - b_{11} + P_t d_{11} - P_t \left(\frac{d\epsilon}{d\alpha}\right) c_{11} f_1 + \bar{h} s_n P_t \left(\frac{d\epsilon}{d\alpha}\right) c_{11} - \bar{d} P_t \left(\frac{d\epsilon}{d\alpha}\right) c_{11} e_1$$

$$A^2_{12} = -\frac{2}{a_w} \frac{dC_{mf}}{d\alpha} \frac{\bar{c}}{2} b_2 - \frac{\bar{c}}{2} b_{12} + P_t \frac{\bar{c}}{2} d_{12} - P_t \left(\frac{d\epsilon}{d\alpha}\right) c_{11} \frac{\bar{c}}{2} f_2 + \bar{h} s_n P_t \left(\frac{d\epsilon}{d\alpha}\right) c_{11} \frac{\bar{c}}{2} g_2$$
$$- \bar{d} P_t \left(\frac{d\epsilon}{d\alpha}\right) c_{11} \frac{\bar{c}}{2} e_2$$

$$A^2_{13} = -\frac{\bar{c}}{2} b_{13} - \bar{d} P_t \left(\frac{d\epsilon}{d\alpha}\right) c_{11} \frac{\bar{c}}{2} f_3 - \bar{e} P_t \left(\frac{d\epsilon}{d\alpha}\right) c_{11} \frac{\bar{c}}{2} c_3 + \bar{d} s_n P_t \left(\frac{d\epsilon}{d\alpha}\right) c_{11} \frac{\bar{c}}{2} e_3$$

$$A^2_{14} = -b_{14} - \bar{f} P_t \left(\frac{d\epsilon}{d\alpha}\right) c_{11} f_4 - \bar{g} P_t \left(\frac{d\epsilon}{d\alpha}\right) c_{11} d_4 + \bar{f} s_n P_t \left(\frac{d\epsilon}{d\alpha}\right) c_{11} e_4$$

$$A^2_{15} = P_t \frac{\bar{c}}{2} d_{15}$$

$$A^2_{16} = P_t d_{16}$$

$$A^2_{20} = \frac{1}{a_w}\frac{dC_{mf}}{d\alpha}\beta\frac{\bar{c}}{2}d_0 - \frac{\bar{c}}{2}b_{20} - P_t\frac{\bar{c}}{2}d_{20} + P_t\left(\frac{d\varepsilon}{d\alpha}\right)c_{21}\frac{\bar{c}}{2}b_0$$

$$A^2_{21} = \frac{1}{a_w}\frac{dC_{mf}}{d\alpha}\beta d_1 - b_{21} - P_t d_{21} + P_t\left(\frac{d\varepsilon}{d\alpha}\right)c_{21}f_1 + \bar{d}\,P_t\left(\frac{d\varepsilon}{d\alpha}\right)c_{21}e_1 - \bar{h}\,s_n P_t\left(\frac{d\varepsilon}{d\alpha}\right)c_{21}$$

$$A^2_{22} = \frac{1}{a_w}\frac{dC_{mf}}{d\alpha}\beta\frac{\bar{c}}{2}d_2 - \frac{\bar{c}}{2}b_{22} - P_t\frac{\bar{c}}{2}d_{22} + P_t\left(\frac{d\varepsilon}{d\alpha}\right)c_{21}\frac{\bar{c}}{2}f_2 + \bar{d}\,P_t\left(\frac{d\varepsilon}{d\alpha}\right)c_{21}\frac{\bar{c}}{2}e_2$$
$$- \bar{h}\,s_n P_t\left(\frac{d\varepsilon}{d\alpha}\right)c_{21}\frac{\bar{c}}{2}g_2$$

$$A^2_{23} = -\frac{\bar{c}}{2}b_{23} + \bar{d}\,P_t\left(\frac{d\varepsilon}{d\alpha}\right)c_{21}\frac{\bar{c}}{2}f_3 + \bar{e}\,P_t\left(\frac{d\varepsilon}{d\alpha}\right)c_{21}\frac{\bar{c}}{2}c_3 - \bar{d}\,s_n P_t\left(\frac{d\varepsilon}{d\alpha}\right)c_{21}\frac{\bar{c}}{2}e_3$$

$$A^2_{24} = -b_{24} + \bar{f}\,P_t\left(\frac{d\varepsilon}{d\alpha}\right)c_{21}f_4 + \bar{g}\,P_t\left(\frac{d\varepsilon}{d\alpha}\right)c_{21}d_4 - \bar{f}\,s_n P_t\left(\frac{d\varepsilon}{d\alpha}\right)c_{21}e_4$$

$$A^2_{25} = -P_t\frac{\bar{c}}{2}d_{25}$$

$$A^2_{26} = -P_t d_{26}$$

$$A^2_{30} = -\frac{\bar{c}}{2}b_{30} \qquad A^2_{40} = -\frac{\bar{c}}{2}b_{40}$$

$$A^2_{31} = -b_{31} \qquad A^2_{41} = -b_{41}$$

$$A^2_{32} = -\frac{\bar{c}}{2}b_{32} \qquad A^2_{42} = -\frac{\bar{c}}{2}b_{42}$$

$$A^2_{33} = -\frac{\bar{c}}{2}b_{33} \qquad A^2_{43} = -\frac{\bar{c}}{2}b_{43}$$

$$A^2_{34} = -b_{34} \qquad A^2_{44} = -b_{44}$$

$$A^2_{35} = 0 \qquad A^2_{45} = 0$$

$$A^2_{36} = 0 \qquad A^2_{46} = 0$$

$$A^2_{50} = -P_t \frac{\bar{c}}{2} d_{50} + P_t \left(\frac{d\varepsilon}{d\alpha}\right) c_{51} \frac{\bar{c}}{2} b_0$$

$$A^2_{51} = -P_t d_{51} + P_t \left(\frac{d\varepsilon}{d\alpha}\right) c_{51} f_1 + \bar{d} P_t \left(\frac{d\varepsilon}{d\alpha}\right) c_{51} e_1 - \bar{h} s_n P_t \left(\frac{d\varepsilon}{d\alpha}\right) c_{51}$$

$$A^2_{52} = -P_t \frac{\bar{c}}{2} d_{52} + P_t \left(\frac{d\varepsilon}{d\alpha}\right) c_{51} \frac{\bar{c}}{2} f_2 + \bar{d} P_t \left(\frac{d\varepsilon}{d\alpha}\right) c_{51} \frac{\bar{c}}{2} e_2 - \bar{h} s_n P_t \left(\frac{d\varepsilon}{d\alpha}\right) c_{51} \frac{\bar{c}}{2} g_2$$

$$A^2_{53} = \bar{d} P_t \left(\frac{d\varepsilon}{d\alpha}\right) c_{51} \frac{\bar{c}}{2} f_3 + \bar{e} P_t \left(\frac{d\varepsilon}{d\alpha}\right) c_{51} \frac{\bar{c}}{2} c_3 - \bar{d} s_n P_t \left(\frac{d\varepsilon}{d\alpha}\right) c_{51} \frac{\bar{c}}{2} e_3$$

$$A^2_{54} = \bar{f} P_t \left(\frac{d\varepsilon}{d\alpha}\right) c_{51} f_4 + \bar{g} P_t \left(\frac{d\varepsilon}{d\alpha}\right) c_{51} d_4 - \bar{f} s_n P_t \left(\frac{d\varepsilon}{d\alpha}\right) c_{51} e_4$$

$$A^2_{55} = -P_t \frac{\bar{c}}{2} d_{55}$$

$$A^2_{56} = -P_t d_{56}$$

$$A^2_{60} = -P_t \frac{\bar{c}}{2} d_{60} + P_t \left(\frac{d\varepsilon}{d\alpha}\right) c_{61} \frac{\bar{c}}{2} b_0$$

$$A^2_{61} = -P_t d_{61} + P_t \left(\frac{d\varepsilon}{d\alpha}\right) c_{61} f_1 - \bar{h} s_n P_t \left(\frac{d\varepsilon}{d\alpha}\right) c_{61} + \bar{d} P_t \left(\frac{d\varepsilon}{d\alpha}\right) c_{61} e_1$$

$$A^2_{62} = -P_t \frac{\bar{c}}{2} d_{62} + P_t \left(\frac{d\varepsilon}{d\alpha}\right) c_{61} \frac{\bar{c}}{2} f_2 + \bar{d} P_t \left(\frac{d\varepsilon}{d\alpha}\right) c_{61} \frac{\bar{c}}{2} e_2 - \bar{h} s_n P_t \left(\frac{d\varepsilon}{d\alpha}\right) c_{61} \frac{\bar{c}}{2} g_2$$

$$A^2_{63} = \bar{d} P_t \left(\frac{d\varepsilon}{d\alpha}\right) c_{61} \frac{\bar{c}}{2} f_3 + \bar{e} P_t \left(\frac{d\varepsilon}{d\alpha}\right) c_{61} \frac{\bar{c}}{2} c_3 - \bar{d} s_n P_t \left(\frac{d\varepsilon}{d\alpha}\right) c_{61} \frac{\bar{c}}{2} e_3$$

$$A^2_{64} = \bar{f} P_t \left(\frac{d\varepsilon}{d\alpha}\right) c_{61} f_4 + \bar{g} P_t \left(\frac{d\varepsilon}{d\alpha}\right) c_{61} d_4 - \bar{f} s_n P_t \left(\frac{d\varepsilon}{d\alpha}\right) c_{61} e_4$$

$$A^2_{65} = -P_t \frac{\bar{c}}{2} d_{65}$$

$$A^2_{66} = -P_t d_{66}$$

The coefficients for the matrix $[A^3]$ are

$$A^3_{00} = 0$$

$$A^3_{01} = -a_{01} - P_t C_{01} + P_t\left(\frac{d\epsilon}{d\alpha}\right)$$

$$A^3_{02} = -\frac{\bar{c}}{2} a_{02} - P_t \frac{\bar{c}}{2} C_{02} + P_t\left(\frac{d\epsilon}{d\alpha}\right)\frac{\bar{c}}{2} q_2$$

$$A^3_{03} = -\frac{\bar{c}}{2} a_{03} + \bar{d}\, P_t\left(\frac{d\epsilon}{d\alpha}\right)\frac{\bar{c}}{2} e_3$$

$$A^3_{04} = -a_{04} + \bar{f}\, P_t\left(\frac{d\epsilon}{d\alpha}\right) e_4$$

$$A^3_{05} = -P_t \frac{\bar{c}}{2} C_{05}$$

$$A^3_{06} = -P_t C_{06}$$

$$A^3_{10} = 0$$

$$A^3_{11} = -\frac{2}{a_w}\frac{dC_{mb}}{d\alpha} - a_{11} + P_t C_{11} - P_t\left(\frac{d\epsilon}{d\alpha}\right) C_{11}$$

$$A^3_{12} = -\frac{2}{a_w}\frac{dC_{mb}}{d\alpha}\frac{\bar{c}}{2} a_2 - \frac{\bar{c}}{2} a_{12} + P_t \frac{\bar{c}}{2} C_{12} - P_t\left(\frac{d\epsilon}{d\alpha}\right) C_{11}\frac{\bar{c}}{2} q_2$$

$$A^3_{13} = -\frac{\bar{c}}{2} a_{13} - \bar{d}\, P_t\left(\frac{d\epsilon}{d\alpha}\right) C_{11}\frac{\bar{c}}{2} e_3$$

$$A^3_{14} = -a_{14} - \bar{f}\, P_t\left(\frac{d\epsilon}{d\alpha}\right) C_{11} e_4$$

$$A^3_{15} = P_t \frac{\bar{c}}{2} C_{15}$$

$$A^3_{16} = P_t C_{16}$$

$$A^3_{20} = 0$$

$$A^3_{21} = \frac{1}{\alpha_w}\frac{dC_{mf}}{d\alpha} c_1 - \alpha_{21} - P_t C_{21} + P_t\left(\frac{d\varepsilon}{d\alpha}\right) c_{21}$$

$$A^3_{22} = \frac{1}{\alpha_w}\frac{dC_{mf}}{d\alpha}\frac{\bar{c}}{2} c_2 - \frac{\bar{c}}{2}\alpha_{22} - P_t \frac{\bar{c}}{2} C_{22} + P_t\left(\frac{d\varepsilon}{d\alpha}\right) c_{21}\frac{\bar{c}}{2} g_2 + k_{22}$$

$$A^3_{23} = -\frac{\bar{c}}{2}\alpha_{23} + \bar{\alpha} P_t\left(\frac{d\varepsilon}{d\alpha}\right) c_{21}\frac{\bar{c}}{2} e_3$$

$$A^3_{24} = -\alpha_{24} + \frac{\bar{\beta}}{\beta} P_t\left(\frac{d\varepsilon}{d\alpha}\right) c_{21} e_4$$

$$A^3_{25} = -P_t \frac{\bar{c}}{2} C_{25}$$

$$A^3_{26} = -P_t C_{26}$$

$$A^3_{30} = 0 \qquad A^3_{40} = 0$$

$$A^3_{31} = -\alpha_{31} \qquad A^3_{41} = -\alpha_{41}$$

$$A^3_{32} = -\frac{\bar{c}}{2}\alpha_{32} \qquad A^3_{42} = -\frac{\bar{c}}{2}\alpha_{42}$$

$$A^3_{33} = -\frac{\bar{c}}{2}\alpha_{33} + k_{33} \qquad A^3_{43} = -\frac{\bar{c}}{2}\alpha_{43}$$

$$A^3_{34} = -\alpha_{34} \qquad A^3_{44} = -\alpha_{44} + k_{44}$$

$$A^3_{35} = 0 \qquad A^3_{45} = 0$$

$$A^3_{36} = 0 \qquad A^3_{46} = 0$$

$$A^3_{50} = 0$$

$$A^3_{51} = -P_t C_{51} + P_t \left(\frac{d\varepsilon}{d\alpha}\right) C_{51}$$

$$A^3_{52} = -P_t \frac{\bar{c}}{2} C_{52} + P_t \left(\frac{d\varepsilon}{d\alpha}\right) C_{51} \frac{\bar{c}}{2} q_2$$

$$A^3_{53} = \bar{d} P_t \left(\frac{d\varepsilon}{d\alpha}\right) C_{51} \frac{\bar{c}}{2} e_3$$

$$A^3_{54} = \bar{f} P_t \left(\frac{d\varepsilon}{d\alpha}\right) C_{51} e_4$$

$$A^3_{55} = -P_t \frac{\bar{c}}{2} C_{55} + k_{55}$$

$$A^3_{56} = -P_t C_{56}$$

$$A^3_{60} = 0$$

$$A^3_{61} = -P_t C_{61} + P_t \left(\frac{d\varepsilon}{d\alpha}\right) C_{61}$$

$$A^3_{62} = -P_t \frac{\bar{c}}{2} C_{62} + P_t \left(\frac{d\varepsilon}{d\alpha}\right) C_{61} \frac{\bar{c}}{2} q_2$$

$$A^3_{63} = \bar{d} P_t \left(\frac{d\varepsilon}{d\alpha}\right) C_{61} \frac{\bar{c}}{2} e_3$$

$$A^3_{64} = \bar{f} P_t \left(\frac{d\varepsilon}{d\alpha}\right) C_{61} e_4$$

$$A^3_{65} = -P_t \frac{\bar{c}}{2} C_{65}$$

$$A^3_{66} = -P_t C_{66} + k_{66}$$

The coefficients

for $[A^4]$ are	and for $[A^5]$ are
$A^4_{00} = 1$	$A^5_{00} = P_t$
$A^4_{01} = 1$	$A^5_{01} = P_t$
$A^4_{12} = 1$	$A^5_{12} = -P_t$
$A^4_{13} = 1$	$A^5_{13} = -P_t$
$A^4_{24} = 1$	$A^5_{24} = P_t$
$A^4_{25} = 1$	$A^5_{25} = P_t$
$A^4_{36} = 1$	$A^5_{5(10)} = P_t$
$A^4_{37} = 1$	$A^5_{5(11)} = P_t$
$A^4_{48} = 1$	$A^5_{6(12)} = P_t$
$A^4_{49} = 1$	$A^5_{6(13)} = P_t$

All other coefficients are zero. The matrices $[A^1]$, $[A^2]$ and $[A^3]$ are of order 7×7 while $[A^4]$ and $[A^5]$ are of order 7×14.

In order to reduce the matrix equation to computational form, the integration formulas derived in Reference 8 are applied at a point $s = n\varepsilon$, as follows:

$$\left\{ y' \right\}_n = \left\{ y' \right\}_{n-1} + \frac{\varepsilon}{2} \left\{ y'' \right\}_n + \frac{\varepsilon}{2} \left\{ y'' \right\}_{n-1} \tag{2.4}$$

$$\left\{ y \right\}_n = \left\{ y \right\}_{n-1} + \varepsilon \left\{ y' \right\}_{n-1} + \frac{\varepsilon^2}{6} \left\{ y'' \right\}_n + \frac{\varepsilon^2}{3} \left\{ y'' \right\}_{n-1} \tag{2.5}$$

In addition, the trapezoidal rule of integration is applied to the convolution integrals of equations (1.25) through (1.32); and, when expressions for the effective angles of attack, $\alpha^{(i)}$, are substituted, there results

$$\{T\}_n = [D^1]\{T\}_{n-1} + [D^2]\{\ddot{\zeta}\}_n + [D^3]\{\dot{\zeta}\}_n + [D^4]\{\ddot{\zeta}\}_{n-1} + [D^5]\{\dot{\zeta}\}_{n-1} \tag{2.6}$$

$$\{T^\gamma\}_n = [C^1]\{T^\gamma\}_{n-1} + [C^2]\{\ddot{\zeta}\}_n + [C^3]\{\dot{\zeta}\}_n + [C^4]\{\ddot{\zeta}\}_{n-1} + [C^5]\{\dot{\zeta}\}_{n-1} \tag{2.7}$$

where

$$D^1_{ii} = e^{-.045\varepsilon}$$

$$D^1_{jj} = e^{-.30\varepsilon}$$

$$D^2_{i0} = .165\frac{\varepsilon}{2}\frac{\bar{c}}{2}b_{\frac{i}{2}0} \qquad D^3_{i0} = 0 \qquad D^4_{i0} = e^{-.045\varepsilon} D^2_{i0}$$

$$D^2_{i1} = .165\frac{\varepsilon}{2}b_{\frac{i}{2}1} \qquad D^3_{i1} = .165\frac{\varepsilon}{2}a_{\frac{i}{2}1} \qquad D^4_{i1} = e^{-.045\varepsilon} D^2_{i1}$$

$$D^2_{i2} = .165\frac{\varepsilon}{2}\frac{\bar{c}}{2}b_{\frac{i}{2}2} \qquad D^3_{i2} = .165\frac{\varepsilon}{2}\frac{\bar{c}}{2}a_{\frac{i}{2}2} \qquad D^4_{i2} = e^{-.045\varepsilon} D^2_{i2}$$

$$D^2_{i3} = .165\frac{\varepsilon}{2}\frac{\bar{c}}{2}b_{\frac{i}{2}3} \qquad D^3_{i3} = .165\frac{\varepsilon}{2}\frac{\bar{c}}{2}a_{\frac{i}{2}3} \qquad D^4_{i3} = e^{-.045\varepsilon} D^1_{i3}$$

$$D^2_{i4} = .165\frac{\varepsilon}{2}b_{\frac{i}{2}4} \qquad D^3_{i4} = .165\frac{\varepsilon}{2}a_{\frac{i}{2}4} \qquad D^4_{i4} = e^{-.045\varepsilon} D^2_{i4}$$

$$D^2_{i5} = D^2_{i6} = 0 \qquad D^3_{i5} = D^3_{i6} = 0 \qquad D^4_{i5} = D^4_{i6} = 0$$

$$D^5_{i0} = 0 \qquad D^2_{j0} = .335\,\frac{\varepsilon}{2}\,\frac{\bar{c}}{2}\,b_{\frac{i}{2}0} \qquad D^3_{j0} = 0$$

$$D^5_{i1} = e^{-.045\varepsilon} D^3_{i1} \qquad D^2_{j1} = .335\,\frac{\varepsilon}{2}\,b_{\frac{i}{2}1} \qquad D^3_{j1} = .335\,\frac{\varepsilon}{2}\,a_{\frac{i}{2}1}$$

$$D^5_{i2} = e^{-.045\varepsilon} D^3_{i2} \qquad D^2_{j2} = .335\,\frac{\varepsilon}{2}\,\frac{\bar{c}}{2}\,b_{\frac{i}{2}2} \qquad D^3_{j2} = .335\,\frac{\varepsilon}{2}\,\frac{\bar{c}}{2}\,a_{\frac{i}{2}2}$$

$$D^5_{i3} = e^{-.045\varepsilon} D^3_{i3} \qquad D^2_{j3} = .335\,\frac{\varepsilon}{2}\,\frac{\bar{c}}{2}\,b_{\frac{i}{2}3} \qquad D^3_{j3} = .335\,\frac{\varepsilon}{2}\,\frac{\bar{c}}{2}\,a_{\frac{i}{2}3}$$

$$D^5_{i4} = e^{-.045\varepsilon} D^3_{i4} \qquad D^2_{j4} = .335\,\frac{\varepsilon}{2}\,b_{\frac{i}{2}4} \qquad D^3_{j4} = .335\,\frac{\varepsilon}{2}\,a_{\frac{i}{2}4}$$

$$D^5_{i5} = D^5_{i6} = 0 \qquad D^2_{j5} = D^2_{j6} = 0 \qquad D^3_{j5} = D^3_{j6} = 0$$

$$D^4_{j0} = e^{-.30\varepsilon} D^2_{j0} \qquad D^5_{j0} = 0$$

$$D^4_{j1} = e^{-.30\varepsilon} D^2_{j1} \qquad D^5_{j1} = e^{-.30\varepsilon} D^3_{j1}$$

$$D^4_{j2} = e^{-.30\varepsilon} D^2_{j2} \qquad D^5_{j2} = e^{-.30\varepsilon} D^3_{j2}$$

$$D^4_{j3} = e^{-.30\varepsilon} D^2_{j3} \qquad D^5_{j3} = e^{-.30\varepsilon} D^3_{j3}$$

$$D^4_{j4} = e^{-.30\varepsilon} D^2_{j4} \qquad D^5_{j4} = e^{-.30\varepsilon} D^3_{j4}$$

$$D^4_{j5} = D^4_{j6} = 0 \qquad D^5_{j5} = D^5_{j6} = 0$$

where $i = 0, 2, 4, 6, 8,$ and $j = i + 1$. The subscript $\frac{i}{2}$ indicates the degree of freedom. All of the D -coefficients are zero when $i = 10, 12$ and when $j = 11, 13$.

Similarly, the coefficients of the C -matrices are defined by

$$C^1_{ii} = e^{-.045\gamma\varepsilon} \qquad C^1_{jj} = e^{-.30\gamma\varepsilon}$$

$$C^2_{i0} = .165\,\frac{\varepsilon}{2}\,\frac{\bar{c}}{2}\,d_{\frac{i}{2}0} \qquad C^3_{i0} = 0 \qquad C^4_{i0} = e^{-.045\gamma\varepsilon}\,C^2_{i0}$$

$$C^2_{i1} = .165\,\frac{\varepsilon}{2}\,d_{\frac{i}{2}1} \qquad C^3_{i1} = .165\,\frac{\varepsilon}{2}\,C_{\frac{i}{2}1} \qquad C^4_{i1} = e^{-.045\gamma\varepsilon}\,C^2_{i1}$$

$$C^2_{i2} = .165\,\frac{\varepsilon}{2}\,\frac{\bar{c}}{2}\,d_{\frac{i}{2}2} \qquad C^3_{i2} = .165\,\frac{\varepsilon}{2}\,\frac{\bar{c}}{2}\,C_{\frac{i}{2}2} \qquad C^4_{i2} = e^{-.045\gamma\varepsilon}\,C^2_{i2}$$

$$C^2_{i5} = .165\,\frac{\varepsilon}{2}\,\frac{\bar{c}}{2}\,d_{\frac{i}{2}5} \qquad C^3_{i5} = .165\,\frac{\varepsilon}{2}\,\frac{\bar{c}}{2}\,C_{\frac{i}{2}5} \qquad C^4_{i5} = e^{-.045\gamma\varepsilon}\,C^2_{i5}$$

$$C^2_{i6} = .165\,\frac{\varepsilon}{2}\,d_{\frac{i}{2}6} \qquad C^3_{i6} = .165\,\frac{\varepsilon}{2}\,C_{\frac{i}{2}6} \qquad C^4_{i6} = e^{-.045\gamma\varepsilon}\,C^2_{i6}$$

$$C^2_{i3} = C^2_{i4} = 0 \qquad C^3_{i3} = C^3_{i4} = 0 \qquad C^4_{i3} = C^4_{i4} = 0$$

$$C^5_{i0} = 0 \qquad C^2_{j0} = .335\,\frac{\varepsilon}{2}\,\frac{\bar{c}}{2}\,d_{\frac{i}{2}0} \qquad C^3_{j0} = 0$$

$$C^5_{i1} = e^{-.045\gamma\varepsilon}\,C^3_{i1} \qquad C^2_{j1} = .335\,\frac{\varepsilon}{2}\,d_{\frac{i}{2}1} \qquad C^3_{j1} = .335\,\frac{\varepsilon}{2}\,C_{\frac{i}{2}1}$$

$$C^5_{i2} = e^{-.045\gamma\varepsilon}\,C^3_{i2} \qquad C^2_{j2} = .335\,\frac{\varepsilon}{2}\,\frac{\bar{c}}{2}\,d_{\frac{i}{2}2} \qquad C^3_{j2} = .335\,\frac{\varepsilon}{2}\,\frac{\bar{c}}{2}\,C_{\frac{i}{2}2}$$

$$C^5_{i5} = e^{-.045\gamma\varepsilon}\,C^3_{i5} \qquad C^2_{j5} = .335\,\frac{\varepsilon}{2}\,\frac{\bar{c}}{2}\,d_{\frac{i}{2}5} \qquad C^3_{j5} = .335\,\frac{\varepsilon}{2}\,\frac{\bar{c}}{2}\,C_{\frac{i}{2}5}$$

$$C^5_{i6} = e^{-.045\gamma\varepsilon}\,C^3_{i6} \qquad C^2_{j6} = .335\,\frac{\varepsilon}{2}\,d_{\frac{i}{2}6} \qquad C^3_{j6} = .335\,\frac{\varepsilon}{2}\,C_{\frac{i}{2}6}$$

$$C^5_{i3} = C^5_{i4} = 0 \qquad C^2_{j3} = C^2_{j4} = 0 \qquad C^3_{j3} = C^3_{j4} = 0$$

$$C^4_{j0} = e^{-.30\gamma\varepsilon}\,C^2_{j0} \qquad C^5_{j0} = 0 \qquad C^4_{j3} = C^4_{j4} = 0$$

$$C^4_{j1} = e^{-.30\gamma\varepsilon}\,C^2_{j1} \qquad C^5_{j1} = e^{-.30\gamma\varepsilon}\,C^3_{j1} \qquad C^5_{j3} = C^5_{j4} = 0$$

$$C^4_{j2} = e^{-.30\gamma\varepsilon}\,C^2_{j2} \qquad C^5_{j2} = e^{-.30\gamma\varepsilon}\,C^3_{j2}$$

$$C^4_{j5} = e^{-.30\gamma\varepsilon}\,C^2_{j5} \qquad C^5_{j5} = e^{-.30\gamma\varepsilon}\,C^3_{j5}$$

$$C^4_{j6} = e^{-.30\gamma\varepsilon}\,C^2_{j6} \qquad C^5_{j6} = e^{-.30\gamma\varepsilon}\,C^3_{j6}$$

where $i = 0, 2, 4, 10, 12$ and $j = i + 1$. The C -coefficients are zero when $i = 6, 8$ and when $j = 7, 9$.

The substitution of equations (2.4), (2.5), (2.6) and (2.7) into equation (2.1) yields the following recurrence formula:

$$\left\{\ddot{y}\right\}_n = [A]^{-1}\left\{ \left\{f^i\right\}_n - [B]\left\{\ddot{y}\right\}_{n-1} - [C]\left\{\dot{y}\right\}_{n-1} - [D]\left\{y\right\}_{n-1} - [E]\left\{T^i\right\}_{n-1} - [F]\left\{T^{(xi)}\right\}_{n-1} \right\} \tag{2.8}$$

where

$$[A] = [A^1] + \frac{\epsilon}{2}[A^2] + \frac{\epsilon^2}{6}[A^3] + [A^4][D^2] + \frac{\epsilon}{2}[A^4][D^3] + [A^5][C^2] + \frac{\epsilon}{2}[A^5][C^3]$$

$$[B] = \frac{\epsilon}{2}[A^2] + \frac{\epsilon^2}{3}[A^3] + [A^4][D^4] + \frac{\epsilon}{2}[A^4][D^3] + [A^5][C^4] + \frac{\epsilon}{2}[A^5][C^3]$$

$$[C] = [A^2] + \epsilon[A^3] + [A^4][D^5] + [A^4][D^3] + [A^5][C^5] + [A^5][C^3]$$

$$[D] = [A^3]$$

$$[E] = [A^4][D^1]$$

$$[F] = [A^5][C^1]$$

The columns of accelerations, velocities, displacements and T -functions are in the same sequence in equation (2.8) as in equation (2.1).

When used alternately, equations (2.8), (2.4), (2.5), (2.6) and (2.7) form a step-by-step recurrence relationship with which the time histories of the airplane responses can be computed. The initial condition for this numerical solution is that

$$\left\{\ddot{\xi}\right\}_0 = \left\{\dot{\xi}\right\}_0 = \left\{\xi\right\}_0 = \left\{T^{(i)}\right\}_0 = \left\{T^{(ai)}\right\}_0 = \left\{0\right\}$$

This computational procedure can be greatly simplified if the unsteady-flow contributions to the motion forces acting on the horizontal tail are neglected ($T^{(ai)} = 0$). This simplification can be made by setting the matrix $[A^5]$ equal to zero in the preceding equations. Certainly, the use of quasi-steady damping for the horizontal tail has only a negligible effect on the motion of the airplane as a whole and probably only a small effect on vibratory response of tail itself.

It has been shown in Reference 8 that the aerodynamic damping forces due to rigid-body motions can be considered as quasi-steady provided that an efficiency factor of $e = 0.75$ is introduced to approximate the reduction in damping due to unsteady flow effects. In all of the example calculations described in Section IV this simplification has been made. The introduction of this efficiency factor into the matrices $[A^2]$ and $[A^3]$ is illustrated in Section III.

III ILLUSTRATION OF COMPUTING STEPS

The present section is concerned with the steps involved to obtain the dynamic stresses in accordance with Section II and Appendix B. A simple two-degrees- of-freedom case (heaving and wing bending) is used for illustrative purposes.

For these two degrees of freedom, equation (2. 8) reduces to

$$\left\{\begin{matrix} y_0'' \\ y_3'' \end{matrix}\right\}_n = [A]^{-1}\left\{ \left\{\begin{matrix} f^0 \\ f^3 \end{matrix}\right\}_n - [B]\left\{\begin{matrix} y_0'' \\ y_3'' \end{matrix}\right\}_{n-1} - [C]\left\{\begin{matrix} y_0' \\ y_3' \end{matrix}\right\}_{n-1} - [D]\left\{\begin{matrix} y_0 \\ y_3 \end{matrix}\right\}_{n-1} - [E]\left\{\begin{matrix} T^1 \\ T^2 \\ T^7 \\ T^8 \end{matrix}\right\}_{n-1} - [F]\left\{\begin{matrix} T^{(21)} \\ T^{(22)} \\ T^{(27)} \\ T^{(28)} \end{matrix}\right\}_{n-1} \right\} \tag{3.1}$$

for a particular time $s = n\varepsilon$. For convergence of the numerical solution the choice of the interval ε depends on the highest natural frequency of the system. The following relation is suggested to assure accuracy and convergence:

$$\varepsilon = \frac{1}{n}\,\frac{\pi}{2k}$$

where

$k = \frac{\omega \bar{c}}{2U}$ is the reduced frequency of the highest mode of vibration

n is the number of intervals per quarter-cycle (not necessarily an integer)

Appendix B of Reference 8 shows that this numerical method will converge for values of n as small as $n = 1$. In computing the results of Section IV, an interval of $\varepsilon = 2$ was used.

The matrices $[A]$, $[B]$, $[C]$, $[D]$, $[E]$, and $[F]$ are defined as functions of the $[A^k]$, $[D^k]$, and $[C^k]$ matrices immediately below equation (2.8). The $[D^k]$ and $[C^k]$ matrices are obtained from equations (2.6) and (2.7) for $\frac{i}{2} = 0, 3$ which corresponds to the heaving and wing-bending degrees of freedom. Thus, there results

$$[D^1] = \begin{bmatrix} D^1_{00} & 0 & 0 & 0 \\ 0 & D^1_{11} & 0 & 0 \\ 0 & 0 & D^1_{66} & 0 \\ 0 & 0 & 0 & D^1_{77} \end{bmatrix} \quad [D^2] = \begin{bmatrix} D^2_{00} & D^2_{03} \\ D^2_{10} & D^2_{13} \\ D^2_{60} & D^2_{63} \\ D^2_{70} & D^2_{73} \end{bmatrix}$$

$$[D^3] = \begin{bmatrix} 0 & D^3_{03} \\ 0 & D^3_{13} \\ 0 & D^3_{63} \\ 0 & D^3_{73} \end{bmatrix} \quad [D^4] = \begin{bmatrix} D^4_{00} & D^4_{03} \\ D^4_{10} & D^4_{13} \\ D^4_{60} & D^4_{63} \\ D^4_{70} & D^4_{73} \end{bmatrix} \quad [D^5] = \begin{bmatrix} 0 & D^5_{03} \\ 0 & D^5_{13} \\ 0 & D^5_{63} \\ 0 & D^5_{73} \end{bmatrix}$$

$$[C^1] = \begin{bmatrix} C^1_{00} & 0 & 0 & 0 \\ 0 & C^1_{11} & 0 & 0 \\ 0 & 0 & 0 & 0 \\ 0 & 0 & 0 & 0 \end{bmatrix} \quad [C^2] = \begin{bmatrix} C^2_{00} & 0 \\ C^2_{10} & 0 \\ 0 & 0 \\ 0 & 0 \end{bmatrix} \quad [C^3] = \begin{bmatrix} C^4_{00} & 0 \\ C^4_{10} & 0 \\ 0 & 0 \\ 0 & 0 \end{bmatrix}$$

$$[C^3] = [C^5] = 0$$

The $[A^k]$ matrices of equation (2.1) are now determined for $i = 0, 3$, and $j = 0, 3$ which corresponds to the heaving and wing-bending degrees of freedom. These are

$$[A^1] = \begin{bmatrix} A^1_{00} & A^1_{03} \\ A^1_{30} & A^1_{33} \end{bmatrix} \quad [A^2] = \begin{bmatrix} A^2_{00} & A^2_{03} \\ A^2_{30} & A^2_{33} \end{bmatrix} \quad [A^3] = \begin{bmatrix} A^3_{00} & A^3_{03} \\ A^3_{30} & A^3_{33} \end{bmatrix}$$

$$[A^4] = \begin{bmatrix} A^4_{00} & A^4_{01} & 0 & 0 \\ 0 & 0 & A^4_{36} & A^4_{37} \end{bmatrix} \quad [A^5] = \begin{bmatrix} A^5_{00} & A^5_{01} & 0 & 0 \\ 0 & 0 & 0 & 0 \end{bmatrix}$$

The forcing functions, f^i, in equation (3.1) are defined in Appendix A. Since the dimensionless time, $s = n\varepsilon$, is measured from the time that the gust front strikes the nose of the fuselage, all of the gust functions for the wing and horizontal tail derived in Appendix A must be translated accordingly.

The reduction of equations (2.4), (2.5), (2.6), and (2.7) for the two degrees of freedom is obvious. The responses per unit $\frac{w}{U}$ can now be found through

the alternate use of equations (3.1), (2.4), (2.5), (2.6) and (2.7) for any number of discrete points $n = 0, 1, 2 \ldots$

This recurrence process is simplified greatly when quasi-steady damping is assumed; i.e., when $T^{(i)} = 0$. It has been shown in Reference 8 that the effects of unsteady flow on the rigid-body damping terms is negligible insofar as the rigid body responses are concerned. Therefore, T^1, T^2, $T^{(r1)}$ and $T^{(r2)}$ will be eliminated; but, as recommended in Section II, an efficiency factor, e, will be incorporated into the matrices $[A^2]$ and $[A^3]$ to compensate for the reduction in rigid-body damping due to unsteady flow effects. It should be noted that the elimination of T^1, T^2, $T^{(r1)}$ and $T^{(r2)}$ is equivalent of setting the coefficients $A^5_{00} = A^5_{01} = A^4_{00} = A^4_{01} = 0$

The coefficients of the matrix $[A^2]$ become

$$A^2_{00} = -e\frac{\bar{c}}{2}b_{00} - e\,P_t\frac{\bar{c}}{2}d_{00} + P_t\left(\frac{d\varepsilon}{d\alpha}\right)\frac{\bar{c}}{2}b_0$$

$$A^2_{03} = -e\frac{\bar{c}}{2}b_{03} + \bar{d}\,s_n P_t\left(\frac{d\varepsilon}{d\alpha}\right)\frac{\bar{c}}{2}f_3 + \bar{e}\,P_t\left(\frac{d\varepsilon}{d\alpha}\right)\frac{\bar{c}}{2}c_3 - \bar{d}\,s_n P_t\left(\frac{d\varepsilon}{d\alpha}\right)\frac{\bar{c}}{2}e_3$$

$$A^2_{30} = -\frac{\bar{c}}{2}b_{30}$$

$$A^2_{33} = -\frac{\bar{c}}{2}b_{33}$$

and those of matrix $[A^3]$ become

$$A^3_{00} = A^3_{30} = 0$$

$$A^3_{03} = -e\,\frac{\bar{c}}{2}\,d_{03} + \bar{d}\,P_t\left(\frac{d\epsilon}{d\alpha}\right)\frac{\bar{c}}{2}\,e_3$$

$$A^3_{33} = -\frac{\bar{c}}{2}\,a_{33} + k_{33}$$

Thus, when quasi-steady damping is used for a particular i^{th} degree of freedom, all of the aerodynamic coefficients a_{ij}, b_{ij}, c_{ij}, and d_{ij} of this i^{th} degree of freedom are multiplied by e except for the c_{ij} coefficients containing the term $\left(\frac{d\epsilon}{d\alpha}\right)$.

After the generalized displacements, velocities, and accelerations have been obtained by the previously described numerical solution, the stresses can be computed with the aid of equations (B. 3) and (B. 4) when quasi-steady damping is used and with equations (B. 5) and (B. 6) when it is desired to include the effects of unsteady flow on the damping forces.

It may be desired to compute the acceleration ratio of the flexible airplane which is usually defined as

$$A.R. = \frac{\eta''_{c.g.}}{\eta''_{ss}} \tag{3.2}$$

where $\eta''_{c.g.}$ is the acceleration of the center of gravity of the deformed airplane and η''_{ss} is the acceleration given by the sharp-edged gust formula as

$$\ddot{\zeta}_{ss} = \frac{1}{2\mu_{oo}} \frac{w}{U}$$

Thus,

$$A.R. = 2\mu_{oo} \ddot{\zeta}_{c.g.} \tag{3.3}$$

For the present two-degree-of-freedom case,

$$\ddot{\zeta}_{c.g.} = \ddot{\zeta}_0 + \frac{M_{03}}{M_{00}} \ddot{\zeta}_3 \tag{3.4}$$

since, from equation (1.11),

$$M_{00} \ddot{q}_{c.g.} = M_{00} \ddot{q}_0 + M_{03} \ddot{q}_3 \tag{3.5}$$

To find the responses or stresses due to an arbitrary gust profile, the time history of the responses or stresses due to a sharp-edged gust must be integrated in convolution with the desired gust profile. If $B(s)$ is the response or stress due to a sharp-edged gust per unit $\frac{w}{U}$, the corresponding response or stress due to an arbitrary gust profile per unit $\frac{w_{max}}{U}$ is

$$C(s) = \int_0^s B(\sigma) F'(s-\sigma)\, d\sigma \tag{3.6}$$

where

$$F(s) = \frac{w(s)}{w_{max}}$$

The application of the trapezoidal rule of integration to equation (3.6) yields

$$C_n = \varepsilon \left(\tfrac{1}{2} B_0 F'_n + B_1 F'_{n-1} + \cdots\cdots + B_{n-1} F'_1 + \tfrac{1}{2} B_n F'_0 \right) \tag{3.7}$$

For a one-minus-cosine gust profile $F(s)$ becomes

$$F(s) = \frac{1}{2} \left(1 - \cos \pi \frac{s}{s_g} \right) \tag{3.8}$$

which after differentiating and substituting $s = n\varepsilon$ yields

$$F'_n = \frac{\pi}{2 s_g} \sin \frac{\pi \varepsilon}{s_g} n \tag{3.9}$$

where s_g is the value of s at the gust peak.

IV RESULTS AND CONCLUSIONS

4.1 Data for Example Airplane

The flexible swept-wing airplane used for illustrative purposes is shown in Figure 4.1. Some of the parameters used to obtain the results of this section are given in Table 4.1. The airplane is operating at an altitude of 11,000 ft. at an equivalent airspeed of 460 mph.

The mode shapes used in the illustrative examples are analytical expressions which approximate the natural cantilever modes of the example airplane. They have the following forms

$$\phi_2(\bar{x}) = \frac{k\,\bar{x}^2}{\left(\frac{\bar{c}}{2}\right)^2\left(\ell_f - \ell_{c.g.}\right)^2}$$ first fuselage bending mode

$$\phi_3(\eta) = \eta^2$$ first wing bending mode along the elastic axis

$$\phi_4(\eta) = \begin{cases} 1.25\,\eta & 0 \le \eta \le .8 \\ 1.00 & .8 \le \eta \le 1.0 \end{cases}$$ first wing torsional mode about the elastic axis

$$\phi_5(\eta) = \eta^2$$ first horizontal tail bending mode along the elastic axis

$$\phi_6(\eta) = \eta$$ first horizontal tail torsion mode about the elastic axis

$$\phi_7(\eta) = \eta^2(4.5\,\eta - 3.5)$$ second wing bending mode along the elastic axis

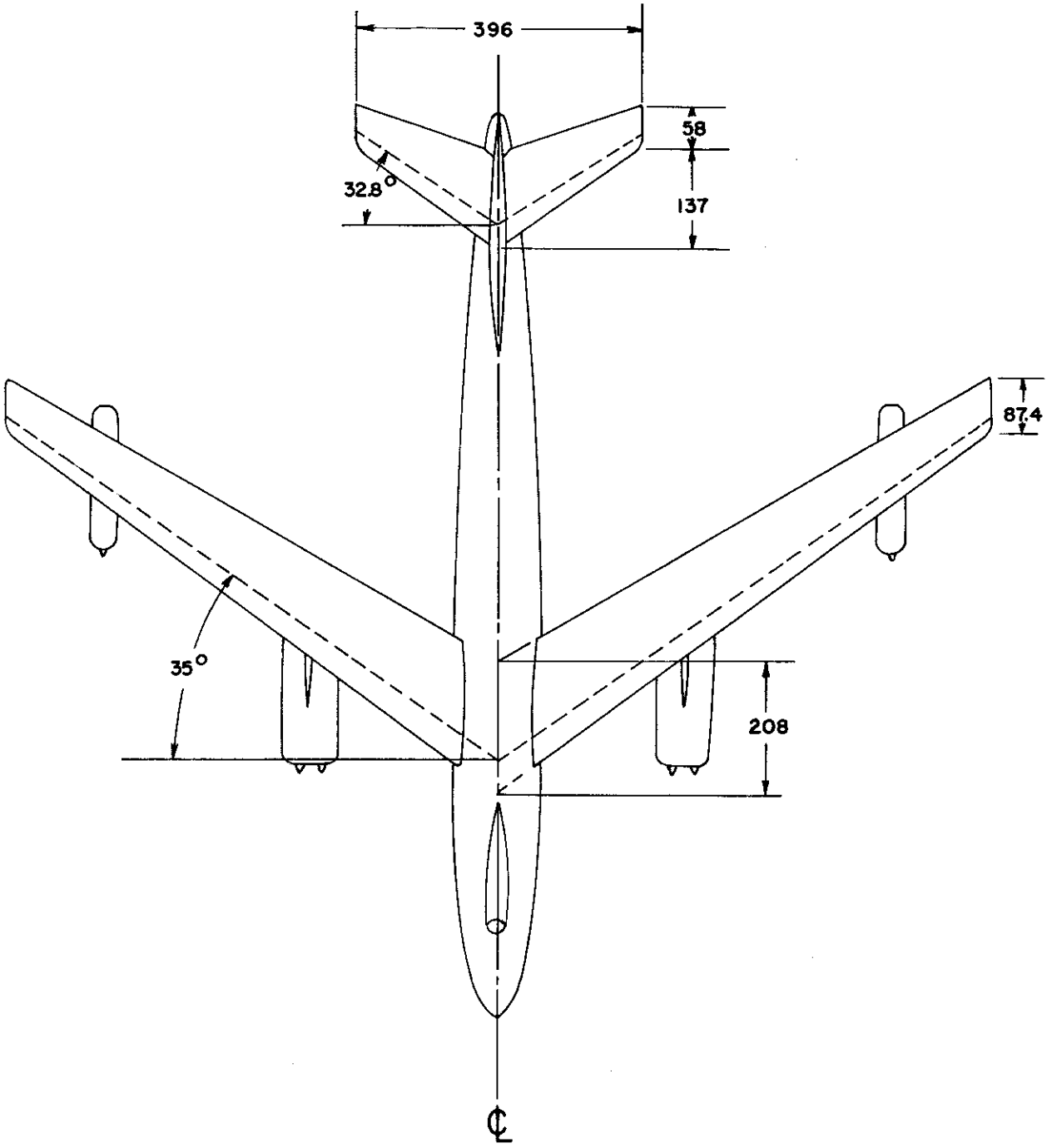

FIGURE 4.1 PLANFORM OF EXAMPLE AIRPLANE

TABLE 4.1

PARAMETERS FOR EXAMPLE AIRPLANE

Basic Parameters

M = 4000 slugs	Λ_o = 36° 38'
I_{yy} = 1.616 × 10^6 slugs ft^2	Λ_1 = 35°
m_1 = 235 slugs (inboard nacelle)	Λ_3 = 31° 32'
m_2 = 100.9 slugs (outboard nacelle)	ⓗ = 34°
ρ = .001702 slugs/ft^3	Λ_{ot} = 36° 40'
b = 116 ft.	Λ_{1t} = 32° 48'
$\bar{c}$ = 12.30 ft.	Λ_{3t} = 23° 58'
$\bar{c}_t$ = 8.32 ft.	ℓ_1 = 3.36
S = 1428 ft^2	ℓ_w = 2.997
S_t = 268 ft.^{2}	ℓ_3 = 1.955
AR = 9.43	$\ell_{c.g.}$ = 8.38
AR_t = 4.06	ℓ_f = 17.46
λ_w = .42	ℓ_{1t} = 6.294
λ_t = .423	ℓ_t = 6.61
$A_{max} = 1.893 \left(\frac{\bar{c}}{2}\right)^2$	ℓ_{3t} = 7.221
$V_f = 23.02 \left(\frac{\bar{c}}{2}\right)^3$	ℓ_{tw} = 7.08

TABLE 4.1 (Cont'd)

Stability Parameters

a_w = 6.01 per rad.

a_t = 4.25 per rad.

$\frac{dC_{mf}}{d\alpha}$ = .363 per rad.

$\frac{d\varepsilon}{d\alpha}$ = .326

$\frac{dC_m}{dC_L}$ = 0

Derived Parameters

β = 7.01

β_t = 3.02

γ = 1.515

P_t = .1327

$\delta_w = 1 - \lambda_w$ = .58

$\delta_t = 1 - \lambda_t$ = .577

A comparison of the assumed modes for the wing with the actual natural modes of the example airplane is made in Figure 4.2. It has been shown in Reference 4 that the fundamental bending modes for typical airplanes can be approximated by parabolas. The assumed second bending mode $\phi_2(\eta)$ was obtained by making it orthogonal to the assumed fundamental mode with respect to the wing mass. The assumed bending mode for the fuselage is compared with the actual normal bending mode in Figure 4.3; and it can be seen that they compare favorably except for a constant factor due to the fact that the assumed mode is cantilevered at the airplane c.g.

4.2 Results

The dynamic stresses for the example swept-wing airplane were obtained by the method outlined in Section III. The results for various numbers of degrees of freedom are presented in Figures 4.4 through 4.22. In all of the illustrative examples the effects of unsteady flow on the damping terms were neglected for the heaving and pitching degrees of freedom, and an efficiency factor $e = .75$ was introduced instead. The bending moments are taken about axes in the streamwise direction while the torques are taken about axes perpendicular to the streamwise direction. The bending moments and torques are normalized in terms of $\frac{1}{2}\rho U^2 S a_w \frac{\bar{c}}{2} \frac{w}{U}$, and the shears in terms of $\frac{1}{2}\rho U^2 S a_w \frac{w}{U}$.

Figure 4.4 shows the acceleration ratios of the center of gravity of the deformed airplane for various numbers of degrees of freedom. It can be seen from this figure that the introduction of a vibratory mode to the heaving degree of freedom greatly alleviates the total load on the airplane but that the inclusion of the airplane

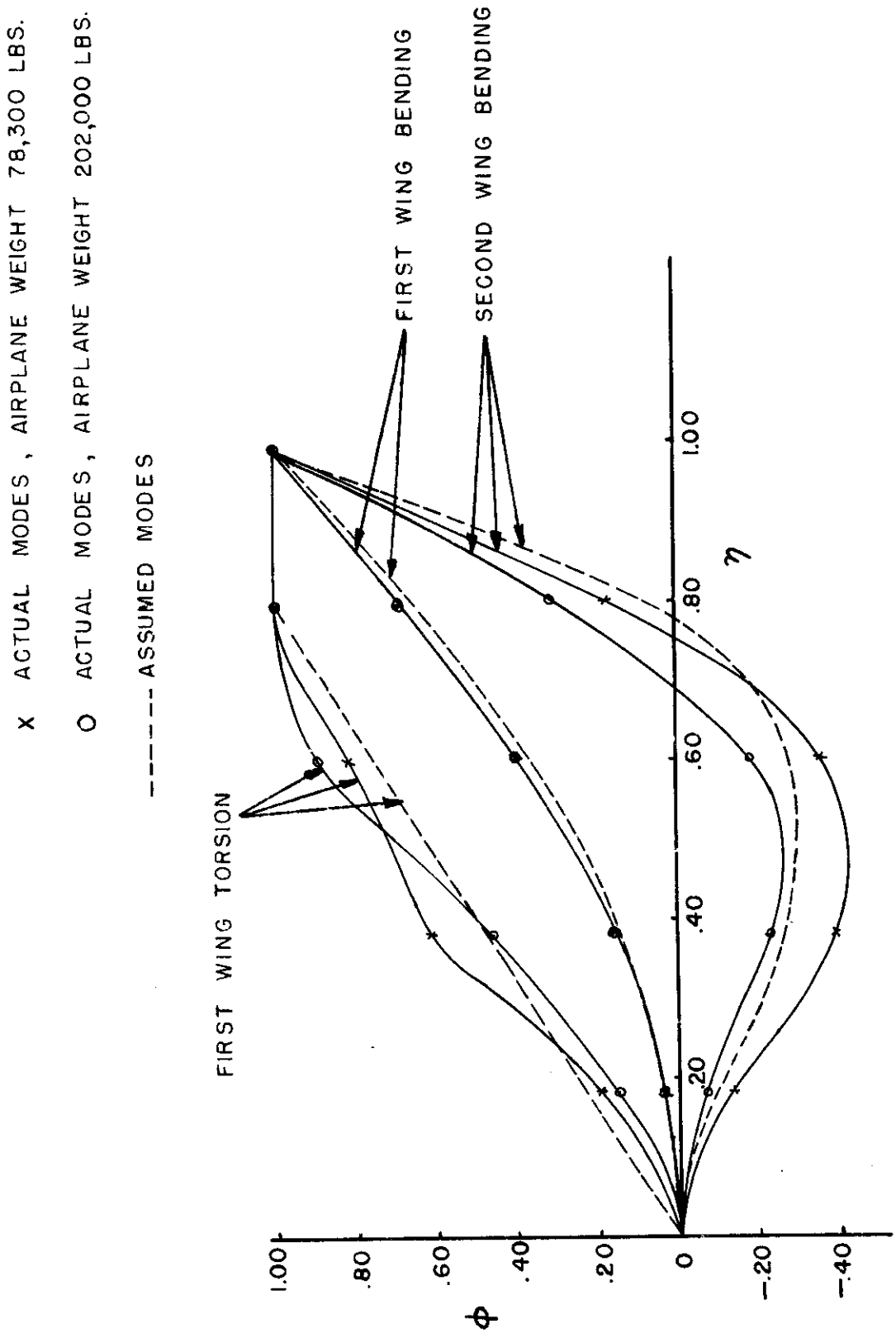

FIGURE 4.2 MODE SHAPES FOR WING OF EXAMPLE AIRPLANE

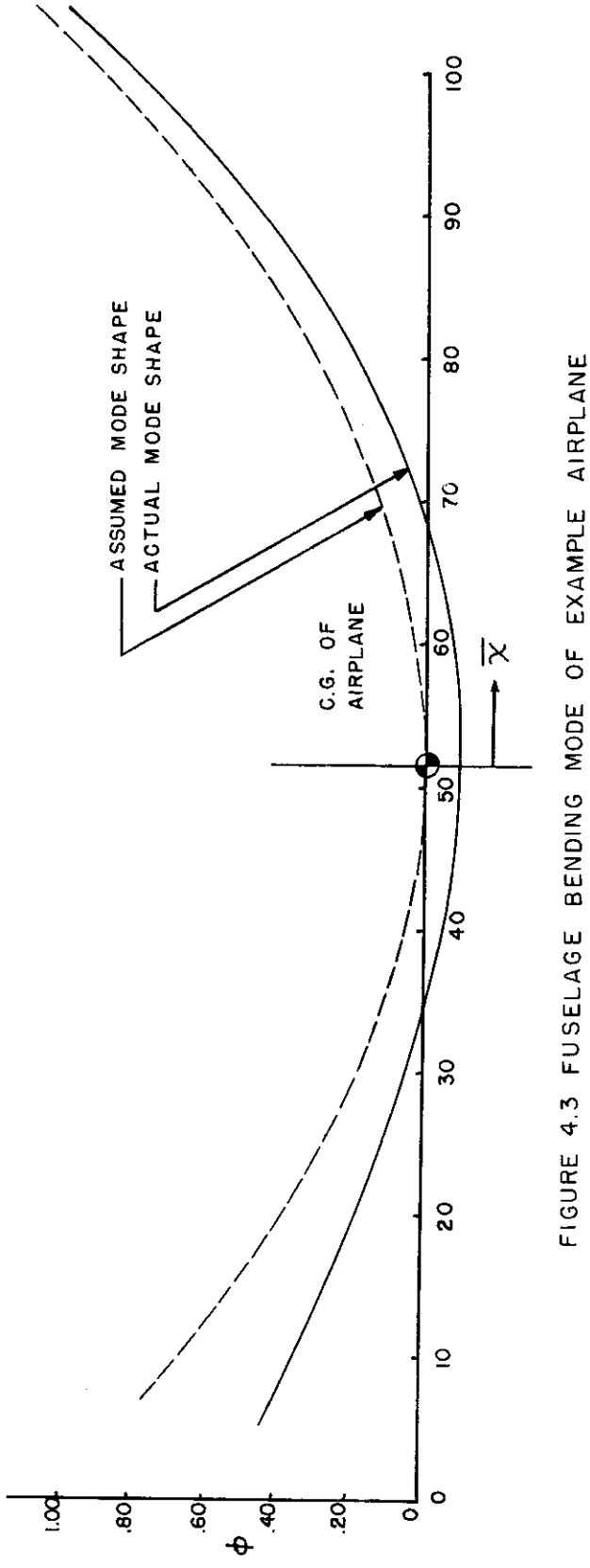

FIGURE 4.3 FUSELAGE BENDING MODE OF EXAMPLE AIRPLANE

pitching motion partially cancels this alleviation.

The sets of curves given in Figures 4.5 through 4.10 give the root shears and bending moments for a sharp-edged gust. In Figures 4.5 and 4.6, the shears and bending moments for the flexible airplane are compared with those of an equivalent rigid airplane when unsteady vibratory damping is used and in Figures 4.7 and 4.8 when vibratory quasi-steady damping is used. These figures clearly show that the alleviation in peak stresses commonly attributed to flexible sweptback wings is always at least partially cancelled by the increased pitching motion of the airplane. It can be seen in these figures that inclusion of the second wing bending mode increases the peak stresses while inclusion of the first torsional mode reduces the peak stresses. For the particular airplane under consideration, the second bending frequency happens to be $\omega_{2nd_B} = 4.5\ \omega_{1st_B}$ while the first torsional frequency is $\omega_{1st_T} = 3.33\ \omega_{1st_B}$; thus, for sinusoidal vibrations the contribution of the second bending mode will be positive when the amplitude of the first bending mode is at its maximum while the contribution of the torsional mode will be negative. This condition may be reversed for other airplanes and should be investigated before additional degrees of freedom are added to the equations of motion.

Figures 4.7 and 4.8 when compared with Figures 4.5 and 4.6 show that the use of quasi-steady aerodynamics for the motion forces due to wing vibrations yields conservative peak stresses. A more direct illustration of this effect is given in Figures 4.9 and 4.10. Also shown in Figures 4.9 and 4.10 is the effect of neglecting the coupling of the wing-bending degree of freedom to the rigid body degree of freedom;

and it can be seen that this yields results which are more unconservative than similar results for unswept-wing airplanes given by the simplified method of Reference 4.

The time histories of the torque at the wing root for different numbers of degrees of freedom is shown in Figure 4.11. The bending moments and torques along and about the elastic axis, respectively, can be obtained by a transfer of axes according to equations (B.13) and (B.14); and a comparison of Figure 4.11 with 4.7 shows that the contribution of the streamwise torque is very small for highly swept wings.

The spanwise variations in peak shear, bending moment, and torque are shown in Figures 4.12, 4.13, 4.14, 4.15 and 4.16. The degrees of freedom used correspond to those used in Figures 4.5, 4.6, 4.7, 4.8, and 4.11, respectively. The discontinuities in shear in Figures 4.13 and 4.15 are caused by the engine nacelles which were considered as concentrated masses; and it will be noticed that these discontinuities are sometimes in a direction opposite to those for the rigid airplane due to the vibratory inertia forces.

In Figure 4.17 the time histories of the wing-root bending moments in response to a one-minus-cosine gust of gradient distance, $s_g = 25$, are shown for the same degrees of freedom as in Figure 4.5. The spanwise variations of peak bending moment are shown in Figure 4.18 for the same one-minus-cosine gust. These results show the same trends as for a sharp-edged gust. The variations of peak wing-root bending moment with gust gradient distance, s_g, is shown in Figure 4.19; and it can be seen that there is never any dynamic overstress in the sense that the dynamic stress is never greater than the rigid-airplane stress. Reference 7 has shown

that a rigid-airplane gust analysis which includes a static aeroelastic correction to the lift-curve slope of swept wings will yield good results for long-graded gusts but will underestimate the stresses due to short-graded gusts.

A comparison of the airplane pitch angles is given in Figure 4.20. It shows that the inclusion structural flexibility in the equations of motion almost doubles the pitching response of the airplane.

Figures 4.21 and 4.22 show the time histories of wing tip deflection in response to a sharp-edged gust; and the same trends as for the wing-root bending moment are observed.

4.3 Discussion

The numerical method of solution of the present report becomes very lengthy and tedious as additional degrees of freedom are added. Consequently, since the solutions were carried out on desk computers, results for only four degrees of freedom were obtained. There is a need for a more practical method of solution because there is some doubt that four degrees of freedom can accurately describe the dynamic stresses. There are at least three alternative methods of solution:

1. Use of the same numerical method on high-speed automatic digital computing machinery.
2. Solution of the equations of motion on an electronic analogue computer.
3. Statistical solutions be means of generalized harmonic analysis.

The present numerical method is readily adaptable to automatic computing machinery because of the step-by-step recurrence process for computing time histories.

Similar gust problems with two degrees of freedom have been solved successfully on automatic digital computing machinery in References 7 and 9. If several degrees of freedom were considered, the program of instructions for an automatic digital computer would be very long and complex; and such a program would not be economically feasible unless the problem became standardized for use over and over again in design studies.

The utility of electronic analogue computers for finding the transient responses of complex physical systems has been well established, and their application to aeroelastic problems has been illustrated in References 10, 11, and 12. References 10 and 12 make use of the differential analyzer or operational analogue type of electronic computer, while Reference 11 makes use of direct electrical analogies. The electronic differential analyzer operates directly on the equations of motion through the use of high-gain d. c. amplifiers as integrators and adders, while the computer of Reference 11 simulates mechanical systems with analogous electrical circuits. For either type of analogue computer the unsteady airforces are taken into account by deriving differential equations or electrical circuits which have solutions given by the convolution integrals involving exponential approximations of the Wagner and Kussner functions.

The equations of motion for the gust response of a flexible swept-wing airplane as formulated in the present report could easily be set up on an electronic differential analyzer; although the number of degrees of freedom which could be handled might be somewhat limited by the number of integrators available in such a

computer. The forcing functions corresponding to the gust penetration of the swept wing and the resulting downwash at the tail cannot be expressed in simple analytical form; and, so, the generation of these functions for an electronic differential analyzer might be a difficult problem.

For the application of the electrical analogy technique of Reference 11, the distributed elastic structure of the airplane must be represented by a system of elastically connected discrete mass particles. The accurate description of an airplane usually requires more degrees of freedom when a lumped mass system is used than when elastic modes are used; however, this type of computer can easily handle a very large number of degrees of freedom. In comparison with electronic differential analyzers, the chief disadvantage of this type of computer is that it is inherently less accurate; its chief advantages are the ability to handle more degrees of freedom and the ability to simulate stresses as well as displacements.

Whether solved numerically or with an analogue computer, the present formulation of the gust problem requires the specification of a standard gust profile; and, since most gusts encountered by aircraft are the result of atmospheric turbulence which is random in character, a standard gust appears to be of doubtful validity. Many recent papers (Reference 13, for example) have described a method for obtaining statistical information on the response of aircraft structures to continuous atmospheric turbulence. In this method, atmospheric turbulence is described by a power spectrum of the random vertical gust velocity. This function, in effect, gives the frequency content of the randomly varying gust velocity; and, together with the frequency

response characteristics of the aircraft structure, it serves to define the power spectrum of the structural response. Such statistical quantities as the root-mean-square stress at a point in the structure can then be found. This method requires the steady-state structural response to sinusoidal gusts which can be computed more accurately and easily than the transient response to discrete gusts. At the present time there are no gust-load specifications based on this power-spectral method. Such a specification awaits the establishment of standards of atmospheric turbulence, if they exist. Also, there is some doubt as to whether reliable limit loads can be found by this method.

4.4 Conclusions and Recommendations

From the results of Section 4.2 and of Appendices C, D and E the following conclusions are drawn:

1. At least three degrees of freedom, heaving, pitching and wing bending, are necessary for the accurate computation of stresses in the wing of a swept-wing airplane.
2. The alleviation of stresses commonly attributed to flexible sweptback wings is always at least partially cancelled by the increased pitching motion of the airplane.
3. The use of quasi-steady damping ($e = 0.75$) in the example calculations always resulted in conservative stresses.
4. The approximate method of Reference 4 for computing dynamic overstresses is not applicable to swept-wing airplanes.

5. The side-bending vibration of an underslung nacelle has a negligible effect on wing stresses except possibly for speeds near the airplane flutter speed.

6. The results of this investigation indicate that the downwash at the tail due to wing vibrations has a negligible effect on the motion of the airplane as a whole and on the resulting stresses in the wing; however, this effect may be important in a dynamic stress analysis of the horizontal tail itself.

7. Due to its combined accuracy and simplicity, the modification of the mode-acceleration method described in Appendix E is recommended for transient stress analyses.

It is the opinion of the authors that any further research on the gust loads problem should investigate the possibility of finding limit loads and stresses by a generalized harmonic analysis.

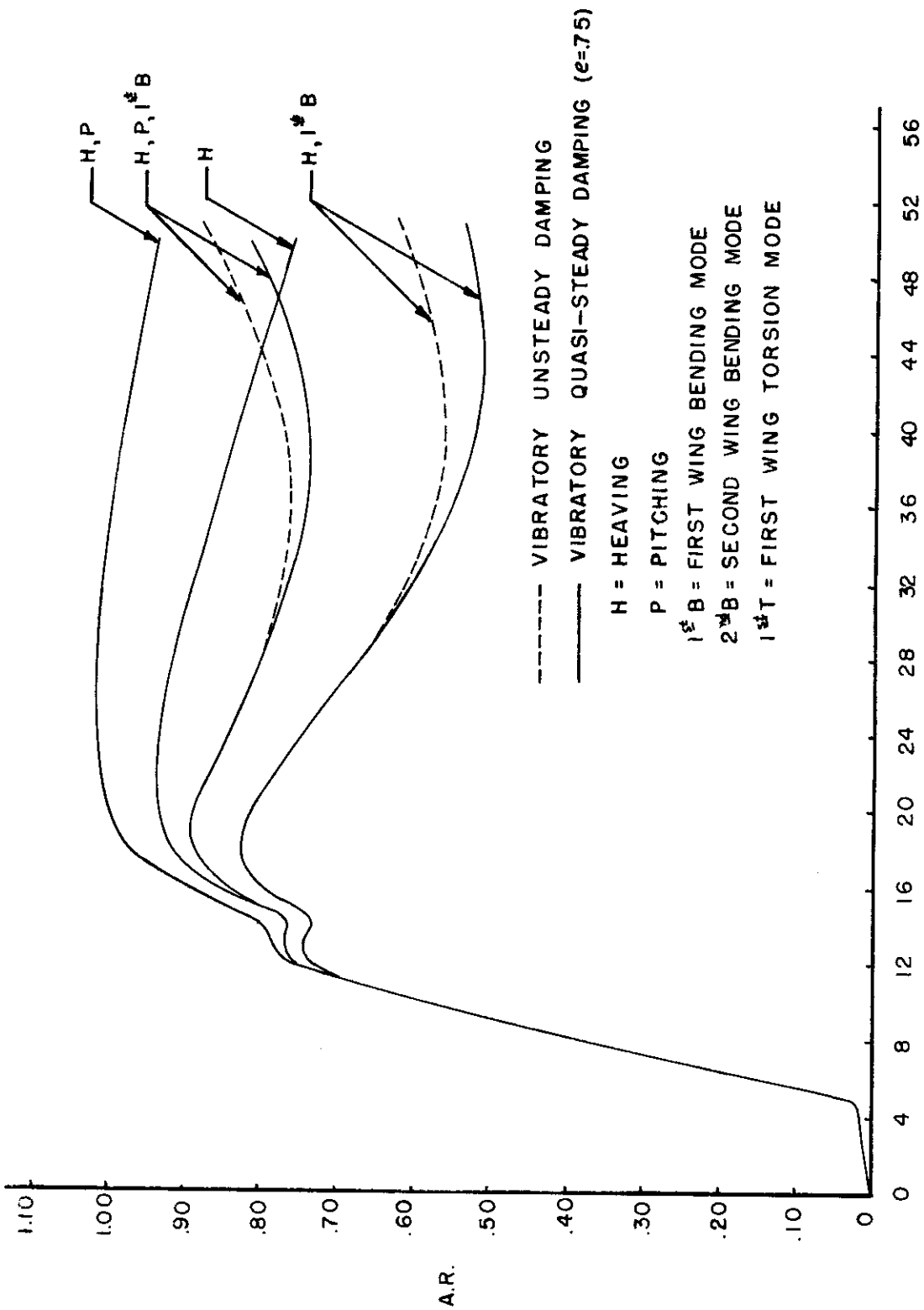

FIGURE 4.4 ACCELERATION RATIOS OF THE CENTER OF GRAVITY OF THE DEFORMED AIRPLANE FOR A SHARP-EDGED GUST

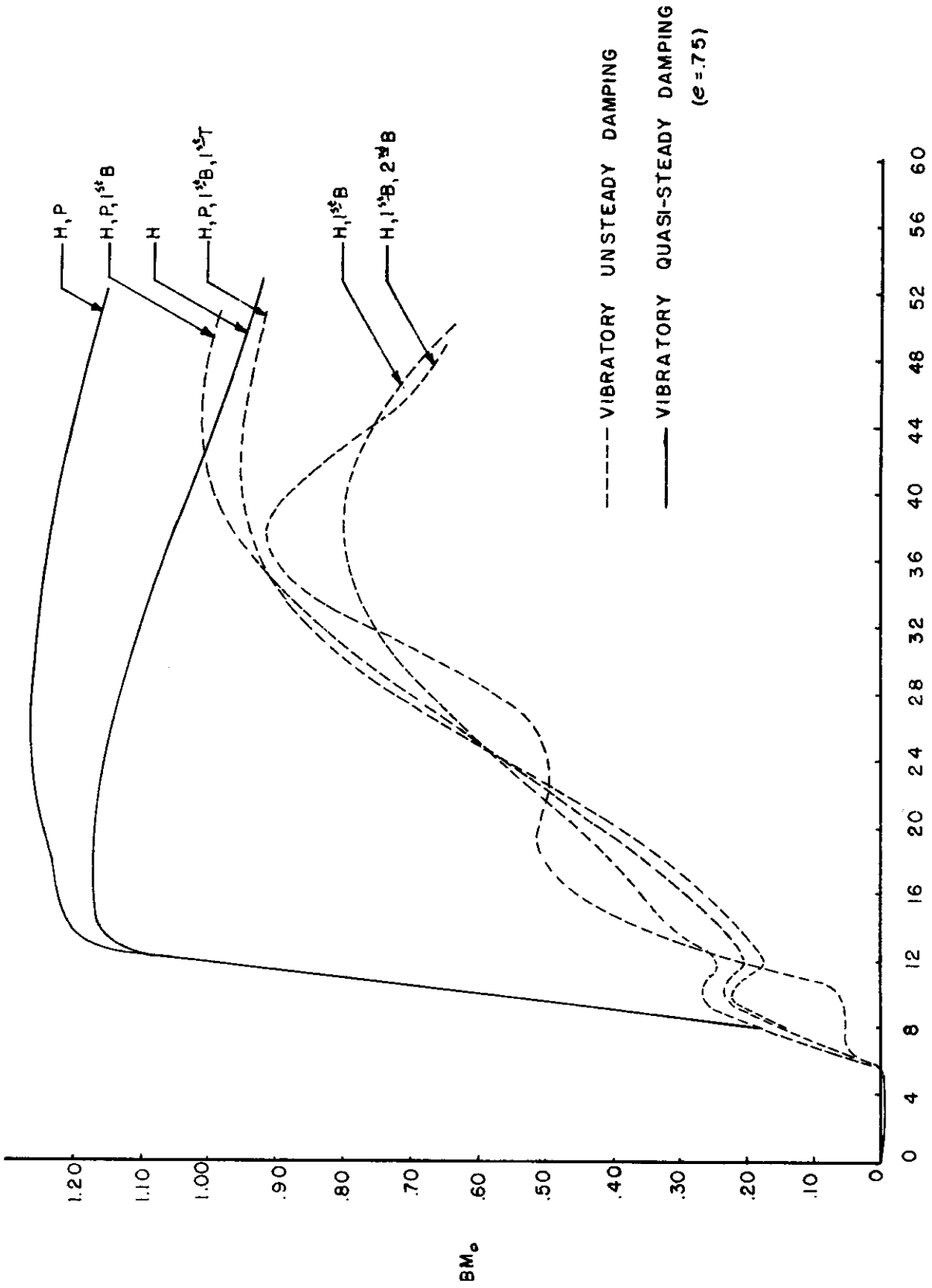

FIGURE 4.5 WING-ROOT BENDING MOMENT FOR A SHARP-EDGED GUST

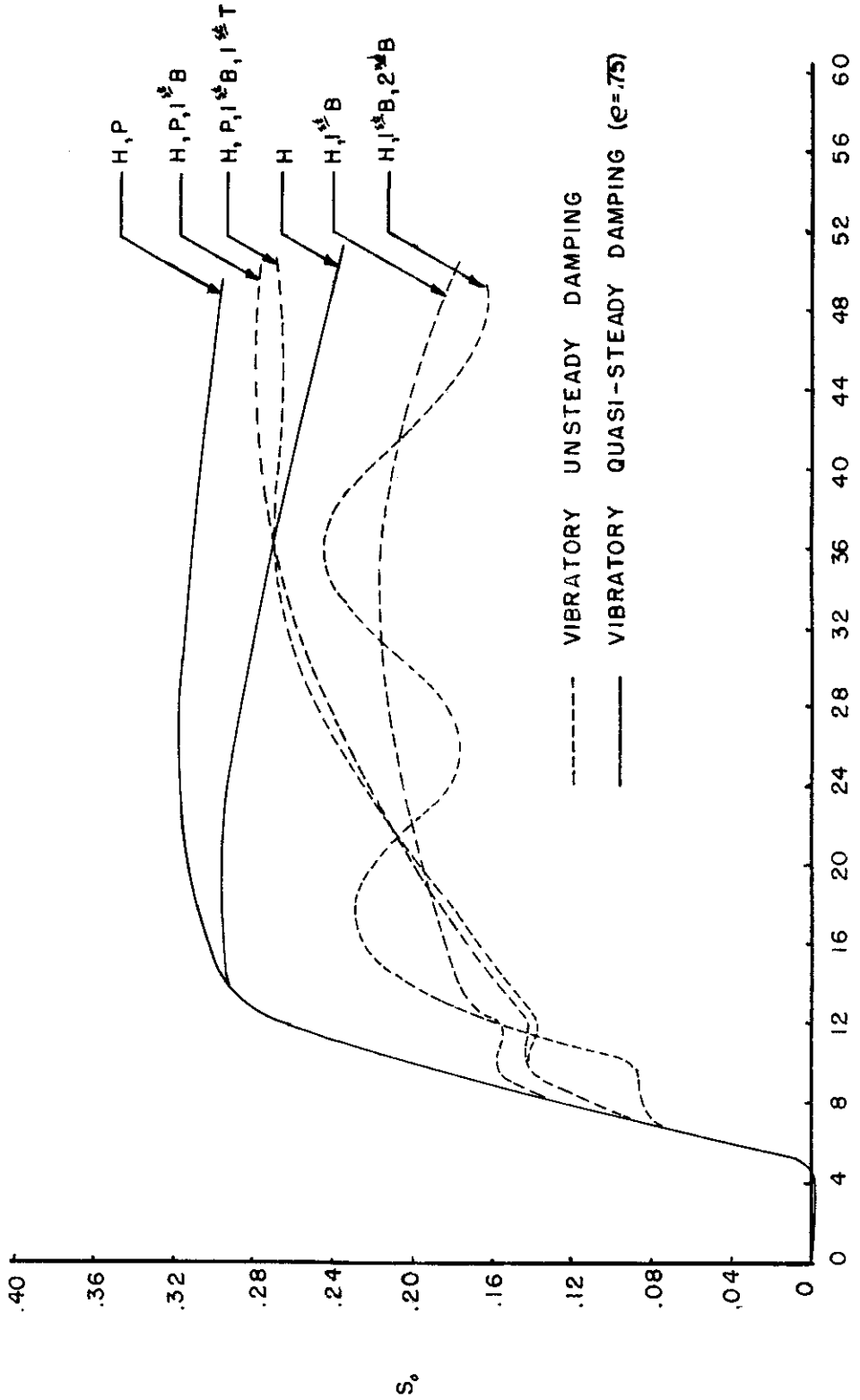

FIGURE 4.6 SHEARS AT WING ROOT FOR A SHARP-EDGED GUST

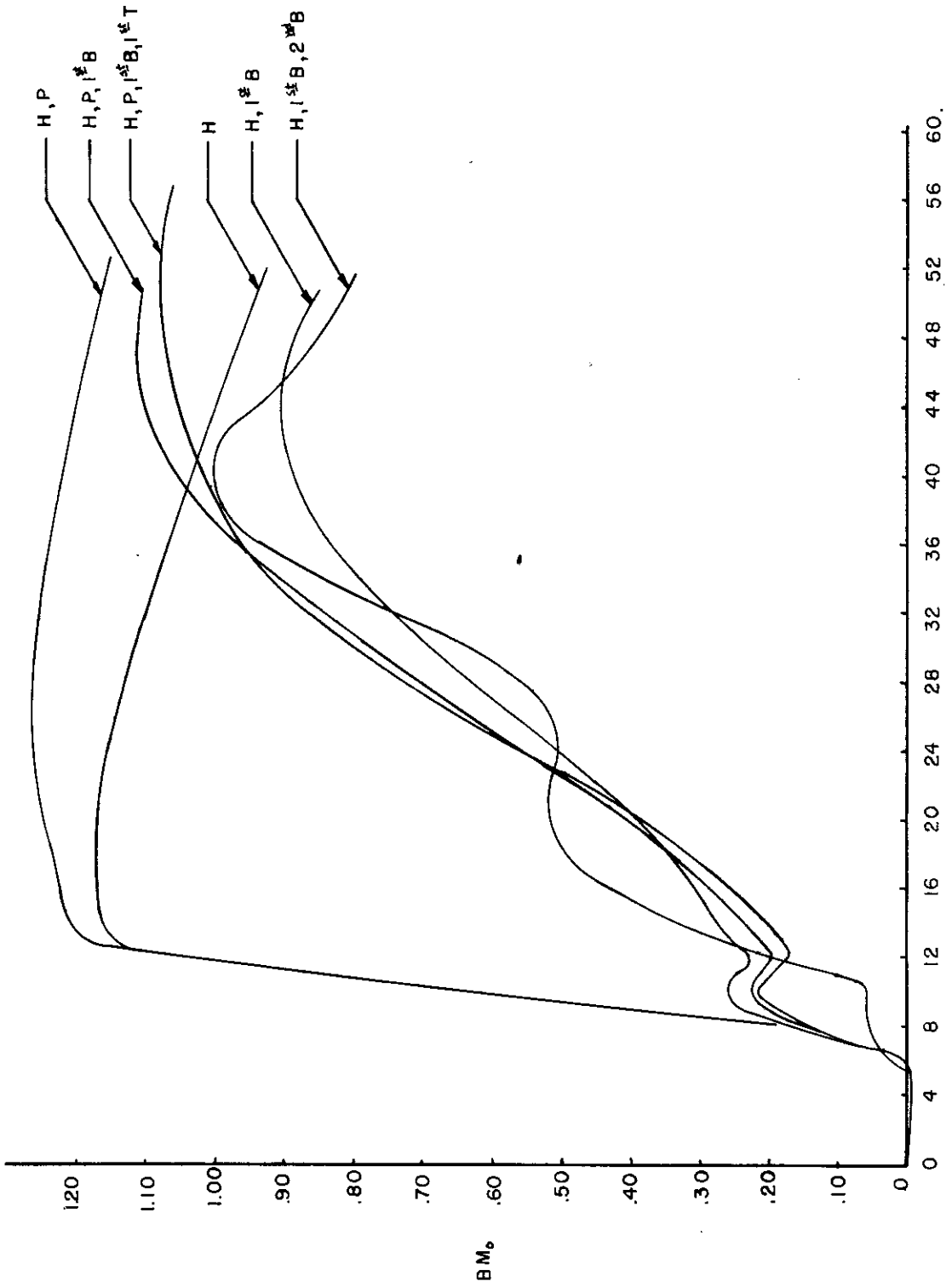

FIGURE 4.7 WING ROOT BENDING MOMENT FOR A SHARP-EDGED GUST, VIBRATORY QUASI-STEADY DAMPING (e=.75)

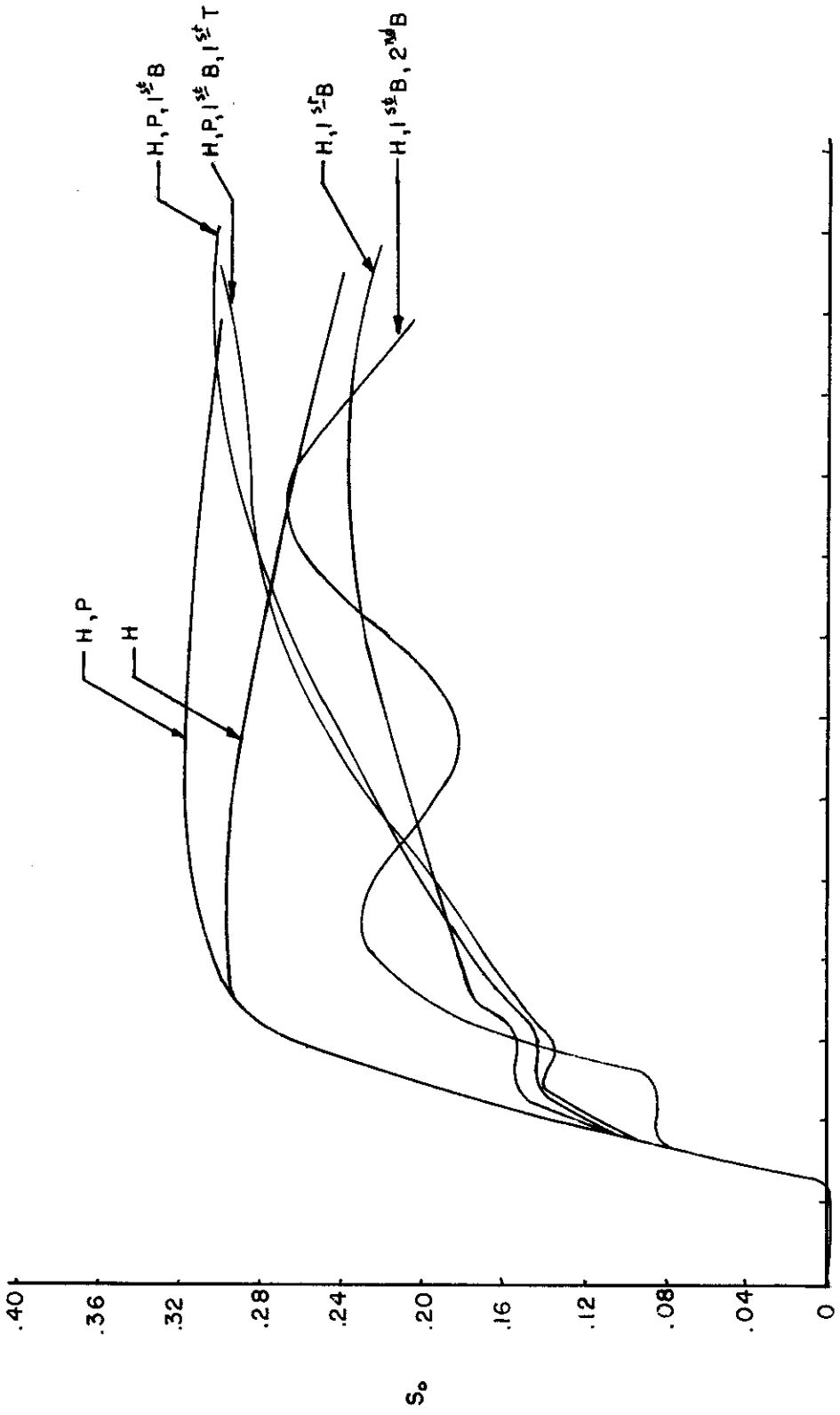

FIGURE 4.8 SHEARS AT WING ROOT FOR A SHARP-EDGED GUST, VIBRATORY QUASI-STEADY DAMPING (ϵ=.75)

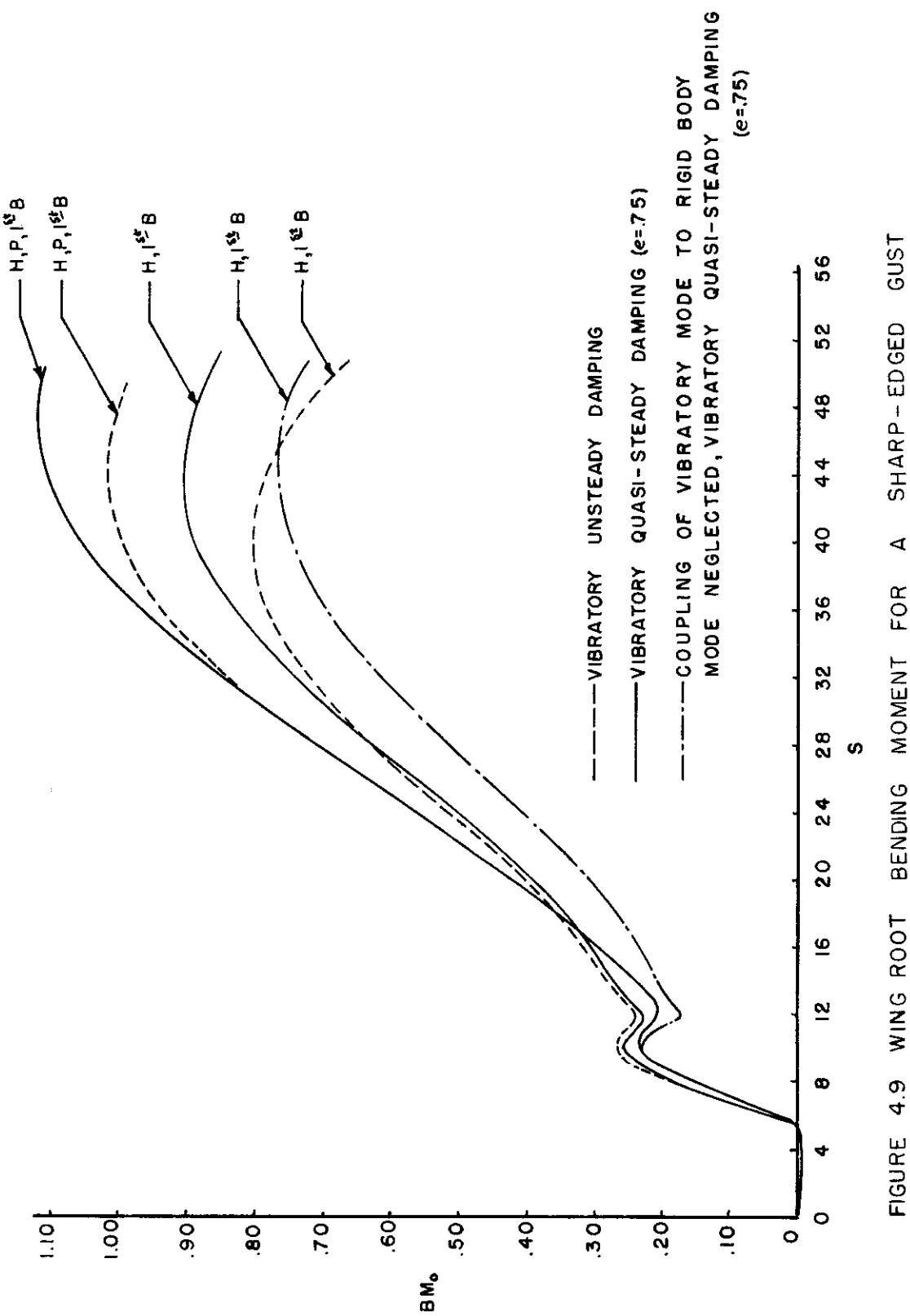

FIGURE 4.9 WING ROOT BENDING MOMENT FOR A SHARP-EDGED GUST

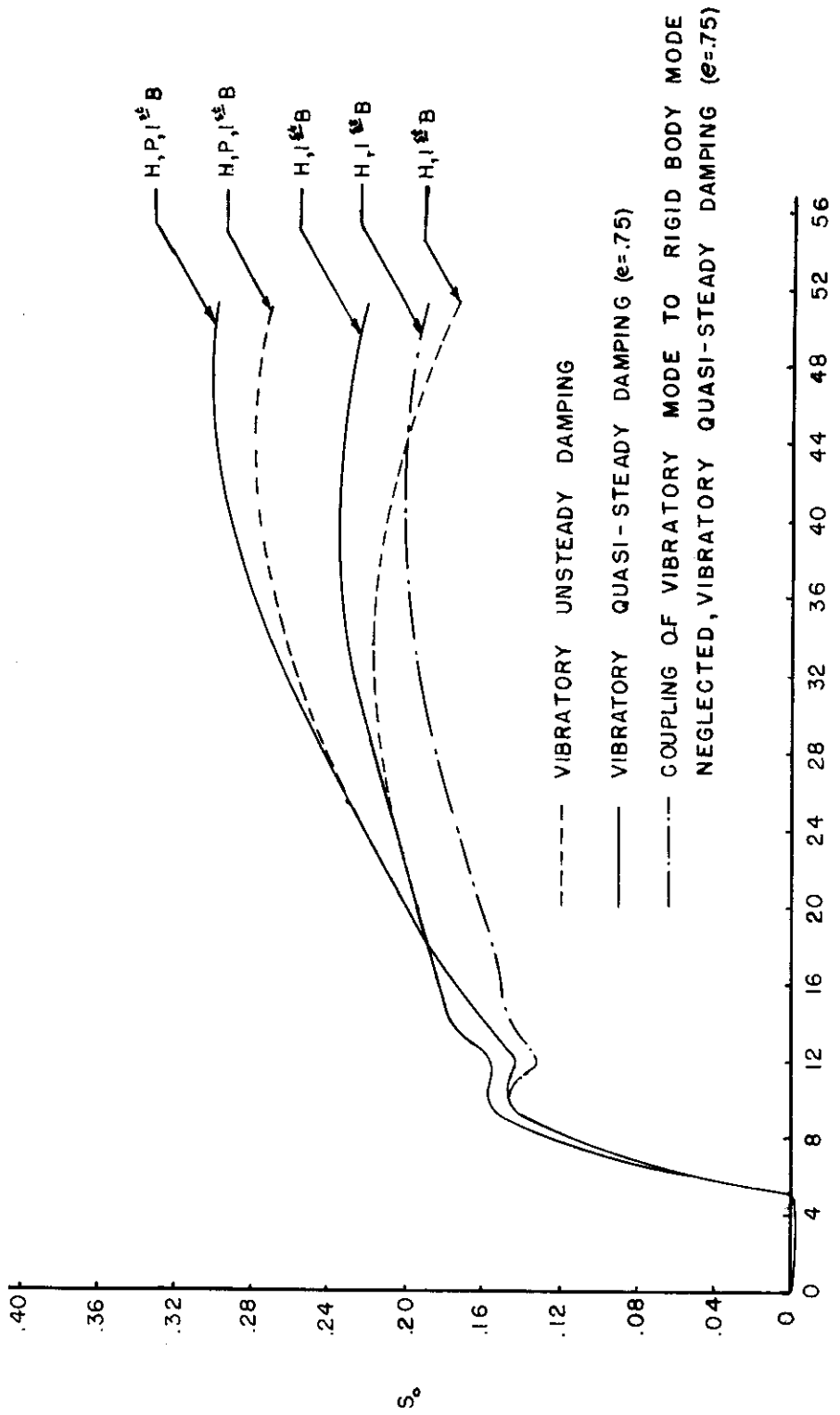

FIGURE 4.10 WING ROOT SHEARS FOR A SHARP-EDGED GUST

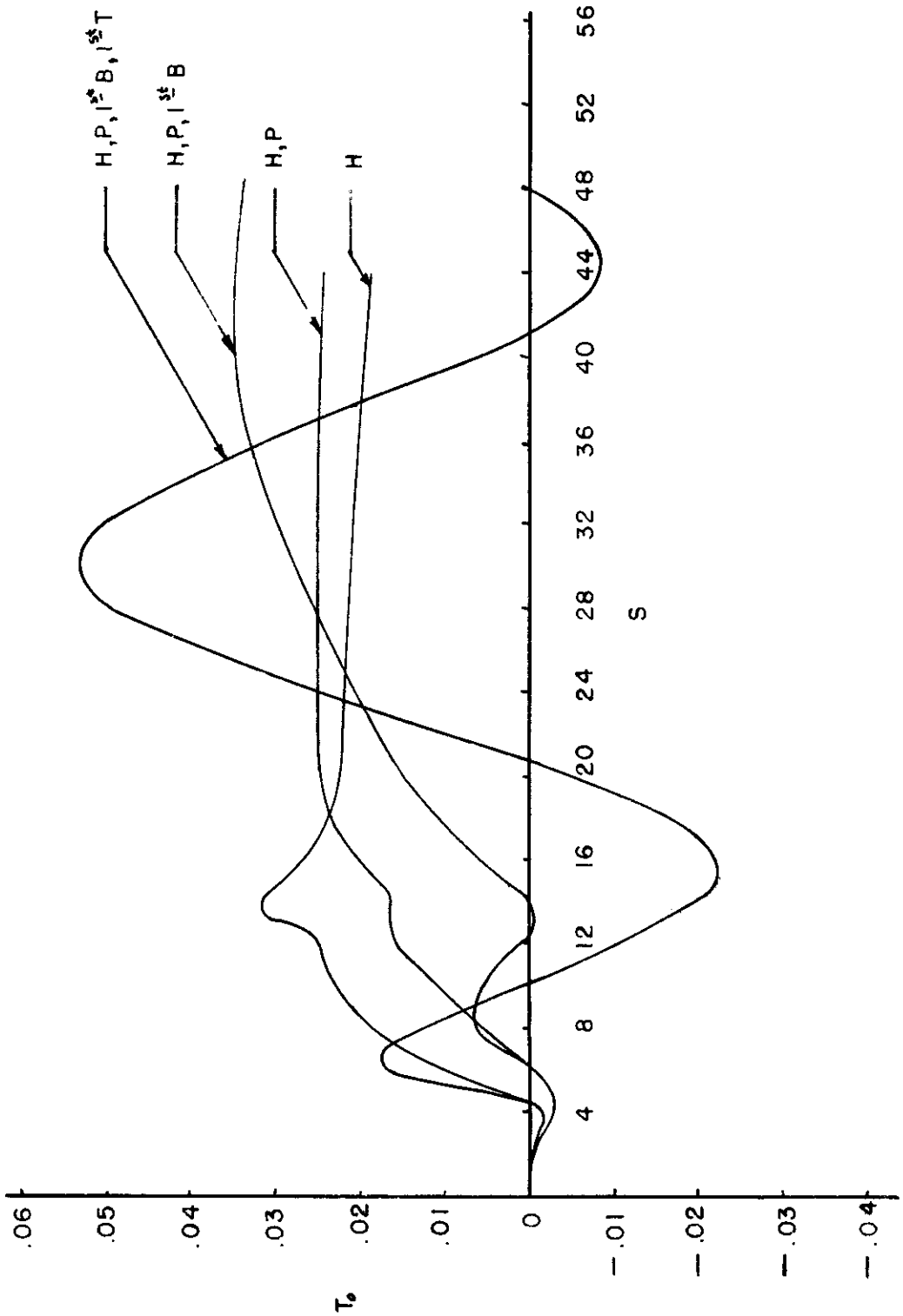

FIGURE 4.11 WING ROOT TORQUES FOR A SHARP-EDGED GUST, VIBRATORY QUASI-STEADY DAMPING (e=.75)

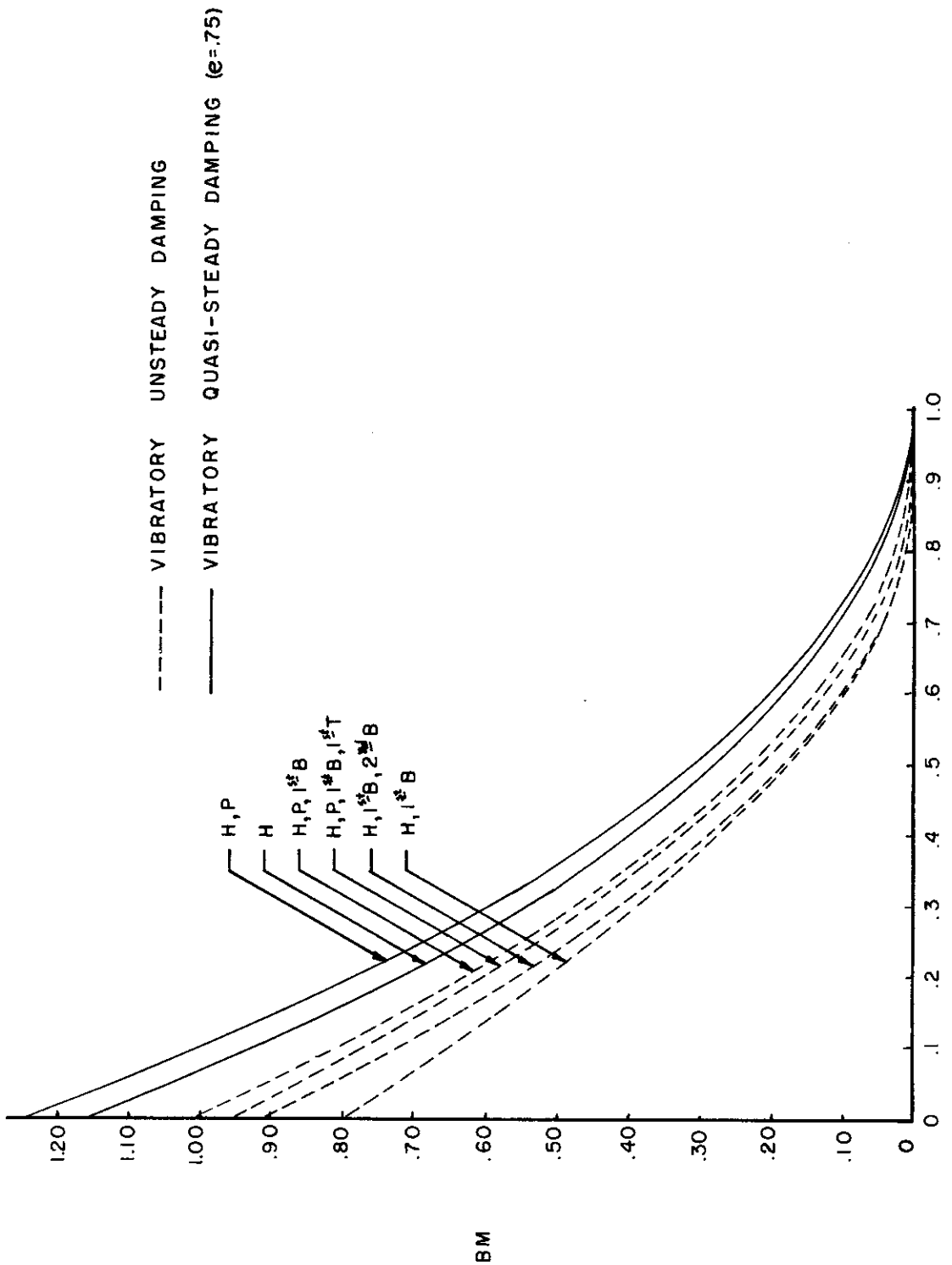

FIGURE 4.12 SPANWISE VARIATION IN PEAK BENDING MOMENT FOR A SHARP-EDGED GUST

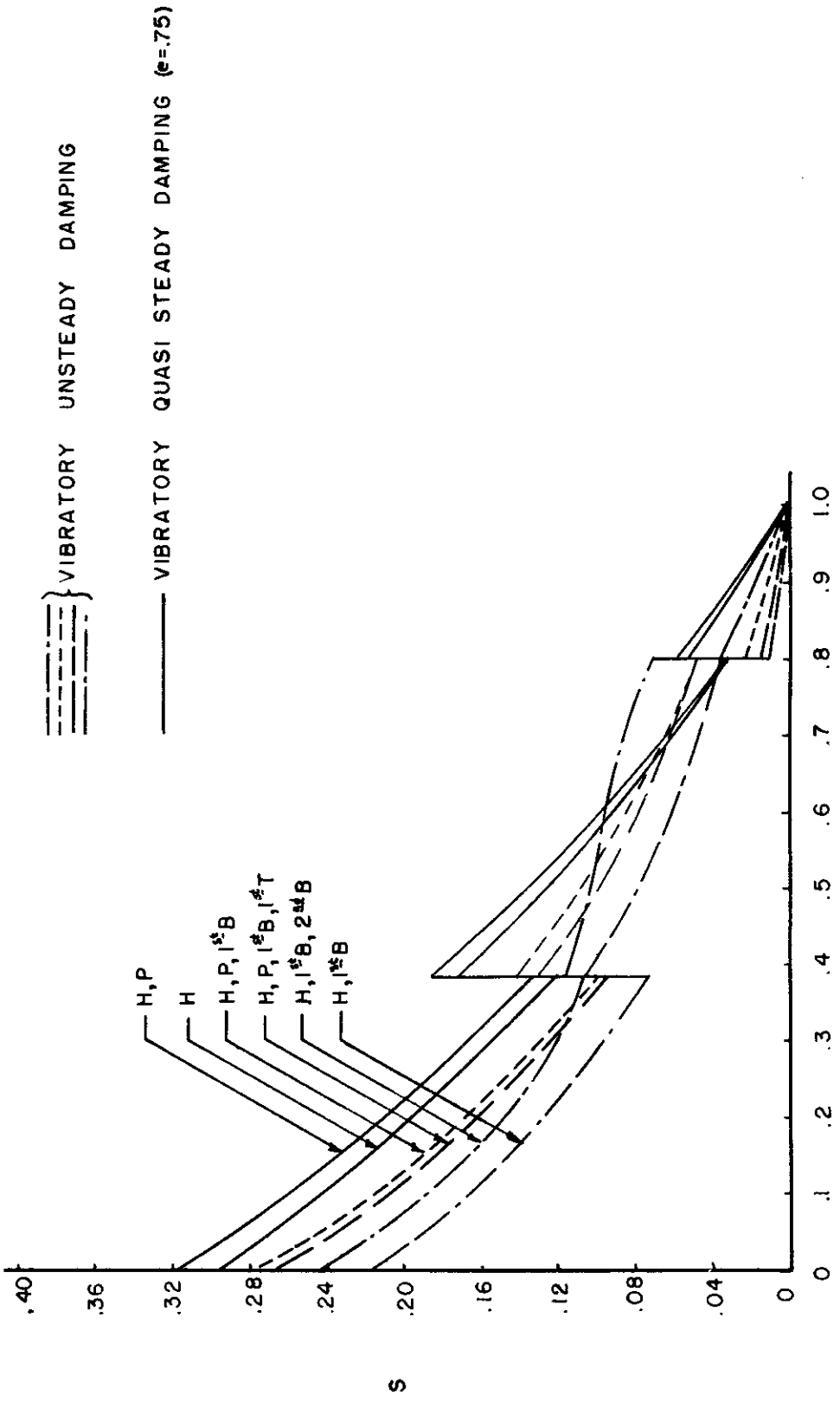

FIGURE 4.13 SPANWISE VARIATION IN PEAK SHEAR FOR A SHARP-EDGED GUST

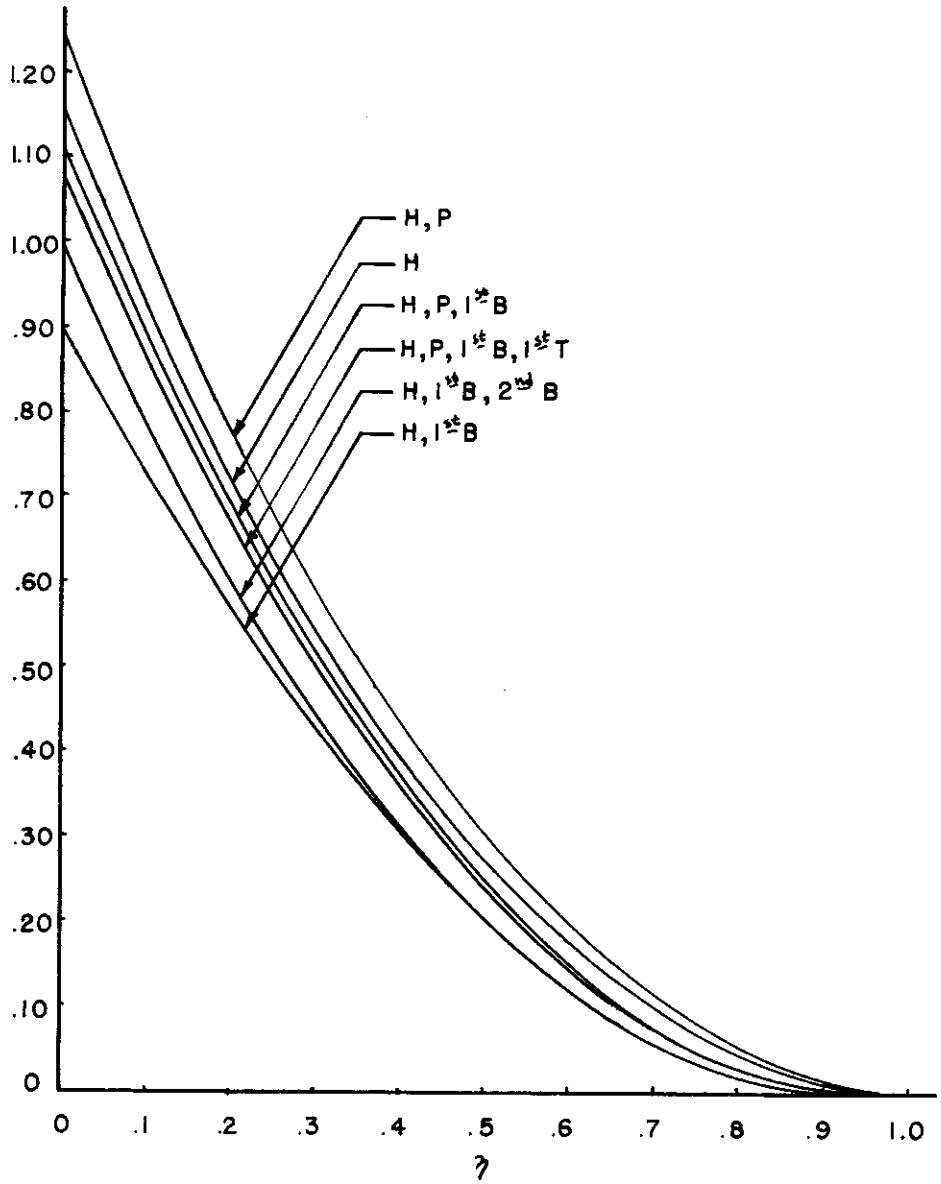

FIGURE 4.14 SPANWISE VARIATION IN PEAK BENDING MOMENT FOR A SHARP-EDGED GUST, VIBRATORY QUASI-STEADY DAMPING (e=.75)

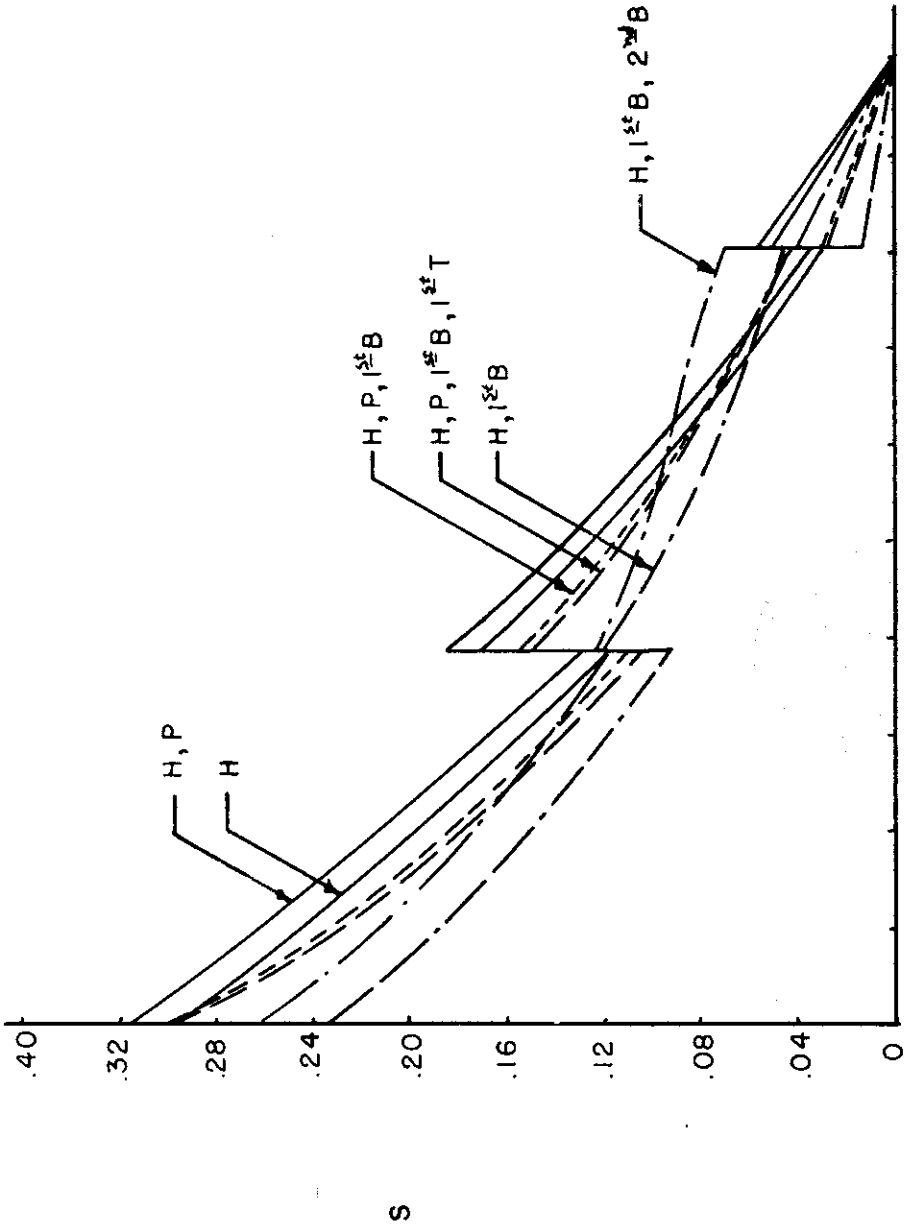

FIGURE 4.15 SPANWISE VARIATION IN PEAK SHEAR FOR A SHARP-EDGED GUST, VIBRATORY QUASI-STEADY DAMPING (e=.75)

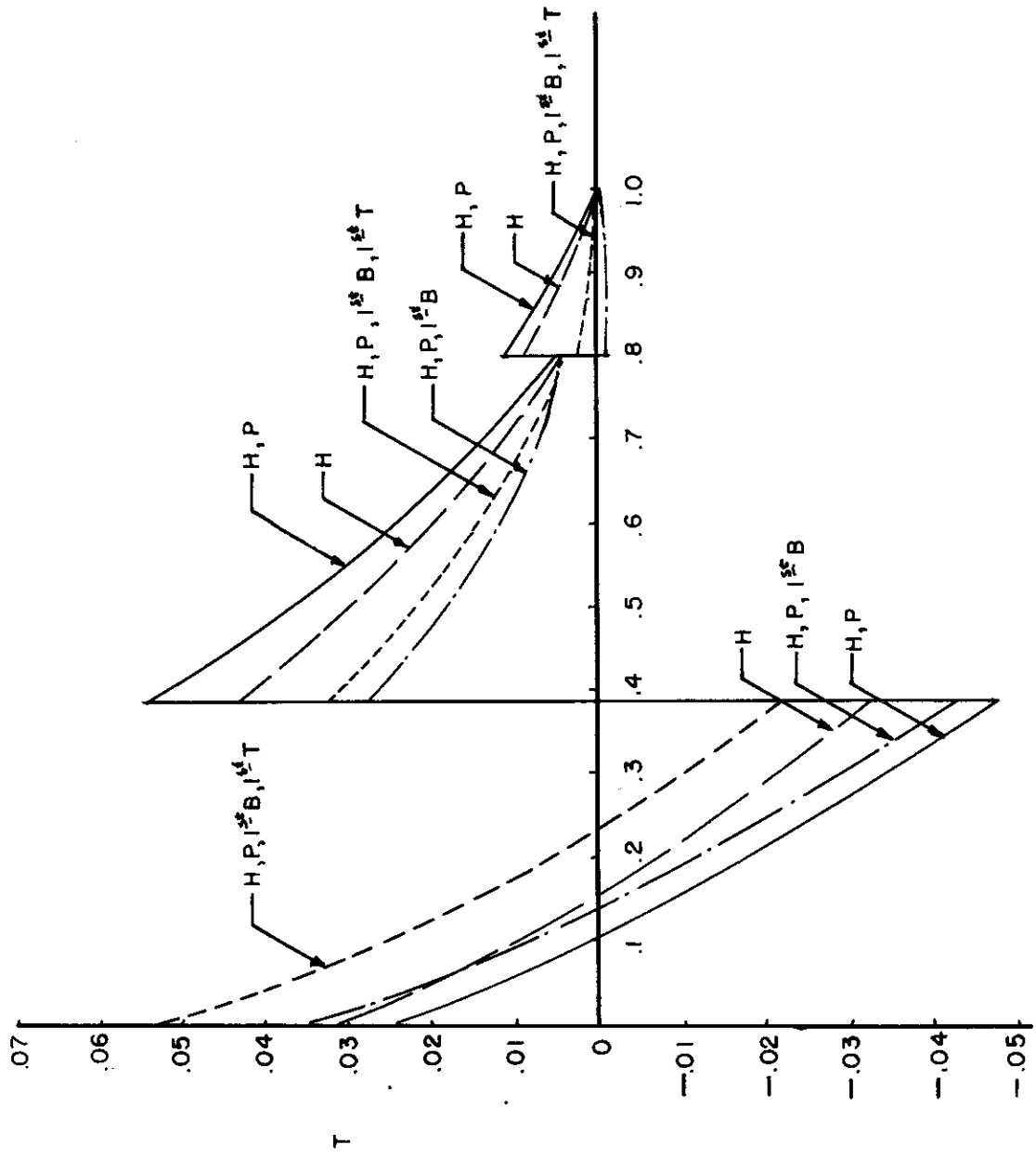

FIGURE 4.16 SPANWISE VARIATION IN PEAK TORQUE FOR A SHARP-EDGED GUST, VIBRATORY QUASI-STEADY DAMPING (e=.75)

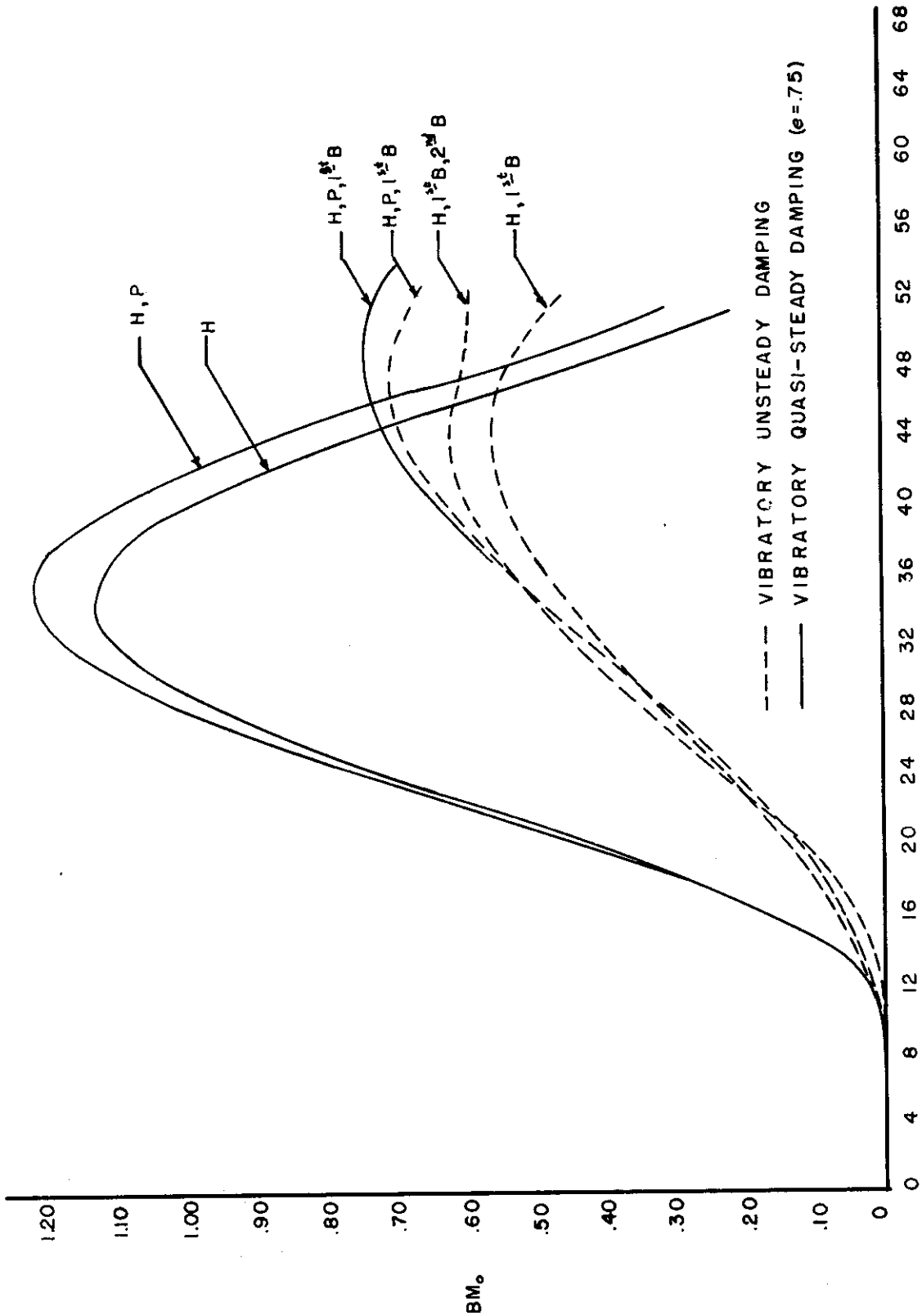

FIGURE 4.17 WING-ROOT BENDING MOMENT FOR ONE-MINUS-COSINE GUST, Sg=25

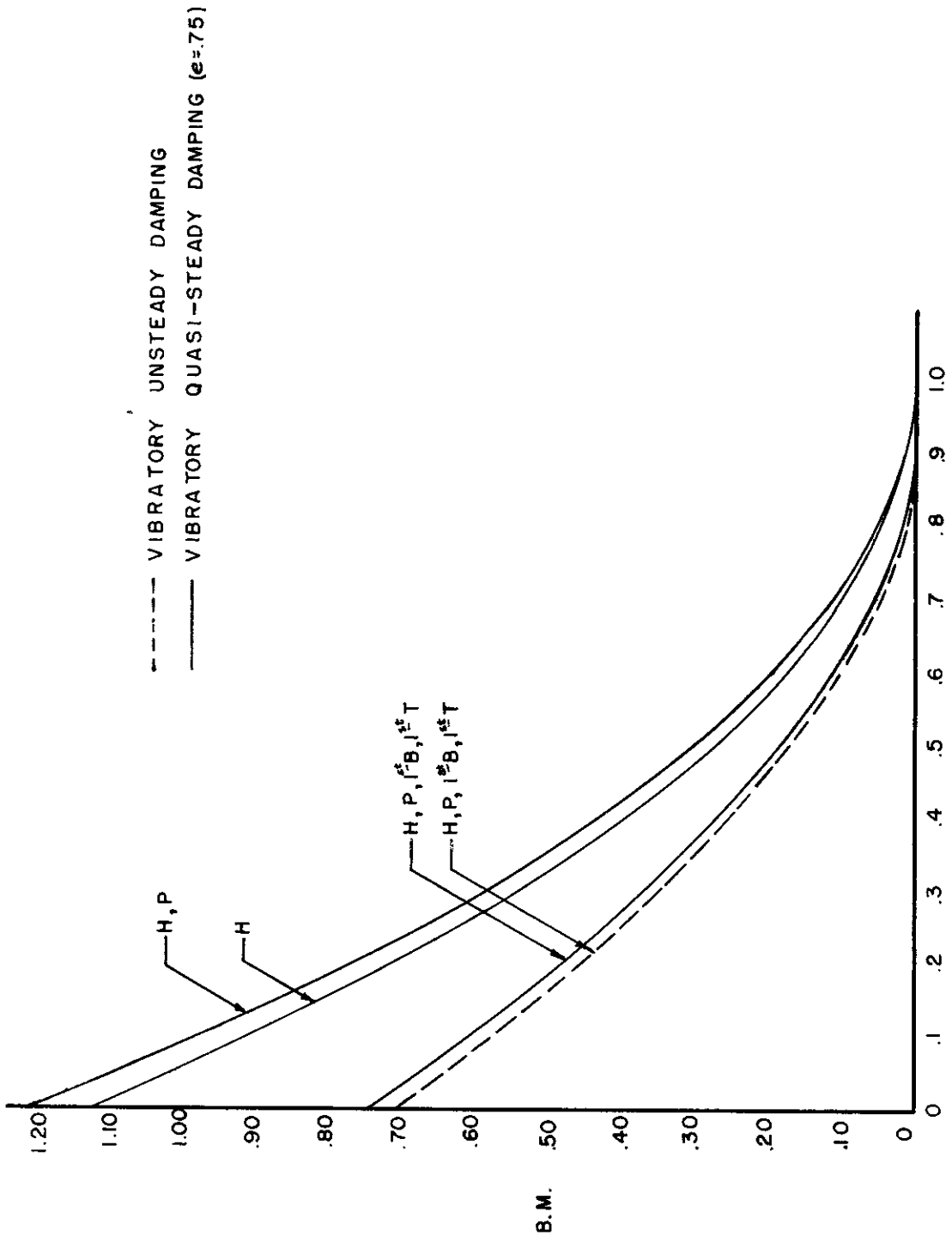

FIGURE 4.18 SPANWISE VARIATION IN PEAK BENDING MOMENT FOR ONE-MINUS-COSINE GUST, Sg = 25

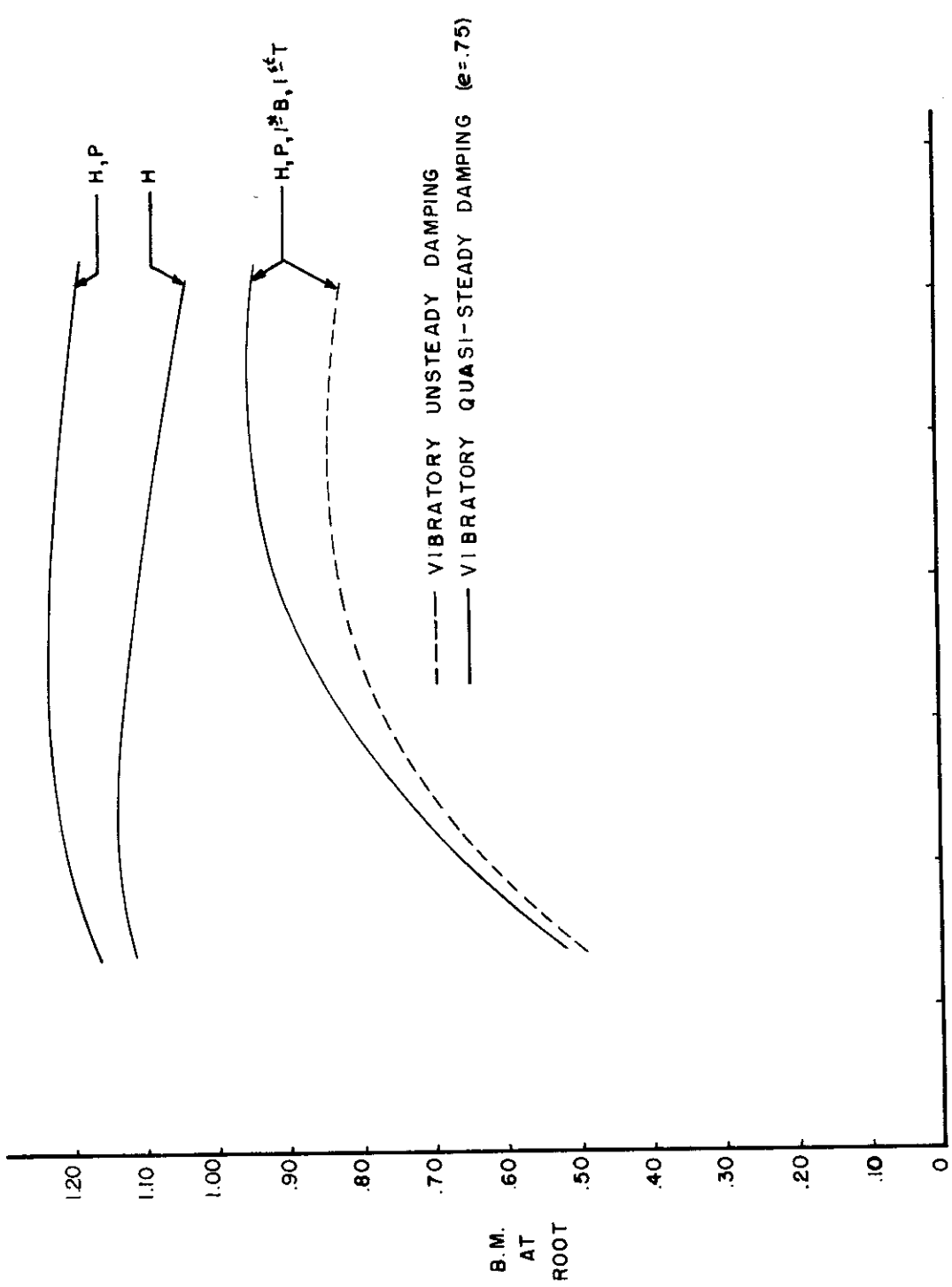

FIGURE 4.19 VARIATION OF PEAK WING-ROOT BENDING MOMENT WITH GUST GRADIENT DISTANCE, ONE-MINUS-COSINE GUST

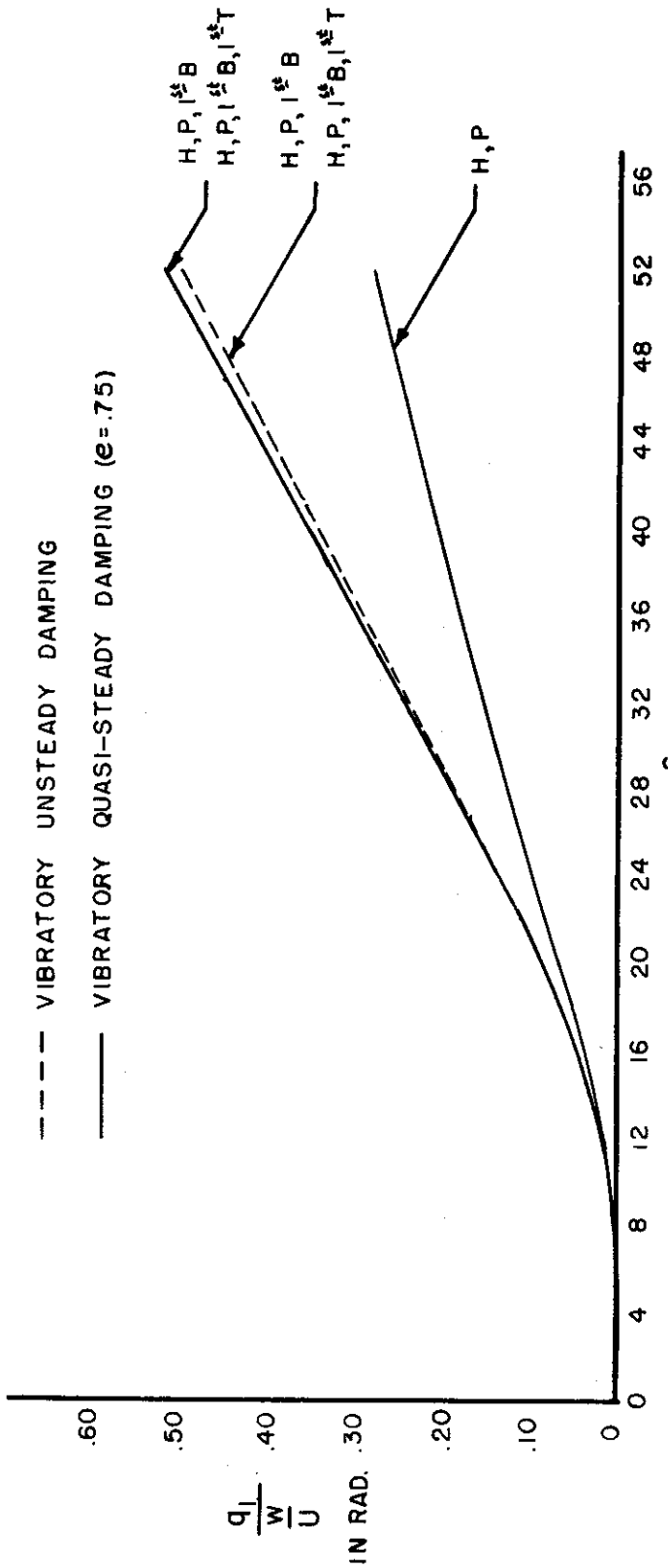

FIGURE 4.20 AIRPLANE PITCH ANGLE FOR A SHARP-EDGED GUST

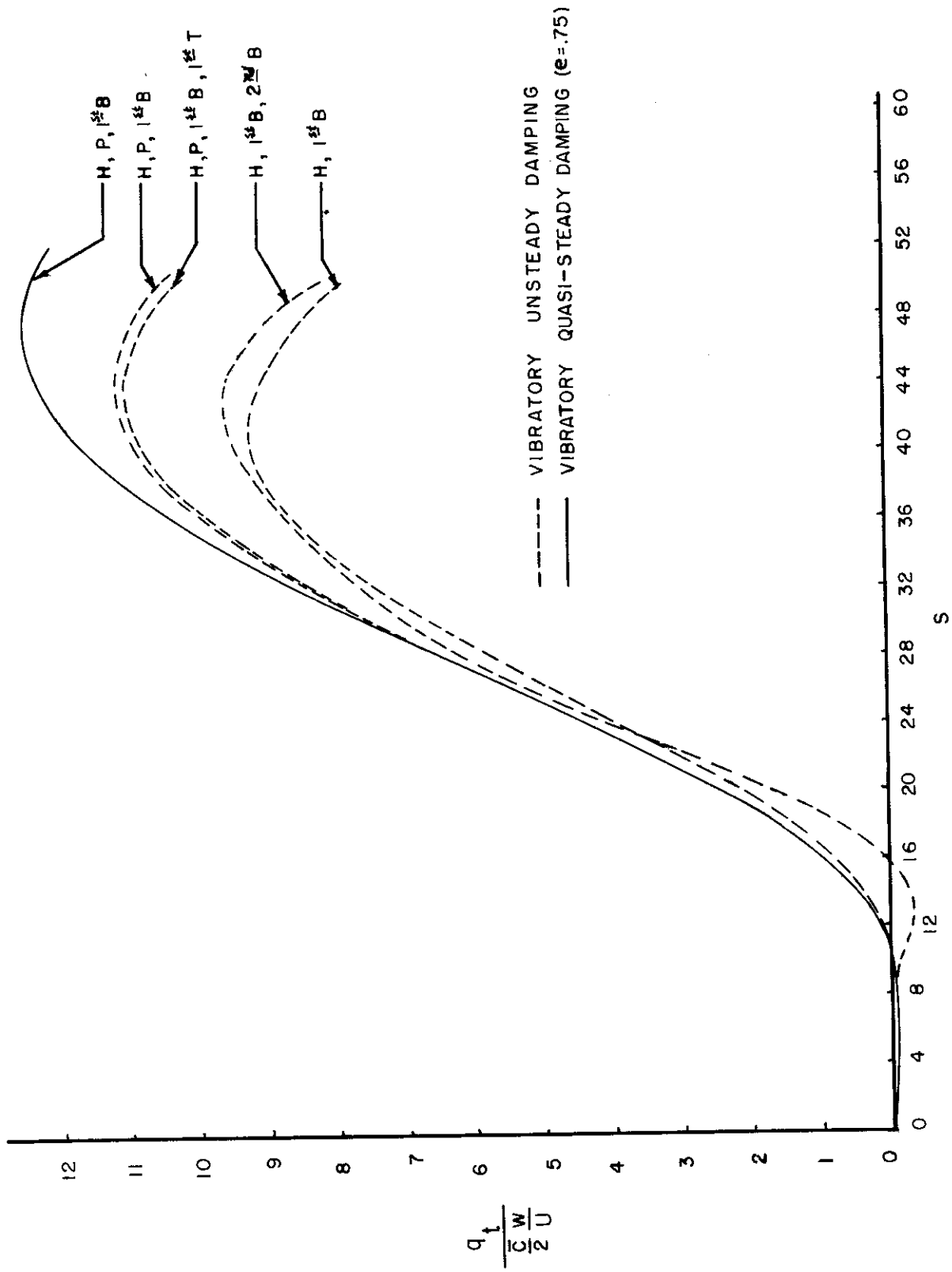

FIGURE 4.21 WING TIP DEFLECTION FOR A SHARP EDGED GUST

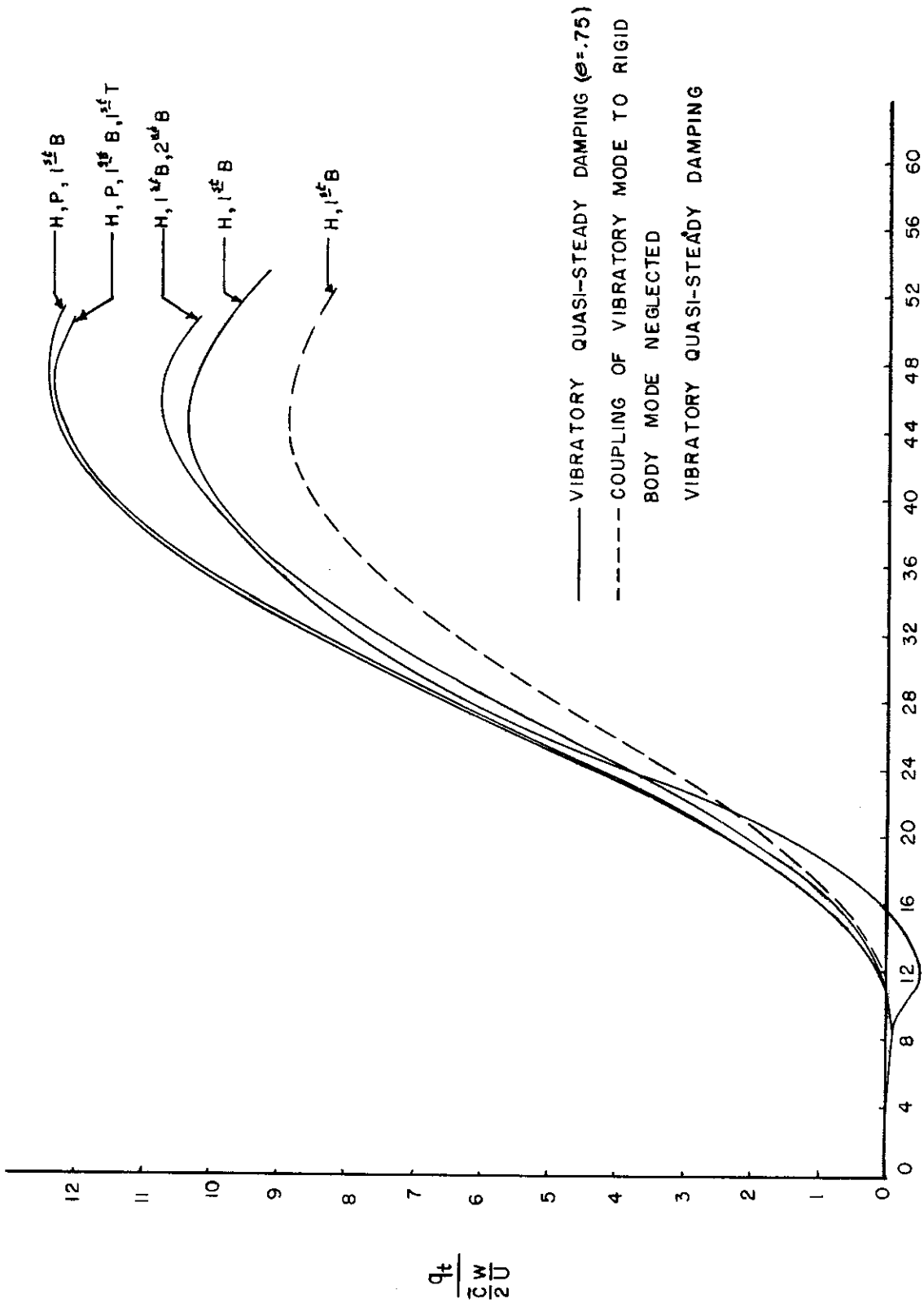

FIGURE 4.22 WING TIP DEFLECTION FOR A SHARP-EDGED GUST

REFERENCES

1. Bisplinghoff, R. L., Isakson, G., Pian, T. H. H., Flomenhoft, H. I., and O'Brien, T. F., An Investigation of Stresses in Aircraft Structures Under Dynamic Loading, Navy Contract NOa(s)-8790, Aeroelastic and Structures Research Laboratory, MIT, January 1949.

2. Houbolt, J. C., A Recurrence Matrix Solution for the Dynamic Response of Aircraft in Gusts, NACA Rept. 1010, 1951.

3. Goland, M., Luke, Y. L., and Kahn, E. A., Prediction of Wing Loads Due to Gusts, Including Aero-Elastic Effects, Part I - Formulation of the Method, Midwest Research Institute, Report No. 1-S36-E-9, July 1947.

4. Pian, T. H. H., and Winter, P. H., Effect of Structural Flexibility on Aircraft Loading, Part XVI - Estimation of the Dynamic Overstress in Straight Wing Airplanes, AF Technical Report No. 6358, Part XVI, February 1954.

5. Houbolt, J. C., and Kordes, E. E., Structural Response to Discrete and Continuous Gusts of an Airplane Having Wing-Bending Flexibility and a Correlation of Calculated and Flight Results, NACA Rept. 1181, March 1954.

6. Codik, A., Lin, H., and Pian, T. H. H., Effect of Flexibility on Aircraft Loading, Part XII - The Gust Response of a Sweptback Tapered Wing Including Bending Flexibility, AF Technical Report No. 6358, Part XII, October 1953.

7. Foss, K. A., Sternlight, D., and Pian, T. H. H., Effect of Structural Flexibility on Aircraft Loading, Part XIX - A Parametric Study of the Gust Response of Swept Wing Airplanes Including a Wing-Bending Degree of Freedom, AF Technical Report No. 6358, Part XIX, March 1954.

8. Foss, K. A., Effects of Structural Flexibility on Gust Loading of Aircraft, Part 1, Gust Loads on Swept-Wing Airplanes Free to Pitch and to Deform Statically, WADC Technical Report No. 54-592, Part 1, March 1955.

9. Brenner, C. W., and Isakson, G., A Parametric Investigation of Gust Loads on Rigid Airplanes in Two Degrees of Freedom, Navy Contract NOa(s)-8790, Aeroelastic and Structures Research Laboratory, Massachusetts Institute of Technology, October 1952.

10. Winson, J., The Solution of Aeroelastic Problems by Electronic Analogue Computation, Journal of the Aeronautical Sciences, Vol. 17, No. 7, pp. 385-395, July 1950.

11. MacNeal, R. H., McCann, G. C., and Wilts, C. H., The Solution of Aeroelastic Problems by Means of Electrical Analogies, Journal of the Aeronautical Sciences, Vol. 18, No. 12, pp. 777-789, December 1951.

12. Brull, M. A., and Howe, R. M., Preliminary Study of the Application of Electronic Differential Analyzers to Aeroelastic Problems, AIR-9, Department of Aeronautical Engineering, University of Michigan, August 1954.

13. Press, H., and Houbolt, J., Some Applications of Generalized Harmonic Analysis to Gust Loads on Airplane, Journal of the Aeronautical Sciences, Vol. 22, No. 1, pp. 17-26, January 1955.

14. Siddall, J. W., and Isakson, G., Approximate Analytical Methods for Determining Natural Modes and Frequencies of Vibration, Navy Contract N5 ori-07833, Aeroelastic and Structures Research Laboratory, Massachusetts Institute of Technology, January 1951.

15. Bisplinghoff, R. L., Isakson, G., and Pian, T. H. H., Methods in Transient Stress Analysis, Journal of the Aeronautical Sciences, Vol 17, No. 5, pp. 259-270, May 1950.

16. Bisplinghoff, R. L., Isakson, G., and O'Brien, T. F., Gust Loads on Rigid and Elastic Airplanes, Navy Contract NOa(s) 8790, Aeroelastic and Structures Research Laboratory, Massachusetts Institute of Technology, July 1950.

17. Calligeros, J. M., A Comparison of Methods of Determining Transient Stresses Due to Gusts, S. M. Thesis, Massachusetts Institute of Technology, June 1955.

APPENDIX A

DERIVATION OF THE GENERALIZED MASSES AND FORCES

A.1 Generalized Masses

The generalized masses of equations (1.11) through (1.17) are given by

$$M_{oo} = \int_{-\frac{\bar{c}}{2}\ell_{c.g.}}^{\frac{\bar{c}}{2}\ell_f} m_f(\bar{x})\,d\bar{x} + 2\int_0^{b/2} m_w(y)\,dy + 2\int_0^{b_t/2} m_t(y)\,dy$$

$$\frac{\bar{c}}{2}M_{o1} = -\int_{-\frac{\bar{c}}{2}\ell_{c.g.}}^{\frac{\bar{c}}{2}\ell_f} m_f(\bar{x})\,\bar{x}\,d\bar{x} + 2\int_0^{b/2} m_w(y)\,c_1(y)\,dy - 2\int_0^{b_t/2} m_t(y)\,c_3(y)\,dy$$

$$M_{o2} = \int_{-\frac{\bar{c}}{2}\ell_{c.g.}}^{\frac{\bar{c}}{2}\ell_f} m_f(\bar{x})\,\phi_2(\bar{x})\,d\bar{x} + 2\int_0^{b/2} m_w(y)\left[\phi_2\left(\tfrac{\bar{c}}{2}\ell_w\right) + \left(\frac{d\phi_2}{d\bar{x}}\right)_{\frac{\bar{c}}{2}\ell_w} c_2(y)\right] dy$$

$$+ 2\int_0^{b_t/2} m_t(y)\left[\phi_2\left(\tfrac{\bar{c}}{2}\ell_t\right) - \left(\frac{d\phi_2}{d\bar{x}}\right)_{\frac{\bar{c}}{2}\ell_t} c_4(y)\right] dy$$

$$M_{o3} = 2\int_0^{b/2} m_w(y)\left[\phi_3(y) - \tfrac{\bar{c}}{2}\,x_{c.g.w}\,\frac{d\phi_3}{dy}\sin\Theta\cos\Theta\right] dy$$

$$\frac{\bar{c}}{2}M_{o4} = 2\int_0^{b/2} m_w(y)\,\tfrac{\bar{c}}{2}\,x_{c.g.w}\,\phi_4(y)\cos\Theta\,dy$$

$$M_{o5} = 2\int_0^{\frac{b_t}{2}} m_t(y)\left[\phi_5(y) - \tfrac{\bar{c}}{2}\,x_{c.g.t}\,\frac{d\phi_5}{dy}\sin\Theta_t\cos\Theta_t\right] dy$$

$$\frac{\bar{c}}{2} M_{06} = 2 \int_0^{b_t/2} m_t(y)\, \frac{\bar{c}}{2} x_{c.g.t}\, \phi_6(y) \cos\Theta_t \, dy$$

$$\left(\frac{\bar{c}}{2}\right)^2 M_{11} = \int_{-\frac{\bar{c}}{2}\ell_{c.g.}}^{\frac{\bar{c}}{2}\ell_f} m_f(\bar{x})\, \bar{x}^2 \, d\bar{x} + 2\int_0^{b/2} m_w(y)\, C_1^2(y)\, dy + 2\int_0^{b_t/2} m_t(y)\, C_3^2(y)\, dy$$

$$+ \int_{-\frac{\bar{c}}{2}\ell_{c.g}}^{\frac{\bar{c}}{2}\ell_f} I_f(\bar{x})\, d\bar{x} + 2\int_0^{b/2} I_w(y)\, dy + 2\int_0^{b_t/2} I_t(y)\, dy$$

$$\frac{\bar{c}}{2} M_{12} = -\int_{-\frac{\bar{c}}{2}\ell_{c.g}}^{\frac{\bar{c}}{2}\ell_f} m_f(\bar{x})\, \phi_2(\bar{x})\, \bar{x}\, d\bar{x} + 2\int_0^{b/2} m_w(y)\, C_1(y) \left[\phi_2\left(\tfrac{\bar{c}}{2}\ell_w\right) + \left(\frac{d\phi_2}{d\bar{x}}\right)_{\frac{\bar{c}}{2}\ell_w} C_2(y)\right] dy$$

$$- 2\int_0^{b_t/2} m_t(y)\, C_3(y) \left[\phi_2\left(\tfrac{\bar{c}}{2}\ell_t\right) - \left(\frac{d\phi_2}{d\bar{x}}\right)_{\frac{\bar{c}}{2}\ell_t} C_4(y)\right] dy + 2\int_0^{b/2} I_w(y) \left(\frac{d\phi_2}{d\bar{x}}\right)_{\frac{\bar{c}}{2}\ell_w} dy$$

$$- 2\int_0^{b_t/2} I_t(y) \left(\frac{d\phi_2}{d\bar{x}}\right)_{\frac{\bar{c}}{2}\ell_t} dy - \int_{-\frac{\bar{c}}{2}\ell_{c.g}}^{\frac{\bar{c}}{2}\ell_f} I_f(\bar{x})\, \frac{d\phi_2}{d\bar{x}}\, d\bar{x}$$

$$\frac{\bar{c}}{2} M_{13} = 2\int_0^{b/2} m_w(y)\, C_1(y) \left[\phi_3(y) - \frac{\bar{c}}{2} x_{c.g.w} \frac{d\phi_3}{dy} \sin\Theta \cos\Theta\right] dy$$

$$- 2\int_0^{b/2} I_w(y)\, \frac{d\phi_3}{dy} \sin\Theta \cos\Theta \, dy$$

$$\left(\frac{\bar{c}}{2}\right)^2 M_{14} = 2\int_0^{b/2} m_w(y)\, c_1(y)\left[\frac{\bar{c}}{2} x_{c.g.w}\, \phi_4(y)\cos\Theta\right] dy + 2\int_0^{b/2} I_w(y)\, \phi_4(y)\cos\Theta\, dy$$

$$\frac{\bar{c}}{2} M_{15} = -2\int_0^{b/2} m_t(y)\, c_3(y)\left[\phi_5(y) - \frac{\bar{c}}{2} x_{c.g.t}\frac{d\phi_5}{dy}\sin\Theta_t\cos\Theta_t\right] dy$$

$$-2\int_0^{b_t/2} I_t(y)\,\frac{d\phi_5}{dy}\sin\Theta_t\cos\Theta_t\, dy$$

$$\left(\frac{\bar{c}}{2}\right)^2 M_{16} = -2\int_0^{b/2} m_t(y)\, c_3(y)\left[\frac{\bar{c}}{2} x_{c.g.t}\,\phi_6(y)\cos\Theta_t\right] dy + 2\int_0^{b_t/2} I_t(y)\,\phi_6(y)\cos\Theta_t\, dy$$

$$M_{22} = \int_{-\frac{\bar{c}}{2}\ell_{c.g.}}^{\frac{\bar{c}}{2}\ell_f} m_f(\bar{x})\,\phi_2^2(\bar{x})\, d\bar{x} + 2\int_0^{b/2} m_w(y)\left[\phi_2\left(\frac{\bar{c}}{2}\ell_w\right) + \left(\frac{d\phi_2}{d\bar{x}}\right)_{\frac{\bar{c}}{2}\ell_w} c_2(y)\right]^2 dy$$

$$+ \int_{-\frac{\bar{c}}{2}\ell_{c.g}}^{\frac{\bar{c}}{2}\ell_f} I_f(\bar{x})\left(\frac{d\phi_2}{d\bar{x}}\right)^2 d\bar{x} + 2\int_0^{b_t/2} m_t(y)\left[\phi_2\left(\frac{\bar{c}}{2}\ell_t\right) - \left(\frac{d\phi_2}{d\bar{x}}\right)_{\frac{\bar{c}}{2}\ell_t} c_4(y)\right]^2 dy$$

$$+ 2\int_0^{b/2} I_w(y)\left(\frac{d\phi_2}{d\bar{x}}\right)^2_{\frac{\bar{c}}{2}\ell_w} dy + 2\int_0^{b_t/2} I_t(y)\left(\frac{d\phi_2}{d\bar{x}}\right)^2_{\frac{\bar{c}}{2}\ell_t} dy$$

$$M_{23} = 2\int_0^{b/2} m_w(y)\left[\phi_3(y) - \frac{\bar{c}}{2} x_{c.g.w}\frac{d\phi_3}{dy}\sin\Theta\cos\Theta\right]\left[\phi_2\left(\frac{\bar{c}}{2}\ell_w\right) + \left(\frac{d\phi_2}{d\bar{x}}\right)_{\frac{\bar{c}}{2}\ell_w} c_2(y)\right] dy$$

$$- 2 \int_0^{b/2} I_w(y) \left(\frac{d\phi_2}{d\bar{x}}\right)_{\frac{\bar{c}}{2}\ell_w} \frac{d\phi_3}{dy} \sin\Theta \cos\Theta \, dy$$

$$\frac{\bar{c}}{2} M_{24} = 2 \int_0^{b/2} m_w(y) \left[\frac{\bar{c}}{2} x_{c.g.w} \phi_4(y) \cos\Theta\right] \left[\phi_2\left(\frac{\bar{c}}{2}\ell_w\right) + \left(\frac{d\phi_2}{d\bar{x}}\right)_{\frac{\bar{c}}{2}\ell_w} C_2(y)\right] dy$$

$$+ 2 \int_0^{b/2} I_w(y) \left(\frac{d\phi_2}{d\bar{x}}\right)_{\frac{\bar{c}}{2}\ell_w} \phi_4(y) \cos\Theta \, dy$$

$$M_{25} = 2 \int_0^{b_t/2} m_t(y) \left[\phi_5(y) - \frac{\bar{c}}{2} x_{c.g.t} \frac{d\phi_5}{dy} \sin\Theta_t \cos\Theta_t\right] \left[\phi_2\left(\frac{\bar{c}}{2}\ell_t\right) - \left(\frac{d\phi_2}{d\bar{x}}\right)_{\frac{\bar{c}}{2}\ell_t} C_4(y)\right] dy$$

$$+ 2 \int_0^{b_t/2} I_t(y) \left(\frac{d\phi_2}{d\bar{x}}\right)_{\frac{\bar{c}}{2}\ell_t} \frac{d\phi_5}{dy} \sin\Theta_t \cos\Theta_t \, dy$$

$$\frac{\bar{c}}{2} M_{26} = 2 \int_0^{b_t/2} m_t(y) \left[\frac{\bar{c}}{2} x_{c.g.t} \phi_6(y) \cos\Theta_t\right] \left[\phi_2\left(\frac{\bar{c}}{2}\ell_t\right) - \left(\frac{d\phi_2}{d\bar{x}}\right)_{\frac{\bar{c}}{2}\ell_t} C_4(y)\right] dy$$

$$- 2 \int_0^{b_t/2} I_t(y) \left(\frac{d\phi_2}{d\bar{x}}\right)_{\frac{\bar{c}}{2}\ell_t} \phi_6(y) \cos\Theta_t \, dy$$

$$M_{33} = 2 \int_0^{b/2} m_w(y) \left[\phi_3(y) - \frac{\bar{c}}{2} x_{c.g.w} \frac{d\phi_3}{dy} \sin\Theta \cos\Theta\right]^2 dy$$

$$+ 2\int_0^{b/2} I_w(y)\left[\frac{d\phi_3}{dy}\sin\Theta\cos\Theta\right]^2 dy$$

$$\frac{\bar{c}}{2}M_{34} = 2\int_0^{b/2} m_w(y)\left[\frac{\bar{c}}{2}x_{c.g.w}\,\phi_4(y)\cos\Theta\right]\left[\phi_3(y) - \frac{\bar{c}}{2}x_{c.g.w}\frac{d\phi_3}{dy}\sin\Theta\cos\Theta\right]dy$$

$$- 2\int_0^{b/2} I_w(y)\,\phi_4(y)\,\frac{d\phi_3}{dy}\sin\Theta\cos^2\Theta\,dy$$

$$\left(\frac{\bar{c}}{2}\right)^2 M_{44} = 2\int_0^{b/2} m_w(y)\left[\frac{\bar{c}}{2}x_{c.g.w}\,\phi_4(y)\cos\Theta\right]^2 dy + 2\int_0^{b/2} I_w(y)\,\phi_4^2(y)\cos^2\Theta\,dy$$

$$M_{55} = 2\int_0^{b_t/2} m_t(y)\left[\phi_5(y) - \frac{\bar{c}}{2}x_{c.g.t}\frac{d\phi_5}{dy}\sin\Theta_t\cos\Theta_t\right]^2 dy + 2\int_0^{b_t/2} I_t(y)\left[\frac{d\phi_5}{dy}\sin\Theta_t\cos\Theta_t\right]^2 dy$$

$$\frac{\bar{c}}{2}M_{56} = 2\int_0^{b_t/2} m_t(y)\left[\frac{\bar{c}}{2}x_{c.g.t}\,\phi_6(y)\cos\Theta_t\right]\left[\phi_5(y) - \frac{\bar{c}}{2}x_{c.g.t}\frac{d\phi_5}{dy}\sin\Theta_t\cos\Theta_t\right]dy$$

$$- 2\int_0^{b_t/2} I_t(y)\,\phi_6(y)\,\frac{d\phi_5}{dy}\sin\Theta_t\cos^2\Theta_t\,dy$$

$$\left(\frac{\bar{c}}{2}\right)^2 M_{66} = 2\int_0^{b_t/2} m_t(y)\left[\frac{\bar{c}}{2}x_{c.g.t}\,\phi_6(y)\cos\Theta_t\right]^2 dy + 2\int_0^{b_t/2} I_t(y)\left[\phi_6(y)\cos\Theta_t\right]^2 dy$$

It should be noted that M_{00} is the total mass of the airplane and $\left(\frac{\bar{c}}{2}\right)^2 M_{11}$ is the total moment of inertia of the airplane about the y-axis. The coefficient $M_{01} = 0$ since the total moment about the center of gravity of the entire airplane is always zero. While for most practical cases the distance from the wing elastic axis to its center of gravity is negligible, care should be taken when large concentrated masses are present such as nacelles whose static unbalance may be very great.

It can be seen from the preceding equations that an additional degree of freedom can be introduced without difficulty. For example, a second bending degree of freedom having a mode shape ϕ_7 would have as generalized masses the above with subscript 3 replaced by 7 plus an additional inertial coupling term given by

$$M_{37} = 2\int_0^{b/2} m_w(y)\left[\phi_3(y) - \frac{\bar{c}}{2} x_{c.g.w} \frac{d\phi_3}{dy} \sin\Phi\cos\Phi\right]\left[\phi_7(y) - \frac{\bar{c}}{2} x_{c.g.w} \frac{d\phi_7}{dy} \sin\Phi\cos\Phi\right] dy$$

$$+ 2\int_0^{b/2} I_w(y) \frac{d\phi_3}{dy} \frac{d\phi_7}{dy} \sin^2\Phi\cos^2\Phi \, dy$$

If the second assumed bending mode is made orthogonal to the first, this coefficient will drop out; although there may still be elastic coupling introduced by the stiffness coefficient,

$$K_{37} = \int_0^{\frac{b}{2\cos\Phi}} E I_w(\bar{y}) \left(\frac{d^2\phi_3}{d\bar{y}^2}\right)\left(\frac{d^2\phi_7}{d\bar{y}^2}\right) d\bar{y}$$

A.2 Unsteady Air Forces

The following analysis is based upon several simplifying assumptions which are explained more fully in Appendix A of Reference 8 (Part 1 of this report) and for which considerable justification is given.

A.2.a Lift on Wing Due to Change in Angle of Attack

Using strip theory, the lift per unit span for a step angle of attack is

$$\ell_w^{\alpha} = \tfrac{1}{2} \rho U^2 c\, a_w\, \varphi(s)\, \alpha_w(y) \tag{A.1}$$

where $\varphi(s)$ is the Wagner function usually approximated for two-dimensional incompressible flow by

$$\varphi(s) = 1 - .165\, e^{-.045 s} - .335\, e^{-.3 s} \tag{A.2}$$

where

$$s = \frac{Ut}{\frac{\bar{c}}{2}} \tag{A.3}$$

and the local chord for a linearly tapered wing is given by

$$c = \frac{2\bar{c}}{1+\lambda_w}\left[1 - (1-\lambda_w)\eta\right] \tag{A.4}$$

where

λ_w is the wing taper ratio

With Duhamel's integral, equation (A. 1), after substituting (A. 4), becomes for an arbitrary angle of attack variation

$$l_w^{\alpha} = \tfrac{1}{2}\rho U^2 \bar{c}\, a_w \frac{2}{1+\lambda_w} \int_0^s \left[1-(1-\lambda_w)\eta\right] \varphi(s-\sigma)\, \alpha_w'(\sigma)\, d\sigma \qquad \text{(A. 5)}$$

where

$\alpha_w(\sigma)$ is the local angle of attack at the 3/4-chord line

a_w is the three-dimensional wing lift-curve slope generally used with strip theory to approximate finite span effects.

The local angle of attack, which can be obtained from equations (1. 6) and (1. 8), is

$$\alpha_w(t) = q_1 + \left(\frac{d\phi_2}{d\bar{x}}\right)_{\frac{\bar{c}}{2}\ell_w} q_2 - \frac{d\phi_3}{dy} \sin\Lambda \cos\Lambda\, q_3 + \phi_4(y) \cos\Lambda\, q_4$$

$$-\frac{1}{U}\left\{\dot{q}_0 + k_6(y)\,\dot{q}_1 + \left[\phi_2\left(\tfrac{\bar{c}}{2}\ell_w\right) + \left(\frac{d\phi_2}{d\bar{x}}\right)_{\frac{\bar{c}}{2}\ell_w} k_7(y)\right]\dot{q}_2 + \phi_3(y)\,\dot{q}_3\right.$$

$$\left. -\left[k_w(y) - k_6(y)\right]\left[\phi_4(y)\cos\Lambda\,\dot{q}_4 - \frac{d\phi_3}{dy}\sin\Lambda\cos\Lambda\,\dot{q}_3\right]\right\} \qquad \text{(A. 6)}$$

After differentiating with respect to s, equation (A. 6) becomes

$$\alpha'_w(s) = \dot{q}_1 + \left(\frac{d\phi_2}{d\bar{x}}\right)_{\frac{\bar{c}}{2}\ell_w} \dot{q}_2 - \frac{d\phi_3}{dy} \sin\Lambda \cos\Lambda\, \dot{q}_3 + \phi_4(y) \cos\Lambda\, \dot{q}_4$$

$$- \frac{2}{\bar{c}} \left\{ \ddot{q}_0 + k_6(y)\ddot{q}_1 + \left[\phi_2\left(\frac{\bar{c}}{2}\ell_w\right) + \left(\frac{d\phi_2}{d\bar{x}}\right)_{\frac{\bar{c}}{2}\ell_w} k_7(y)\right]\ddot{q}_2 + \phi_3(y)\ddot{q}_3 \right.$$

$$\left. - \left[k_w(y) - k_6(y)\right]\left[\phi_4(y)\cos\Lambda\,\ddot{q}_4 - \frac{d\phi_3}{dy}\sin\Lambda\cos\Lambda\,\ddot{q}_3\right] \right\}$$

(A.7)

where

$$k_6(y) = \frac{\bar{c}}{2}\left(\ell_3 - \frac{y}{\frac{\bar{c}}{2}}\tan\Lambda_3\right)$$

$$k_7(y) = \frac{\bar{c}}{2}\left(\ell_3 - \ell_w - y/\frac{\bar{c}}{2}\tan\Lambda_3\right)$$

$y = \frac{b}{2}\eta$ is the distance measured along the y axis

The distance ℓ_3 and the sweep angle Λ_3 are defined in Figure 1.1; and the prime mark denotes differentiation with respect to s.

A.2.b Lift on Tail Due to Change in Angle of Attack

By analogy with the wing lift, the horizontal tail lift per unit span for an arbitrary angle of attack variation is

$$\ell_t^{\alpha} = \frac{1}{2}\rho U^2 \bar{c}_t a_t \frac{2}{1+\lambda_t} \int_0^s \left[1-(1-\lambda_t)\eta\right] \varphi(\gamma s - \gamma\sigma)\, \alpha'_t(\sigma)\, d\sigma$$

(A.8)

where

$$\alpha_t'(s) = \dot{q}_1 - \left(\frac{d\phi_2}{d\bar{x}}\right)_{\frac{\bar{c}}{2}\ell_t} \dot{q}_2 - \frac{d\phi_5}{dy} \sin\Phi_t \cos\Phi_t \dot{q}_5 + \phi_6(y) \cos\Phi_t \dot{q}_6$$

$$-\frac{2}{\bar{c}} \left\{ \ddot{q}_0 - k_8(y) \ddot{q}_1 + \left[\phi_2\left(\frac{\bar{c}}{2}\ell_t\right) + \left(\frac{d\phi_2}{d\bar{x}}\right)_{\frac{\bar{c}}{2}\ell_t} k_9(y) \right] \ddot{q}_2 + \phi_5(y) \ddot{q}_5 \right.$$

$$\left. - \left[k_8(y) - k_5(y) \right] \left[\phi_6(y) \cos\Phi_t \ddot{q}_6 - \frac{d\phi_5}{dy} \sin\Phi_t \cos\Phi_t \ddot{q}_5 \right] \right\}$$

(A. 9)

and where

$$k_5(y) = \frac{\bar{c}}{2}\left(\ell_t + y/\frac{\bar{c}}{2} \tan\Phi_t\right)$$

$$k_8(y) = \frac{\bar{c}}{2}\left(\ell_{3t} + y/\frac{\bar{c}}{2} \tan\Lambda_{3t}\right)$$

$$k_9(y) = \frac{\bar{c}}{2}\left(\ell_{3t} - \ell_t + y/\frac{\bar{c}}{2} \tan\Lambda_{3t}\right)$$

A. 2. c Lift on Fuselage Due to Change in Angle of Attack

It is shown in Reference 8 that the lift per unit length on a slender fuselage due to a change in angle of attack can be approximated by

$$\ell_f^\alpha = \frac{d}{dt}\left(\rho A U \alpha_f\right) = U \frac{\partial}{\partial x}\left(\rho A U \alpha_f\right) + \frac{\partial}{\partial t}\left(\rho A U \alpha_f\right)$$

(A. 10)

where A is the local cross-sectional area of an equivalent body of revolution having the same width. The local angle of attack of the fuselage including the fuselage bending mode is

$$\alpha_f = q_1 - \frac{d\phi_2}{d\bar{x}} q_2 - \frac{\dot{q}_0}{U} + \bar{x}\,\frac{\dot{q}_1}{U} - \phi_2(\bar{x})\,\frac{\dot{q}_2}{U} \tag{A.11}$$

Neglecting apparent mass terms, the lift per unit length on the fuselage is, then,

$$\ell_f^{\alpha} = \rho U^2 \frac{d}{d\bar{x}} \left\{ A\left(q_1 - \frac{d\phi_2}{d\bar{x}} q_2 - \frac{2}{\bar{c}} \dot{q}_0 + \frac{2\bar{x}}{\bar{c}} \dot{q}_1 - \frac{2\phi_2(\bar{x})}{\bar{c}} \dot{q}_2 \right) \right\} \tag{A.12}$$

A. 2. d Lift on Wing Due to Gust Penetration

The lift per unit span on the wing after penetrating a symmetrical sharp-edged gust can be written as

$$\ell_w^G = \frac{1}{2} \rho U^2 c\, a_w \frac{w}{U}\, \psi(s) \tag{A.13}$$

where

w is the gust velocity

$\psi(s)$ is the Kussner lift-growth function

The Kussner function is defined in such a way that s must be measured from the leading edge of each wing strip. However, it is shown in Reference 8 that, insofar as generalized forces are concerned, the effect of a swept wing penetrating a sharp-edged gust can be approximated with the following expression for ℓ_w^G:

$$\left.\begin{aligned} \ell_w^G &= \tfrac{1}{2}\rho U^2 \bar{c}\, a_w \frac{2}{1+\lambda_w}\left[1-(1-\lambda_w)\eta\right]\frac{w}{U}\,\psi\left(\tfrac{s}{2}\right), \quad \eta < \frac{s}{\beta} \\ &= 0 \qquad\qquad\qquad\qquad\qquad\qquad\qquad\qquad\quad , \quad \eta > \frac{s}{\beta} \end{aligned}\right\} s \le \beta$$

$$\ell_w^G = \tfrac{1}{2}\rho U^2 \bar{c}\, a_w \frac{2}{1+\lambda_w}\left[1-(1-\lambda_w)\eta\right]\frac{w}{U}\,\psi\left(s-\tfrac{\beta}{2}\right) \quad , \quad s \ge \beta \qquad \text{(A.14)}$$

where

$$\beta = AR \tan \Lambda_o \qquad \text{(A.15)}$$

and Λ_o is the sweep angle of the leading edge of the wing.

Approximate means for including three-dimensional effects in this build up of lift is discussed in Reference 8.

A.2.e Lift on Tail Due to Gust Penetration

By analogy with the lift on the wing, the horizontal-tail lift per unit span after penetrating a sharp edged gust is given by

$$\left.\begin{aligned} l_t^G &= \tfrac{1}{2}\rho U^2 \bar{c}_t a_t \frac{2}{1+\lambda_t}\left[1-(1-\lambda_t)\eta_t\right]\frac{w}{U}\,\psi\left(\frac{\gamma s}{2}\right), \quad \eta_t < \frac{\gamma s}{\beta_t} \\ &= 0 \qquad\qquad\qquad\qquad\qquad\qquad\qquad\qquad\quad , \quad \eta_t > \frac{\gamma s}{\beta_t} \end{aligned}\right\} \; s \le \frac{\beta_t}{\gamma}$$

$$l_t^G = \tfrac{1}{2}\rho U^2 \bar{c}_t a_t \frac{2}{1+\lambda_t}\left[1-(1-\lambda_t)\eta_t\right]\frac{w}{U}\,\psi\left(\gamma s - \frac{\beta_t}{2}\right) \quad , \quad s \ge \frac{\beta_t}{\gamma} \qquad \text{(A. 16)}$$

where

$$\beta_t = AR_t \tan \Lambda_{ot}$$

$$\gamma = \frac{\bar{c}}{\bar{c}_t}$$

A. 2. f Lift on Fuselage Due to Gust Penetration

From equation (A. 10), the lift on the fuselage per unit length due to a sharp-edged gust becomes

$$l_f^G = \frac{d}{dt}\left(\rho A U \frac{w}{U}\right) = \rho U^2 \frac{dA}{d\bar{x}}\frac{w}{U} \qquad \text{(A. 17)}$$

where

$$\frac{w}{U} = \text{const.} \quad , \qquad \bar{x} + \frac{\bar{c}}{2} l_{c.g.} \le \frac{\bar{c}}{2} s$$

$$= 0 \quad , \qquad \bar{x} + \frac{\bar{c}}{2} l_{c.g.} \ge \frac{\bar{c}}{2} s$$

$\frac{\bar{c}}{2} l_{c.g}$ is the distance from the nose of the fuselage to the center of gravity of the airplane

The lift due to penetration of gusts with other profiles can be obtained by employing Duhamel's integral.

A. 2. g Lift on Tail Due to Wing Downwash

The section tail lift due to wing downwash is usually written for a constant angle of attack of the wing as

$$\ell_{tw}^{\alpha} = -\tfrac{1}{2}\rho U^2 c_t a_t \left(\frac{d\varepsilon}{d\alpha}\right)\alpha_w \tag{A. 18}$$

where

$\frac{d\varepsilon}{d\alpha}$ is the rate of change of effective downwash angle at the tail with respect to wing angle of attack

The unsteady downwash at the tail due to a time variation of angle of attack of the wing will modify equation (A. 18) to the following form:

$$\ell_{tw}^{\alpha} = -\tfrac{1}{2}\rho U^2 \bar{c}_t a_t \left(\frac{d\varepsilon}{d\alpha}\right)\frac{2}{1+\lambda_t}\left[1-(1-\lambda_t)\eta_t\right]\sum_i \int_0^s \alpha'_{ti}(\sigma)\, \varphi_i^{\alpha}(\eta_t, s-\sigma)\, d\sigma \tag{A. 19}$$

and for the wing entering a sharp edge gust to

$$\ell_{tw}^{G} = -\tfrac{1}{2}\rho U^2 \bar{c}_t a_t \left(\frac{d\varepsilon}{d\alpha}\right)\frac{2}{1+\lambda_t}\left[1-(1-\lambda_t)\eta_t\right]\frac{w}{U}\,\varphi^{G}(\eta_t, s) \tag{A. 20}$$

where

$\varphi_i^{\alpha}(\eta_t, s)$ are normalized lift-growth functions for the tail after a step increase in angle of attack of the wing

$\varphi^{G}(\eta_t, s)$ is a normalized lift-growth function for the tail after entry of the wing into a sharp-edged gust

α'_{ti} are the wing tip angles of attack obtained when equation (A.7) is resolved into various span-wise distributions of angle of attack across the wing span

The wing angle-of-attack distributions are referred to the tip to normalize the φ -functions.

It is assumed here that the indicial lift-growth functions φ_i^{α} and φ^{G} are not functions of the spanwise coordinate η_t and that they can be approximated by the lift-growth functions derived in Reference 8 for the total lift on the tail. Thus,

$$\varphi_i^{\alpha} = \frac{1}{w_n(\infty)} \int_0^s \psi'_{\lambda t}(s-\sigma) \int_0^{\sigma} w_{ni}(\sigma')\, \psi'(\sigma-\sigma')\, d\sigma' d\sigma \qquad \text{(A.21)}$$

and

$$\varphi^{G} = \frac{1}{w_n(\infty)} \int_0^s \psi'_{\lambda t}(s-\sigma) \int_0^{\sigma} w_n(\sigma')\, \chi'(\sigma-\sigma')\, d\sigma' d\sigma \qquad \text{(A.22)}$$

where

$W_{ni}(s)$ are the variations in downwash at the 3/4-chord point of the horizontal-tail M. A. C. due to a step change in circulation of the wing

$\psi(s)$ is the Kussner function which describes the growth in circulation on the wing due to a step increase in angle of attack

$\chi(s)$ is the circulation-growth function for a wing which enters a sharp-edged gust

$\psi_{At}(s)$ is the lift-growth function for horizontal tail entry into a sharp-edged gust

A procedure for computing the time history of downwash at the tail is described in Reference 8.

Equations (A. 21) and (A. 22) assume that the downwash variation over the horizontal tail is constant. Although for a constant spanwise angle of attack of the wing the downwash is approximately constant over the horizontal tail, Figure A. 1 shows that the steady-state downwash angle for a linearly varying angle of attack of the wing results in negative downwash at the root and positive at the tip. This indicates that, for the various distributions of angle of attack in equation (A. 7), the variation in downwash along the tail span should be computed. Such computations, however, are extremely time consuming; and, in the present analysis, the downwash at the 3/4-M. A. C. of the horizontal tail is considered to be an effective overall downwash.

With this approximation and the assumption made in Reference 8 that the downwash field acts as a gust travelling over the horizontal tail, the indicial lift-growth functions, ψ_i^{α} , thus calculated, must be displaced by an amount Δx

in order for the downwash field to start at the apex of the horizontal tail, where

Δx is the streamwise distance from the apex of the horizontal tail to its 3/4-M. A. C. measured in wing mean geometric semichords

Figure A. 2 shows these lift-growth functions for the example swept-wing airplane. The various wing angle-of-attack distributions are the ones used in the example calculations of this report.

$$\alpha'_w = \alpha'_{t1} + \alpha'_{t2}\eta + \alpha'_{t3}\eta^2 + \alpha'_{t4}\frac{\eta}{i} + \alpha'_{t5}\eta\left(\frac{\eta}{i}\right) \tag{A.23}$$

where

α'_{t1} is the wing-tip angle of attack for a constant angle of attack across the span

α'_{t2} is the wing-tip angle of attack for a linear twist

α'_{t3} is the wing-tip angle of attack for parabolic twist

α'_{t4} is the wing-tip angle of attack for a linear twist to station i and constant from i to the tip

α'_{t5} is the wing-tip angle of attack for a parabolic twist to station i and linear from i to the tip

Also shown in Figure A. 2 is a comparison of $\mathcal{J}_1^{\varphi\alpha}$ as obtained in Reference 8 for downwash at the apex of the tail with $\mathcal{J}_1^{\alpha}$ for downwash at the M. A. C.

It can be seen from Figure A. 2 that the lift-growth functions for wing angle-of-attack distributions other than constant contribute very little to the total tail lift. For this reason, step functions were assumed. In addition to the expressions given in Reference 8 for a constant wing angle of attack, the following expressions

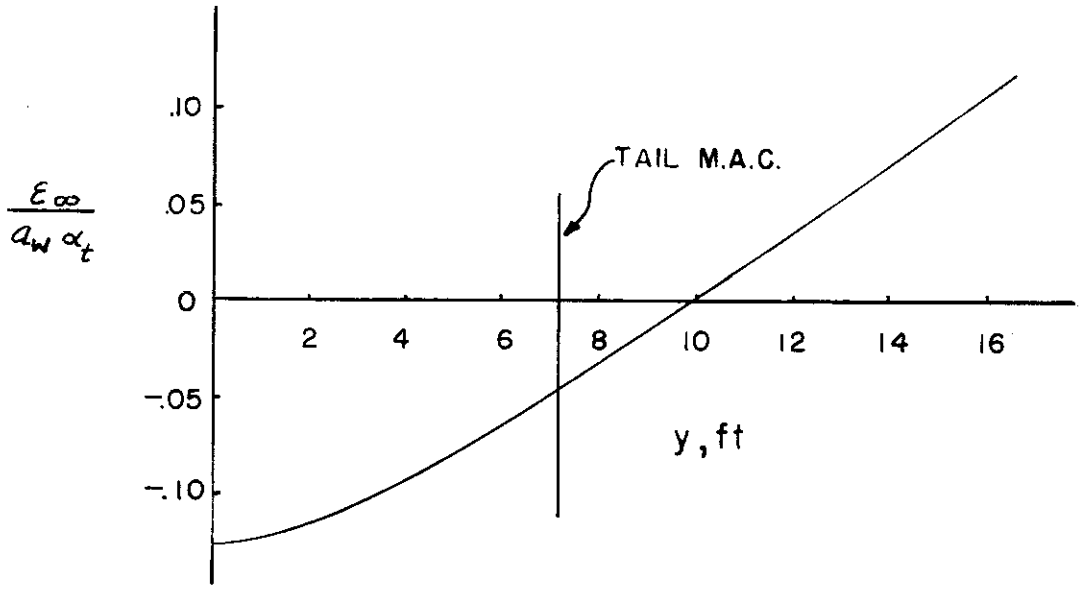

FIGURE A.I STEADY-STATE DOWNWASH ANGLE AT HORIZONTAL TAIL DUE TO A LINEAR SPANWISE VARIATION OF WING ANGLE OF ATTACK

are used:

$$\begin{aligned} \varphi_1^{\alpha} &= -.20 && s < s_n \\ \varphi_1^{\alpha} &= \varphi_1^{\alpha}(\infty) = 1.00 && s > s_n \end{aligned} \qquad \text{(A.24)}$$

$$\varphi_{2,3,4,5}^{\alpha} = 0 \qquad s < s_n \qquad \text{(A.25)}$$

$$\left.\begin{aligned} \varphi_2^{\alpha} &= -.20 \\ \varphi_3^{\alpha} &= -.15 \\ \varphi_4^{\alpha} &= -.25 \\ \varphi_5^{\alpha} &= -.19 \end{aligned}\right\} \quad s > s_n \qquad \text{(A.26)}$$

$$\begin{aligned} \varphi^{G} &= 0 && s < 1.5 \\ \varphi^{G} &= -.16 && 1.5 < s < s_n + 1.5 \\ \varphi^{G} &= 1.00 && s > s_n + 1.5 \end{aligned} \qquad \text{(A.27)}$$

where

$$s_n = \ell_{tw} + \frac{\beta_t}{2\gamma} + 1.6 \qquad \text{(A.28)}$$

A.3 Generalized Forces

In the following derivation, the generalized forces will be separated into two components, a contribution due to angle of attack (or motion) Q_i^{M} and

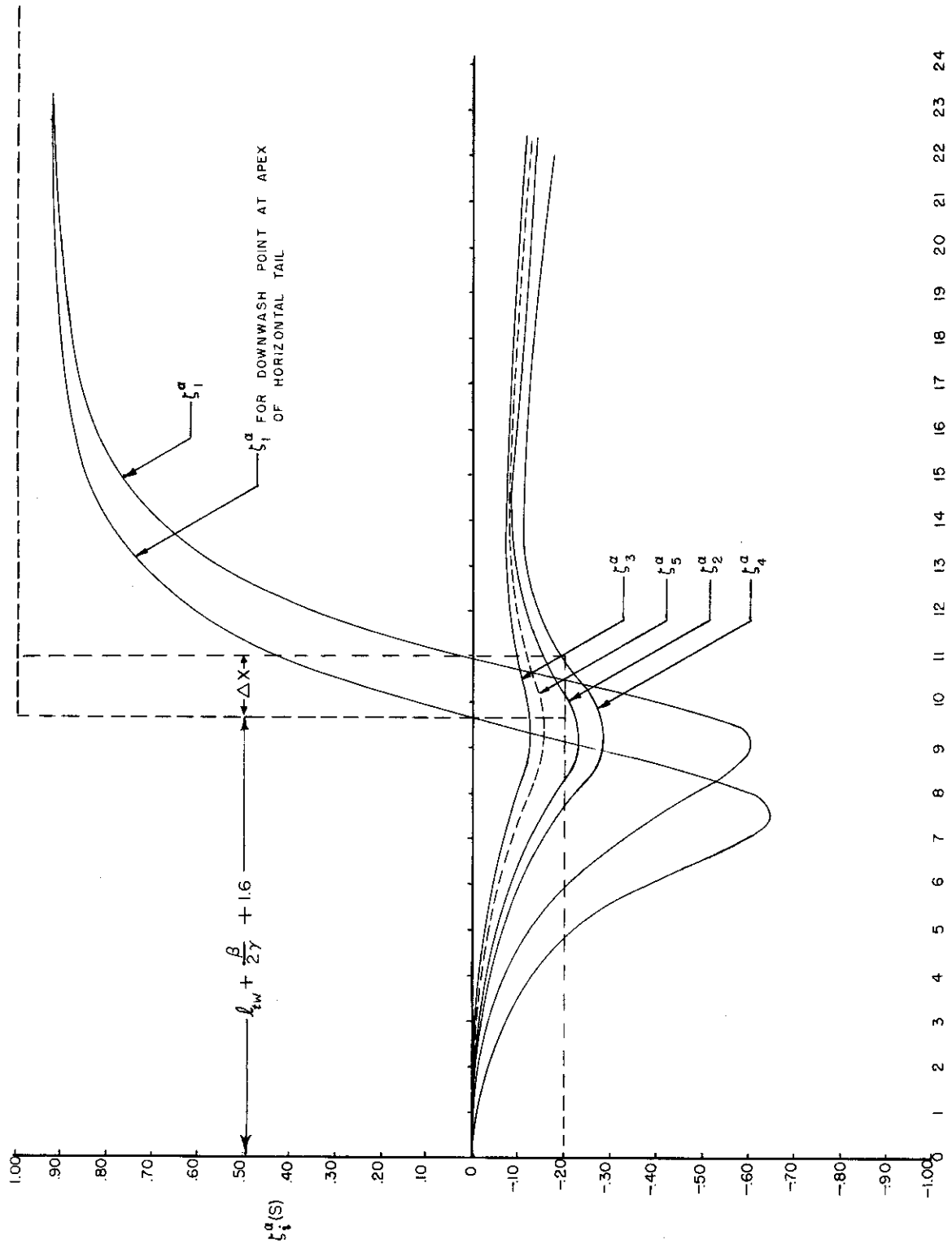

FIGURE A.2 NORMALIZED LIFT GROWTH ON TAIL DUE TO DOWNWASH FROM AN ABRUPT ANGLE OF ATTACK CHANGE OF THE WING

a contribution due to the gust Q_i^D . The local lifts due to motion and gust penetration derived in the preceding sections can now be integrated for the generalized forces given in Section I. Thus,

$$Q_i = Q_i^M + Q_i^D \tag{A.29}$$

where

$$Q_i^M = \int_{-\frac{\bar{c}}{2}\ell_{c.g}}^{\frac{\bar{c}}{2}\ell_f} \ell_f^\alpha A_i(\bar{x})\, d\bar{x} + b\int_0^1 \ell_w^\alpha B_i(\eta)\, d\eta + b_t\int_0^1 (\ell_t^\alpha + \ell_{tw}^\alpha) C_i(\eta)\, d\eta \tag{A.30}$$

and

$$Q_i^D = \int_{-\frac{\bar{c}}{2}\ell_{c.g}}^{\frac{\bar{c}}{2}\ell_f} \ell_f^G A_i(\bar{x})\, d\bar{x} + b\int_0^1 \ell_w^G B_i(\eta)\, d\eta + b_t\int_0^1 (\ell_t^G + \ell_{tw}^G) C_i(\eta)\, d\eta \tag{A.31}$$

The A_i , B_i , and C_i functions are

$$A_0 = 1 \qquad A_1 = -\bar{x} \qquad A_2 = \phi_2(\bar{x})$$

$$A_3 = A_4 = A_5 = A_6 = 0$$

$$B_0 = 1$$

$$B_1 = k_1(\eta)$$

$$B_2 = \left[\phi_2\left(\tfrac{\bar{c}}{2}\ell_w\right) + \left(\frac{d\phi_2}{d\bar{x}}\right)_{\frac{\bar{c}}{2}\ell_w} k_2(\eta)\right]$$

$$B_3 = \left\{\phi_3(\eta) - \frac{d\phi_3}{d\eta}\,\frac{\sin\Theta\cos\Theta}{b/2}\left[k_1(\eta) - k_w(\eta)\right]\right\}$$

$$B_4 = \left[k_1(\eta) - k_w(\eta)\right]\phi_4(\eta)\cos\Theta$$

$$B_5 = 0$$

$$B_6 = 0$$

$$C_0 = 1$$

$$C_1 = -k_3(\eta)$$

$$C_2 = \left[\phi_2\left(\tfrac{\bar{c}}{2}\ell_t\right) + \left(\frac{d\phi_2}{d\bar{x}}\right)_{\frac{\bar{c}}{2}\ell_t} k_4(\eta)\right]$$

$$C_3 = 0$$

$$C_4 = 0$$

$$C_5 = \left\{\phi_5(\eta) - \frac{d\phi_5}{d\eta}\,\frac{\sin\Theta_t\cos\Theta_t}{b_t/2}\left[k_5(\eta) - k_3(\eta)\right]\right\}$$

$$C_6 = \left[k_5(\eta) - k_3(\eta)\right]\phi_6(\eta)\cos\Theta_t$$

A. 3. a Heaving

When equations (A. 5), (A. 8), (A. 12) and (A. 19) are substituted into equation (A 30), the generalized force due to heaving motion becomes

$$Q_o^M = \tfrac{1}{2}\rho U^2 S a_w \int_0^s \varphi(s-\sigma)\Big\{ a_{01}\dot{q}_1 + a_{02}\dot{q}_2 + a_{03}\dot{q}_3 + a_{04}\dot{q}_4 + b_{00}\ddot{q}_0 + b_{01}\ddot{q}_1 + b_{02}\ddot{q}_2 + b_{03}\ddot{q}_3 + b_{04}\ddot{q}_4 \Big\} d\sigma$$

$$+ \tfrac{1}{2}\rho U^2 S_t a_t \int_0^s \varphi(\gamma s - \gamma\sigma)\Big\{ c_{01}\dot{q}_1 + c_{02}\dot{q}_2 + c_{05}\dot{q}_5 + c_{06}\dot{q}_6 + d_{00}\ddot{q}_0 + d_{01}\ddot{q}_1 + d_{02}\ddot{q}_2 + d_{05}\ddot{q}_5 + d_{06}\ddot{q}_6 \Big\} d\sigma$$

$$- \tfrac{1}{2}\rho U^2 S_t a_t \left(\frac{d\varepsilon}{d\alpha}\right) \sum_{i=1}^{n} \int_0^s \varphi_i^{\alpha}(s-\sigma)\, \alpha'_{ti}(\sigma)\, d\sigma \qquad \text{(A. 32)}$$

From equation (A. 12), it can be seen that

$$\int_{-\frac{\bar{c}}{2}\ell_{c.g}}^{\frac{\bar{c}}{2}\ell_f} \ell_f^{\alpha}\, d\bar{x} = \int_{-\frac{\bar{c}}{2}\ell_{c.g}}^{\frac{\bar{c}}{2}\ell_f} \frac{dz}{d\bar{x}}\, d\bar{x} = z \Big|_{-\frac{\bar{c}}{2}\ell_{c.g}}^{\frac{\bar{c}}{2}\ell_f} = 0 \qquad \text{(A. 33)}$$

where

$$Z = \rho U^2 A \left(q_1 - \frac{d\phi_2}{d\bar{x}} q_2 - \frac{2}{\bar{c}} \dot{q}_0 + \frac{2\bar{x}}{\bar{c}} \dot{q}_1 - \frac{2\phi_2(\bar{x})}{\bar{c}} \dot{q}_2 \right)$$

Thus, the lift on the fuselage due to angle of attack is zero since the area at the nose and the tail vanishes.

The coefficients a_{ij}, b_{ij}, c_{ij}, and d_{ij} for equation (A. 32) and for the subsequent motion forces and moments are

$$a_{i1} = \frac{2}{1+\lambda_w} \int_0^1 \left[1 - \delta_w \eta\right] B_i(\eta)\, d\eta$$

$$a_{i2} = \frac{2}{1+\lambda_w} \int_0^1 \left[1 - \delta_w \eta\right] B_i(\eta) \left(\frac{d\phi_2}{d\bar{x}}\right)_{\frac{\bar{c}}{2}\ell_w} d\eta$$

$$a_{i3} = -\frac{2}{1+\lambda_w} \int_0^1 \left[1 - \delta_w \eta\right] B_i(\eta) \frac{d\phi_3}{d\eta} \frac{\sin\Theta\cos\Theta}{b/2}\, d\eta$$

$$a_{i4} = \frac{2}{1+\lambda_w} \int_0^1 \left[1 - \delta_w \eta\right] B_i(\eta)\, \phi_4(\eta) \cos\Theta\, d\eta$$

$$b_{i0} = -\frac{2}{\bar{c}} \cdot \frac{2}{1+\lambda_w} \int_0^1 \left[1 - \delta_w \eta\right] B_i(\eta)\, d\eta$$

$$b_{i1} = -\frac{2}{1+\lambda_w}\int_0^1 [1-\delta_w\eta]\, B_i(\eta)\, k_6(\eta)\, d\eta$$

$$b_{i2} = -\frac{2}{\bar{c}}\cdot\frac{2}{1+\lambda_w}\int_0^1 [1-\delta_w\eta]\left[\phi_2\left(\tfrac{\bar{c}}{2}\ell_w\right) + \left(\frac{d\phi_2}{d\bar{x}}\right)_{\frac{\bar{c}}{2}\ell_w} k_7(\eta)\right] B_i(\eta)\, d\eta$$

$$b_{i3} = -\frac{2}{\bar{c}}\cdot\frac{2}{1+\lambda_w}\int_0^1 [1-\delta_w\eta]\left\{\phi_3(\eta) + [k_w(\eta)-k_6(\eta)]\frac{d\phi_3}{d\eta}\frac{\sin\Theta\cos\Theta}{b/2}\right\} B_i(\eta)\, d\eta$$

$$b_{i4} = \frac{2}{\bar{c}}\cdot\frac{2}{1+\lambda_w}\int_0^1 [1-\delta_w\eta][k_w(\eta)-k_6(\eta)]\, B_i(\eta)\, \phi_4(\eta)\cos\Theta\, d\eta$$

$$C_{i1} = \frac{2}{1+\lambda_t}\int_0^1 [1-\delta_t\eta]\, C_i(\eta)\, d\eta$$

$$C_{i2} = -\frac{2}{1+\lambda_t}\int_0^1 [1-\delta_t\eta]\left(\frac{d\phi_2}{d\bar{x}}\right)_{\frac{\bar{c}}{2}\ell_t} C_i(\eta)\, d\eta$$

$$C_{i5} = -\frac{2}{1+\lambda_t}\int_0^1 [1-\delta_t\eta]\, C_i(\eta)\, \frac{d\phi_5}{d\eta}\frac{\sin\Theta_t\cos\Theta_t}{b_t/2}\, d\eta$$

$$C_{i6} = \frac{2}{1+\lambda_t}\int_0^1 [1-\delta_t\eta]\, C_i(\eta)\, \phi_6(\eta)\cos\Theta_t\, d\eta$$

$$a_{i0} = \frac{2}{1+\lambda_t}\int_0^1 [1-\delta_t \eta]\, C_i(\eta)\, d\eta$$

$$a_{i1} = \frac{2}{1+\lambda_t}\int_0^1 [1-\delta_t \eta]\, C_i(\eta)\, k_8(\eta)\, d\eta$$

$$a_{i2} = -\frac{2}{\bar{c}}\cdot\frac{2}{1+\lambda_t}\int_0^1 [1-\delta_t \eta]\left[\phi_2\left(\tfrac{\bar{c}}{2}\ell_t\right) + \left(\frac{d\phi_2}{d\bar{x}}\right)_{\frac{\bar{c}}{2}\ell_t} k_9(\eta)\right] C_i(\eta)\, d\eta$$

$$a_{i5} = -\frac{2}{\bar{c}}\cdot\frac{2}{1+\lambda_t}\int_0^1 [1-\delta_t \eta]\left\{\phi_5(\eta) + \left[k_8(\eta) - k_5(\eta)\right]\frac{d\phi_5}{d\eta}\,\frac{\sin\Theta_t\cos\Theta_t}{b_t/2}\right\} C_i(\eta)\, d\eta$$

$$a_{i6} = \frac{2}{\bar{c}}\cdot\frac{2}{1+\lambda_t}\int_0^1 [1-\delta_t \eta]\left[k_8(\eta) - k_5(\eta)\right] C_i(\eta)\, \phi_6(\eta)\cos\Theta_t\, d\eta$$

for $i = 0, 1, 2, 3, 4, 5, 6.$

After substitution of equations (A. 14), (A. 16), (A. 17) and (A. 20) into (A. 31), the forcing function for the heaving motion becomes

$$Q_o^D = \tfrac{1}{2}\rho U^2 S a_w \frac{w}{U}\left\{\frac{2A_{max}}{S a_w}\psi_f^{LO}(s) + \psi_\lambda^{LO}(s) + \frac{S_t a_t}{S a_w}\psi_{\lambda t}^{LO}(s) - \frac{S_t a_t}{S a_w}\left(\frac{d\varepsilon}{d\alpha}\right)\psi^G(s)\right\} \qquad \text{(A. 34)}$$

where the term in braces corresponds to f_s^o in equation (1. 18).

$$\psi_f^{(0)}(s) = \frac{A(s)}{A_{max}} \qquad s < \frac{\bar{c}}{2} l_f$$

$$\psi_f^{(0)}(s) = 0 \qquad s > \frac{\bar{c}}{2} l_f$$

$A(s)$ = cross sectional area of equivalent body of revolution at the gust front

A_{max} = maximum cross sectional area

$$\psi_\lambda^{(i)} = \frac{2}{1+\lambda_w} \int_0^{s/\beta} [1 - \delta_w \eta] B_i(\eta) \psi\left(\frac{s}{2}\right) d\eta \qquad s \le \beta$$

$$\psi_\lambda^{(i)} = a_{i1} \psi\left(s - \frac{\beta}{2}\right) \qquad s \ge \beta \qquad \text{(A. 34a)}$$

$$\psi_{\lambda t}^{(i)} = \frac{2}{1+\lambda_t} \int_0^{\frac{\gamma s}{\beta_t}} [1 - \delta_t \eta] C_i(\eta) \psi\left(\frac{\gamma s}{2}\right) d\eta \qquad s \le \frac{\beta_t}{\gamma}$$

$$\psi_{\lambda t}^{(i)} = c_{i1} \psi\left(\gamma s - \frac{\beta_t}{2}\right) \qquad s \ge \frac{\beta_t}{\gamma} \qquad \text{(A. 34b)}$$

$\mathcal{J}^{(c)}(s)$ is given by equation (A. 27).

A. 3. b Pitching

The generalized force associated with the pitching motion is given by equations (A. 30) and (A. 31) for $i = 1$. The fuselage moment due to motion forces is

$$-\int_{-\frac{\bar{c}}{2} l_{c.g}}^{\frac{\bar{c}}{2} l_f} l_f^{\alpha} \bar{x}\, d\bar{x} = -\int_{-\frac{\bar{c}}{2} l_{c.g}}^{\frac{\bar{c}}{2} l_f} \frac{dz}{d\bar{x}} \bar{x}\, d\bar{x} = -z\bar{x}\Big|_{-\frac{\bar{c}}{2} l_{c.g}}^{\frac{\bar{c}}{2} l_f} + \int_{-\frac{\bar{c}}{2} l_{c.g}}^{\frac{\bar{c}}{2} l_f} z\, d\bar{x}$$

but since $-z\bar{x}\Big|_{-\frac{\bar{c}}{2} l_{c.g}}^{\frac{\bar{c}}{2} l_f} = 0$ from equation (A. 33), there results for the fuselage moment

$$-\int_{-\frac{\bar{c}}{2}\ell_{c.g}}^{\frac{\bar{c}}{2}\ell_f} \ell_f^{\alpha}\,\bar{x}\,d\bar{x} = \rho U^2\left\{-q_2\int_{-\frac{\bar{c}}{2}\ell_{c.g}}^{\frac{\bar{c}}{2}\ell_f}\frac{d\phi_2}{d\bar{x}}A\,d\bar{x} - \frac{2}{\bar{c}}\dot{q}_2\int_{-\frac{\bar{c}}{2}\ell_{c.g}}^{\frac{\bar{c}}{2}\ell_f}\phi_2(\bar{x})A\,d\bar{x}\right.$$

$$\left. + \frac{2}{\bar{c}}\dot{q}_1\int_{-\frac{\bar{c}}{2}\ell_{c.g}}^{\frac{\bar{c}}{2}\ell_f}A\bar{x}\,d\bar{x} + q_1\int_{-\frac{\bar{c}}{2}\ell_{c.g}}^{\frac{\bar{c}}{2}\ell_f}A\,d\bar{x} - \frac{2}{\bar{c}}\dot{q}_0\int_{-\frac{\bar{c}}{2}\ell_{c.g}}^{\frac{\bar{c}}{2}\ell_f}A\,d\bar{x}\right\} \qquad \text{(A. 35)}$$

Upon placing $\bar{x} = x - \frac{\bar{c}}{2}\ell_{c.g}$ and $d\bar{x} = dx$, the pitching moment on the fuselage due to motion forces becomes

$$-\int_{-\frac{\bar{c}}{2}\ell_{c.g}}^{\frac{\bar{c}}{2}\ell_f} \ell_f^{\alpha}\,\bar{x}\,d\bar{x} = \tfrac{1}{2}\rho U^2 S\,\frac{\bar{c}}{2}\left(2\frac{dC_{mf}}{d\alpha}\right)\left\{q_1 + a_0\dot{q}_0 + b_1\dot{q}_1 + a_2 q_2 + b_2\dot{q}_2\right\} \qquad \text{(A. 36)}$$

where

$V_f = \int_0^{\frac{\bar{c}}{2}\ell_f} A\,dx$ = total volume of the equivalent body of revolution

$a_0 = -\frac{2}{\bar{c}}$ $\qquad \frac{dC_{mf}}{d\alpha} = \frac{2V_f}{\bar{c}S}$

$b_1 = (\bar{\ell}_f - \ell_{c.g})$ $\qquad a_2 = -\dfrac{\int_0^{\frac{\bar{c}}{2}\ell_f}\frac{d\phi_2}{dx}A\,dx}{V_f}$

$\bar{\ell}_f = \dfrac{\int_0^{\frac{\bar{c}}{2}\ell_f} A\,x\,dx}{\frac{\bar{c}}{2}V_f}$ = distance from the nose of fuselage to the centroid of the volume of the equivalent body of revolution measured in wing mean geometric semichords

$$b_2 = - \frac{\int_0^{\frac{\bar{c}}{2} l_f} \phi_2(x)\, A\, dx}{\frac{\bar{c}}{2} V_f}$$

Equation (A. 30) can now be written for Q_1^M as

$$Q_1^M = \tfrac{1}{2}\rho U^2 S \tfrac{\bar{c}}{2}\left(2\tfrac{dC_{mf}}{d\alpha}\right)\left\{ q_1 + a_2 q_2 + a_0 \dot{q}_0 + b_1 \dot{q}_1 + b_2 \dot{q}_2 \right\}$$

$$+ \tfrac{1}{2}\rho U^2 S a_w \tfrac{\bar{c}}{2} \int_0^s \varphi(s-\sigma)\left\{ a_{11}\dot{q}_1 + a_{12}\dot{q}_2 + a_{13}\dot{q}_3 + a_{14}\dot{q}_4 + b_{10}\ddot{q}_0 \right.$$

$$\left. + b_{11}\ddot{q}_1 + b_{12}\ddot{q}_2 + b_{13}\ddot{q}_3 + b_{14}\ddot{q}_4 \right\} d\sigma$$

$$+ \tfrac{1}{2}\rho U^2 S_t a_t \tfrac{\bar{c}}{2} \int_0^s \varphi(\gamma s - \gamma\sigma)\left\{ c_{11}\dot{q}_1 + c_{12}\dot{q}_2 + c_{15}\dot{q}_5 + c_{16}\dot{q}_6 + d_{10}\ddot{q}_0 \right.$$

$$\left. + d_{11}\ddot{q}_1 + d_{12}\ddot{q}_2 + d_{15}\ddot{q}_5 + d_{16}\ddot{q}_6 \right\} d\sigma \qquad \text{(A. 37)}$$

$$+ \tfrac{1}{2}\rho U^2 S_t a_t \tfrac{\bar{c}}{2}\left(\tfrac{d\varepsilon}{d\alpha}\right) c_{11} \sum_{i=1}^{n} \int_0^s \varphi_i^{\alpha}(s-\sigma)\, \alpha_{ti}'(\sigma)\, d\sigma$$

It should be noticed in the above moment equation that a term $\frac{\bar{c}}{2}$ has been taken outside the braces for the purpose of nondimensionalizing the equations of motion in Section I. With this term outside the braces, the coefficients a_{ij}, b_{ij}, c_{ij}, and d_{ij} in Section A. 3. a should be divided by $\frac{\bar{c}}{2}$ for $i = 1, 4, 6$. This has the effect of dividing B_1, B_4, C_1, C_6, which have

the dimensions of length, by $\frac{\bar{c}}{2}$.

The pitching moment due to gust entry of the fuselage is from equation (A. 17) and (A. 31)

$$-\int_{-\frac{\bar{c}}{2}\ell_{c.g}}^{\frac{\bar{c}}{2}\ell_f} \ell_f^G \bar{x}\, d\bar{x} = -\rho U^2 \frac{w}{U} \int_0^{\frac{\bar{c}}{2}s} \frac{dA}{dx}\left[x - \tfrac{\bar{c}}{2}\ell_{c.g}\right] dx$$

$$= -\rho U^2 \frac{w}{U}\left[A(x)\left[x - \tfrac{\bar{c}}{2}\ell_{c.g}\right] - \int_0^x A(x)\,dx \right]_0^{\frac{\bar{c}}{2}s}$$

$$= -\rho U^2 \frac{w}{U}\left[V_f(s) - \tfrac{\bar{c}}{2}(s - \ell_{c.g})A(s)\right] \qquad \text{(A. 38)}$$

The total pitching moment due to gust entry then becomes

$$Q_1^D = \tfrac{1}{2}\rho U^2 S a_w \frac{\bar{c}}{2}\frac{w}{U}\left\{ \frac{2}{a_w}\frac{dC_{mf}}{d\alpha}\psi_f^{L'}(s) + \psi_A^{L'}(s) - \frac{S_t a_t}{S a_w}\psi_{At}^{L'}(s) + \frac{S_t a_t}{S a_w}\left(\frac{d\epsilon}{d\alpha}\right) C_{11}\, \varphi^G(s) \right\} \qquad \text{(A. 39)}$$

where

$$\psi_f^{L'}(s) = \frac{V_f(s)}{V_f} - \frac{\bar{c}}{2}(s - \ell_{c.g})\frac{A(s)}{A_{max}}\cdot\frac{A_{max}}{V_f}$$

and the term in braces corresponds to f'_s in equation (1. 19).

A. 3. c Fuselage Bending

The generalized force for fuselage bending is obtained from the first term of equation (A. 30) and is

$$\int_{-\frac{\bar{c}}{2}\ell_f}^{\frac{\bar{c}}{2}\ell_f} \ell_f^{\alpha}\,\phi_2(\bar{x})\,d\bar{x} = \int_{-\frac{\bar{c}}{2}\ell_{c.g}}^{\frac{\bar{c}}{2}\ell_f} \frac{dz}{d\bar{x}}\,\phi_2(\bar{x})\,d\bar{x} = Z\,\phi_2(\bar{x})\Big|_{-\frac{\bar{c}}{2}\ell_{c.g}}^{\frac{\bar{c}}{2}\ell_f} - \int_{-\frac{\bar{c}}{2}\ell_{c.g}}^{\frac{\bar{c}}{2}\ell_f} Z\,\frac{d\phi_2}{d\bar{x}}\,d\bar{x} \tag{A. 40}$$

which, after introducing Z from equation (A. 33), becomes

$$\int_{-\frac{\bar{c}}{2}\ell_{c.g}}^{\frac{\bar{c}}{2}\ell_f} \ell_f^{\alpha}\,\phi_2(\bar{x})\,d\bar{x} = -\frac{1}{2}\rho U^2 S\,a_w\left(\frac{1}{a_w}\,\frac{dC_{mf}}{d\alpha}\right)\left\{c_1 q_1 + c_2 q_2 + d_0\dot{q}_0 + d_1\dot{q}_1 + d_2\dot{q}_2\right\} \tag{A. 40 cont'd}$$

where

$$c_1 = \frac{\bar{c}}{V_f}\int_0^{\frac{\bar{c}}{2}\ell_f} A(x)\,\frac{d\phi_2}{dx}\,dx$$

$$c_2 = -\frac{\bar{c}}{V_f}\int_0^{\frac{\bar{c}}{2}\ell_f} A(x)\left(\frac{d\phi_2}{dx}\right)^2 dx$$

$$d_0 = -\frac{2}{\bar{c}}\,c_1$$

$$d_1 = \frac{2}{V_f}\int_0^{\frac{\bar{c}}{2}\ell_f} A(x)\,\frac{d\phi_2}{dx}\left[x - \frac{\bar{c}}{2}\ell_{c.g}\right] dx$$

$$d_2 = -\frac{2}{V_f}\int_0^{\frac{\bar{c}}{2}\ell_f} A(x)\,\phi_2(x)\left(\frac{d\phi_2}{dx}\right) dx$$

With equation (A. 40), the generalized force due to motion for fuselage bending can now be written

$$Q_2^M = -\frac{1}{2}\rho U^2 S a_w \left(\frac{1}{a_w}\frac{dC_{mf}}{d\alpha}\right)\left\{c_1 q_1 + c_2 q_2 + d_0 \dot{q}_0 + d_1 \dot{q}_1 + d_2 \dot{q}_2\right\}$$

$$+ \frac{1}{2}\rho U^2 S a_w \int_0^s \varphi(s-\sigma)\left\{a_{21}\dot{q}_1 + a_{22}\dot{q}_2 + a_{23}\dot{q}_3 + a_{24}\dot{q}_4 + b_{20}\ddot{q}_0\right.$$

$$\left. + b_{21}\ddot{q}_1 + b_{22}\ddot{q}_2 + b_{23}\ddot{q}_3 + b_{24}\ddot{q}_4\right\} d\sigma$$

$$+ \frac{1}{2}\rho U^2 S_t a_t \int_0^s \varphi(\gamma s - \gamma\sigma)\left\{c_{21}\dot{q}_1 + c_{22}\dot{q}_2 + c_{25}\dot{q}_5 + c_{26}\dot{q}_6 + d_{20}\ddot{q}_0\right.$$

$$\left. + d_{21}\ddot{q}_1 + d_{22}\ddot{q}_2 + d_{25}\ddot{q}_5 + d_{26}\ddot{q}_6\right\} d\sigma$$

$$- \frac{1}{2}\rho U^2 S_t a_t \left(\frac{d\varepsilon}{d\alpha}\right) c_{21} \sum_{i=1}^{n} \int_0^s \varphi_i^{\alpha}(s-\sigma)\,\alpha_{ti}'(\sigma)\, d\sigma \qquad \text{(A. 41)}$$

and the generalized force due to gust entry from equation (A. 31) as

$$Q_2^D = \frac{1}{2}\rho U^2 S a_w \frac{w}{U}\left\{\frac{2A_{max}}{S a_w}\psi_f^{i2}(s) + \psi_A^{i2}(s) + \frac{S_t a_t}{S a_w}\psi_{At}^{i2}(s)\right.$$

$$\left. - \frac{S_t a_t}{S a_w}\left(\frac{d\varepsilon}{d\alpha}\right) c_{21}\,\varphi^G(s)\right\} \qquad \text{(A. 42)}$$

where

$$\psi_f^{\prime 2}(s) = \left[\phi_2(s)\, A(s) - \int_0^{\frac{\xi}{2}s} \frac{d\phi_2}{dx}\, A(x)\, dx \right] \frac{1}{A_{max}}$$

The functions $\psi_\lambda^{\prime 2}(s)$ and $\psi_{\lambda t}^{\prime 2}(s)$ are given by equations (A. 34a) and (A. 34b). The term in braces in equation (A. 42) corresponds to f_s^2 of equation (1. 20).

A. 3. d Wing Bending

Since the fuselage forces and moments are non-existent for $i = 3, 4, 5,$ and 6, equation (A. 30) and (A. 31) can now be written directly for the generalized force for wing bending; thus

$$Q_3^M = \tfrac{1}{2}\rho U^2 S a_w \int_0^s \varphi(s-\sigma) \Big\{ a_{31}\dot{q}_1 + a_{32}\dot{q}_2 + a_{33}\dot{q}_3 + a_{34}\dot{q}_4 + b_{30}\ddot{q}_0 + b_{31}\ddot{q}_1 + b_{32}\ddot{q}_2 + b_{33}\ddot{q}_3 + b_{34}\ddot{q}_4 \Big\}\, d\sigma \qquad \text{(A. 43)}$$

and

$$Q_3^D = \tfrac{1}{2}\rho U^2 S a_w \frac{w}{U} \psi_\lambda^{\prime 3}(s) \qquad \text{(A. 44)}$$

where $\psi_\lambda^{\prime 3}(s)$ is obtained from equation (A. 34a) and is equal to f_s^3 of equation (1. 21).

A. 3. e Wing Torsion

As for the pitching moment, the function B_4 must be divided by $\frac{\bar{c}}{2}$ to get the proper a_{4j} and b_{4j} coefficients. Equations (A. 30) and (A. 31) become for the generalized force due to wing torsion

$$Q_4^M = \tfrac{1}{2}\rho U^2 S a_w \tfrac{\bar{c}}{2} \int_0^S \varphi(s-\sigma)\Big\{a_{41}\dot{q}_1 + a_{42}\dot{q}_2 + a_{43}\dot{q}_3 + a_{44}\dot{q}_4 + b_{40}\ddot{q}_0 + b_{41}\ddot{q}_1 + b_{42}\ddot{q}_2 + b_{43}\ddot{q}_3 + b_{44}\ddot{q}_4\Big\}\, d\sigma \qquad \text{(A. 45)}$$

and

$$Q_4^D = \tfrac{1}{2}\rho U^2 S a_w \tfrac{\bar{c}}{2} \tfrac{w}{U} \psi_\lambda^{44}(s) \qquad \text{(A. 46)}$$

where $\psi_\lambda^{44}(s) = f_s^4$ in equation (1. 22) and is given by equation (A. 34a).

A. 3. f Horizontal Tail Bending

By analogy to the wing bending equations, the generalized force associated with horizontal tail bending becomes

$$Q_5^M = \tfrac{1}{2}\rho U^2 S_t a_t \int_0^S \varphi(\gamma s - \gamma\sigma)\Big\{c_{51}\dot{q}_1 + c_{52}\dot{q}_2 + c_{55}\dot{q}_5 + c_{56}\dot{q}_6 + d_{50}\ddot{q}_0 + d_{51}\ddot{q}_1 + d_{52}\ddot{q}_2 + d_{55}\ddot{q}_5 + d_{56}\ddot{q}_6\Big\}\, d\sigma$$
$$- \tfrac{1}{2}\rho U^2 S_t a_t \left(\tfrac{d\varepsilon}{d\alpha}\right) c_{51} \sum_{i=1}^{n} \int_0^S \varphi_i^\alpha(s-\sigma)\alpha_{ti}'(\sigma)\, d\sigma \qquad \text{(A. 47)}$$

and

$$Q_5^D = \tfrac{1}{2}\rho U^2 S a_w \frac{w}{U}\left\{\frac{S_t a_t}{S a_w}\psi_{\lambda t}^{L5}(s) - \frac{S_t a_t}{S a_w}\left(\frac{d\varepsilon}{d\alpha}\right)c_{51}\mathcal{J}^G(s)\right\} \tag{A.48}$$

where the term in braces corresponds to f_s^5 in equation (1.23) and is given by equation (A.34b).

A.3.g Horizontal Tail Torsion

When the coefficient C_6 is divided by $\frac{\bar{c}}{2}$, the generalized force for horizontal tail torsion is

$$Q_6^M = \tfrac{1}{2}\rho U^2 S_t a_t \tfrac{\bar{c}}{2}\int_0^s \varphi(\gamma s-\gamma\sigma)\Big\{c_{61}\dot{q}_1 + c_{62}\dot{q}_2 + c_{65}\dot{q}_5 + c_{66}\dot{q}_6 + d_{60}\ddot{q}_0$$

$$+ d_{61}\ddot{q}_1 + d_{62}\ddot{q}_2 + d_{65}\ddot{q}_5 + d_{66}\ddot{q}_6\Big\}d\sigma$$

$$- \tfrac{1}{2}\rho U^2 S_t a_t \tfrac{\bar{c}}{2}\left(\frac{d\varepsilon}{d\alpha}\right)c_{61}\sum_{i=1}^{n}\int_0^s \mathcal{J}_i^{\alpha}(s-\sigma)\,\alpha'_{ti}(\sigma)\,d\sigma \tag{A.49}$$

and

$$Q_6^D = \tfrac{1}{2}\rho U^2 S a_w \tfrac{\bar{c}}{2}\frac{w}{U}\left\{\frac{S_t a_t}{S a_w}\psi_{\lambda t}^{L6}(s) - \frac{S_t a_t}{S a_w}\left(\frac{d\varepsilon}{d\alpha}\right)c_{61}\mathcal{J}^G(s)\right\} \tag{A.50}$$

where $\psi_{\alpha t}^{66}(s)$ is given by equation (A. 34b), and the term in braces of equation (A. 50) corresponds to f_s^6 of equation (1. 24).

A. 3. h Additional Bending Mode

If an additional bending mode is introduced, having a mode shape ϕ_7, coupling terms will be added into the original generalized forces, and there will be an additional generalized force Q_7 .

The coefficients to be introduced into the various generalized forces due to motion are

$$a_{i7} = -\frac{2}{1+\lambda_w}\int_0^1 [1-\delta_w\eta]\, B_i(\eta)\, \frac{d\phi_7}{d\eta}\, \frac{\sin\Phi\cos\Phi}{b/2}\, d\eta$$

$$b_{i7} = -\frac{2}{1+\lambda_w}\cdot\frac{2}{\bar{c}}\int_0^1 [1-\delta_w\eta]\left\{\phi_7(\eta) + [k_w(\eta)-k_6(\eta)]\frac{d\phi_7}{d\eta}\,\frac{\sin\Phi\cos\Phi}{b/2}\right\} B_i(\eta)\, d\eta$$

The functions $A_7 = C_7 = 0$ in equations (A. 30) and (A. 31), and

$$B_7 = \left\{\phi_7(\eta) - \frac{d\phi_7}{d\eta}\,\frac{\sin\Phi\cos\Phi}{b/2}\,[k_1(\eta)-k_w(\eta)]\right\}$$

The generalized motion force due to the second bending mode are

$$Q_7^M = \tfrac{1}{2}\rho U^2 S a_w \int_0^s \varphi(s-\sigma)\left\{a_{71}\dot{q}_1 + a_{72}\dot{q}_2 + a_{73}\dot{q}_3 + a_{74}\dot{q}_4 + a_{77}\dot{q}_7\right.$$

$$\left. + b_{70}\ddot{q}_0 + b_{71}\ddot{q}_1 + b_{72}\ddot{q}_2 + b_{73}\ddot{q}_3 + b_{74}\ddot{q}_4 + b_{77}\ddot{q}_7\right\} d\sigma \qquad \text{(A. 51)}$$

and

$$Q_7^D = \tfrac{1}{2}\rho U^2 S a_w \frac{w}{U} \psi_\lambda^{47}(s) \qquad \text{(A. 52)}$$

where $\psi_\lambda^{47}(s) = f_s^7$ is given by equation (A. 34a) and is the forcing function for the additional equation of motion with this new mode.

A. 3. i Forces and Moments Due to Wing Downwash

The forces and moments due to downwash from the wing on the horizontal tail given in equations (A. 32), (A. 37), (A. 47) and (A. 49) will now be expanded for the particular case at hand for the purpose of illustration. The common term in all these equations has the following form:

$$\sum_{i=1}^{n} \int_0^s \varphi_i^\alpha (s-\sigma)\, \alpha'_{ti}(\sigma)\, d\sigma \qquad \text{(A. 53)}$$

which will be simplified by approximating the φ_i^α -functions by step functions as given in equations (A. 24) to (A. 28). By interchanging the variables in the convolution integral, equation (A. 54) can be written as

$$\sum_{i=1}^{n} \int_0^s \varphi_i^\alpha (s-\sigma)\, \alpha'_{ti}(\sigma)\, d\sigma = -\sum_{i=1}^{n} \int_0^s \varphi_i^\alpha (\sigma)\, \alpha'_{ti}(s-\sigma)\, d\sigma \qquad \text{(A. 54)}$$

The purpose of interchanging variables becomes apparent when equation (A. 53) is integrated with the functions φ_i^α as given by equations (A. 24) to (A. 28). The resulting expressions would contain $\alpha_{ti}(s_n)$ terms which are unknown, and the numerical procedure of Section II could not be applied since the responses depend on

their previous time histories. On the other hand, with equation (A. 54), the resulting terms have the form $\alpha_{ti}(s - s_n)$ which can be expanded in a Taylor's series as shown in Section II.

Substituting equations (A. 24) through (A. 28) into (A. 54), there results

$$-\sum_{i=1}^{n}\int_0^s \varphi_i^{\alpha}(\sigma)\,\alpha_{ti}'(s-\sigma)\,d\sigma = -\sum_{i=1}^{n}\varphi_i^{\alpha}\alpha_{ti}(s-\sigma)\Big|_0^{s_n} - \sum_{i=1}^{n}\varphi_i^{\alpha}\alpha_{ti}(s-\sigma)\Big|_{s_n}^{s} \tag{A. 55}$$

or

$$-\sum_{i=1}^{n}\int_0^s \varphi_i^{\alpha}(\sigma)\,\alpha_{ti}'(s-\sigma)\,d\sigma = -\Big\{\bar{b}\,\alpha_{t1}(s-s_n) - \bar{b}\,\alpha_{t1}(s) + (\bar{h}+\bar{b})\alpha_{t1}(s)$$

$$-(\bar{h}+\bar{b})\alpha_{t1}(s-s_n) + \bar{d}\,\alpha_{t2}(0) - \bar{d}\,\alpha_{t2}(s-s_n) + \bar{e}\,\alpha_{t3}(0) - \bar{e}\,\alpha_{t3}(s-s_n)$$

$$+\bar{f}\,\alpha_{t4}(0) - \bar{f}\,\alpha_{t4}(s-s_n) + \bar{g}\,\alpha_{t5}(0) - \bar{g}\,\alpha_{t5}(s-s_n)\Big\} \tag{A. 56}$$

where

$$\bar{b} = \varphi_1^{\alpha} \qquad s < s_n$$

$$\bar{h}+\bar{b} = \varphi_1^{\alpha}(\infty) \qquad s > s_n$$

$$\bar{d} = \varphi_2^{\alpha}(\infty) \qquad s > s_n$$

$$\bar{e} = \varphi_3^{\alpha}(\infty) \qquad s > s_n$$

$$\bar{f} = \varphi_4^{\alpha}(\infty) \qquad s > s_n$$

$$\bar{g} = \varphi_5^{\alpha}(\infty) \qquad s > s_n$$

Since initially, the angles $\alpha_{ti}(0) = 0$, equation (A. 56) becomes

$$-\sum_{i=1}^{n}\int_{0}^{s} g_i^{\alpha}(\sigma)\,\alpha'_{ti}(s-\sigma)\,d\sigma = \bar{b}\,\alpha_{t1}(s) + \bar{h}\,\alpha_{t1}(s-s_n) + \bar{d}\,\alpha_{t2}(s-s_n)$$

$$+ \bar{e}\,\alpha_{t3}(s-s_n) + \bar{f}\,\alpha_{t4}(s-s_n) + \bar{g}\,\alpha_{t5}(s-s_n) \qquad \text{(A. 57)}$$

For the assumed mode shapes used in the example calculations of Section IV the angles $\alpha_{ti}(s)$ are

$$\alpha_{t1}(s-s_n) = \left\{ q_1 + g_2 q_2 + b_0 \dot{q}_0 + f_1 \dot{q}_1 + f_2 \dot{q}_2 \right\}_{s-s_n} \qquad \text{(A. 58)}$$

$$\alpha_{t2}(s-s_n) = \left\{ e_3 q_3 + e_1 \dot{q}_1 + e_2 \dot{q}_2 + f_3 \dot{q}_3 \right\}_{s-s_n} \qquad \text{(A. 59)}$$

$$\alpha_{t3}(s-s_n) = \left\{ c_3 \dot{q}_3 \right\}_{s-s_n} \qquad \text{(A. 60)}$$

$$\alpha_{t4}(s-s_n) = \left\{ e_4 q_4 + f_4 \dot{q}_4 \right\}_{s-s_n} \qquad \text{(A. 61)}$$

$$\alpha_{t5}(s-s_n) = \left\{ d_4 \dot{q}_4 \right\}_{s-s_n} \qquad \text{(A. 62)}$$

where

$$g_2 = \left(\frac{d\phi_2}{d\bar{x}}\right)_{\frac{\bar{c}}{2}} \ell_w$$

$$b_0 = -\frac{2}{\bar{c}}$$

$$c_3 = -\frac{2}{\bar{c}} + \frac{4}{b}\left[AR\tan\Theta - AR\tan\Lambda_3\right]\sin\Theta\cos\Theta$$

$$d_4 = AR\cos\Theta\left(\tan\Lambda_3 - \tan\Theta\right)$$

$$e_1 = AR\tan\Lambda_3$$

$$e_2 = \left(\frac{d\phi_2}{d\bar{x}}\right)_{\frac{\bar{c}}{2}\ell_w} AR\tan\Lambda_3$$

$$e_3 = -\frac{4}{b}\sin\Theta\cos\Theta$$

$$e_4 = \cos\Theta$$

$$f_1 = -\ell_3$$

$$f_2 = \left(\frac{d\phi_2}{d\bar{x}}\right)_{\frac{\bar{c}}{2}\ell_w}\left[\ell_w - \ell_3\right] - \frac{2}{\bar{c}}\phi_2\left(\frac{\bar{c}}{2}\ell_w\right)$$

$$f_3 = \frac{4}{b}\left[\ell_3 - \ell_w\right]\sin\Theta\cos\Theta$$

$$f_4 = \left(\ell_w - \ell_3\right)\cos\Theta$$

With equations (A. 58) through (A. 62) substituted into (A. 57), the final expression for the convolution integral used in the equations of motion in Section I is obtained.

A. 4 Internal Energy in Terms of Influence or Stiffness Coefficients

The internal energy expression in Section I can also be formulated in terms of influence or stiffness coefficients if available. In this case, equation (1. 3) can be written as

$$U_i = U_{iw} + U_{it} + U_{if} \qquad \text{(A. 63)}$$

where

U_{iw} is the internal energy of the wing

U_{it} is the internal energy of the horizontal tail

U_{if} is the internal energy of the fuselage

The internal energies of the wing, fuselage, and horizontal tail in terms of influence coefficients are

$$U_{iw} = \sum_{i=1}^{n}\sum_{j=1}^{n} C_{ij}^{zz} Q_i^w Q_j^w + \sum_{i=1}^{n}\sum_{j=1}^{n} C_{ij}^{\theta\theta} Q_i^w Q_j^w + 2\sum_{i=1}^{n}\sum_{j=1}^{n} C_{ij}^{z\theta} Q_i^w Q_j^w \tag{A.64}$$

$$U_{it} = \sum_{i=1}^{n}\sum_{j=1}^{n} C_{ij}^{zz} Q_i^t Q_j^t + \sum_{i=1}^{n}\sum_{j=1}^{n} C_{ij}^{\theta\theta} Q_i^t Q_j^t + 2\sum_{i=1}^{n}\sum_{j=1}^{n} C_{ij}^{z\theta} Q_i^t Q_j^t \tag{A.65}$$

$$U_{if} = \frac{1}{2}\sum_{i=1}^{n}\sum_{j=1}^{n} C_{ij}^{zz} Q_i^f Q_j^f \tag{A.66}$$

To obtain the equations of motion, however, the internal energies must be expressed in terms of stiffness coefficients which can be obtained by inverting the matrices of influence coefficients. Thus,

$$U_{iw} = \sum_{i=1}^{n}\sum_{j=1}^{n} k_{ij}^{zz} Z_i^w Z_j^w + \sum_{i=1}^{n}\sum_{j=1}^{n} k_{ij}^{\theta\theta} \theta_i^w \theta_j^w + 2\sum_{i=1}^{n}\sum_{j=1}^{n} k_{ij}^{z\theta} Z_i^w \theta_j^w \tag{A.67}$$

$$U_{it} = \sum_{i=1}^{n}\sum_{j=1}^{n} k_{ij}^{zz} Z_i^t Z_j^t + \sum_{i=1}^{n}\sum_{j=1}^{n} k_{ij}^{\theta\theta} \theta_i^t \theta_j^t + 2\sum_{i=1}^{n}\sum_{j=1}^{n} k_{ij}^{z\theta} Z_i^t \theta_j^t \tag{A.68}$$

$$U_{if} = \frac{1}{2}\sum_{i=1}^{n}\sum_{j=1}^{n} k_{ij}^{zz} Z_i^f Z_j^f \tag{A.69}$$

where

C_{ij}^{zz} is the linear displacement at station i due to a unit load applied at j on the elastic axis

$C_{ij}^{\theta\theta}$ is the angular rotation at station i due to a unit torque applied at j about the elastic axis

$C_{ij}^{z\theta}$ is the linear displacement at station i due to a unit torque applied at j about the elastic axis, and which has the property that $C_{ij}^{z\theta} = C_{ij}^{\theta z}$

k_{ij}^{zz} is the load required to prevent displacement at i when a unit displacement is given at j along the elastic axis and all other coordinates held fixed

$k_{ij}^{\theta\theta}$ is the torque required to prevent angular rotation at i when a unit angular rotation is given at j about the elastic axis and all other coordinates are held fixed

$k_{ij}^{z\theta}$ is the load required to prevent a linear displacement at i when a unit angular rotation is given at j about the elastic axis and all other coordinates are held fixed and which have the property that $k_{ij}^{z\theta} = k_{ij}^{\theta z}$

$Z_{i,j}^{w}$ is the bending displacement of the wing elastic axis at i or j

$\theta_{i,j}^{w}$ is the torsional rotation about the wing elastic axis at i or j

In the particular case when assumed modes are used, the displacements and rotations are

$$Z_{i,j}^{w} = \phi_{3i} q_3 \, , \, \phi_{3j} q_3 \qquad \theta_{i,j}^{w} = \phi_{4i} q_4 \, , \, \phi_{4j} q_4$$

$$Z_{i,j}^{t} = \phi_{5i} q_5 \, , \, \phi_{5j} q_5 \qquad \theta_{i,j}^{t} = \phi_{6i} q_6 \, , \, \phi_{6j} q_6$$

$$Z_{i,j}^{f} = \phi_{2i} q_2 \, , \, \phi_{2j} q_2 \qquad \theta_{i,j}^{f} = 0 \qquad \text{(A.70)}$$

If equations (A.70) are substituted into equations (A.67), (A.68) and (A.69), the internal energy in terms of stiffness coefficients is

$$U_i = \frac{1}{2}\sum_{i=1}^{n}\sum_{j=1}^{n} k_{ij}^{zz}(\phi_{2i}\phi_{2j})q_2^2 + \sum_{i=1}^{n}\sum_{j=1}^{n} k_{ij}^{zz}(\phi_{3i}\phi_{3j})q_3^2$$
$$+ \sum_{i=1}^{n}\sum_{j=1}^{n} k_{ij}^{\theta\theta}(\phi_{4i}\phi_{4j})q_4^2 + 2\sum_{i=1}^{n}\sum_{j=1}^{n} k_{ij}^{z\theta}(\phi_{3i}\phi_{4j})q_3 q_4$$
$$+ \sum_{i=1}^{n}\sum_{j=1}^{n} k_{ij}^{zz}(\phi_{5i}\phi_{5j})q_5^2 + \sum_{i=1}^{n}\sum_{j=1}^{n} k_{ij}^{\theta\theta}(\phi_{6i}\phi_{6j})q_6^2$$
$$+ 2\sum_{i=1}^{n}\sum_{j=1}^{n} k_{ij}^{z\theta}(\phi_{5i}\phi_{6j})q_5 q_6 \qquad \text{(A.71)}$$

When equation (A.71) is used instead of equation (1.3), the elastic coupling between bending and torsion in a swept wing is taken into account.

APPENDIX B

DETERMINATION OF TRANSIENT STRESSES

In Appendix E, three different methods for computing transient stresses are described; and, of these, the so-called "mode acceleration method" is recommended because of its combined simplicity and accuracy. For the assumed cantilever modes chosen in Section I, however, this method is not directly applicable; and so, the more accurate and more complex "force summation method" is employed here.

With the force summation method (Appendix E) the shears and bending moments along the span for the elastic airplane are computed as

$$S(\eta,s)_e = \frac{b}{2}\int_{\eta}^{1} \ell_w^e \, d\eta + \frac{b}{2}\int_{\eta}^{1} \ell_w^a \, d\eta - \left(\frac{U}{\frac{\varepsilon}{2}}\right)^2 \frac{b}{2}\int_{\eta}^{1} m_w(\eta)\, V_w'(s,\eta)\, d\eta \qquad \text{(B. 1)}$$

$$BM(\eta,s)_e = \frac{b}{2}\int_{\eta}^{1} S(\eta,s)_e \, d\eta \qquad \text{(B. 2)}$$

where V_w' is given by equation (1.6). The prime denotes differentiation with respect to s.

After substituting ℓ_w^e and ℓ_w^a from Appendix A and non-dimensionalizing equation (B. 1) in terms of $\frac{1}{2}\rho U^2 S\, a_w \frac{w}{U}$ and (B. 2) in terms of $\frac{1}{2}\rho U^2 S\, a_w \frac{\varepsilon}{2}\frac{w}{U}$, the shears and bending moments at any station η along the wing can be written in matrix form as

$$\left\{S(\eta,s)_e\right\} = \left[K^1_\eta\right]\left\{\psi(s), \ddot{\xi}\right\} + \left[K^2_\eta\right]\left\{\dot{\xi}\right\} + \left[K^3_\eta\right]\left\{\xi\right\} \tag{B. 3}$$

$$\left\{BM(\eta,s)_e\right\} = \left[K^4_\eta\right]\left\{\psi(s), \ddot{\xi}\right\} + \left[K^5_\eta\right]\left\{\dot{\xi}\right\} + \left[K^6_\eta\right]\left\{\xi\right\} \tag{B. 4}$$

for $s \geq \beta$

where the columns are defined by

$$\left\{\psi(s), \ddot{\xi}\right\} = \begin{Bmatrix} \psi(s) \\ \ddot{\xi}_0 = \ddot{q}_1 \\ \ddot{\xi}_2 \\ \ddot{\xi}_3 \\ \ddot{q}_4 \end{Bmatrix} \quad \left\{\dot{\xi}\right\} = \begin{Bmatrix} \dot{\xi}_0 \\ \dot{q}_1 \\ \dot{\xi}_2 \\ \dot{\xi}_3 \\ \dot{q}_4 \end{Bmatrix} \quad \left\{\xi\right\} = \begin{Bmatrix} q_1 \\ \xi_2 \\ \xi_3 \\ q_4 \end{Bmatrix} \tag{B. 5}$$

In the above equations, an efficiency factor e can be introduced after the manner of Section III to take into account the reduction in damping forces due to unsteady aerodynamics; for which case the stresses at anytime do not depend on their previous time histories and they need not be calculated for $s \leq \beta$. In this case the matrices $\left[K^2_\eta\right]$, $\left[K^3_\eta\right]$, $\left[K^4_\eta\right]$ and $\left[K^6_\eta\right]$ in equations (B. 3) and (B. 4) are multiplied by e.

Using strip theory, the K -coefficients are

$$K'_{\eta 1} = \frac{1}{1+\lambda_w}\int_{\eta}^{1}\left[1-\delta_w\eta\right]d\eta$$

$$K'_{\eta 2} = -\frac{1}{2\rho\left(\frac{\bar{c}}{2}\right)^2 a_w}\int_{\eta}^{1} m(\eta)\,d\eta \;-\; \frac{1}{\rho b\left(\frac{\bar{c}}{2}\right)^2 a_w}\sum_{j=1}^{n} m_j$$

$$K'_{\eta 3} = -\frac{1}{2\rho\left(\frac{\bar{c}}{2}\right)^2 a_w}\int_{\eta}^{1} m(\eta)C(\eta)\,d\eta - \frac{1}{\rho b\left(\frac{\bar{c}}{2}\right)^2 a_w}\sum_{j=1}^{n} m_j C(\eta_j)$$

$$K'_{\eta 4} = -\frac{1}{2\rho\left(\frac{\bar{c}}{2}\right)^2 a_w}\int_{\eta}^{1} m(\eta)\phi_{22}(\eta)\,d\eta - \frac{1}{\rho b\left(\frac{\bar{c}}{2}\right)^2 a_w}\sum_{j=1}^{n} m_j \phi_{22}(\eta_j)$$

$$K'_{\eta 5} = -\frac{1}{2\rho\left(\frac{\bar{c}}{2}\right)^2 a_w}\int_{\eta}^{1} m(\eta)\phi_{33}(\eta)\,d\eta - \frac{1}{\rho b\left(\frac{\bar{c}}{2}\right)^2 a_w}\sum_{j=1}^{n} m_j \phi_{33}(\eta_j)$$

$$K'_{\eta 6} = -\frac{1}{2\rho\left(\frac{\bar{c}}{2}\right)^2 a_w}\int_{\eta}^{1} m(\eta)\phi_{44}(\eta)\,d\eta - \frac{1}{\rho b\left(\frac{\bar{c}}{2}\right)^2 a_w}\sum_{j=1}^{n} m_j \phi_{44}(\eta_j)$$

$$K^2_{\eta 1} = -\frac{1}{1+\lambda_w}\int_{\eta}^{1}\left[1-\delta_w\eta\right]d\eta$$

$$K^2_{\eta 2} = -\frac{1}{1+\lambda_w}\int_{\eta}^{1}\left[1-\delta_w\eta\right]\left(\ell_3 - AR\,\eta\tan\lambda_3\right)d\eta$$

$$K^2_{\eta 3} = -\frac{1}{1+\lambda_w}\int_\eta^1 [1-\delta_w\eta]\left[\phi_2\left(\tfrac{\bar{c}}{2}\ell_w\right) + \left(\frac{d\phi_2}{d\bar{x}}\right)_{\frac{\bar{c}}{2}\ell_w} k_7(\eta)\right] d\eta$$

$$K^2_{\eta 4} = -\frac{1}{1+\lambda_w}\int_\eta^1 [1-\delta_w\eta]\left\{\phi_3(\eta) + [k_w(\eta)-k_6(\eta)]\frac{d\phi_3}{d\eta}\,\frac{\sin\Lambda\cos\Lambda}{b/2}\right\} d\eta$$

$$K^2_{\eta 5} = -\frac{1}{1+\lambda_w}\int_\eta^1 [1-\delta_w\eta][k_w(\eta)-k_6(\eta)]\,\phi_4(\eta)\cos\Lambda\, d\eta$$

$$K^3_{\eta 1} = -K^2_{\eta 1}$$

$$K^3_{\eta 2} = \frac{\bar{c}}{2}\frac{1}{1+\lambda_w}\int_\eta^1 [1-\delta_w\eta]\left(\frac{d\phi_2}{d\bar{x}}\right)_{\frac{\bar{c}}{2}\ell_w} d\eta$$

$$K^3_{\eta 3} = -\frac{\bar{c}}{2}\frac{1}{1+\lambda_w}\int_\eta^1 [1-\delta_w\eta]\,\frac{d\phi_3}{d\eta}\,\frac{\sin\Lambda\cos\Lambda}{b/2}\, d\eta$$

$$K^3_{\eta 4} = \frac{1}{1+\lambda_w}\int_\eta^1 [1-\delta_w\eta]\,\phi_4(\eta)\cos\Lambda\, d\eta$$

where

$$C(\eta) = (x_{c.g.w} + \ell_w - AR\,\eta\tan\Lambda)$$

$m(\eta)$ is the mass per unit length of the wing without nacelles

m_j is the mass of the j^{th} nacelle

$$\phi_{22}(\eta) = \left[\phi_2\left(\tfrac{\bar{c}}{2}\ell_w\right) + \left(\frac{d\phi_2}{d\bar{x}}\right)_{\frac{\bar{c}}{2}\ell_w} \frac{\bar{c}}{2}\left(x_{c.g.w} - AR\,\eta \tan\Lambda\right)\right]$$

$$\phi_{33}(\eta) = \left[\phi_3(\eta) - x_{c.g.w} \frac{d\phi_3}{d\eta} \frac{\sin\Lambda\cos\Lambda}{AR} \right]$$

$$\phi_{44}(\eta) = x_{c.g.w}\,\phi_4(\eta)\cos\Lambda$$

$$\psi(s) = \psi\left(s - \frac{\beta}{2}\right) \qquad s \geq \beta$$

The coefficients for equation (B. 4) are

$$K^4_{\eta i} = AR \int_\eta^1 K^1_{\eta i}\, d\eta$$

$$K^5_{\eta i} = AR \int_\eta^1 K^2_{\eta i}\, d\eta$$

$$K^6_{\eta i} = AR \int_\eta^1 K^3_{\eta i}\, d\eta$$

When unsteady aerodynamic effects are included in the damping forces, the stresses at any time depend upon the previous time histories of the responses; and the coefficients $K^1_{\eta i}$ and $K^4_{\eta i}$ have to be modified for a time $s \leq \beta$. In this case they become

$$K'_{\eta_1} = \frac{1}{1+\lambda_w}\int_{\eta}^{s/\beta}\left[1-\delta_w\eta\right]d\eta \qquad \eta\beta \le s \le \beta$$

$$K''_{\eta_1} = AR\int_{\eta}^{s/\beta} K'_{\eta_1}\,d\eta \qquad \eta\beta \le s \le \beta$$

$$\psi(s) = \psi\left(\frac{s}{2}\right) \qquad s \le \beta$$

and the matrices for the shears and bending moments including unsteady aerodynamic effects are

$$\left\{S(\eta,s)_e\right\} = \left\{\text{ equation (B. 3) }\right\} - \left[K^o\right]\left\{T^i\right\} \tag{B.5}$$

$$\left\{BM(\eta,s)_e\right\} = \left\{\text{ equation (B. 4) }\right\} - \left[K^o\right]\left\{L^i\right\} \tag{B.6}$$

where the functions T^i and L^i are similar to equations (1. 25) and (1. 26) which, after integration, have the forms of equation (2. 6).

Thus, the functions T^i and L^i become for the stresses at a time $s = n\varepsilon$

$$\left\{T^i\right\}_n = \left[K^1\right]\left\{T^i\right\}_{n-1} + \left[K^2\right]\left[K^2_n\right]\left\{\begin{matrix} q_0 = \dot{u}_0 \\ q_1 = \dot{u}_1 \\ q_2 = \dot{u}_2 \\ q_3 = \dot{u}_3 \\ q_4 = \dot{u}_4 \end{matrix}\right\}_n + \left[K^2\right]\left[K^3_n\right]\left\{\begin{matrix} \dot{q}_1 \\ \dot{u}_2 \\ \dot{u}_3 \\ \dot{q}_4 \end{matrix}\right\}_n$$

$$+ \left[K^3\right]\left[K^2_n\right]\left\{\begin{matrix} q_0 = \dot{u}_0 \\ q_1 = \dot{u}_1 \\ q_2 = \dot{u}_2 \\ q_3 = \dot{u}_3 \\ q_4 = \dot{u}_4 \end{matrix}\right\}_{n-1} + \left[K^3\right]\left[K^3_n\right]\left\{\begin{matrix} \dot{q}_1 \\ \dot{u}_2 \\ \dot{u}_3 \\ \dot{q}_4 \end{matrix}\right\}_{n-1} \qquad \text{(B. 7)}$$

and

$$\left\{L^i\right\}_n = \left[K^1\right]\left\{L^i\right\}_{n-1} + \left[K^2\right]\left[K^5_n\right]\left\{\begin{matrix} q_0 = \dot{u}_0 \\ q_1 = \dot{u}_1 \\ q_2 = \dot{u}_2 \\ q_3 = \dot{u}_3 \\ q_4 = \dot{u}_4 \end{matrix}\right\}_n + \left[K^2\right]\left[K^6_n\right]\left\{\begin{matrix} \dot{q}_1 \\ \dot{u}_2 \\ \dot{u}_3 \\ \dot{q}_4 \end{matrix}\right\}_n$$

$$+ \left[K^3\right]\left[K^5_n\right]\left\{\begin{matrix} q_0 = \dot{u}_0 \\ q_1 = \dot{u}_1 \\ q_2 = \dot{u}_2 \\ q_3 = \dot{u}_3 \\ q_4 = \dot{u}_4 \end{matrix}\right\}_{n-1} + \left[K^3\right]\left[K^6_n\right]\left\{\begin{matrix} \dot{q}_1 \\ \dot{u}_2 \\ \dot{u}_3 \\ \dot{q}_4 \end{matrix}\right\}_{n-1} \qquad \text{(B. 8)}$$

In the above equations, since T^i and L^i occur in pairs for a given spanwise station η, i will be twice the number of stations taken along the wing. The matrices in equations (B.7) and (B.8) are as follows:

$$[K^0] = \begin{bmatrix} 1 & 1 & 0 & 0 & 0 & 0 & \cdots \\ 0 & 0 & 1 & 1 & 0 & 0 & \cdots \\ 0 & 0 & 0 & 0 & 1 & 1 & \\ \vdots & \vdots & \vdots & \vdots & & & \end{bmatrix}$$

$$[K^1] = \begin{bmatrix} e^{-.045\varepsilon} & 0 & 0 & 0 & \cdots \\ 0 & e^{-.30\varepsilon} & 0 & 0 & \cdots \\ 0 & 0 & e^{-.045\varepsilon} & 0 & \cdots \\ \vdots & \vdots & & & \end{bmatrix}$$

$$[K^2] = \begin{bmatrix} .165\frac{\varepsilon}{2} & 0 & 0 & 0 & \cdots \\ 0 & .335\frac{\varepsilon}{2} & 0 & 0 & \cdots \\ 0 & 0 & .165\frac{\varepsilon}{2} & 0 & \cdots \\ 0 & 0 & 0 & .335\frac{\varepsilon}{2} & \\ \vdots & \vdots & \vdots & & \end{bmatrix}$$

$$[K^3] = [K^1][K^2]$$

By analogy with the shears and bending moments, the torque about the y-axis at the wing elastic axis, is

$$T(\eta,s)_e = \frac{b}{2}\int_\eta^1 \ell_w^\delta \left[k_1(\eta)-k_w(\eta)\right]d\eta + \frac{b}{2}\int_\eta^1 \ell_w^\alpha \left[k_1(\eta)-k_w(\eta)\right]d\eta$$
$$-\left(\frac{U}{\frac{\bar c}{2}}\right)^2 \frac{b}{2}\int_\eta^1 m_w(\eta)\, V_w'(\eta,s)\, \frac{\bar c}{2}\, x_{c.g.w}\, d\eta$$
$$-\left(\frac{U}{\frac{\bar c}{2}}\right)^2 \frac{b}{2}\int_\eta^1 I_w(\eta)\, \ddot\theta_w\, d\eta \qquad \text{(B. 9)}$$

where $\ddot\theta_w$ is obtained from equation (1. 8). Dividing equation (B. 9) by $\frac{1}{2}\rho U^2 S a_w \frac{\bar c}{2}\frac{w}{U}$, the dimensionless torques about the y-axis in matrix form are

$$\left\{T(\eta,s)_e\right\} = \left[J_\eta^1\right]\left\{\psi(s), \ddot\psi\right\} + \left[J_\eta^2\right]\left\{\dot\psi\right\} + \left[J_\eta^3\right]\left\{\psi\right\} \qquad s \geq \beta \qquad \text{(B. 10)}$$

In the same manner as for the shears and bending moments, if an efficiency factor e is introduced, the matrices $\left[J_\eta^2\right]$ and $\left[J^3{}_\eta\right]$ are multiplied by e. The matrix coefficients for equation (B. 10) are

$$J'_{\eta,1} = \frac{1}{1+\lambda_w}\int_\eta^1 \left[1-\delta_w\eta\right]\frac{2}{\bar c}\left[k_1(\eta)-k_w(\eta)\right]d\eta \qquad \text{when} \quad s \geq \beta$$

$$\psi(s) = \psi\left(s-\frac{\beta}{2}\right) \qquad \text{when} \quad s \geq \beta$$

$$J'_{\eta_1} = \frac{1}{1+\lambda_w}\int_{\eta}^{s/\beta}\left[1-\delta_w\eta\right]\frac{2}{c}\left[k_1(\eta)-k_w(\eta)\right]d\eta \qquad \eta\beta \le s \le \beta$$

$$\psi(s) = \psi\left(\frac{s}{2}\right) \qquad s \le \beta$$

$$J'_{\eta_2} = -\frac{1}{2\rho\left(\frac{c}{2}\right)^2 a_w}\int_{\eta}^{1} m(\eta)\, x_{c.g.w}\, d\eta \; - \frac{1}{\rho b\left(\frac{c}{2}\right)^2 a_w}\sum_{j=1}^{n} m_j\, x_{c.g.j}$$

$$J'_{\eta_3} = -\frac{1}{2\rho\left(\frac{c}{2}\right)^2 a_w}\int_{\eta}^{1} m(\eta)\, C(\eta)\, x_{c.g.w}\, d\eta - \frac{1}{\rho b\left(\frac{c}{2}\right)^2 a_w}\sum_{j=1}^{n} m_j\, C(\eta_j)\, x_{c.g.j}$$

$$- \frac{1}{2\rho\left(\frac{c}{2}\right)^4 a_w}\int_{\eta}^{1} I_{c.g}(\eta)\, d\eta \; - \frac{1}{\rho b\left(\frac{c}{2}\right)^4 a_w}\sum_{j=1}^{n} I_{c.g.j}$$

$$J'_{\eta_4} = -\frac{1}{2\rho\left(\frac{c}{2}\right)^2 a_w}\int_{\eta}^{1} m(\eta)\,\phi_{22}(\eta)\, x_{c.g.w}\, d\eta - \frac{1}{\rho b\left(\frac{c}{2}\right)^2 a_w}\sum_{j=1}^{n} m_j\,\phi_{22}(\eta_j)\, x_{c.g.j}$$

$$- \frac{1}{2\rho\left(\frac{c}{2}\right)^3 a_w}\int_{\eta}^{1} I_{c.g}(\eta)\left(\frac{d\phi_2}{d\bar{x}}\right)_{\frac{c}{2}\ell_w} d\eta \; - \frac{1}{\rho b\left(\frac{c}{2}\right)^3 a_w}\sum_{j=1}^{n} I_{c.g.j}\left(\frac{d\phi_2}{d\bar{x}}\right)_{\frac{c}{2}\ell_w}$$

$$J'_{\eta_5} = -\frac{1}{2\rho\left(\frac{c}{2}\right)^2 a_w}\int_{\eta}^{1} m(\eta)\,\phi_{33}(\eta)\, x_{c.g.w}\, d\eta - \frac{1}{\rho b\left(\frac{c}{2}\right)^2 a_w}\sum_{j=1}^{n} m_j\,\phi_{33}(\eta_j)\, x_{c.g.j}$$

$$+ \frac{1}{2\rho\left(\frac{c}{2}\right)^4 a_w}\int_{\eta}^{1} I_{c.g.}(\eta)\frac{d\phi_3}{d\eta}\,\frac{\sin\Theta\cos\Theta}{AR}\,d\eta \; + \frac{\sin\Theta\cos\Theta}{\rho b\left(\frac{c}{2}\right)^4 a_w AR}\sum_{j=1}^{n} I_{c.g.j}\left(\frac{d\phi_3}{d\eta}\right)_j$$

$$J'_{\eta 6} = -\frac{1}{2\rho\left(\frac{\bar{c}}{2}\right)^2 a_w}\int_{\eta}^{1} m(\eta)\,\phi_{44}(\eta)\,x_{c.g.w}\,d\eta \;-\; \frac{1}{\rho b\left(\frac{\bar{c}}{2}\right)^2 a_w}\sum_{j=1}^{n} m_j\,\phi_{44}(\eta_j)\,x_{c.g.j}$$

$$-\frac{1}{2\rho\left(\frac{\bar{c}}{2}\right)^4 a_w}\int_{\eta}^{1} I_{c.g}(\eta)\,\phi_4(\eta)\cos\Phi\,d\eta \;-\; \frac{\cos\Phi}{\rho b\left(\frac{\bar{c}}{2}\right)^4 a_w}\sum_{j=1}^{n} I_{c.g.j}\,\phi_4(\eta_j)$$

where

$I_{c.g}(\eta)$ is the moment of inertia of the wing without nacelles per unit length about an axis through its c. g. and perpendicular to the streamwise direction

$I_{c.g.j}$ is the moment of inetia of the j^{th} nacelle about an axis through its c. g. and perpendicular to the streamwise direction

$x_{c.g.j}$ is the streamwise distance from the c. g. of the j^{th} nacelle to the elastic axis measured in mean geometric wing semichords, positive if in front of the elastic axis

The $J^2_{\eta i}-$ and $J^3_{\eta i}-$ coefficients follow directly from the $K^2_{\eta i}-$ and $K^3_{\eta i}-$ coefficients where the terms under the integral signs are multiplied by $\frac{2}{\bar{c}}\left[k_1(\eta) - k_w(\eta)\right]$.

In the case when unsteady aerodynamic effects are included in the damping forces, the procedure is identical to that for the shears and bending moments. Thus

$$\left\{T(\eta,s)_e\right\} = \left\{\quad \text{equation (B. 10)} \quad\right\} - \left[K^o\right]\left\{J^i\right\} \qquad \text{(B. 11)}$$

where

$$\left\{J^{i}\right\}_{m} = \left[K^{1}\right]\left\{J^{i}\right\}_{m-1} + \left[K^{2}\right]\left[J^{2}_{\eta}\right]\left\{\begin{matrix} \zeta_{0} = \zeta_{0} \\ \zeta_{1} = q_{1} \\ \zeta_{2} = \zeta_{2} \\ \zeta_{3} = \zeta_{3} \\ q_{4} = \zeta_{4} \end{matrix}\right\}_{m} + \left[K^{2}\right]\left\{J^{3}_{\eta}\right\}\left\{\begin{matrix} \dot{q}_{1} \\ \dot{\zeta}_{2} - \zeta_{2} \\ \dot{\zeta}_{3} \\ \dot{q}_{4} \end{matrix}\right\}_{m}$$

$$+ \left[K^{3}\right]\left[J^{2}_{\eta}\right]\left\{\begin{matrix} \zeta_{0} = \zeta_{0} \\ q_{1} = \zeta_{1} \\ \zeta_{2} = \zeta_{2} \\ \zeta_{3} = \zeta_{3} \\ q_{4} = \zeta_{4} \end{matrix}\right\}_{m-1} + \left[K^{3}\right]\left[J^{3}_{\eta}\right]\left\{\begin{matrix} \dot{q}_{1} \\ \dot{\zeta}_{2} - \zeta_{2} \\ \dot{\zeta}_{3} \\ \dot{q}_{4} \end{matrix}\right\}_{m-1} \qquad \text{(B. 12)}$$

The previously defined bending moments and shears are taken in planes parallel to the air stream. The bending moments along the elastic axis and the torques about the elastic axis are, then, given by

$$BM_{e.a} = BM\cos\theta - T\sin\theta \qquad \text{(B. 13)}$$

$$T_{e.a} = BM\sin\theta + T\cos\theta \qquad \text{(B. 14)}$$

APPENDIX C

EFFECT OF NACELLE FLEXIBILITY ON WING STRESSES

To find the effect of the side-bending vibration of an underslung nacelle on wing stresses, a simplified analysis is made to determine its contribution to the root bending moment. Figure C. 1 shows the simplified model for this analysis which approximates a cantilevered wing by three elastically connected point masses with a strut-mounted nacelle located at a distance d below the wing.

The kinetic energy of this system can be written as

$$T = \tfrac{1}{2} m_1' \dot{q}_1^2 + \tfrac{1}{2} m_2 \dot{q}_2^2 + \tfrac{1}{2} m_3 \dot{q}_3^2 + \tfrac{1}{2} m_4 (\dot{q}_1^2 + \dot{q}_4^2) \qquad \text{(C. 1)}$$

where

q_1, q_2, q_3, q_4 are generalized coordinates

m_1', m_2, m_3 are the point masses

m_4 is the mass of the nacelle

The internal energy is

$$U_i = \tfrac{1}{2} \sum_{i=1}^{4} \sum_{j=1}^{4} C_{ij} Q_i Q_j = \tfrac{1}{2} \sum_{i=1}^{4} \sum_{j=1}^{4} K_{ij} q_i q_j \qquad \text{(C. 2)}$$

where

C_{ij} are flexibility influence coefficients

K_{ij} are stiffness influence coefficients

$Q_{i,j}$ are generalized forces

The work done on the system is given by

$$Q_i \delta q_i = F_i(t) \delta q_i \qquad i = 1, 2, 3 \tag{C.3}$$

Using Lagrange's equation of motion

$$\frac{d}{dt}\left(\frac{\partial T}{\partial \dot{q}_i}\right) + \frac{\partial U_i}{\partial q_i} = Q_i \tag{C.4}$$

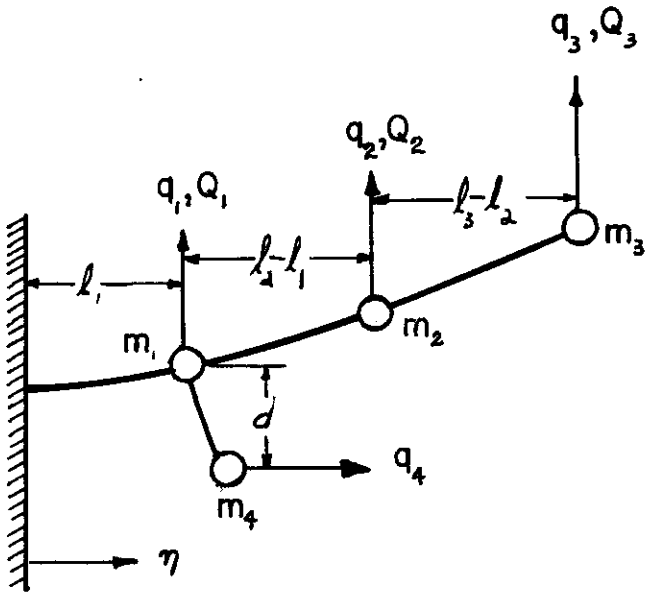

FIGURE C.1 SIMPLIFIED MODEL OF CANTILEVERED WING WITH FLEXIBLE NACELLE

and substituting equations (C. 1), (C. 2) and (C. 3) into (C. 4), the equations of motion in matrix form are

$$\{m_i \ddot{q}_i\} + [K_{ij}]\{q_j\} = \{Q_i\} \tag{C.5}$$

For free vibrations $\{Q_i\} = 0$, and equation (C. 5) after multiplying through by $[C_{ij}]$ reduces to

$$[C_{ij}]\{m_j \ddot{q}_j\} + \{q_i\} = 0 \qquad \text{for} \quad i = 1, 2, 3, 4 \tag{C.6}$$

where m_1 is the sum of $m_1' + m_4$ because the mass m_4 moves with m_1' in the q_1 direction. The matrix $[C_{ij}]$ has the property that $[C_{ij}] = [K_{ij}]^{-1}$.

Substituting $q_i = A_i \sin(\omega t + \psi)$ into (C. 5), there results

$$-\omega^2 [D_{ij}]\{A_j\} + \{A_i\} = 0 \tag{C.7}$$

which after normalizing becomes

$$[D_{ij}]\{\phi_j\} = \frac{1}{\omega^2}\{\phi_i\} \tag{C.8}$$

where

$$[D_{ij}] = [C_{ij}][m_j]$$

$\{\phi_j\}$ are the mode shapes.

Reference 14 gives a method of iteration and sweeping by which the natural modes of vibration and frequencies are obtained. Due to the accumulation of the errors when using the orthogonality condition in sweeping, the following equation was used to obtain the higher frequencies and mode shapes:

$$\left[D'_{ij}\right]\left\{\phi_j\right\} = \omega^2\left\{\phi_i\right\} \tag{C.9}$$

where

$$\left[D'_{ij}\right] = \left[\frac{1}{m_j}\right]\left[K_{ij}\right]$$

The normalized equations of motion then become for the r^{th} mode

$$M_r \ddot{\eta}_r + M_r \omega_r^2 \eta_r = \overline{\overline{F}}_r \tag{C.10}$$

where

$$M_r = \sum_{i=1}^{4} m_i \left(\phi_i^{(r)}\right)^2$$

$$\overline{\overline{F}}_r = \sum_{i=1}^{4} F_i(t)\, \phi_i^{(r)}$$

and using the force summation method, the dimensionless bending moment at the root becomes

$$\frac{BM_e}{BM_r} = 1 - \frac{\sum_{r=1}^{4} \frac{\overline{\overline{F}}_r}{M_r} \cos\omega_r t}{\sum_{i=1}^{3} F_i l_i}\left[\sum_{i=1}^{3} m_i \phi_i^{(r)} l_i + m_4 d\, \phi_4^{(r)}\right] \tag{C.11}$$

when the forcing functions $F_i(t)$ are step functions.

Wing data for the example airplane of Section IV are also used in this numerical example. The pertinent data are given in Table C. 1. The bending stiffnessess of the nacelle struts were calculated on the assumption that the stiffness is constant over the distance d ; and the choice of values used was determined from the relationship of a weightless cantilever beam with a tip mass in such a way that the nacelle frequencies correspond to the first wing bending frequency and the actual frequency of the nacelle. For this relationship, we have $m_4 \omega_4^2 = K_{44}$, where the stiffness coefficient $K_{44} = \frac{3EI_m}{d^3}$. In this manner only the cantilever frequency of the nacelle has to be known. The coefficients k_i given in Figure C. 2 are then obtained in the form

$$k_i = \frac{m_4 \omega_i^2 a e^3}{3} \qquad i = 1, 2 \tag{C. 12}$$

where

$k_i = \frac{EI_{mi}}{EI_{.5}}$ are the ratios of the nacelle stiffnesses to the wing stiffness at mid-span associated with a particular nacelle frequency given by equation (C. 12)

$e = \frac{d}{b/2\cos\Phi}$ is the ratio of the nacelle distance below the wing elastic axis to the wing semispan

$a = \frac{\left(b/2\cos\Phi\right)^3}{EI_{.5}}$

$\frac{b}{2\cos\Phi}$ = wing semispan measured along the wing elastic axis

Two additional k's were used, k_0 which represents the system with nacelle attached at the wing elastic axis ($d = 0$) and k_∞ which represents an infinitely stiff nacelle.

The $[C_{ij}]$ matrix coefficients were calculated from the approximate equation

$$EI_w(\eta) = \frac{EI_{.5}}{10\eta^3 - 2.5\eta^2 + .25\eta + .25} \qquad \text{(C. 13)}$$

TABLE C. 1

DATA FOR EXAMPLE WING

ℓ_1 = 22. 22 ft.	$b/2\cos\Theta$ = 70 ft.
ℓ_2 = 34. 80 ft.	b = 116 ft.
ℓ_3 = 46. 40 ft.	Θ = 35°
m_1' = 198. 44 slugs	$EI_{.5}$ = 19. 1 x 10^7 lb. ft^2
m_2 = 42. 86 slugs	EI_{n1} = 4. 85 x 10^5 lb. ft^2
m_3 = 103. 63 slugs	EI_{n2} = 1. 62 x 10^6 lb. $ft.^2$ (actual)
m_4 = 235 slugs	d = 4. 67 ft.
$m_1 = m_1' + m_4$ = 433. 44 slugs	$\omega_{NACELLE}$ = 14. 24 rad./sec.

With equation (C. 13), the C_{ij} – coefficients used in equation (C. 8) become

$$C_{ij} = a\left\{\eta_j\left(\frac{1}{2}\eta_i^5 - \frac{2.5}{12}\eta_i^4 + \frac{.25}{6}\eta_i^3 + \frac{.25}{2}\eta_i^2\right) - \left(\frac{1}{3}\eta_i^6 - \frac{2.5}{20}\eta_i^5 + \frac{.25}{12}\eta_i^4 + \frac{.25}{6}\eta_i^3\right)\right\}$$

$$C_{14} = \alpha e \left\{ \frac{1}{2}\eta_1^5 - \frac{2.5}{12}\eta_1^4 + \frac{.25}{6}\eta_1^3 + \frac{.25}{2}\eta_1^2 \right\}$$

$$C_{24} = \alpha e \left\{ \left(\frac{1}{2}\eta_1^5 - \frac{2.5}{12}\eta_1^4 + \frac{.25}{6}\eta_1^3 + \frac{.25}{2}\eta_1^2 \right) + (\eta_2 - \eta_1)\left(\frac{10}{4}\eta_1^4 - \frac{2.5}{3}\eta_1^3 + \frac{.25}{2}\eta_1^2 + .25\eta_1 \right) \right\}$$

$$C_{34} = \alpha e \left\{ \left(\frac{1}{2}\eta_1^5 - \frac{2.5}{12}\eta_1^4 + \frac{.25}{6}\eta_1^3 + \frac{.25}{2}\eta_1^2 \right) + (\eta_3 - \eta_2)\left(\frac{10}{4}\eta_1^4 - \frac{2.5}{3}\eta_1^3 + \frac{.25}{2}\eta_1^2 + .25\eta_1 \right) \right\}$$

$$C_{44} = \alpha e^2 \left\{ \left(\frac{10}{4}\eta_1^4 - \frac{2.5}{3}\eta_1^3 + \frac{.25}{2}\eta_1^2 + .25\eta_1 \right) + \frac{e}{3k_i} \right\}$$

where

$$\eta_{i,j} = \frac{\ell_{i,j}}{b/2\cos\Phi} \qquad i,j = 1,2,3$$

The natural frequencies of the wing calculated from equations (C. 8) and (C. 9) are listed in Table C. 2 for the various nacelle conditions. The forcing functions used in equation (C. 11) were step functions concentrated at stations 1, 2 and 3 which represent a uniform spanwise distribution of force.

The time histories of wing-root bending moment obtained from equation (C. 11) are plotted in Figure C. 2 for different values of nacelle frequency. These results show that the effect of the side-bending vibration of the nacelle is negligible in this particular case. It appears, then, that a gust response analysis need not consider the vibration of a nacelle except possibly for speeds near the airplane flutter speed when the phase shifts between the natural modes of vibration are important.

TABLE C. 2

NATURAL FREQUENCIES OF WING

		k_0	k_1	k_2	k_∞
ω_1	(rad/sec)	7.79	7.41	7.74	7.45
ω_2	(rad/sec)	25.25	8.18	14.28	25.25
ω_3	(rad/sec)	110.92	25.28	25.32	99.06
ω_4	(rad/sec)	-	110.86	110.96	179.05

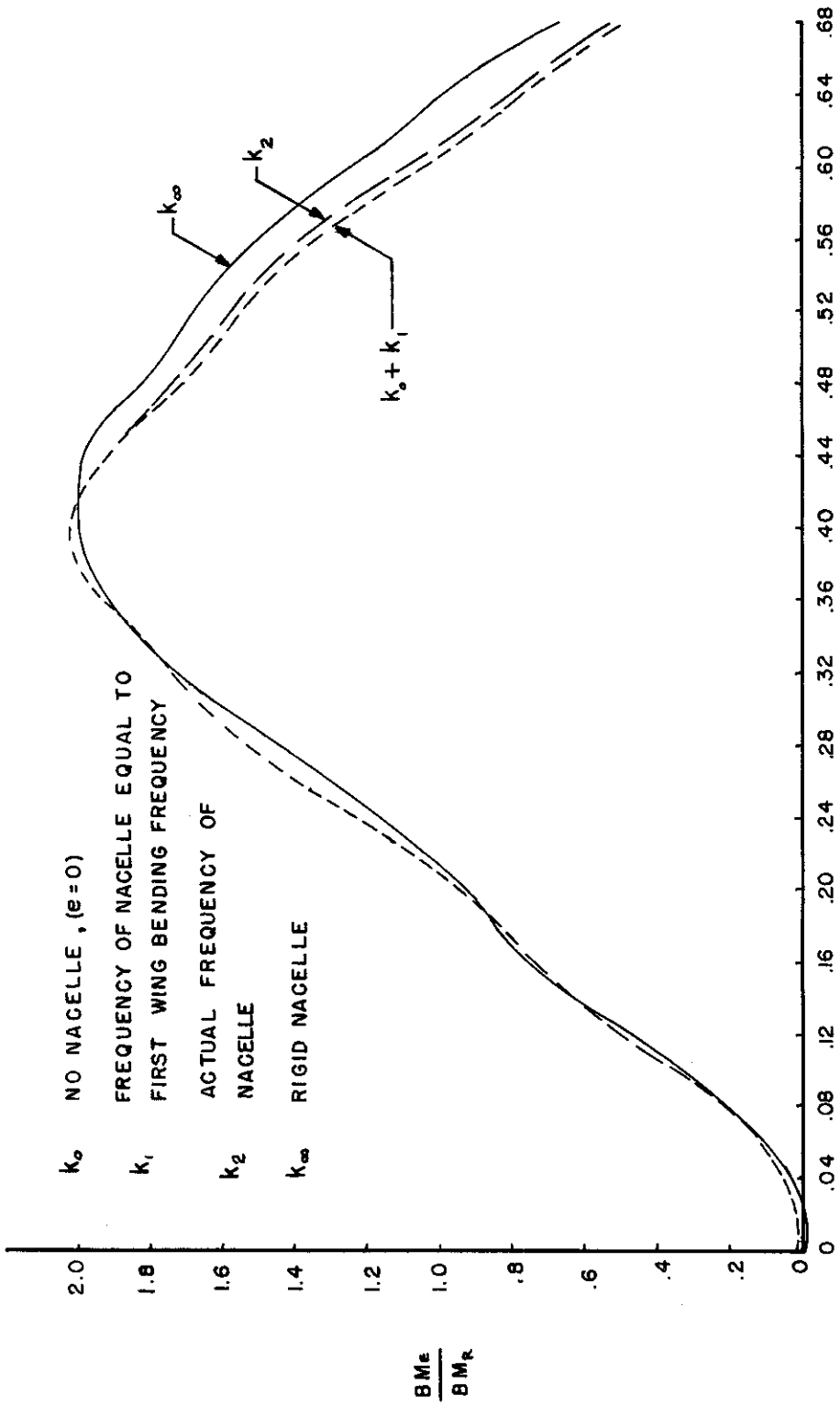

FIGURE C.2 COMPARISON OF WING-ROOT BENDING MOMENTS FOR VARIOUS NACELLE CONDITIONS

APPENDIX D

EFFECT OF VIBRATORY DOWNWASH AT THE HORIZONTAL TAIL

The expressions for the generalized forces derived in Appendix A. 3 are greatly simplified if the lift on the horizontal tail due to the downwash caused by vibrations of the wing can be neglected. The small error in the wing stresses of the example airplane of Section IV introduced by this simplification is illustrated in Figures D. 1 and D. 2. Thus, it appears that this vibratory downwash has only a secondary effect on the stresses in the wing.

In an attempt to determine the generality of the above conclusion, the effect of this simplification on the total lift of the horizontal tail will be found for the example airplane of Section IV when two degrees of freedom, heaving and wing bending, are considered. From equations (A. 8), (A. 16) and (A. 17) this lift is

$$L_t = \tfrac{1}{2}\rho U^2 S_t a_t \int_0^s \varphi(\gamma s - \gamma\sigma)\left\{\tfrac{\bar{c}}{2} b_{00} \overset{11}{\varphi}_0\right\} d\sigma$$
$$- \tfrac{1}{2}\rho U^2 S_t a_t \left(\frac{d\varepsilon}{d\alpha}\right) \sum_{i=1}^{3} \int_0^s \overset{\alpha}{\varphi}_i (s-\sigma)\alpha'_{ti}(\sigma)\, d\sigma$$
$$+ \tfrac{1}{2}\rho U^2 S_t a_t \left\{ \psi_{it}^{10}(s) - \left(\frac{d\varepsilon}{d\alpha}\right) \overset{G}{\varphi}(s) \right\} \qquad \text{(D. 1)}$$

where the functions $\overset{\alpha}{\varphi}_1$, $\overset{\alpha}{\varphi}_2$, $\overset{\alpha}{\varphi}_3$ and $\overset{G}{\varphi}$ are given in Figure A. 2. When quasi-steady damping is used with an efficiency factor of $e = 0.75$ to account for the reduction in damping due to unsteady flow effects, equation (D. 1) can be easily integrated; and the total lift on the tail becomes

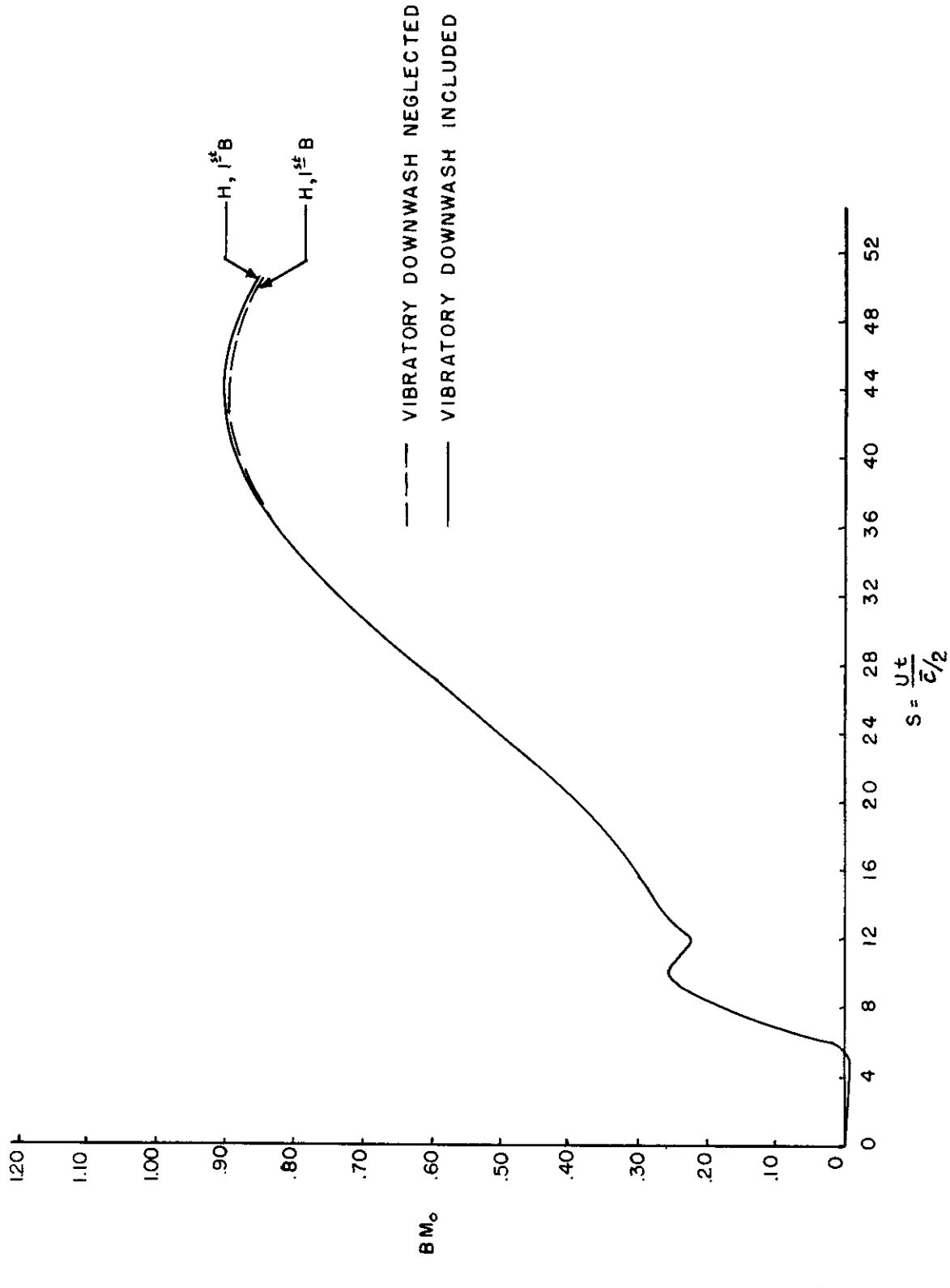

FIGURE D.1 EFFECT OF VIBRATORY DOWNWASH ON WING-ROOT BENDING MOMENT, SHARP-EDGED GUST

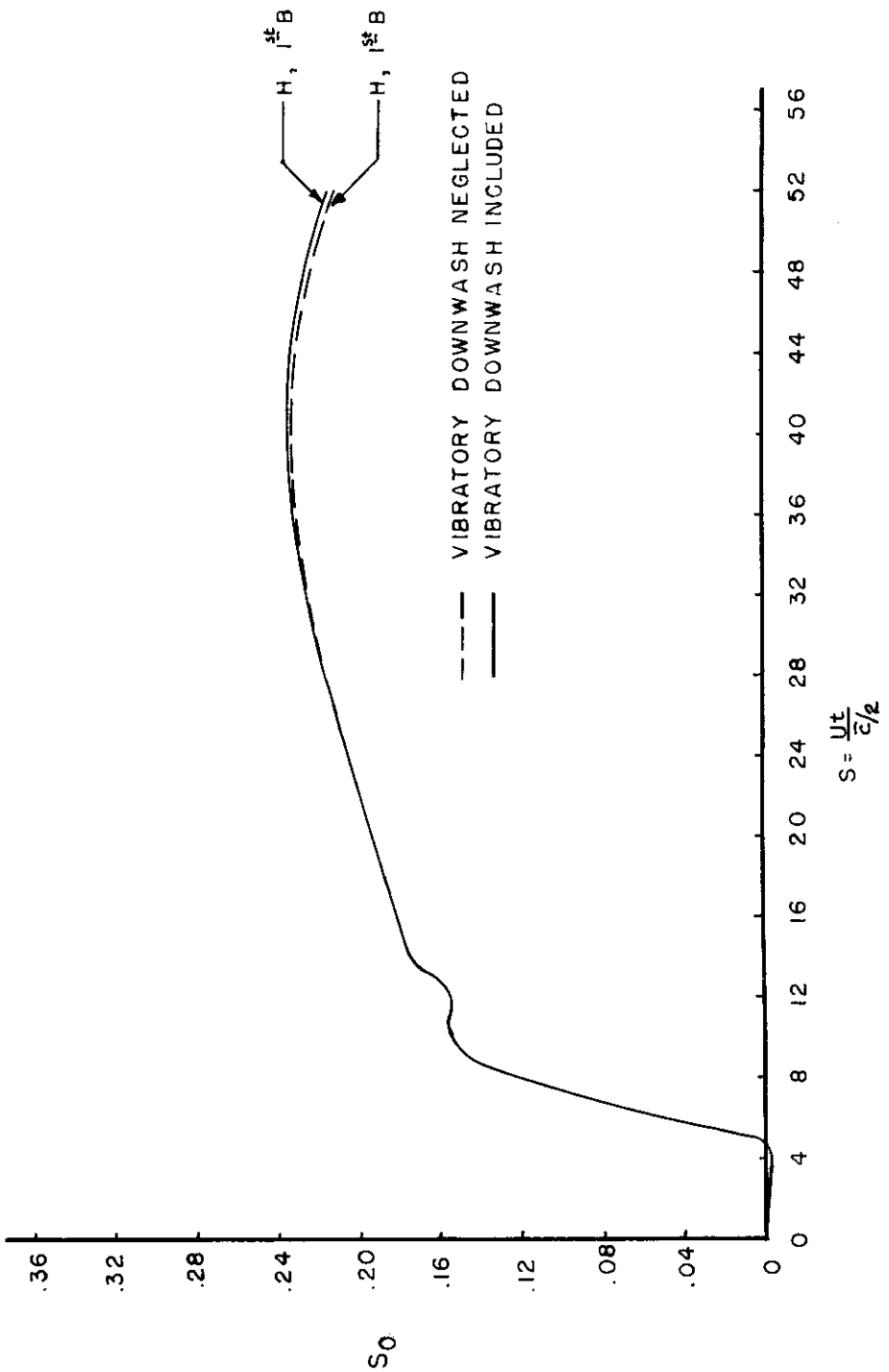

FIGURE D.2 EFFECT OF VIBRATORY DOWNWASH ON WING-ROOT SHEAR, SHARP-EDGED GUST

$$\frac{L_t}{\frac{1}{2}\rho U^2 S_t a_t} = e\,\frac{\bar{c}}{2}\,b_{00}\,\psi_0' - \left(\frac{d\epsilon}{d\alpha}\right)\left\{\frac{\bar{c}}{2}\,b_{00}\,\psi_0' - \bar{h}\,\frac{\bar{c}}{2}\,b_{00}\,\psi_0'(s_n)\right.$$

$$+ \bar{d}\left(\frac{\bar{c}}{2}\,e_3\,\psi_3 + \frac{\bar{c}}{2}\,f_3\,\psi_3' - \frac{\bar{c}}{2}\,e_3\,\psi_3(s_n) - \frac{\bar{c}}{2}\,f_3\,\psi_3'(s_n)\right)$$

$$\left. + \bar{e}\left(\frac{\bar{c}}{2}\,c_3\,\psi_3' - \frac{\bar{c}}{2}\,c_3\,\psi_3'(s_n)\right)\right\} + \psi_{at}^{\alpha_0} - \left(\frac{d\epsilon}{d\alpha}\right)\psi^G \qquad \text{(D.2)}$$

The contribution of the downwash caused by wing vibrations to the total lift on the horizontal tail is shown in Figure D. 3 for independent variations of the wing-mass to airplane-mass ratio and of the reduced frequency, $k_3 = \frac{\omega_3 \bar{c}}{2U}$ of the wing. Although the natural frequency of the wing is a function of its mass when its stiffness is held constant, its reduced frequency can be varied independently by varying the airplane speed, U . The total tail load used in Figure D. 3 is that which occurs at the peak vibratory downwash contribution, and is plotted in Figure D. 4. This vibratory downwash contribution never exceeds 20% of the total tail load which itself has only a small effect on the stresses in the wing.

As explained in Appendix A, the means for taking into account the downwash at the tail due to wing vibrations is very crude because the large spanwise variation in downwash at the tail is not considered. Nevertheless, the results of this Appendix indicate that the effects of vibratory downwash on the tail load may be neglected when computing wing stresses or the motion of the airplane as a whole.

However, the spanwise variation in vibratory downwash at the tail would probably be very important in a dynamic stress analysis of the horizontal tail itself.

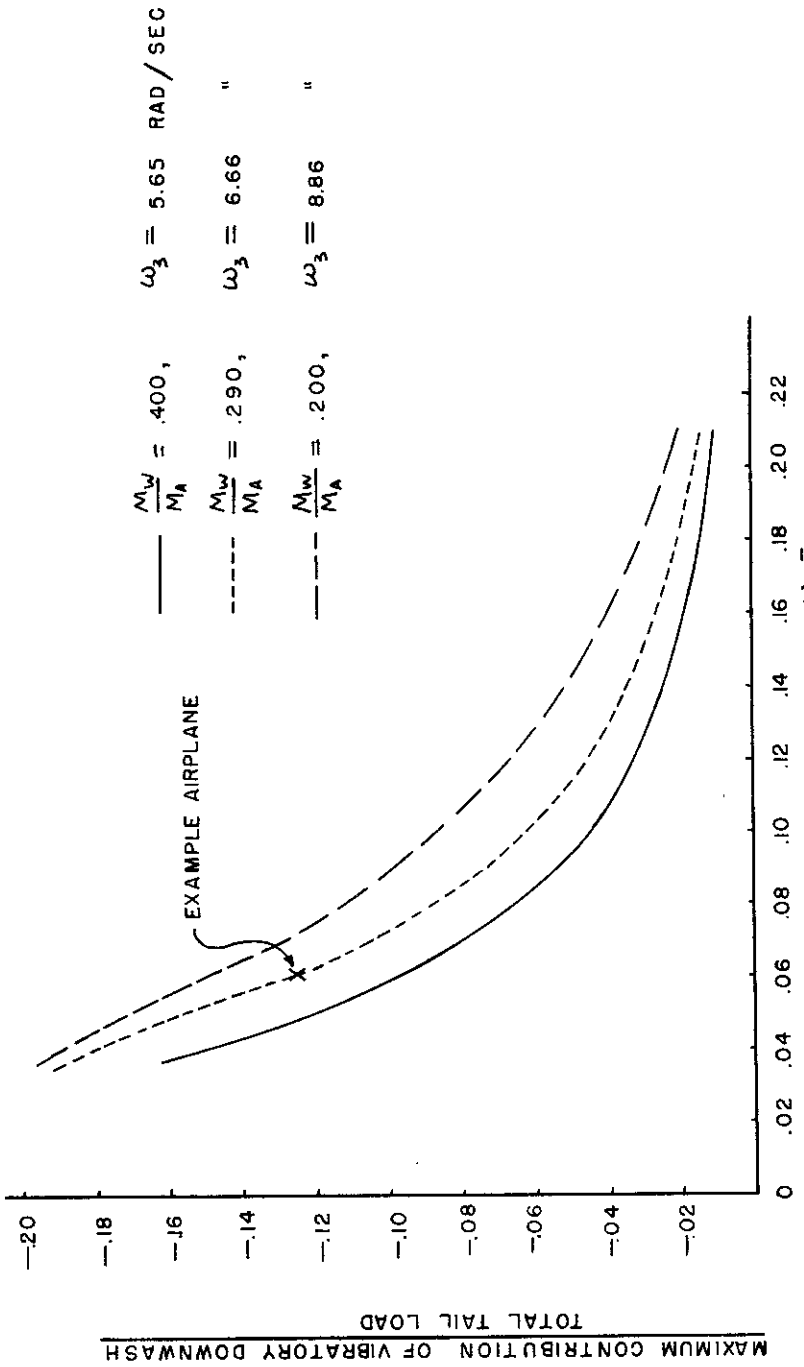

FIGURE D.3 CONTRIBUTION OF VIBRATORY DOWNWASH TO TOTAL TAIL LOAD, SHARP-EDGED GUST

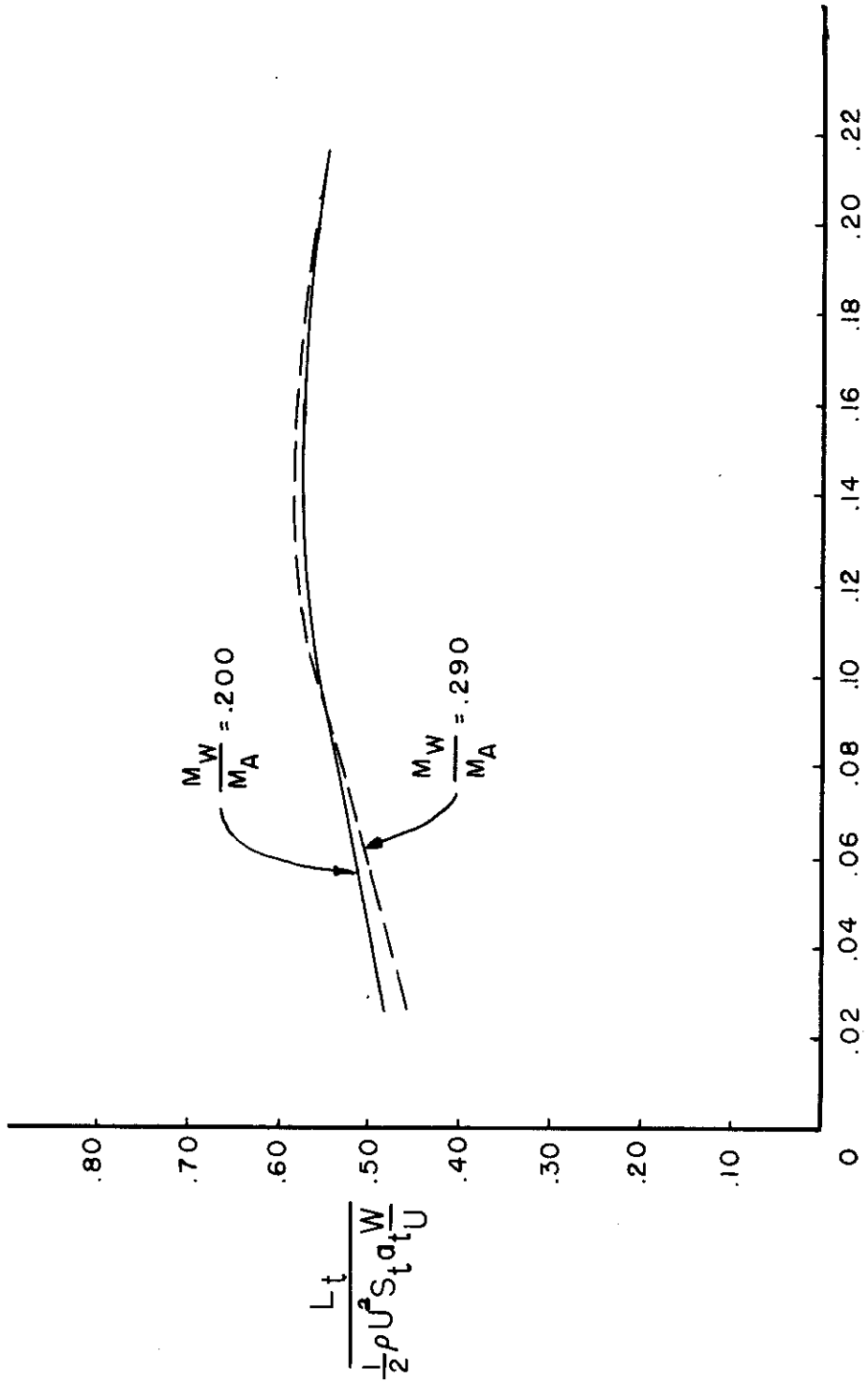

FIGURE D.4 TOTAL LIFT ON HORIZONTAL TAIL, SHARP-EDGED GUST

APPENDIX E

THE CONVERGENCE OF TRANSIENT STRESS METHODS

Due to aerodynamic coupling the solution of the equations of motion for the gust response of flexible airplanes represents the major computing task; however, there is still considerable labor involved in finding the transient stresses after the structural response is known. The analysis presented in the main body of the present report makes use of what might be called the force-summation method of transient stress analysis. In this method, the stress at a point in the structure is obtained by superimposing the stresses due to the external disturbing forces, the inertia forces, and the motion-dependent forces. The purpose of this appendix is to investigate two other methods and to compare their convergence and ease of application with the force summation method.

E. 1 Normal Modes

The three methods are best described in terms of equations of motion which are based on the displacements of normal modes.

$$M_r \ddot{\eta}_r + M_r \omega_r^2 \eta_r = \Pi_r^D(t) + \Pi_r^M(\eta_1, \cdots, \dot{\eta}_1, \cdots, \ddot{\eta}_1, \cdots) \tag{E. 1}$$

where

$r = 1, \cdots, m$ are rigid body modes $(\omega_r = 0)$

$r = m+1, \cdots, n$ are deformation modes

$\eta_r(t)$ is the displacement of r^{th} mode

$\Xi_r^D(t)$ is the generalized force corresponding to the prescribed disturbing force

Ξ_r^M is the generalized force corresponding to the motion dependent forces

The mode displacement method has been described in Reference 15.

The stress at a point in the structure is computed by summing the stresses due to the displacement of each normal mode such that

$$\sigma_i = \sum_{r=m+1}^{n} A_i^{(r)} \eta_r(t) \qquad \text{(E. 2)}$$

where

σ_i is the stress at point i

A_i is the stress at point i due to a unit displacement of the r^{th} normal mode, $\eta_r(t)$

For example, when an airplane wing is considered as a simple beam, the shear at y due a unit displacement of the r^{th} normal mode, $\phi_r(y)$, is

$$A^{(r)}(y) = \omega_r^2 \int_y^{\frac{b}{2}} m(y)\,\phi_r(y)\,dy \qquad \text{(E. 3)}$$

in terms of inertia loadings, or

$$A^{(r)}(y) = EI(y)\,\frac{d^3\phi_r}{dy^3} \qquad \text{(E. 4)}$$

in terms of elastic forces.

The mode acceleration method is also described in Reference 15. This method is easily derived by rearranging the equations of motion as

$$\ddot{\eta}_r(t) = \frac{\Pi_r^D}{\omega_r^2 M_r} + \frac{\Pi_r^M}{\omega_r^2 M_r} - \frac{\ddot{\eta}_r}{\omega_r^2} \tag{E.5}$$

The substitution of this into equation (E. 2) yields

$$\sigma_i = \sum_{r=m+1}^{n} A_i^{(r)} \frac{\Pi_r^D}{\omega_r^2 M_r} + \sum_{r=m+1}^{n} A_i^{(r)} \left(\frac{\Pi_r^M}{\omega_r^2 M_r} - \frac{\ddot{\eta}_r}{\omega_r^2} \right) \tag{E.6}$$

The first summation represents the stress resulting from the static application of the disturbing forces, and it can be computed more accurately by a static stress analysis which in effect carries the summation to $r = \infty$. Thus, equation (E. 6) can be rewritten as

$$\sigma_i = (\sigma_i)_{STATIC} + \sum_{r=m+1}^{n} A_i^{(r)} \left(\frac{\Pi_r^M}{\omega_r^2 M_r} - \frac{\ddot{\eta}_r}{\omega_r^2} \right) \tag{E.7}$$

which expresses the mode acceleration method. Since Π_r^M itself is a summation of integrated motion forces, the summation in equation (E. 7) is very laborious to calculate, particularly, when unsteady aerodynamics is taken into account. However, Professor J. W. Mar of M. I. T. has pointed out that the mode acceleration method can be greatly simplified by again rearranging the equations of motion in the form

$$\ddot{\eta}_r - \frac{\Pi_r^D}{\omega_r^2 M_r} = \frac{\Pi_r^M}{\omega_r^2 M_r} - \frac{\ddot{\eta}_r}{\omega_r^2} \tag{E.8}$$

The substitution of this expression into equation (E. 7) results in an alternative version of the mode acceleration method:

$$\sigma_i = (\sigma_i)_{STATIC} + \sum_{r=m+1}^{n} A_i^{(r)} \left(\ddot{\eta}_r - \frac{\Pi_r^D}{\omega_r^2 M_r} \right) \tag{E.9}$$

In this form, the unwieldly motion terms have been eliminated.

The force summation method for the case of shear in a wing considered as a simple beam can be expressed as

$$S(y) = \int_y^{\frac{b}{2}} \ell^D(y,t)\, dy + \int_y^{\frac{b}{2}} \ell^M(y,t)\, dy - \sum_{r=1}^{n} \ddot{\eta}_r \int_y^{\frac{b}{2}} m(y)\, \phi_r(y)\, dy \tag{E.10}$$

where

$\ell^D(y,t)$ is the local disturbing load

$\ell^M(y,t)$ is the local load due to motion

To compare the convergence of this method with that of the mode acceleration method, $\ell^M(y,t)$ can be expanded into a series of normal loadings by considering the definition of the generalized motion forces. Thus,

$$\ell^M(y,t) = \sum_{r=1}^{\infty} \frac{\Pi_r^M}{M_r} m(y)\, \phi_r(y) \tag{E.11}$$

When this asummation is substituted into equation (E. 10) there results

$$S(y) = \int_y^{\frac{b}{2}} \ell^D(y,t)\, dy + \sum_{r=1}^{\infty} \frac{\Pi_r^M}{M_r} \int_y^{\frac{b}{2}} m(y)\, \phi_r(y)\, dy - \sum_{r=1}^{n} \ddot{\eta}_r \int_y^{\frac{b}{2}} m(y)\, \phi_r(y)\, dy \tag{E.12}$$

or

$$S(y) = [S(y)]_{STATIC} + \sum_{r=m+1}^{\infty} \frac{\Xi_r^M}{\omega_r^2 M_r} A^{(r)}(y) - \sum_{r=m+1}^{\infty} \frac{\ddot{\eta}_r}{\omega_r^2} A^{(r)}(y) \qquad \text{(E. 13)}$$

where

$$[S(y)]_{STATIC} = \int_y^{\frac{b}{2}} \ell^D(y,t)\, dy + \sum_{r=1}^{m} \left(\frac{\Xi_r^M}{M_r} - \ddot{\eta}_r \right) \int_y^{\frac{b}{2}} m(y)\, \phi_r(y)\, dy$$

$$= \int_y^{\frac{b}{2}} \ell^D(y,t)\, dy - \sum_{r=1}^{m} \frac{\Xi_r^D}{M_r} \int_y^{\frac{b}{2}} m(y)\, \phi_r(y)\, dy \qquad \text{(E. 14)}$$

A comparison of equation (E. 13) with (E. 7) reveals that the only difference between the force summation and mode acceleration methods lies in the summation giving the stress due to motion forces; and, since the force summation method carries this expansion to infinity, it is the more accurate method. Also, equation (E. 14) shows that in the mode acceleration method the static-stress term must include the rigid-body inertia forces which would result from a static application of the disturbing force, since

$$\frac{\Xi_r^D}{M_r} = \left(\ddot{\eta}_r \right)_{STATIC} \quad , \text{ when} \quad r = 1, \ldots, m \qquad \text{(E. 15)}$$

From convergence considerations, the preceding analysis has shown that the accuracy of the mode acceleration method lies somewhere between that of the force summation method and the mode displacement method depending upon the

relative importance of the disturbing forces and the motion forces. In its alternative form, the mode acceleration method is much easier to apply than the force summation method and only slightly more difficult than the mode displacement method.

For a numerical comparison, each of the three methods have been applied to an idealized wing consisting of a uniform beam with a center mass to represent the fuselage. The airplane has a fuselage mass equal to the total wing mass. The equations of motion for this system are

$$M \ddot{\eta}_0 = \Xi^D_0(t) + \Xi^M_0 \tag{E. 16}$$

for the free-body vertical motion, and

$$M \ddot{\eta}_r + M \omega_r^2 \eta_r = \Xi^D_r(t) + \Xi^M_r \tag{E. 17}$$

for the normal modes in bending. The bending modes are so normalized that the generalized masses are equal to the total mass of the airplane. The airplane is subjected to a step-load gust constant along the span so that the disturbing force is

$$\ell^D(t) = \tfrac{1}{2} \rho U^2 c a_w \frac{w}{U} 1(t) \tag{E. 18}$$

The motion force is given by quasi-steady aerodynamics with an efficiency factor e to account for the loss in lift due to unsteady flow effects, such that

$$\ell^M = -\tfrac{1}{2} \rho U c e a_w \sum_{r=0}^{n} \phi_r(y) \dot{\eta}_r \tag{E. 19}$$

The natural frequencies and mode shapes for this wing were obtained from Reference 16 in which the classical solution of a free-free beam with a central mass is given. The equations of motion were put in dimensionless form by defining dimensionless mass, frequency, and time parameters which were given typical values of

$$\mu = \frac{2M}{\rho c S a_w} = 40.9$$

$$k = \frac{c\omega}{2U} \qquad (k_1 = 0.0505)$$

$$s = \frac{2U}{c} t \qquad \left(\frac{2U}{c} = 144 \text{ per sec.}\right)$$

Equations (E. 16) and (E. 17) were solved by means of Laplace tranforms for one and two vibrational degrees of freedom. The details of this solution and of the application of the three stress methods are given in Reference 17.

The time histories of the bending moment at the wing root obtained by the three methods are shown in Figures E. 1 and E. 2. Figure E. 1 represents results for one vibrational mode and Figure E. 2 for two vibration modes; in both figures, the reference bending moment is the maximum bending moment for an equivalent rigid airplane. These results illustrate the close agreement between the force summation and mode acceleration methods; in fact, when two vibration modes are used, the two methods almost coincide. The spanwise variation in peak bending moment is shown in Figures E. 3 and E. 4; and again the close agreement between the force summation and mode acceleration methods is illustrated. Similar results for the shear distribution in the wing were obtained in Reference 17.

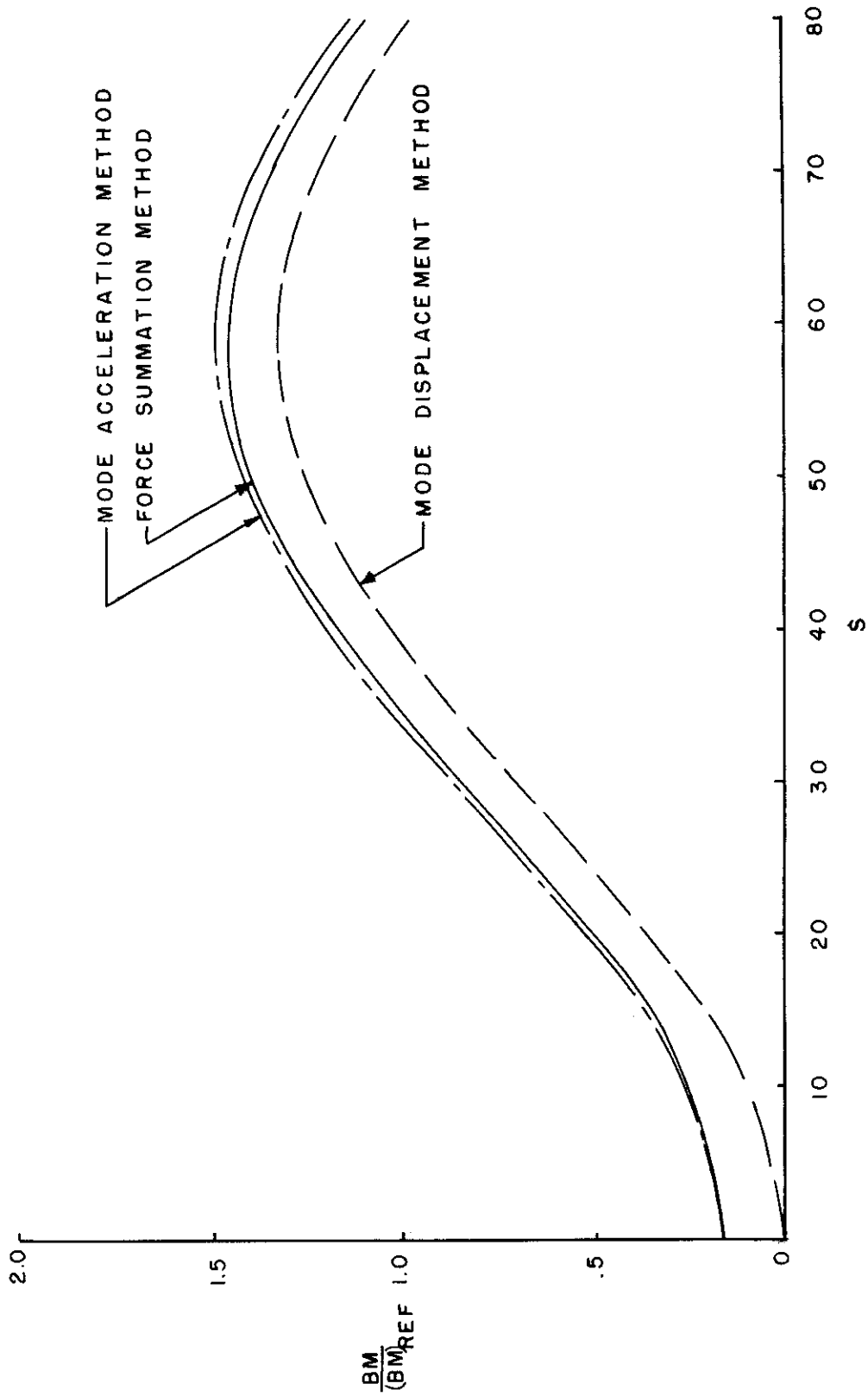

FIGURE E.1 COMPARISON OF STRESS METHODS, WING ROOT BENDING MOMENT, ONE NORMAL BENDING MODE

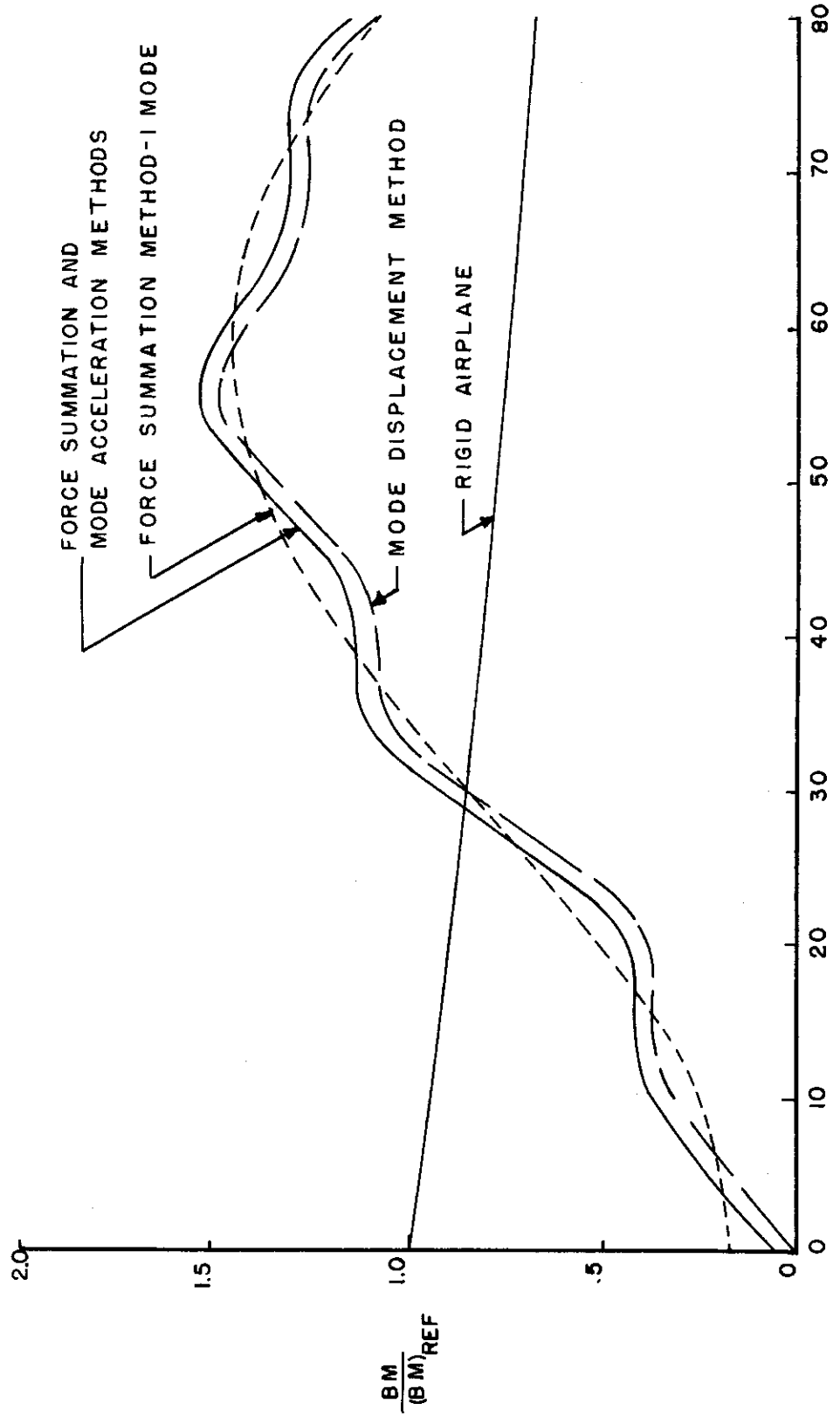

FIGURE E.2 COMPARISON OF STRESS METHODS, WING-ROOT BENDING MOMENT, TWO NORMAL BENDING MODES

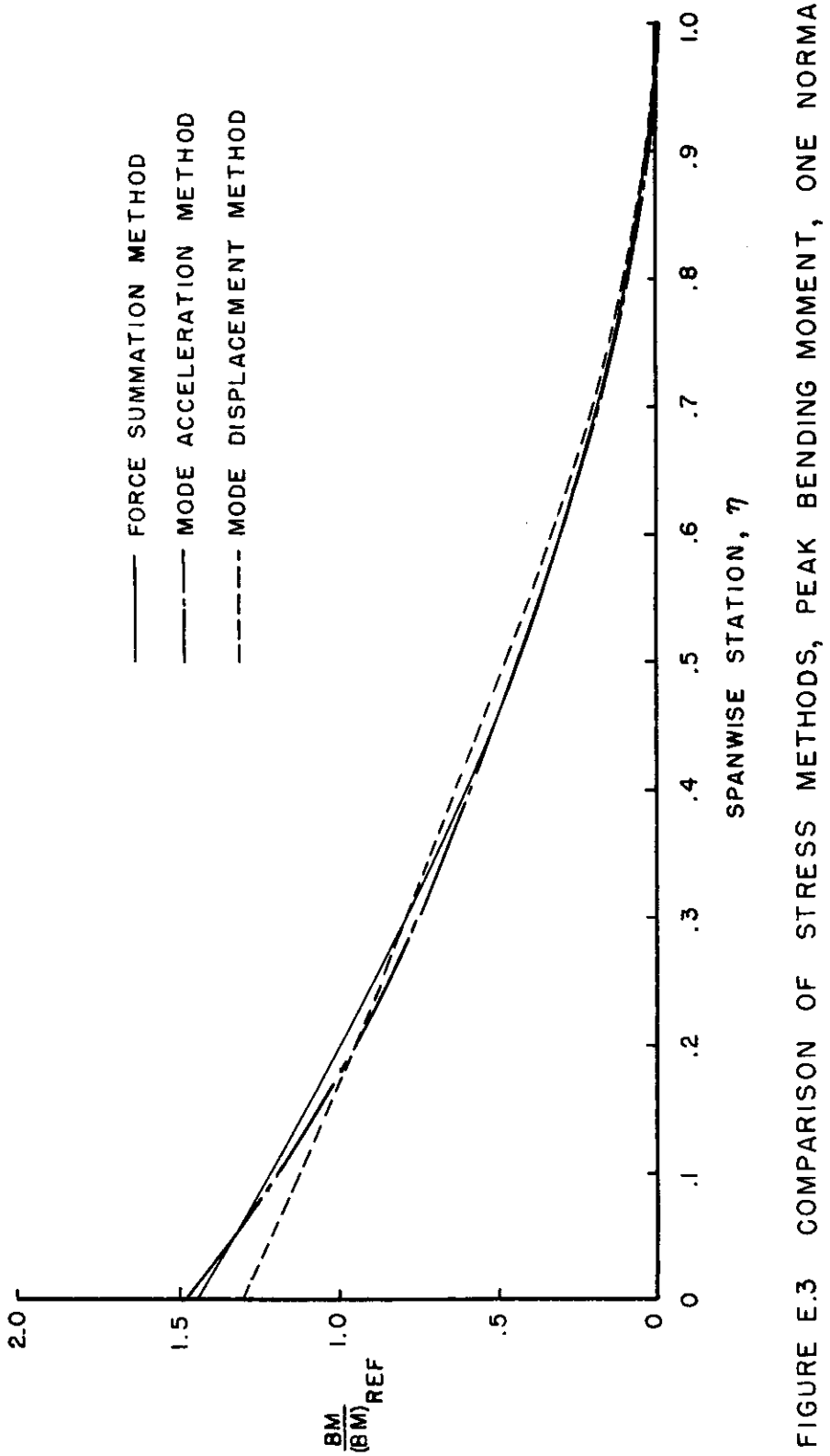

FIGURE E.3 COMPARISON OF STRESS METHODS, PEAK BENDING MOMENT, ONE NORMAL BENDING MODE

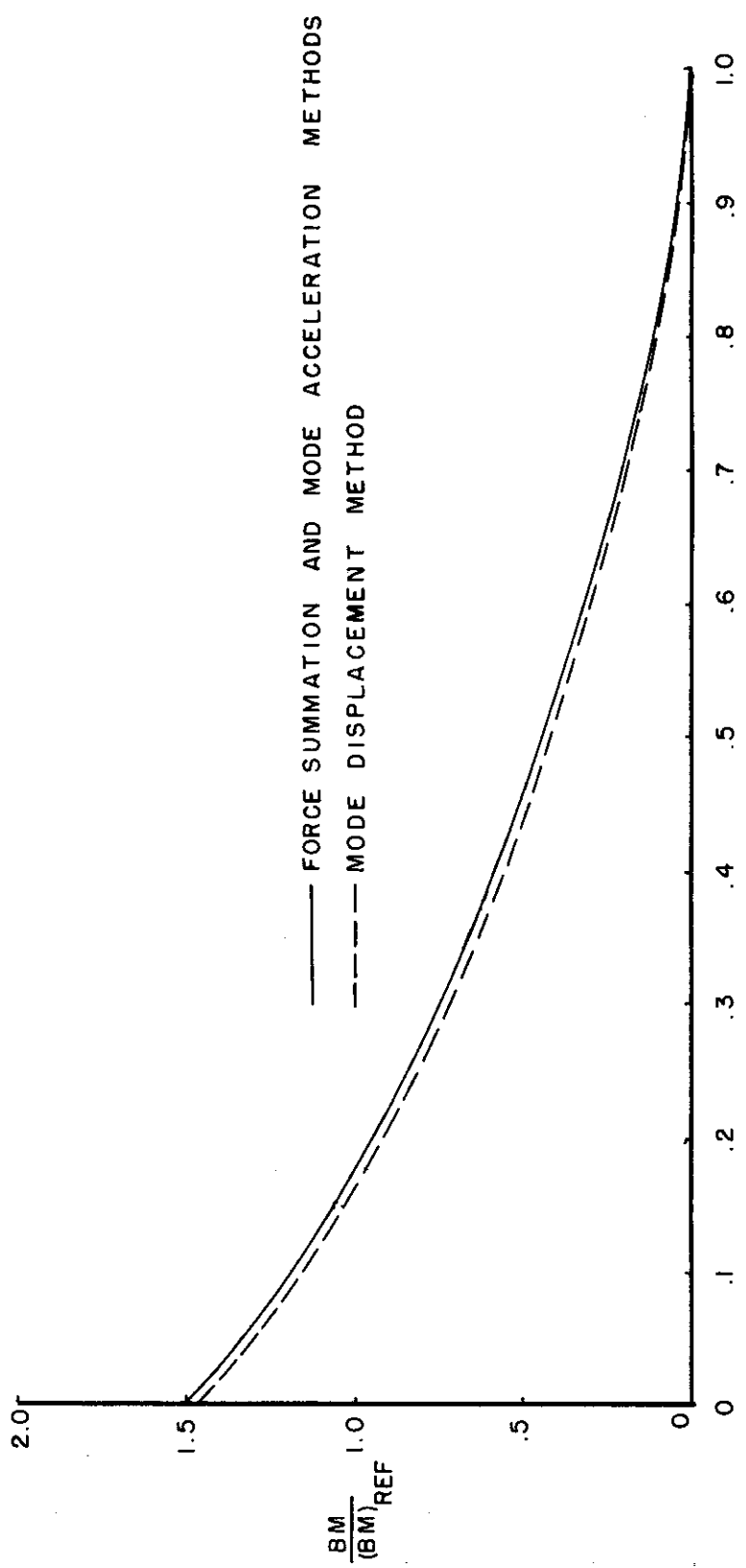

FIGURE E.4 COMPARISON OF STRESS METHODS, PEAK BENDING MOMENT, TWO NORMAL BENDING MODES

E. 2 Assumed Modes

When the normal modes of an airplane are not known, it is often more convenient to derive equations of motion similar to equations (E. 1) for assumed modes of deformation. This can be done by the application of the principle of virtual work through the form known as Lagrange's equations (Reference 15); and equations of the following form result:

$$\sum_{j=1}^{m} M_{rj}\ddot{q}_j = Q_r^D(t) + Q_r^M \qquad (r = 1, \cdots, m) \tag{E. 20}$$

$$\sum_{j=1}^{n} M_{rj}\ddot{q}_j + \sum_{j=m+1}^{n} K_{rj} q_j = Q_r^D(t) + Q_r^M \qquad (r = m+1, \cdots, n) \tag{E. 21}$$

It will be noted that these equations are more complicated than equations (E. 1) because of the inertial and elastic coupling terms; however, when there is coupling between the normal-mode equations of motion due to motion forces, these equations are not much more difficult to solve. The convergence of assumed-mode solutions usually compares favorably with that of normal-mode solutions depending upon how well the assumed modes satisfy the boundary conditions and upon their completeness in the mathematical sense.

The mode displacement method for assumed modes is the same as for normal modes and is expressed by

$$\sigma_i = \sum_{r=m+1}^{n} A_i^{(r)} q_r(t) \tag{E. 22}$$

However, equations (E. 3) and (E. 4) are no longer equivalent; and the shear in a simple beam resulting from a unit displacement of the r^{th} assumed mode must be found from

$$A_i^{(r)} = EI(y) \frac{d^3\phi_r}{dy^3} \tag{E. 23}$$

Since this expression involves the third derivative (the second derivative for bending moments) of the assumed function, it seems doubtful that this method can converge very rapidly.

The mode acceleration method for assumed modes can be derived by arbitrarily expressing the displacement of the r^{th} mode as

$$q_r = (q_r)_{STATIC} + \left[q_r - (q_r)_{STATIC} \right] \tag{E. 24}$$

When this is substituted into equation (E. 22), there results

$$\sigma_i = (\sigma_i)_{STATIC} + \sum_{r=m+1}^{n} A_i^{(r)} \left[q_r - (q_r)_{STATIC} \right] \tag{E. 25}$$

The static stress is the same as in the normal mode case since it does not require any knowledge of the deformation modes. The static displacements, however, are more difficult to obtain and must be found from the following set of simultaneous equations:

$$\sum_{j=1}^{m} M_{rj} (\ddot{q}_j)_{STATIC} + \sum_{j=m+1}^{n} K_{rj} (q_j)_{STATIC} = Q_r^o(t) \quad (r = m+1, \cdots, n) \tag{E. 26}$$

There is obviously considerable simplification if the modes are chosen so that there is no inertial coupling between the rigid-body and vibration modes and no elastic coupling in the elastic modes. In this case, equation (E. 26) reduces to

$$(q_r)_{STATIC} = \frac{Q_r^P(t)}{K_{rr}} \qquad \text{(E. 27)}$$

As in the normal mode case the mode acceleration method will converge more rapidly than the mode displacement method because the static portion of the stress is accounted for more accurately.

The force summation method for assumed modes is exactly the same as that for normal modes (equation (E. 10)). The convergence of this method depends upon the particular deformation modes which are assumed; but, when the same assumed modes are used, it should be more accurate than the mode acceleration method because it considers the motion-dependent forces explicitly and because it does not require spanwise derivatives of the assumed modes.

Each of the three methods using assumed modes have been applied to the idealized airplane described in Appendix E. 1. The first symmetrical wing bending mode was taken as

$$\phi_1(\eta) = C_1 + C_2 \eta^2 \qquad \text{(E. 28)}$$

The coefficients C_1 and C_2 were determined from the following conditions:

(a) Condition that $\phi_1(\eta)$ is orthogonal to the rigid-body displacement

$$\int_0^1 m(\eta)\, \phi_1(\eta)\, d\eta = 0$$

(b) Condition that the generalized mass is equal to the total mass of the airplane

$$b \int_0^1 m(\eta)\, \phi_1^2(\eta)\, d\eta = M$$

The second symmetrical wing bending mode was taken as

$$\phi_2(\eta) = C_1 + C_2 \eta^2 + C_3 \eta^3 \qquad \text{(E. 29)}$$

where the coefficients were again determined from conditions (a) and (b) and in addition from either

(c) Condition that there is no inertial coupling between the vibration modes

$$\int_0^1 m(\eta)\, \phi_1(\eta)\, \phi_2(\eta)\, d\eta = 0$$

or

(d) Condition that there is no elastic coupling between the vibration modes

$$\int_0^1 EI\, \frac{d^2\phi_1}{d\eta^2}\, \frac{d^2\phi_2}{d\eta^2}\, d\eta = 0$$

The mode shapes so obtained are compared with the equivalent normal modes in Figures E. 5 and E. 6. The assumed modes are very similar to the normal modes except for the case where elastic coupling has been eliminated; however, the two assumed second bending modes results in the same stresses because they are linear combination of each other, that is,

$$\phi_2^{(d)}(\eta) = K_1 \phi_2^{(c)}(\eta) + K_2 \phi_1(\eta) + K_3 \phi_0(\eta)$$

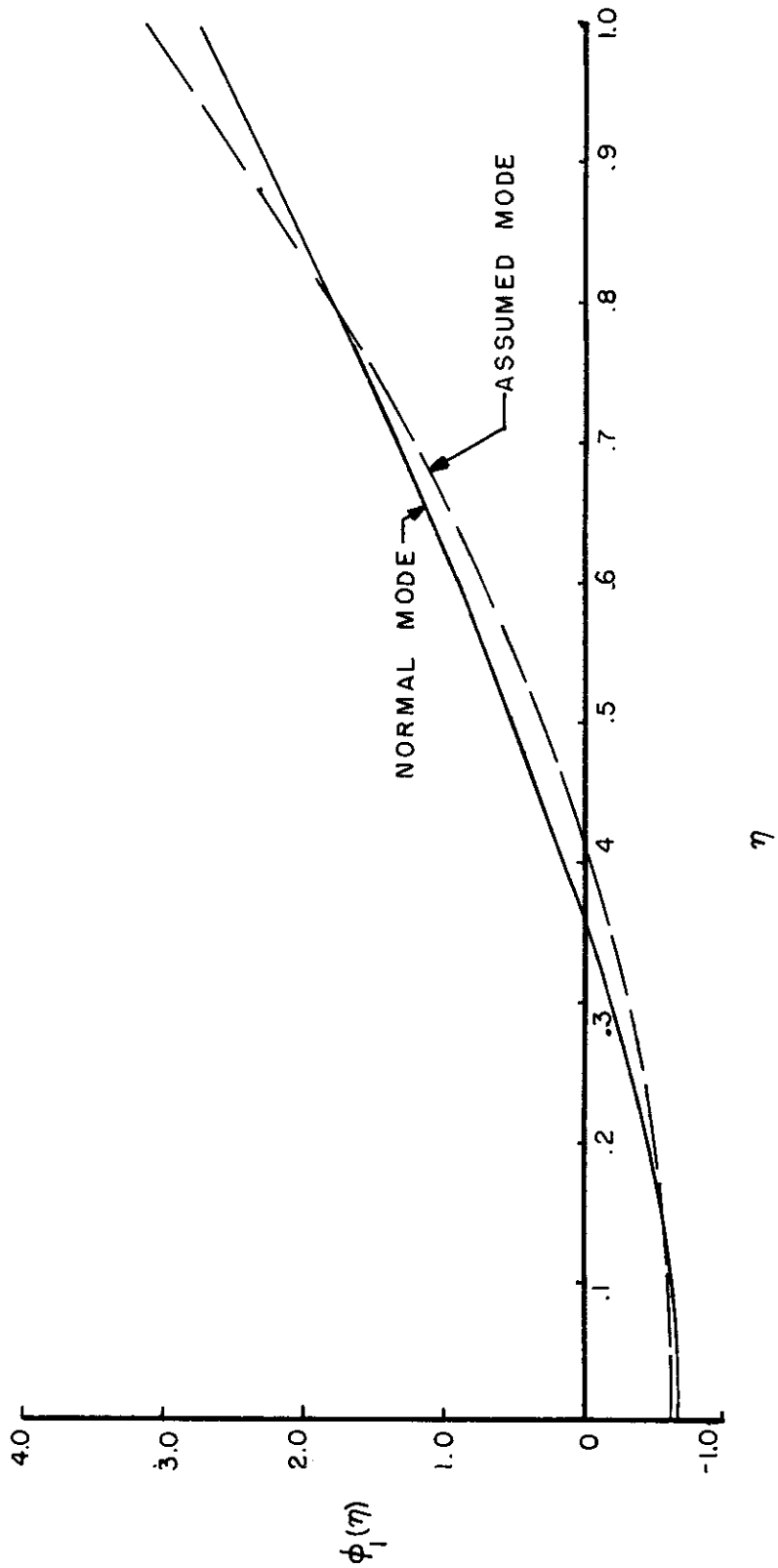

FIGURE E.5 COMPARISON OF NORMAL AND ASSUMED FIRST SYMMETRICAL WING BENDING MODES

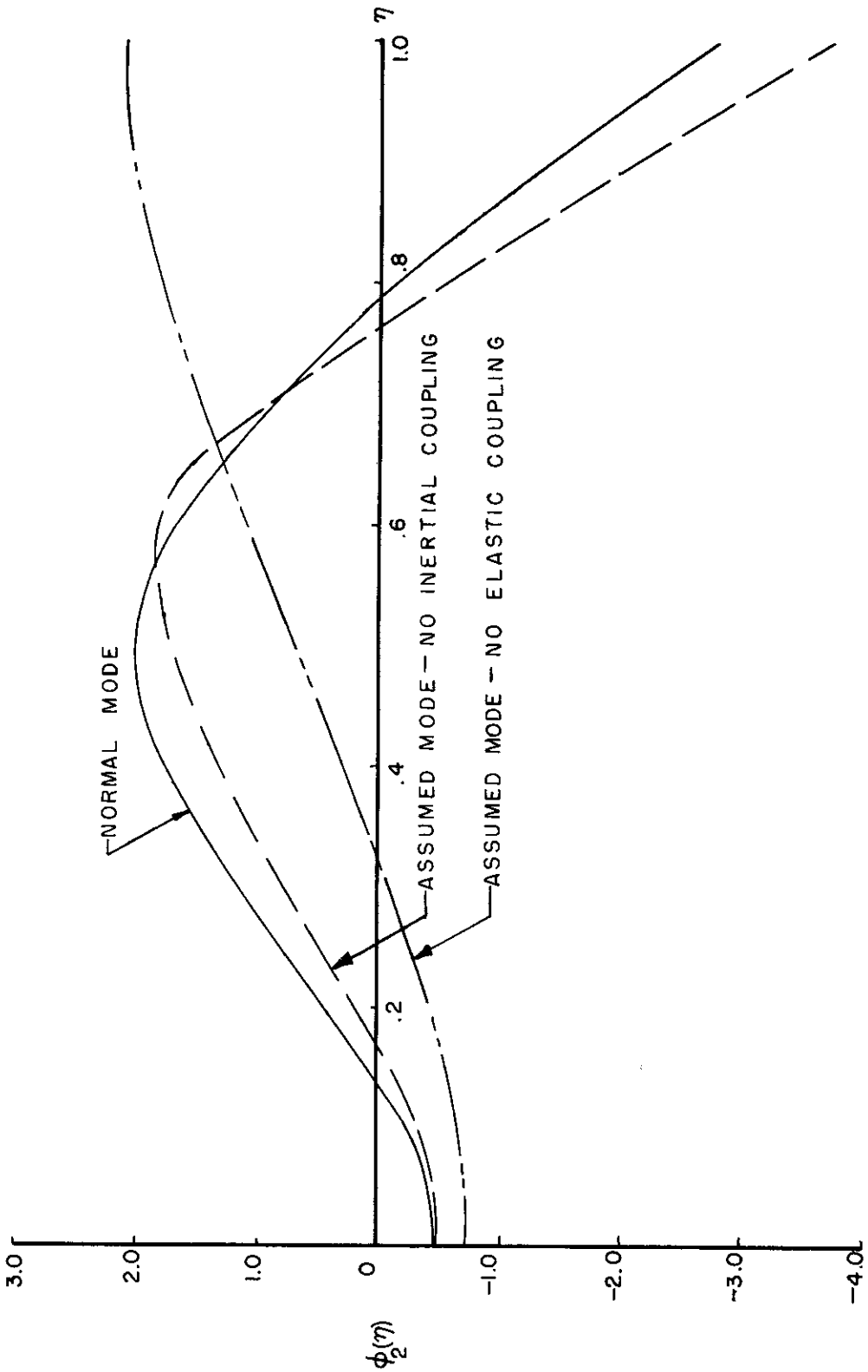

FIGURE E.6 COMPARISON OF NORMAL AND ASSUMED SECOND SYMMETRICAL WING BENDING MODES

Furthermore, when condition (d) is used, the mode acceleration method is simpler because equation (E. 27) can be used rather than equation (E. 26).

The time histories of the bending moment at the wing root obtained by using the assumed modes of deformation are shown in Figures E. 7 and E. 8. By comparing these results with the normal-mode results of Figures E. 1 and E. 2, one can see that there is somewhat more dispersion among the three stress methods when assumed modes are used; although the agreement between the mode-acceleration and force-summation methods is still quite satisfactory. Similar favorable results are presented in Reference 17 for other spanwise stations. A comparison of assumed-mode with normal-mode results is shown in Figure E. 9; and the time histories of wing-root bending moment are in good agreement, except that the second bending frequency for the assumed mode case is slightly higher. This agreement is quite surprising since the assumed modes did not satisfy the boundary conditions at the wing tip (zero shear and zero bending moment).

E. 3 Conclusions

By considerations of convergence and by numerical examples the utility of the mode acceleration method for computing transient stresses has been demonstrated. Even when motion forces are present, this method in its alternative form has a simplicity approaching that of the mode displacement method while maintaining an accuracy approaching that of the force summation method. It has also been shown that the mode acceleration method can easily be applied to systems described by assumed modes of vibration if these modes are properly chosen. However, when a limited

number of modes are used, the mode acceleration method for assumed modes may not always represent a distinct improvement over the mode displacement method because spanwise derivatives of the assumed functions are still required.

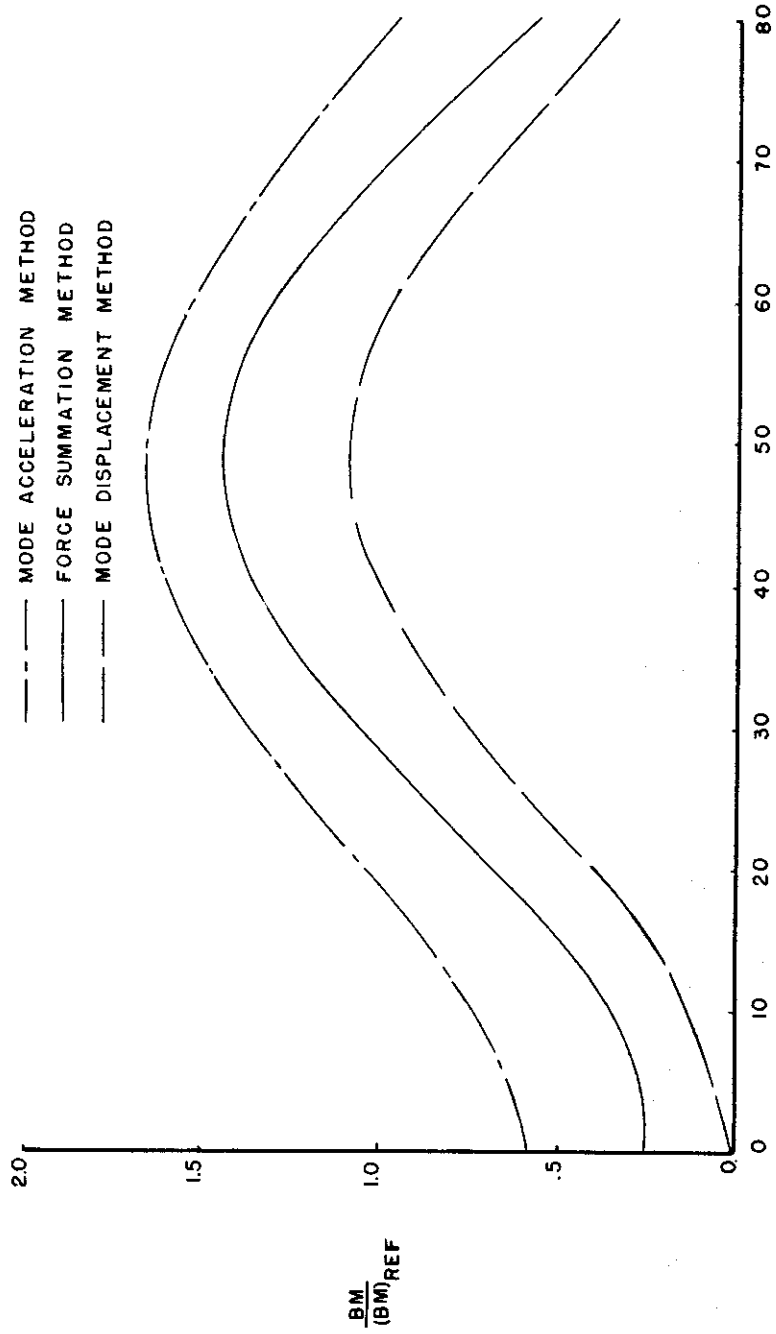

FIGURE E.7 COMPARISON OF STRESS METHODS, WING ROOT BENDING MOMENT, ONE ASSUMED BENDING MODE

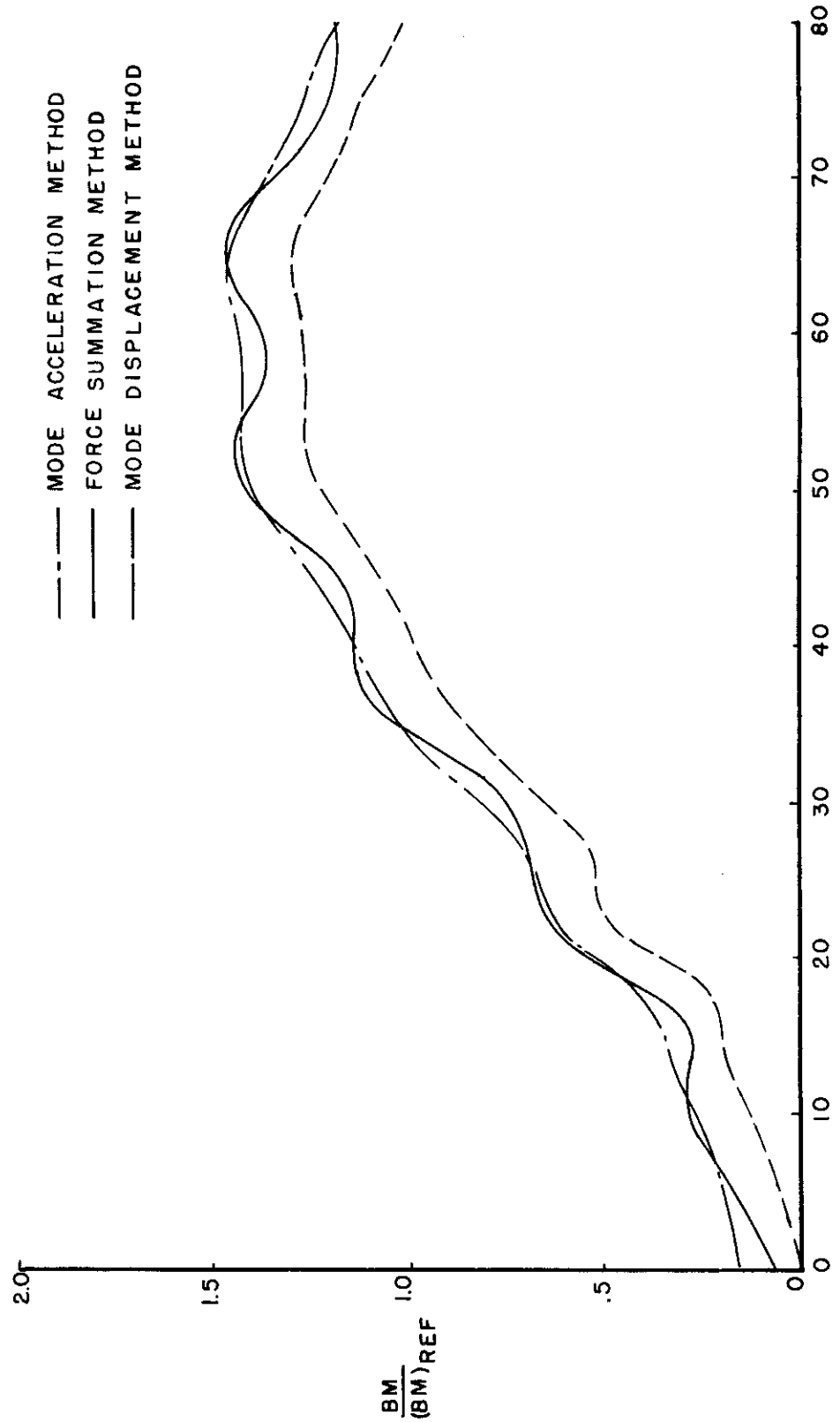

FIGURE E.8 COMPARISON OF STRESS METHODS, WING ROOT BENDING MOMENT, TWO ASSUMED BENDING MODES

FIGURE E.9 COMPARISON OF ASSUMED-MODE WITH NORMAL-MODE RESULTS, WING ROOT BENDING MOMENT, FORCE SUMMATION METHOD

APPENDIX F

INVESTIGATION OF OPTIMUM NACELLE LOCATION

The location of a heavy concentrated mass such as a power-plant nacelle or an external fuel tank near the wing tip of an airplane often has a beneficial effect on the wing stresses due to flight loads because the stresses due to the inertia of the concentrated mass tend to cancel those due to the applied air loads. However, the question arises as to whether the dynamic stresses are increased by the presence of this concentrated mass when the wing is subjected to suddenly applied air loads. An attempt is made in this appendix to find the effects of varying the spanwise location of a heavy concentrated mass on the dynamic response of an unswept wing.

A simplified unswept-wing airplane will be used as an example. The spanwise mass distribution of the half-airplane is illustrated in Figure F. 1. This consists of the fuselage mass M_F, a concentrated mass M_c located at a distance y_c from the airplane center line, and the distributed mass of the wing $m_D(y)$. The distributed mass is linearly tapered and is given by

$$m_D(y) = m_D(0)\left(1 - \frac{3}{4}\frac{y}{b/2}\right) \tag{F. 1}$$

$$m_D(\eta) = m_D(0)\left(1 - \frac{3}{4}\eta\right) \tag{F. 2}$$

where

$$\eta = \frac{y}{b/2} \tag{F. 3}$$

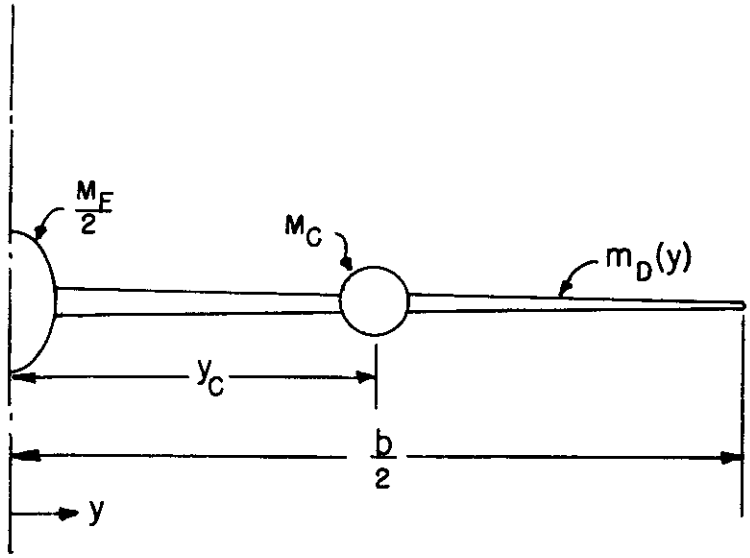

FIGURE F.1 SPANWISE MASS DISTRIBUTION OF EXAMPLE AIRPLANE

Furthermore, the concentrated mass is set equal to the distributed mass of the half-wing, i.e.,

$$M_c = \int_0^{\frac{b}{2}} m_0(y)\, dy \tag{F.4}$$

Therefore,

$$\frac{M_c}{M} = \frac{1}{4}\,\frac{M_w}{M} \tag{F.5}$$

and

$$\frac{M_F}{M} = 1 - \frac{M_w}{M} \tag{F.6}$$

where

M_w is the total mass of the wing

M is the total mass of the airplane

Thus, the spanwise mass distribution of the airplane can be specified by the two parameters $\frac{M_w}{M}$ and η_c, where

$$\eta_c = \frac{y_c}{b/2} \tag{F.7}$$

The wing is linearly tapered with a taper ratio of one half such that the chord distribution is given by

$$c = \frac{4}{3}\bar{c}\left(1 - \frac{1}{2}\eta\right) \tag{F.8}$$

where $\bar{c}$ is the mean geometric chord.

The stiffness distribution is

$$EI(\eta) = EI(.5)(4 - 6\eta) \quad , \text{when} \quad \eta \leq .5$$

$$= EI(.5)\frac{1}{8\eta^3} \quad , \text{when} \quad \eta \geq .5 \tag{F.9}$$

The approximate method of Reference 4 is used to find the response of the wing to a suddenly applied distributed load. In this reference, the following equation is derived:

$$\ddot{q}_1 + 2\zeta_2\dot{q}_1 + q_1 = \Phi_1\ddot{q}_0(\tau) \tag{F.10}$$

where

q_1 is the displacement of the first normal bending mode, $\phi_1(\eta)$, which is so normalized that the generalized mass is equal to the total mass of the airplane

$\ddot{q}_0$ is the acceleration of the center of gravity of the deformed airplane

$$\Phi_1 = \int_0^1 \frac{c(\eta)}{\bar{c}} \phi_1(\eta)\, d\eta \qquad \text{(F. 11)}$$

$$\mathcal{J}_2 = \frac{e}{2\mu k_1} \int_0^1 \frac{c(\eta)}{\bar{c}} \phi_1^2(\eta)\, d\eta \qquad \text{(F. 12)}$$

$$\mu = \frac{2M}{\rho a_w \bar{c} S} \qquad \text{(F. 13)}$$

$$k_1 = \frac{\bar{c}\omega_1}{U} \qquad \text{(F. 14)}$$

ω_1 is the natural frequency of the first normal bending mode

e is the efficiency factor to account for unsteady flow effects

The prime mark indicates differentiation with respect to τ, where

$$\tau = \omega_1 t$$

The derivation of equation (F. 10) in Reference 4 includes the following assumptions:

1. The unsteady air forces are given by quasi-steady aerodynamic theory with an efficiency factor e to account for the reduction due to unsteady flow effects.

2. The spanwise distribution of lift is given by strip theory.

3. Only the first bending vibration mode of the wing is excited.

4. The center-of-gravity acceleration, $\ddot{q}_0$, is the same as that of a rigid airplane; i.e., the coupling of the elastic mode to the rigid-body degree of freedom can be neglected with only a small error as shown in Reference 4.

In order to apply equation (F. 10) to the present problem, ω_1, and ϕ_1 must be found for the mass and stiffness characteristics described by equations (F. 2) through (F. 9). It would be very difficult to compute them exactly; but, Reference 4 shows that, for existing aircraft, the fundamental bending mode can be approximated by

$$\phi_1(\eta) = \phi_1(0) + \left[\phi_1(1) - \phi_1(0)\right]\eta^2 \tag{F. 15}$$

where the coefficients $\phi_1(1)$ and $\phi_1(0)$ are determined from the following two conditions:

(a) Condition that $\phi_1(\eta)$ is orthogonal to the rigid-body displacement

$$\frac{\ell}{2}\int_0^1 m_0(\eta)\,\phi_1(\eta)\,d\eta + \frac{M_F}{2}\phi_1(0) + M_c\,\phi_1(\eta_c) = 0 \tag{F. 16}$$

(b) Condition that the generalized mass is equal to the total mass of the airplane

$$\ell\int_0^1 m_0(\eta)\,\phi_1^2(\eta)\,d\eta + M_F\,\phi_1^2(0) + 2\,M_c\,\phi_1^2(\eta_c) = M \tag{F. 17}$$

The combination of equations (F. 2), (F. 4), (F. 5), (F. 6), (F. 15), (F. 16) and (F. 17) yields

$$\phi_1(1) = \frac{1-\sigma}{\sqrt{\beta-\sigma^2}} \tag{F. 18}$$

$$\phi_1(0) = \frac{-\sigma}{\sqrt{\beta-\sigma^2}} \tag{F. 19}$$

where

$$\sigma = \frac{M_w}{M}\left(\frac{7}{60} + \frac{1}{2}\eta_c^2\right) \tag{F. 20}$$

$$\beta = \frac{M_w}{M}\left(\frac{9}{150} + \frac{1}{2}\eta_c^4\right) \tag{F. 21}$$

An approximate fundamental bending frequency can be obtained by using this mode shape in Rayleigh's method. This yields

$$\omega_1^2 = \frac{\left(\frac{2}{\ell}\right)^3 \int_0^1 EI(\eta)\left(\frac{d^2\phi_1}{d\eta^2}\right)^2 d\eta}{\frac{M}{2}} \tag{F. 22}$$

The substitution of equations (F. 9) and (F. 15) into equation (F. 22) yields

$$\omega_1 = \sqrt{\frac{23}{2}}\sqrt{\frac{EI(.5)}{M\left(\frac{\ell}{2}\right)^3}}\left[\phi_1(1) - \phi_1(0)\right] \tag{F. 23}$$

Typical values of the parameter $EI(.5)/M\left(\frac{\ell}{2}\right)^3$ range from about 0.1 to 10.

The substitution of equations (F. 8) and (F. 15) into equations (F. 11) and (F. 12) yields for the damping parameters Φ_1 and $\mathcal{G}_2$

$$\Phi_1 = \frac{5}{18}\phi_1(1) + \frac{13}{18}\phi_1(0) \tag{F. 24}$$

$$\mathcal{G}_2 = \frac{e}{2\mu k_1}\left[\frac{7}{45}\phi_1^2(1) + \frac{11}{45}\phi_1(1)\phi_1(0) + \frac{3}{5}\phi_1^2(0)\right] \tag{F. 25}$$

To evaluate $\mathcal{G}_2$ the following typical values were assumed:

μ = 40

$\frac{U}{c}$ = 50 per sec.

e = 3/4

This yields

$$\mathcal{G}_2 = \frac{7\phi_1^2(1) + 11\phi_1(1)\phi_1(0) + 27\phi_1^2(0)}{96\omega_1} \tag{F. 26}$$

The vibratory response of the wing can now be found from equation (F. 10) for any time variation of the rigid body acceleration. In Reference 4, the dynamic response factor for a one-minus-cosine time history of rigid body acceleration was found from this equation for various values of the damping parameter, $\mathcal{G}_2$, and the time ratio, t_1/T, and the resulting chart is reproduced here as Figure F. 2. The time ratio, t_1/T, is the ratio of the time to reach maximum rigid-body acceleration to the natural period of vibration, $T = 2\pi/\omega_1$. The dynamic response factor is the ratio of the maximum displacement of the bending mode under

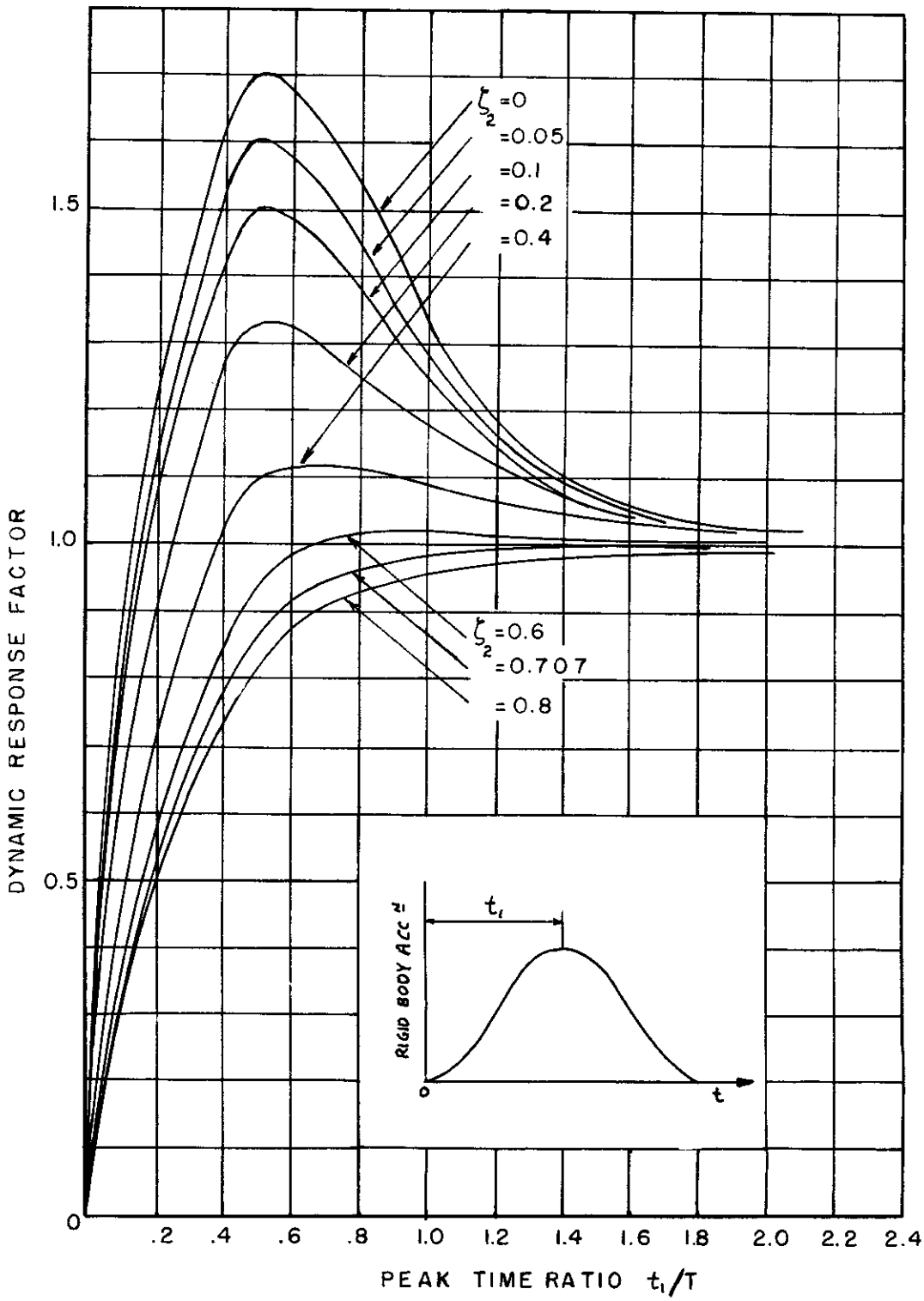

FIGURE F.2 DYNAMIC RESPONSE FACTOR WITH ONE-MINUS-COSINE FORCING FUNCTION

dynamic loading to its maximum displacement when the same loading is applied statically; i.e.,

$$DRF = \frac{(q_1)_{MAX}}{(q_{1\,RIGID})_{MAX}} \qquad \text{(F. 27)}$$

The variation of dynamic response factor with the spanwise location of the concentrated mass was found for two values of M_w/M and for two values of the stiffness parameter, $EI(.5)/M\left(\frac{b}{2}\right)^3$, and the results are presented in Figure F. 3. The solid lines show the variation in dynamic response factor when t_1 is specified as the time for the airplane to travel 12.5 chord lengths, and the dashed lines show the variation in dynamic response factor when t_1 is chosen for maximum response. The value of $EI(.5)/M\left(\frac{b}{2}\right)^3 = .223$ represents a "soft" wing such that, when $t_1 = 12.5\,\frac{\bar{c}}{U}$, t_1/T is always less then 1/2, while $EI(.5)/M\left(\frac{b}{2}\right)^3 = 1.840$ represents a relatively stiff wing such that t_1/T is always greater than 1/2. When t_1 is chosen for maximum response, the dynamic response factor is always greatest when the concentrated mass is at the tip; when $t_1 = 12.5\,\frac{\bar{c}}{U}$, the dynamic response factor for the stiff wing increases very rapidly as the concentrated mass is moved toward the tip, whereas the response factor for the "soft" wing decreases.

Except for the lag in rigid body response, the value of $t_1 = 12.5\,\frac{\bar{c}}{U}$ corresponds to the standard one-minus-cosine gust used in gust load specifications. From the viewpoint of random atmospheric turbulence (Reference 13), such a specification implies that gusts with other gradient distances have less intensity. If this

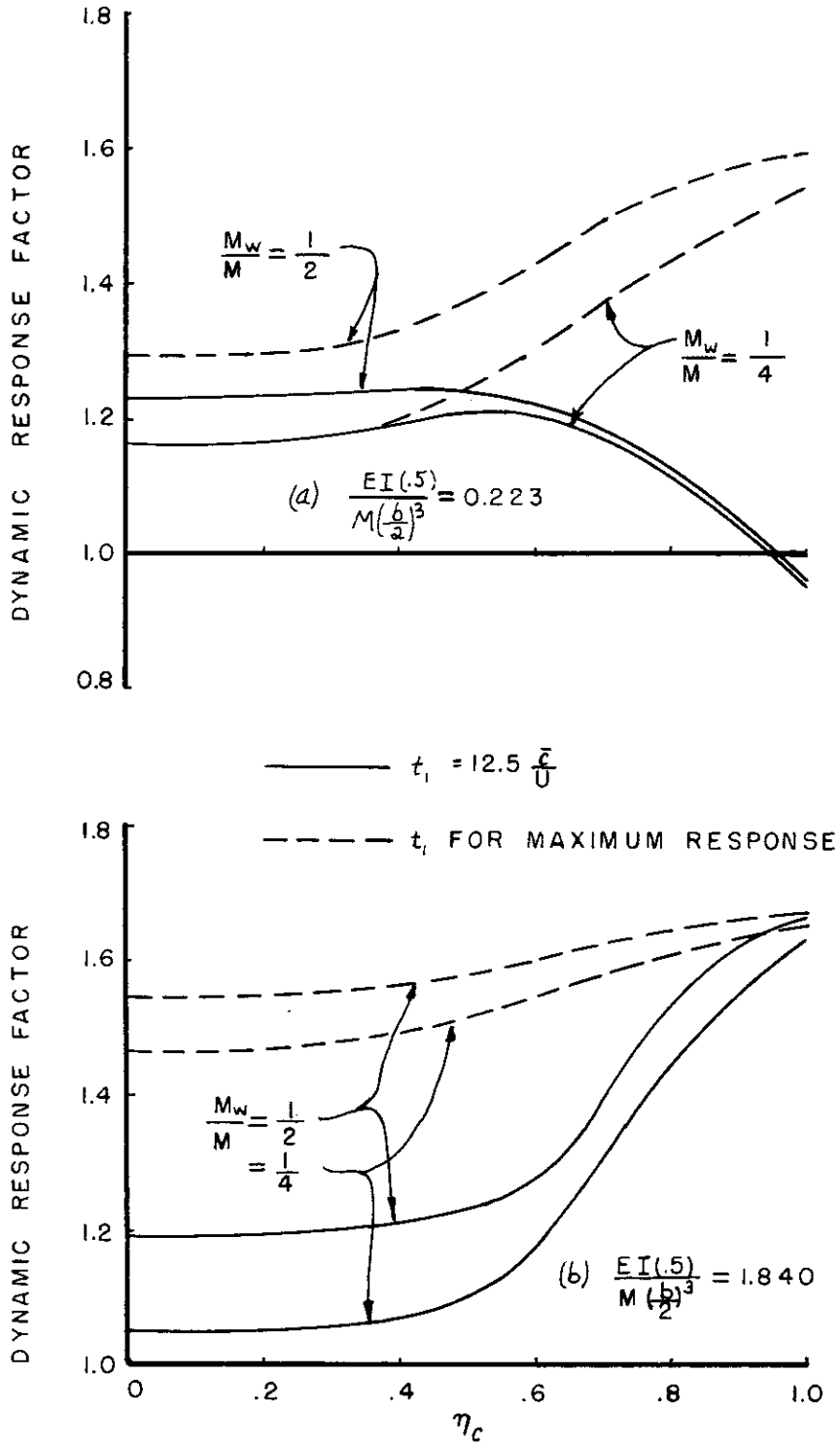

FIGURE F.3 EFFECT OF SPANWISE LOCATION OF CONCENTRATED MASS ON DYNAMIC RESPONSE.

is true, then the actual reponse of the wing probably should be represented by lines which lie somewhere between the solid and dashed curves of Figure F. 3; in which case, for minimum dynamic response, the concentrated mass should be located at an inboard location on the relatively stiff wing, whereas there is no clear-out location on the very flexible wing.

The dynamic response factor of Figure F. 3 is a crude measure of the dynamic overstresses in the wing; in fact, if the vibratory stresses in the wing were distributed in the same manner as those for a rigid airplane, this dynamic reponse factor would be the dynamic overstress in both shear and bending moment. However, the actual dynamic overstresses have spanwise variations and can be estimated by methods outlined in Reference 4. Two methods commonly used for computing dynamic stresses are the mode displacement and force summation methods. (The force summation method is called the "mode acceleration" method in Reference 4). In the mode displacement method, the spanwise distribution of stress is the same as that which results from the inertia forces that maintain the natural mode of vibration while the variation with time is determined from the amplitude, q_1 , of the vibration mode. From Reference 4, for the example wing, the bending moment is then

$$BM(\eta) = \omega_1^2 \frac{b}{2} q_1 \left[\frac{b}{2} \int_{\eta}^{1} \int_{\eta}^{1} m_D(\eta)\, \phi_1(\eta)\, d\eta\, d\eta + M_c (\eta_c - \eta)\, \phi_1(\eta_c) \right] \qquad \text{(F. 28)}$$

In the force summation method, the stresses are found from the air and inertia loads acting on the wing. Again from Reference 4, the bending moment is

$$BM(\eta) = \left[BM(\eta)\right]_{RIGID} - \omega_1^2\left[\dot{q}_1\left\{\frac{eM}{24k_1}\frac{b}{2}\int_\eta^1\int_\eta^1\frac{c}{\bar{c}}\phi_1(\eta)\,d\eta\,d\eta\right\}\right.$$

$$\left. + \ddot{q}_1\left\{\left(\frac{b}{2}\right)^2\int_\eta^1\int_\eta^1 m_0(\eta)\phi_1(\eta)\,d\eta\,d\eta - \frac{b}{2}M_c(\eta_c-\eta)\,\phi(\eta_c)\right\}\right] \qquad \text{(F. 29)}$$

where

$$\left[BM(\eta)\right]_{RIGID} = \omega_1^2\,\ddot{q}_0\left\{\frac{Mb}{4}\int_\eta^1\int_\eta^1\frac{c}{\bar{c}}\,d\eta\,d\eta - \left(\frac{b}{2}\right)^2\int_\eta^1\int_\eta^1 m_0(\eta)\,d\eta\,d\eta - \frac{b}{2}M_c(\eta_c-\eta)\right\} \qquad \text{(F. 30)}$$

The mode acceleration method described in Appendix E can also be applied to this simplified system. In comparison with the mode displacement method, only the stresses due to flexibility are computed from the distribution of vibratory inertia forces, and the bending moment is

$$BM(\eta) = \left[BM(\eta)\right]_{RIGID} + \omega_1^2\,\frac{b}{2}\left(q_1 - q_{1\,RIGID}\right)\left[\frac{b}{2}\int_\eta^1\int_\eta^1 m_0(\eta)\,\phi_1(\eta)\,d\eta\,d\eta\right.$$

$$\left. + M_c(\eta_c-\eta)\,\phi_1(\eta_c)\right] \qquad \text{(F. 31)}$$

When $\ddot{q}_0(\tau)$ is normalized so that its maximum value is unity, these three methods yield the following expressions for the dynamic overstress in bending:

(1) Mode displacement method,

$$\frac{\left[BM(\eta)\right]_{MAX}}{\left[BM(\eta)\right]_{RIGID\,MAX}} = q_{1\,MAX}\,B(\eta) \qquad \text{(F. 32)}$$

(2) Mode acceleration method,

$$\frac{[BM(\eta)]_{MAX}}{[BM(\eta)]_{RIGID_{MAX}}} = \left[\ddot{q}_0 + (q_1 - \Phi_1 \ddot{q}_0) B(\eta)\right]_{MAX} \qquad \text{(F. 33)}$$

(3) Force summation method,

$$\frac{[BM(\eta)]_{MAX}}{[BM(\eta)]_{RIGID_{MAX}}} = \left[\ddot{q}_0 - \dot{q}_1 A(\eta) - \ddot{q}_1 B(\eta)\right]_{MAX} \qquad \text{(F. 34)}$$

where

$$A(\eta) = \frac{\frac{eM}{24 k_1}\int_\eta^1\int_\eta^1 \frac{c}{\bar{c}}\phi_1(\eta)\,d\eta\,d\eta}{\frac{M}{2}\int_\eta^1\int_\eta^1 \frac{c}{\bar{c}}\,d\eta\,d\eta - \frac{b}{2}\int_\eta^1\int_\eta^1 m_0(\eta)\,d\eta\,d\eta - M_c(\eta_c - \eta)} \qquad \text{(F. 35)}$$

$$B(\eta) = \frac{\frac{b}{2}\int_\eta^1\int_\eta^1 m_0(\eta)\,\phi_1(\eta)\,d\eta\,d\eta + M_c(\eta_c - \eta)\,\phi_1(\eta_c)}{\frac{M}{2}\int_\eta^1\int_\eta^1 \frac{c}{\bar{c}}\,d\eta\,d\eta - \frac{b}{2}\int_\eta^1\int_\eta^1 m_0(\eta)\,d\eta\,d\eta - M_c(\eta_c - \eta)} \qquad \text{(F. 36)}$$

These three methods were applied to the example wing with $\eta_c = \frac{1}{4}$, $\frac{M_w}{M} = \frac{1}{4}$ $EI(.5)/M\left(\frac{b}{2}\right)^3 = 0.223$ and $t_1 = 12.5\,\frac{\bar{c}}{U}$ and the results are illustrated in Figure F. 4. There is considerable discrepancy in the three methods; and, although the force summation and mode acceleration methods are known to converge more rapidly than the mode displacement method, it is not known whether one bending mode gives sufficient convergence by either of the methods. For this reason a

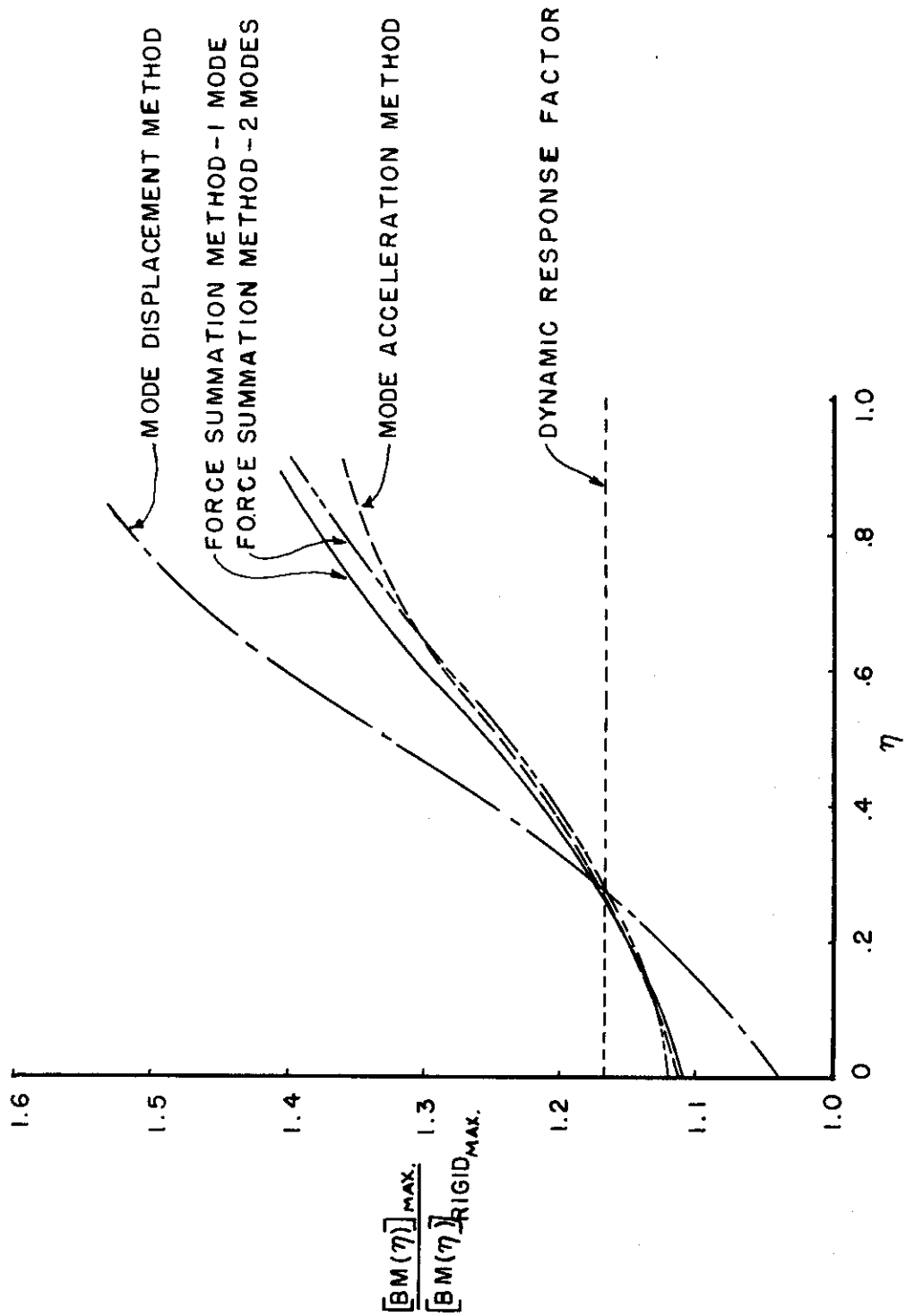

FIGURE F.4 COMPARISON OF STRESS METHODS FOR EXAMPLE WING, ONE BENDING MODE, $\eta_c = \frac{1}{4}$, $\frac{M_w}{M} = \frac{1}{4}$, $\frac{EI(.5)}{M(\frac{b}{2})^3} = 0.223$, $t_1 = 12.5\frac{\bar{c}}{U}$

similar analysis involving two bending modes of vibration was carried out.

Mode shapes for the second bending mode were estimated by two different methods. For the first method the mode shape was assumed as

$$\phi_2(\eta) = C_1 + C_2\eta^2 + C_3\eta^3 \qquad \text{(F. 37)}$$

The constants, C_1, C_2, and C_3 were determined from the conditions described by equations (F. 16) and (F. 17) together with the condition that $\phi_2(\eta)$ be orthogonal to $\phi_1(\eta)$; i.e.,

$$\frac{\ell}{2}\int_0^1 m_D(\eta)\,\phi_1(\eta)\,\phi_2(\eta)\,d\eta + \frac{M_F}{2}\phi_1(0)\,\phi_2(0) + M_C\,\phi_1(\eta_c)\,\phi_2(\eta_c) = 0 \qquad \text{(F. 38)}$$

An approximate second bending frequency was obtained from Rayleigh's method as in equation (F. 22).

For the second method the cubic polynomial of equation (F. 37) was assumed for both the first and second bending mode shapes; and the constants were determined by a Rayleigh-Ritz procedure which not only satisfied the orthogonality conditions of equations (F. 17) and (F. 38) but also satisfied the condition of no elastic coupling,

$$\int_0^1 EI(\eta)\,\frac{d^2\phi_1}{d\eta^2}\,\frac{d^2\phi_2}{d\eta^2}\,d\eta = 0 \qquad \text{(F. 39)}$$

A comparison of these mode shapes and frequencies is made in Figure F. 5. The close agreement between the second mode shapes and frequencies is probably

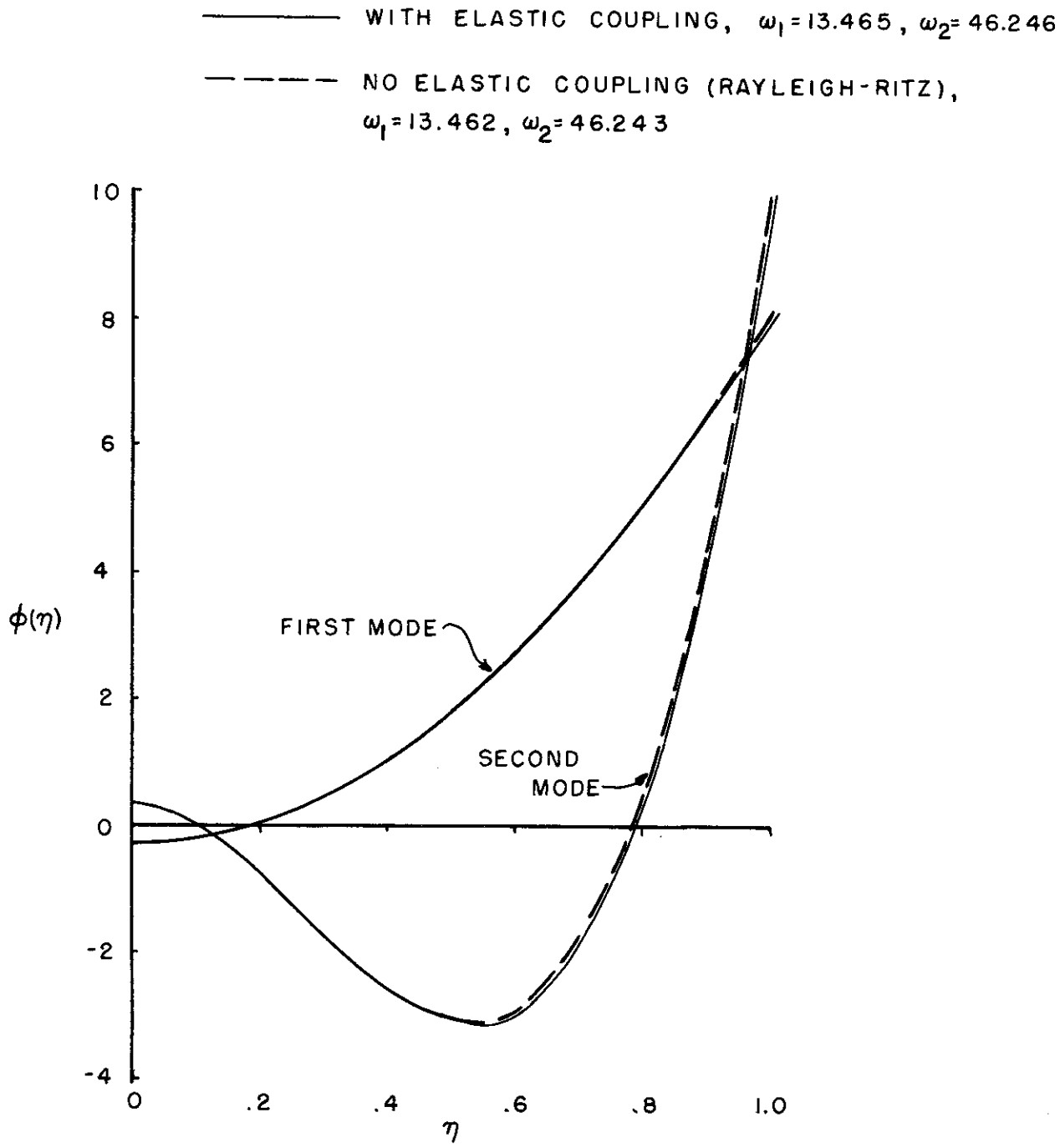

FIGURE F.5 COMPARISON OF ASSUMED MODE SHAPES, $\eta_c = \frac{1}{4}$, $\frac{M_w}{M} = \frac{1}{4}$

a coincidence. The difference in the response of the system for the two sets of mode shapes is negligible.

The dynamic overstress in bending moment when two bending degrees of freedom are considered is shown in Figure F. 6. The two-mode result by the force summation method is also plotted in Figure F. 4 for comparison. These results indicate that the dynamic overstress is given fairly accurately by both the force summation and the mode acceleration methods when only one bending mode is used.

Through the use of the mode acceleration method, the variation in dynamic overstress in bending with the location of the concentrated mass on the "soft" wing was found. These results are shown in Figure F. 7, and it can be seen that only the dynamic overstress near the root varies in the same manner as the dynamic response factor of Figure F. 3. When the concentrated mass is located at the wing tip, the dynamic overstress becomes infinite near the tip because the bending moment in the rigid wing changes sign rather than because the bending moment in the flexible wing is excessive. The bending moments in the wing are plotted on an absolute basis in Figure F. 8 for a better comparison between the elastic and rigid stresses.

From the results obtained in this study one may conclude that, for minimum dynamic overstress, a concentrated mass should be located at an inboard location on a relatively stiff unswept wing ($\frac{b_1}{T} > \frac{1}{2}$). For a relatively "soft" wing, there appears to be no clear-cut conclusion. These results are not applicable to swept wings because the bending slope of a swept wing introduces an angle of attack, and the bending vibration of the wing has a large influence on the rigid-body acceleration.

A similar investigation for swept wings would be even more inconclusive because of the additional parameters introduced by wing sweep.

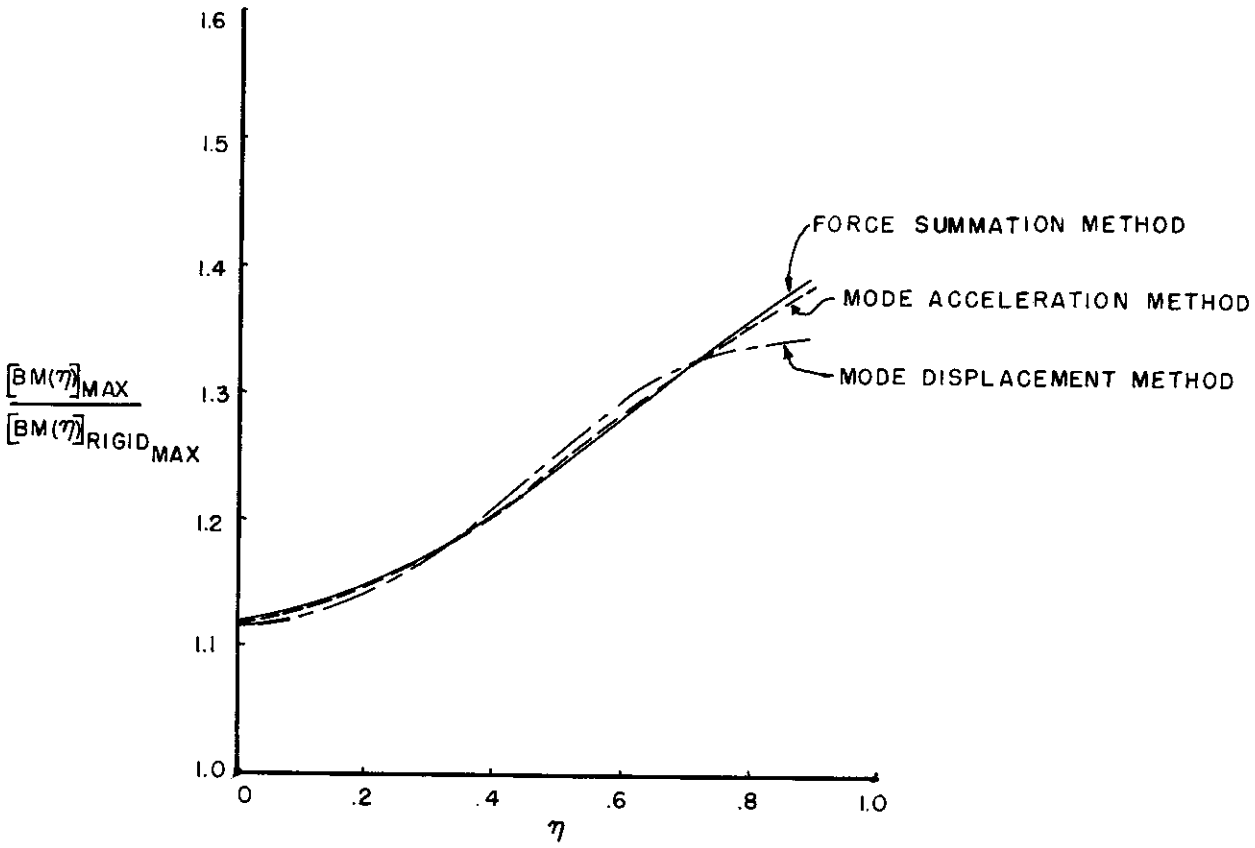

FIGURE F.6 COMPARISON OF STRESS METHODS FOR EXAMPLE WING, TWO BENDING MODES, $\eta_c = \frac{1}{4}$, $\frac{M_w}{M} = \frac{1}{4}$, $\frac{EI(.5)}{M(\frac{b}{2})^3} = 0.223$, $t_1 = 12.5 \frac{\bar{c}}{U}$

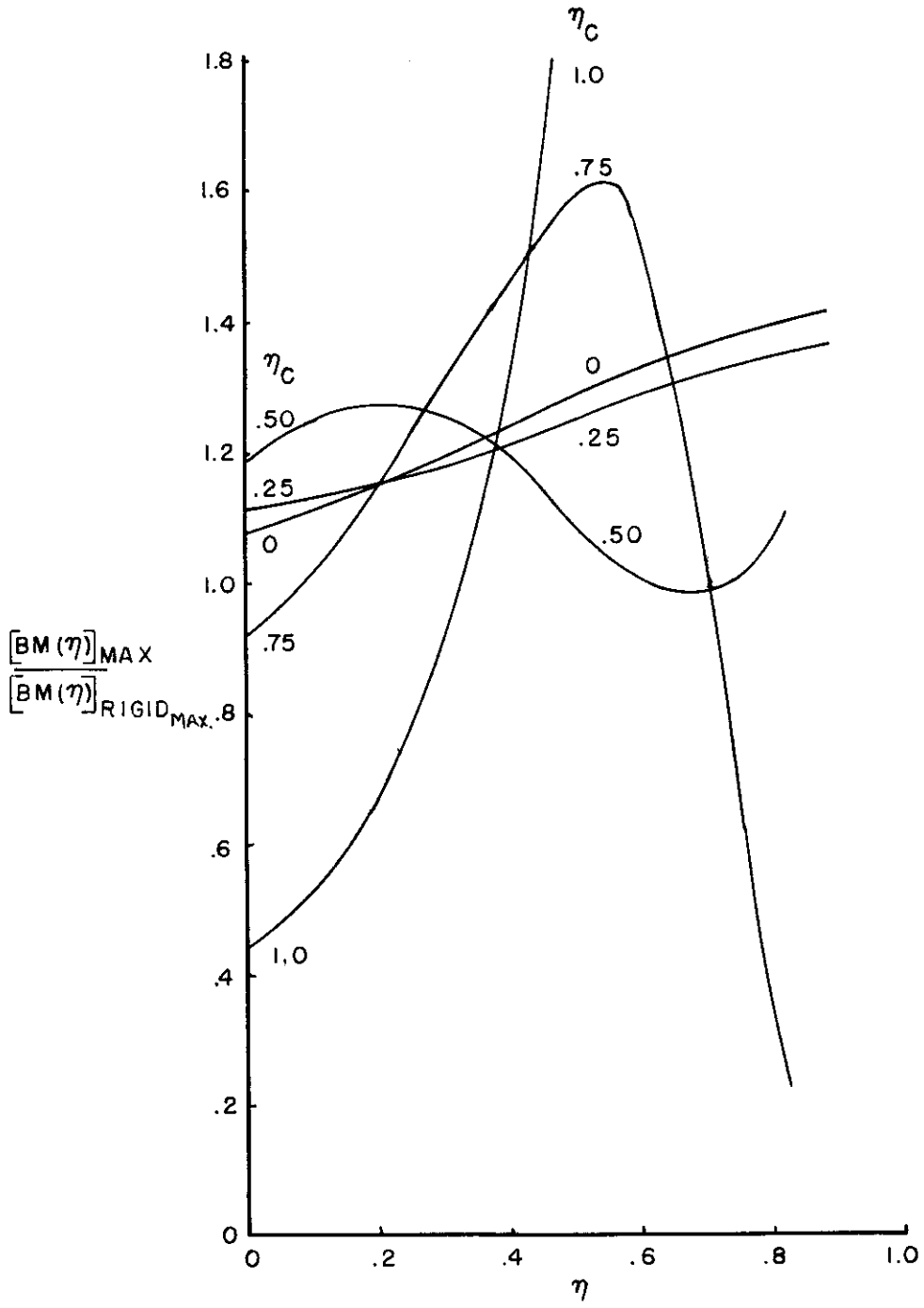

FIGURE F.7 VARIATION OF DYNAMIC OVERSTRESS IN BENDING WITH LOCATION OF CONCENTRATED MASS,

$\frac{M_W}{M} = \frac{1}{4}$, $\frac{EI(.5)}{M(\frac{b}{2})^3} = 0.223$, $t_1 = 12.5 \frac{\bar{c}}{U}$

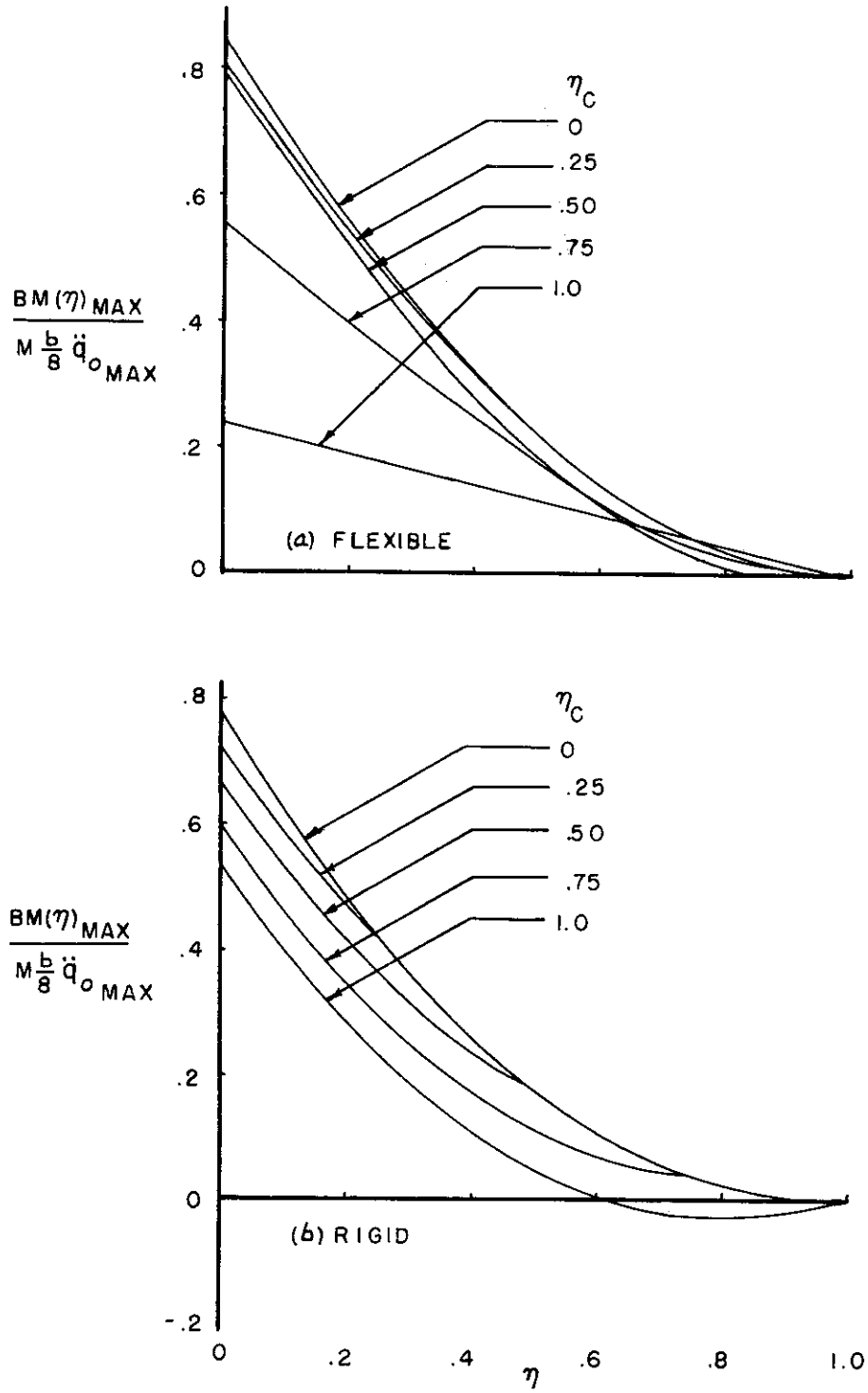

FIGURE F.8 VARIATION OF DYNAMIC STRESSES IN BENDING WITH LOCATION OF CONCENTRATED MASS,

$\frac{M_W}{M} = \frac{1}{4}$, $\frac{EI(.5)}{M(\frac{b}{2})^3} = 0.223$, $t_1 = 12.5\frac{\bar{c}}{U}$